MEMBRANE DISTILLATION OF CONCENTRATED BRINES

Lynette Mariah
BSc(Hons), (Natal)

Submitted in fulfillment of the academic
requirements for the degree of
Doctor of Philosophy
in the
School of Chemical Engineering
University of KwaZulu-Natal, Durban

March 2006

The fear of the LORD *is* the beginning of knowledge:
but fools despise wisdom and instruction.

Proverbs 1:7

To my Father

ACKNOWLEDGEMENTS

To God Almighty, the Lord Jesus Christ, without whom nothing is possible. For being my rock and my fortress and granting me the fortitude to live each day.

To my parents, for my very existence, and nurturing me in an upright way, giving me the opportunities to reach for my goals even though it meant painful sacrifices at times. Ma, hopefully now your nights will be a bit more restful.

To my siblings, my brother for being my brains and my sister my mouth so that I always had someone to count on no matter what the situation. My nephew Keenan – your presence in my life has alleviated more than one stressful and somber moments.

To Antonio, my soulmate, *"Tra sparare o sparire, scelgo ancora di sperare, finché ho te da respirare" (C. Baglioni).*
Grazie per tutti i sacrifici che hai sofferto per la nostra favola.

I would like to express my thanks and utmost gratification to my supervisor and co-supervisors:

Prof. Chris Buckley, for being more than just an instructor and curator but granting me grand opportunities which have aided my development into the individual that I've become.

Prof. Deogratius Jaganyi whose benevolence to co-supervise me has highly facilitated the progression of my studies. Your *hospitality* and unhesitating advice is most graciously appreciated.

Mr. Chris Brouckaert for helping me out when things got tough!

I wish to express my thanks to the following people and organizations:

The members of Staff at the School of Chemistry at Pietermaritzburg for laying the foundations of this work. The thermodynamics research unit at the Howard College campus, for their assistance during the experimentation that was performed in these labs.

To Prof. Drioli, for granting me the opportunity to work at his laboratories and the continuous assistance and collaboration during this work. To Efrem, for guiding me during the initial stages of an unbeknown area of work and, not to mention, an unknown habitat! To my Italian friends, Fausta, Silvia, Anna, Luca, Jurian (Olandese) and others, for making my stay in a foreign country much more easier and lots of fun at times.

"È sempre doloroso separarsi dalle persone che si conoscono da poco. Si può sopportare l'assenza di vecchi amici con animo sereno. Ma perfino una momentanea separazione da qualcuno a cui si è appena stati presentati risulta quasi insopportabile" Oscar Wilde

My friends, Gaish, Jess, Uresh, Jaz, Judith, Vish and others for keeping the laughter strong. Venashree and Keshika, for enabling more than one lonely and sad moments of being far from home, pass with much more ease, Desigan for watching my back as long as I needed and all others who have assisted me through the years in more than one way. Thanks.

Finally, these studies would have not been possible without the financial support of Sasol, the National Research Foundation (NRF) and The Technology and Human Resources for Industry Programme (THRIP).

ABSTRACT

Salinity is one of the most critical environmental problems for water scarce countries, deteriorating water quality and threatening economic and social consequences. This research encompasses the investigation of a system to appropriately manage concentrated aqueous brines. Membrane distillation and crystallisation is a useful adjunct to seawater and other desalination processes in order to further process the resulting brine streams. This technique becomes particularly valuable when treating solutions of extremely high concentration which other processes such as reverse osmosis are incapable of handling. The process uses low grade heat (which is often present in excess in many industries) and operates at about atmospheric pressure. This work demonstrates how membrane distillation and crystallisation was used to obtain pure crystalline products and water from solutions of sodium chloride and magnesium sulphate of concentrations near to saturation (exceeding 5 m).

A problem that is faced during membrane distillation is that of a rapid decline in distillate flux once crystal disengagement begins, after which the flux diminishes to zero. In order to gain a better understanding of the process, a new approach to the modelling of the membrane distillation process enables the prediction of driving force for the process by estimating the vapour pressure from chemical speciation calculations. The measurement of the vapour pressure is not readily achieved during the course of the experiment itself. The calculations were verified by performing experimental vapour pressure measurements in a dynamic vapour liquid equilibrium still.

The modelling of vapour pressures and hence driving force enabled it to be compared with the distillate flux. The thermodynamics of high ionic strength solutions were used to arrive at this correlation. This comparison revealed a marked similarity between driving force and distillate flux implying that reduction in the driving force is one of the mechanisms which causes the distillate flux to fall zero, along with membrane fouling and crystallisation on the membrane. Further simulations were performed which illustrates how membrane distillation could be used to recover solid products from a mixed solution of salts whilst maintaining a positive driving force at extremely high solute concentrations thus reducing both the cost and environmental impacts of brine disposal while being an energy conserving process. It was found that in order for reverse osmosis to operate at these concentrations, pressures exceeding 45 MPa have to be applied in order to overcome the osmotic pressure barrier.

PREFACE

I, Lynette Mariah, declare that unless indicated, this thesis is my own work and that it has not been submitted, in whole or in part, for a degree at another University or Institution.

.....

Lynette Mariah

March 2006

CONTENTS

FIGURES

TABLES

NOMENCLATURE

Symbols

a	solvent activity
b	universal empirical parameter
$\mathbf{A_\gamma}$	Debye-Hückel parameter for activity coefficient
$\mathbf{A_\phi}$	Debye-Hückel parameter for osmotic coefficient
B	geometric factor determined by pore structure (in Equation 2.27)
$\mathbf{B_s}$	solute permeability coefficient
$B_{ij}(I)$	second virial coefficients
B_{MX}	functions of ionic strength
c	molar concentration of ions
C	membrane mass transfer coefficient
$C_{ijk}(I)$	third virial coefficients respectively
C_{MX}	single electrolyte third virial coefficients
CV	Coefficient of variation
$\mathbf{d_w}$	density
D	diffusion coefficient
$\mathbf{D_w}$	dielectric constant of water
F	cumulative crystal size distribution
f(I)	Debye-Hückel type term in Equation 4.9
$\mathbf{G_{ex}}$	excess free energy
H	effective heat transfer coefficient
ΔH_{vap}	molar heat of vaporisation

I	ionic strength of the solution
J	mass flux
k_m	thermal conductivity of porous membrane
K_p	equilibrium constant for the p^{th} phase
K_{sp}	solubility product
ℓ	parameter which expresses the distance at which the electrostatic energy for singly charged ions in the dielectric just equals thermal energy (Equation 4.6b)
m	molality
M	molecular weight
n_w	mass of water
N_0	Avagadro's number
p	solute permeability
P	water vapour pressure
∇p_i	gradient in partial pressure
∇P	gradient in the total pressure
ΔP_{lm}	logarithmic mean vapour pressure
ΔP_{appl}	applied pressure
P_{net}	net pressure
Q	heat flux
r	pore radius
r_{max}	largest pore radius
R	universal gas constant
R_{rej}	rejection coefficient
T	temperature
Y_{in}	mole fraction of air
x	mole fraction

X	salt mass fraction of a solution
z	charge on an ion

Subscripts

a	anion
avg	average
c	cation
b	bulk
C	conductive heat
D	molecular diffusion model
f	feed
h	heat
K	Knudsen diffusion model
L	latent heat
m	membrane surface
P	Poiseuille flow model
p	permeate
s	solute
Th	threshold
w	water
x	mole fraction of dissolved species
MX	mixed electrolyte
DH	Debye Hückel

Superscripts

D	diffusive flux
f	feed
p	permeate
V	viscous flux

Greek Symbols

α	activity
χ	pore tortuosity
δ	membrane thickness
ε	membrane porosity
Φ_{ij}	mixed electrolyte coefficient
γ	concentration polarisation coefficient
γ_L	liquid surface tension
$\gamma_{\pm}$	mean activity coefficient
η	gas viscosity
λ	thermal or heat conductivity
$\lambda_{ij}(I)$	second virial coefficient (Equation 4.9)
μ	fluid viscosity
μ_{ijk}	third virial coefficient (Equation 4.9)
π	osmotic pressure
θ	liquid-solid contact angle

θ_{ij}	single parameter for each pair of anions or cations (Equation 4.13)
σ_r	reflection coefficient
σ	function in Equation 4.5b
τ	temperature polarisation coefficient
ψ_{ijk}	mixed electrolyte coefficient
ν	number of ions
ϕ	osmotic coefficient

ABBREVIATIONS

General Abbreviations

AGMD	Air Gap Membrane Distillation
CAPS	Compact Accelerated Precipitation Softening
CPC	Concentration Polarisation Coefficient
CSD	Crystal Size Distribution
CV	Coefficient of Variation
DCMD	Direct Contact Membrane Distillation
DGM	Dusty Gas Model
ED	Electrodialysis
EDR	Electrodialysis Reversal
GFW	gram formula weight
IAP	ion activity product
MC	Membrane Contactor
MCr	Membrane Crystalliser
MD	Membrane Distillation
MDC	Membrane Distillation Concentration
MED	Multi-Effect Distillation
MF	Microfiltration
MOD	Membrane Osmotic Distillation
MSF	Multi-Stage Flash (distillation)
NF	Nanofiltration
OD	Osmotic Distillation
OPPT	Office of Pollution Prevention and Toxics
PE	Polyethylene
PP	Polypropylene
PTFE	Polytetrafluoroethylene
PVC	Polyvinyl Chloride
PVDF	Polyvinylidene Fluoride
RO	Reverse Osmosis
SGL	Stripped Gas Liquor
SGMD	Sweeping Gas Membrane Distillation

SHMP	Sodium Hexametaphosphate
SI	Saturation Index
SPARRO	Slurry Precipitation and Recycle Reverse Osmosis
SRO	Seeded Reverse Osmosis
SSF	Sasol Synthetic Fuels
SWRO	Spiral Wound Reverse Osmosis
TDS	Total Dissolved Solids
TPC	Temperature Polarisation Coefficient
TRO	Tubular Reverse Osmosis
UF	Ultrafiltration
UNEP	United Nations Environment Programme
USGS	United States Geological Survey
VCD	Vapour Compression Distillation
VLE	Vapour liquid equilibrium
VMD	Vacuum Membrane Distillation

List of Minerals

Anhydrite	$CaSO_4$
Calcite	$CaCO_3$
Epsom Salt	$MgSO_4.7H_2O$ (Magnesium sulphate heptahydrate)
Gypsum	$(CaSO_4.2H_2O)$
Halite	NaCl
Mirabilite	$(Na_2SO_4.10H_2O)$
Magnesium sulphate	$MgSO_4$
Sodium chloride	NaCl
Sepiolite	$[MgSi_3O_6(OH)_2]$

Chapter 1

Chapter 1

INTRODUCTION

This research encompasses the investigation of a system to appropriately manage concentrated aqueous brines. In this thesis, the main process being investigated is the membrane distillation of concentrated brine solutions for the recovery of crystalline products from brine effluents. This chapter provides a background to this work. Section 1.1 serves as an overview of the water situation in South Africa. The utilisation and distribution of water within the Sasol industrial complex is specifically discussed. Section 1.2 addresses the issue of salinity in South Africa as a whole, and in industry in particular. Section 1.3 introduces the concepts of green chemistry and sustainable development and discusses their indispensability in any research or thought process in general. Section 1.4 summarises the various approaches that industry have adopted and those still under consideration in order to address the issue of salinity and brine disposal. Section 1.5 lays down the hypotheses and project objectives, and briefly describes the technique of membrane distillation that would be used to reach these objectives. Also described in Section 1.5 is the series of methods that would be followed to achieve the overall goal. This chapter concludes with the outline of this thesis in Section 1.6.

1.1 THE INDUSTRIAL WATER SCENARIO

Water is the backbone of the country's economy. The demand for pure water is on the rise within the social and economic sectors, whilst the availability of pure water is on the downward trend. South Africa experiences an average rainfall of 500 mm per year and, together with other natural resources such as rivers and lakes, is still inadequate to meet these demands (FAO, 2005). Industry poses as one of the chief consumers of large volumes of water together with the generation of vast quantities of wastewater (Mann and Liu, 1999). Industrial water traverses various operational arrays within the industrial domain.

The Sasol group of companies encompasses a diverse field of manufacturing and marketing operations within the sphere of fuels and chemicals. Sasol is world leading in the conversion of

low-grade coal to fuels, chemicals and gas and in so doing is South Africa's single largest industrial investor directly contributing about R 40 billion (ca 4 %) to South Africa's annual gross domestic product during the year (SASOL, 2005). The unique Fischer-Tropsch technology is the heart of this process. The initial stage in this process, known as gasification, requires coal to be reacted under pressure and high temperature and, following exposure to steam and oxygen, is converted into crude synthesis feed. As such, Sasol utilises large volumes of fresh water for the various operations which includes steam generation, process cooling and generation of electricity. The Sasol operations in South Africa alone consume water in excess of 300 Mℓ/d (Ginster and Jeevaratnam, 2003). Figure 1.1 is a schematic representation of Sasol's incoming water supplies and how these various water sources are distributed within the plant.

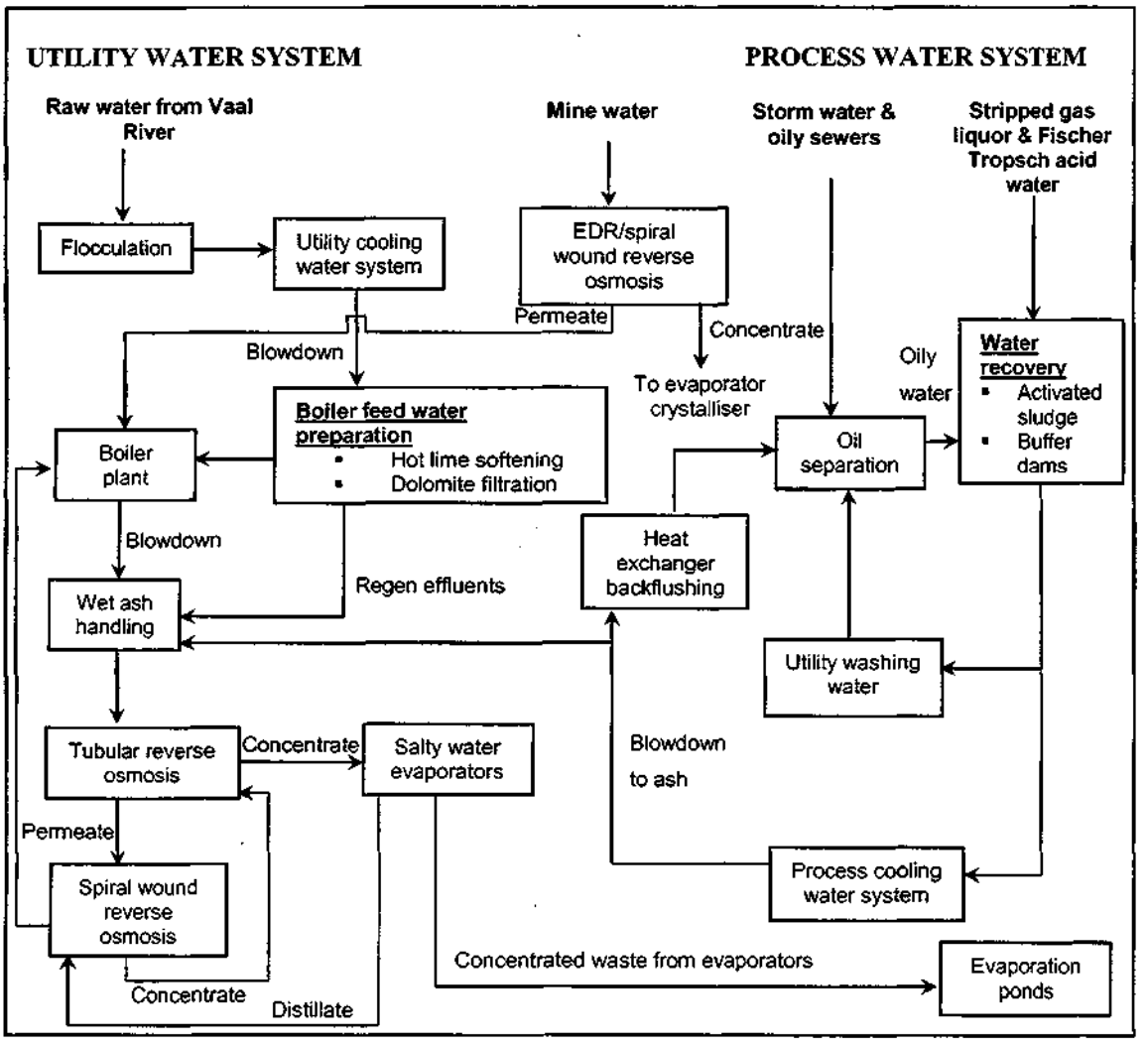

Figure 1.1: *Schematic diagram of the Sasol Secunda complex water distribution systems (Phillips and du Toit, 2002)*

Three main organic effluent streams arise from Sasol's operations:

(i) Stripped Gas Liquor (SGL) is the largest effluent stream. SGL emanates from the condensate of gasification which has undergone separation processes such as gravity separation, liquid-liquid extraction and steam stripping in order to retrieve by-products.

(ii) Oily sewer water, resulting from plant drainage from the operations, gives rise to the second largest effluent stream.

(iii) Fischer-Tropsch acid water forms the third largest of these effluent streams. Residual water emanating from the Fischer-Tropsch reaction is rich in organic compounds. These compounds are recovered by distillation, concomitantly yielding a distillate stream rich in organic acid (C_1 to C_6). This stream is known as the Fischer-Tropsch acid water.

Appropriate treatment of these organic effluent streams renders possible the recycling of these effluents as process cooling water. The majority of the blowdown from the process cooling water system is sent to the wet ash handling system and the remainder is recycled to the water recovery plant. The reason for the large flow of blowdown to the ash system initially arose from low rates of evaporation from the evaporation ponds. In order to overcome this hurdle, all initial downstream unit processes at the water recovery plant, such as clarification, filtration and ion exchange, were eliminated which facilitated a reduction in saline effluents. However, to compensate for the reduced quality of make-up to the process cooling water system, the cycles of concentration in the cooling system were reduced with the net effect of doubling the blowdown to the ash system.

1.1.1 The Ash Water System

Ash is a residue of coal combustion. Sasol produces large quantities of utility boiler ash comprising a mixture of *fly ash* and *bottom ash*. Sasol adopts a wet ash handling system. In this system the ash is conveyed to the ash heaps as a slurry. The excess water is recovered and stored in a series of dams prior to re-use. To overcome the positive water balances in the wet ash water system (due to the increased load from the process cooling water system), a combined reverse osmosis (RO) plant comprising of a primary tubular reverse osmosis (TRO) unit and a secondary spiral wound reverse osmosis (SWRO) unit has been installed to treat clear ash effluent (Figure 1.1). Regeneration effluents from the boiler feed water preparation plant is sent

to the ash handling system. Permeate from the SWRO unit is recycled as boiler feed water. The chemistry of the ash water (TRO brine) is similar to that of mine water, with sulphate and sodium forming the major components. Some iron, potassium, manganese, copper and silica are also present in small amounts. Most of the ash produced in South Africa is disposed on landfills. However, the rapidly increasing size of the ash systems is becoming a mounting threat to industries.

1.1.2 The Mine Water System

South Africa holds fifth position on a global basis as a coal producing country (Azzie, 2001). Moreover, Sasol alone operates one of the world's largest underground coal mining complexes. Coal mining requires large volumes of water for operations including, amongst others, drilling, dust suppression, environmental cooling and hydropower generation. The remains of these activities tend to increase the contamination of mine water which collects in the underground mining complex. The characteristic mine water can be typified as acidic, saline and containing high metal concentrations. A system was installed to purify this water for re-use as boiler feed water. It consisted of an electrodialysis reversal (EDR) plant followed by a SWRO plant (Figure 1.1). A major portion of the chemistry of the EDR and mine water constitutes sulphate, sodium, calcium, chloride and magnesium, in order. A small fraction of potassium and silicate are also present giving rise to a total dissolved solids (TDS) content of 20 g/ℓ and 5 g/ℓ for EDR and mine water, respectively. Depending on the particular treatment technology that the mine water undergoes, the correspondent waste residue stream may be in the following forms (Du Plessis, 2005):

- Neutralization sludges with a typical composition of metal hydroxides, carbonates and gypsum.
- Sulphur sludges from biological treatment processes.
- Softening sludges with a high calcium carbonate content.
- Brines with variable concentrations of various salts dependent on the chemical profile of the mine water feed.

Despite the recovery and re-use of the mine water, another problem which will be aggravated over the years is that of seepage of surface and underground water into the mined-out areas. A proposal for the treatment of this water to produce water which could substitute or complement

the raw water stream is being analysed, however the capital and operating costs of this process may make the system uneconomic.

A generic water balance, developed by Pulles et al. (2001) for the South African coal mining industries, explicitly describes the industry-wide patterns of water sources, water utilisation and water disposal around coal mines. This water balance enables industries or other role players to set benchmarks that can be used to evaluate the water management performance of individual mines. With the accumulation of mine water being on the increase, it seems improbable that the solution to the problem lies simply in the treatment of this water. An alternative and possibly innovative strategy needs to be devised before this challenge can be overcome.

1.2 THE SALINATION SCENARIO

Salinity is the general term associated with the build-up of salts in soil or water. Saline water, in particular, refers to water containing dissolved solids which are in excess of the limits of potable water (U.S. Bureau of Reclamation and Sandia National Laboratories, 2003). Salinity has become one of South Africa's most critical challenges, threatening economic and social consequences. Saline waters have two major origins - natural and anthropogenic (DWAF, 2005). The salination of river water is a natural, inevitable cause borne by the geology of the land. Man-made causes are manifold. The large volumes of aqueous waste that are discharged by industries represents one of the sources of salts. However, a greater predicament is that of diffuse pollution as it impacts over a much larger area on the water resource. This scattered form of pollution has its origins from, amongst others, poor or deficient administration of urban settlements, land pollution from waste deposits and accumulation of the remains of mining activities.

The Sasol operations alone contribute two of the major sources of saline aqueous effluents, i.e. internal to the water circuits and ash systems or external on the mining operations. Figure 1.2 is an illustration of the distribution of water and salt within the Sasol Synthetic Fuels (SSF) complex together with an indication of the quantity of these streams that pass through the plant on a daily basis.

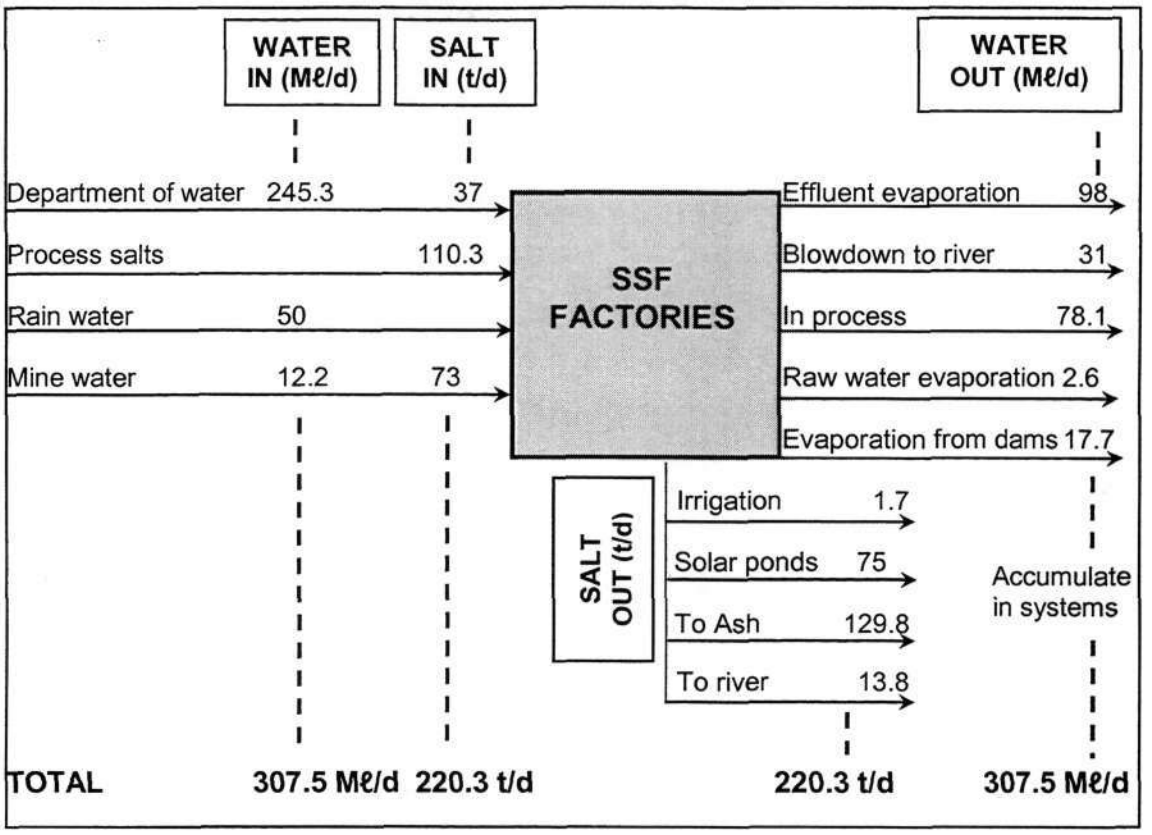

Figure 1.2: *Average daily figures of water and salt flows within the SSF complex (SASOL, 2004)*

The internal salt generation arises from water treatment processes such as desalination for water recovery, ion exchange regeneration for water softening to produce boiler feed water and cooling systems which produce blow down. Furthermore, when ash comes into contact with water a saline alkaline leachate is formed.

With the increase in the demand of fresh water in South Africa, particularly within the industrial sector, and with salination reducing the availability of pure water, an urgent need arises for the clean-up or prevention of saline effluents. Numerous measures against salination are being implemented both in industry and on the urban frontier. These include reducing salts in the water supply and during domestic and industrial use, proper management of water resources (release of part of the water resource to sea), suitable irrigation systems and practices, soil conditioning and desalination of water and wastewater (Juanicó, 2005). However, if one would consider treatment of the source of the problem in the first instance, this would ultimately prevent build-up and a dilemma at the end-of-pipe stage.

1.3 GREEN CHEMISTRY AND SUSTAINABLE DEVELOPMENT

The United States Pollution Prevention Act of 1990 prompted the U.S. Environmental Protection Agency to take action and develop preventative approaches against pollution (Nameroff et al., 2004). The Office of Pollution Prevention and Toxics (OPPT) was founded and focuses on being able to improve existing infrastructure and to prevent the recurrence of previous shortcomings in new developments (Hjeresen et al., 2000). It was the U.S. Environmental Protection Agency who first introduced the concept of Green Chemistry and defined it as *the utilization of a set of principles that reduces or eliminates the use or generation of hazardous substances in the design, manufacture and application of chemical products* (EHSC, 2002). Globalisation of the concept of green chemistry has expanded this definition and it now covers a wider range of issues than those reflected in the original statement. The green chemistry programme has impinged on many areas of society and developed various collaborations with academia, industry and other governmental agencies such that green chemistry is now being envisaged as a way to think rather than just a new branch of science. Over the years it has been realised that through the implementation of various sub-disciplines of chemistry and molecular sciences, there is a rising positive reception that this flourishing area of chemistry is needed in the design and attainment of *sustainable development.*

In 1987, the United Nation's Brundtland Commission defined sustainable development as *meeting the needs of the present without compromising the ability of future generations to meet their own needs* (United Nation's General Assembly, 1987). This definition is very broad and could have many different interpretations. As such, there have been many debates over the definition of sustainability. Since the Brundtland Report, sustainability has been given numerous definitions as (i) maintaining intergenerational well-being, (ii) maintaining the subsistence of the humankind, (iii) satisfying the productivity of economic systems, (iv) maintaining biodiversity, and (v) maintaining evolutionary prospective (Tisdell, 1991). However, despite these various ways of defining sustainability this is a concept that is vague by nature. The concept of sustainability may assist in decision making for the establishment or progression toward a sustainable business, enterprise or society; however the ambivalent character of the concept, i.e. trying to sustain something that exists in a milieu of perpetual change, is both theoretically and functionally challenging. But if one considers that life itself revolves around change, it is not surprising then, that sustainability is a principle of life about both sustaining a particular resilient state and adjusting to changing internal conditions (Köhn et

al., 2000). Over the years sustainable development has become an accepted aim of the world. This paradigm may also be explained by the perception, from the late 1960s, that the world is facing a meta crisis, including crises of development, environment and security (Kirkby et al., 1995).

With *Green Chemistry* and *Chemical Engineering*, one works toward *sustainable development* by inventing, designing and implementing chemical products that fulfil the following ideologies of overcoming the environmental pollution hurdle (Anastas and Warner, 1998; Frederick, 2005 and ACS, 1987):

- Preventative approach – seizing the problem at the roots thus preventing aggravation with time and adversity at maturity.
- Atom economy – making maximum use of starting materials to yield the final product.
- Minimisation of the use of hazardous products – a synthetic route should be planned so as to prevent the use and generation of harmful or toxic reagents and products or, if certain auxiliaries are indispensable, the minimum quantities should be used.
- Design of safer chemicals and chemistry – chemical products should be designed with reduced toxicity and potential for chemical accidents, while still maintaining efficacy in functionality.
- Energy conservation and waste minimisation – energy and use of non-renewal resources should be reduced as much as possible during the manufacture and use phases of a product.
- Less hazardous solvents and auxiliaries – selecting the most appropriate solvents with minimum toxicity.
- Design of appropriate starting materials and products – a raw material or feedstock should carry renewable end properties while products should be biodegradable.
- Reduction in derivatives – use of protection / deprotection groups and blocking groups during chemical syntheses should be minimal or avoided if possible as such steps generate additional waste.
- Efficient use of catalysts – selective catalysts should be preferred wherever possible.
- Real-time analysis for pollution prevention – development of analytical methods to allow for real-time in-process monitoring and control prior to hazardous material formation.

If the above mentioned principles are adhered to, particularly by industry, it is proposed that within two decades the following should be possible (Sanghi, 2000):

- Complete eradication of emissions from polymer manufacturing and processing.
- Substitution of all environmentally hazardous solvents and acid-based catalysts with solids or more eco-friendly alternatives.
- Waste reduction between 30 and 40 %.
- More than 50 % reduction in the amount of plastics in landfills.

Recently, a strategy for implementing the relationships between industry and academia has been proposed. This philosophy known as the *triple bottom line* predicts that an enterprise or business association would be economically sustainable if the objectives of environmental protection, societal benefit, and market advantage are all satisfied (Tundo et al., 2000). This three fold philosophy is a strong hypothesis for evaluating the success of industry or environmental technologies.

Industry would be a good starting point for the promotion and implementation of green chemistry thus providing the pathway for others to follow to a cleaner and greener country. Recent advancements to Sasol's industrial chemical plant have proved to be making valuable progress in this direction. A project involving the utilisation of natural gas, brought in from Mozambique, as a substitute to their large coal requirements as a source of energy, lead to significant reductions in this industries overall environmental emissions. The use of natural gas has decreased Sasol's coal requirements by a factor of 60 to 70 % and was said to yield significant environmental benefits (BCSD, 2003).

Any technical solution to the problem of salinity needs to be assessed by applying the principles of green chemistry and sustainable development.

1.4 INDUSTRIAL APPROACH TO SALINITY

Desalination technologies have been recognised as the primary method of generating surplus water supplies and is so rapidly developing that the efficiency of desalination technologies evolves at a rate of approximately four percent per year (U.S. Bureau of Reclamation and Sandia National Laboratories, 2003). It is therefore this approach of desalination that industries

have adopted in order to produce freshwater from saline effluents for re-use or recycling and forms an attractive approach, especially if the particular industry is situated within water scarce catchments. **Section 1.4.1** lists some of the desalination technologies that are currently in use. However, it must be realised that every desalination and water purification technology generates two process streams – a water product stream and a brine or concentrate stream. The latter contains species that did not pass through the membrane during desalination using membrane technologies or of the backwash from low pressure processing. These waste streams contain high concentration of salts and other contaminants. Disposal of these streams is currently posing a major problem to industries. Some approaches that have been considered by industries for brine handling and disposal is discussed in **Section 1.4.2.**

1.4.1 Desalination Technologies

Recent years have seen significant progress in the improvement of desalination technologies in industry and mining and a number of new desalination plans are currently being devised. Listed below are some of the technologies that are used for the desalination and purification of saline water.

- Membrane technologies – makes use of semi-permeable or selective membranes in order to remove contaminants during the desalination or purification of water. Examples include microfiltration, ultrafiltration, nanofiltration, reverse osmosis and electrodialysis (these are discussed in detail in Chapter 2).
- Thermal technologies – requires energy (heating or cooling) for selective retention of contaminants with the production of pure water.
- Reuse / Recycling technologies – modified membrane or alternate technologies which are appropriately adjusted to accommodate for increased contaminant loads due to their end applications (valuable or saleable products).

The basis of all desalination technologies is conversion of part of the inlet feedwater flow into fresh water. This inevitably results in a stream of water which is relatively concentrated in dissolved salts. This concentrated stream is a major obstacle which creates uncertainty and hinders the implementation of desalination technologies, as the management and containment of these inorganic waste products (sludges and brines) pose a serious problem.

1.4.2 Brine handling options

In the past most of the waste streams arising from the various mining and manufacturing activities were discharged to surface waters or the ocean. However, more rigid current and future environmental regulations will make these disposal routes less feasible, therefore other disposal options need to be sought. It seems that technologies that are available for managing these waste products are either prohibitively uneconomic (exceeding the cost of water treatment or desalination) or unsatisfactory because of long term liabilities and associated risks they pose to water resources (Du Plessis, 2005).

Andrews and Witts (1993) have discussed some options concerning the handling of RO concentrates and, more recently, Du Plessis (2005) has suggested future trends in brine disposal. Apart from surface water discharge, they have described the following as typical means of concentrate disposal:

- Spray irrigation / land application.
- Deep well injection in appropriate geological environments.
- Waste water treatment facilities which are capable of accommodating concentrate loads without disturbing its own treatment operations.
- Thermal evaporation and solar evaporation ponds.
- Drain fields and boreholes where discharge is to the surficial aquifers.
- Disposal in old underground mine workings, similar to existing backfill operations.
- Solidification and deposit in underground vaults.

However, the extent of use of these methods is subject to the composition or, in some instances, quality of the concentrate, government regulations, economic implications and site-specific factors.

Table 1.1 lists an evaluation of some brine disposal options considered by industry, together with the advantages and disadvantages associated with these technologies.

Table 1.1: *Summary of the various brine handling technologies at Sasol (Ginster et al., 2003)*

Name	Description	Advantages	Disadvantages
Brine to Brick	In this process an ash cement brick which is more economical is made from brine.	• A stronger brick as opposed to bricks manufactured using tap water.	• Performance over prolonged periods is unknown and requires further investigation.
Evaporator / crystalliser	Further concentration of brine coming from EDR membrane desalination.	• Tried and tested. • A dry product is produced which is preferred for land disposal.	• The crystallised salts do not carry high saleable value. • Added cost for salt disposal. • Little or no further brine handling options.
Waste backfilling	Co-disposal of brine with ash backfills into mine workings.	• The formation of acid rock drainage is suppressed and less water can seep into the mine. • Mine-life can be prolonged.	• This concept has been well-applied internationally; however, local implementation is limited. • Pumping and flow rates are limited. • Requires cementitous agent to bind the salt.
Salt splitting	Uses bi-polar membranes to split salts of sodium sulphate to sodium hydroxide and sulphuric acid.	• Generation of reagents that can be re-used within process streams.	• Bi-polar membranes are intolerant to certain impurities such as iron and silica present in brine effluents.
Solar ponds	Modification of existing salt storage ponds.	• Widely used. • Operationally economic.	• Contamination to groundwater. • Temporary solution.

Considering the two major sources of saline aqueous effluents within the Sasol complex discussed in **Section 1.2**, the internal salt generation needs to be addressed through a range of

interventions including waste minimisation, process optimisation and water pinch but ultimately concentrated brine streams will be produced. Considering the mining operations there are three ways to respond to salinity:

i) A preventative approach – by changing land use practices responsible for the aggravation of the problem and to prevent further damage.
ii) Management and containment – by schemes such as salt interception to control the groundwater movement through the subsurface or by lowering the water tables.
iii) Considering the salts as a sustainable resource for the next two thousand years – instead of viewing salinity as a problem, it could be viewed as an opportunity to obtain value while simultaneously improving the situation.

Much work has been performed on being able to solve this salinity crisis. However, bearing in mind the concept of sustainable development, the third tactic to this problem of salinity forms an attractive approach. We can view these saline waters as an environmental problem or we can turn this environmental problem into an economic resource by viewing these saline waters as a sustainable resource of salts (Mariah et al., 2004). Several of the waste streams contain potentially recoverable and saleable products. Sustainable salt sinks can be achieved by considering the formation of valuable salts when designing a saline water circuit and the composition of the streams that enter the circuit. The separation and concentration processes need to be combined to produce high value products.

1.5 PROJECT OBJECTIVES

Based on the premise that inorganic concentrates can be separated into high purity chemicals and reusable water, this research addresses the need for industries such as Sasol to ensure an adequate supply of water of sufficient quality while at the same time being able to manage the inorganic brines arising from its manufacturing and mining activities. The chlor alkali salt preparation circuit is an example of a process that requires a pure sodium chloride feed for a subsequent synthesis step (electrolysis) (Gianadda, 2002). Suitably purified and concentrated brine streams could substitute for the imported raw salt which is used as the feed chemical. A technique is therefore required in order to separate and recover these concentrates with the concomitant release of pure water. **Section 1.5.1** discusses a membrane technique which is proposed. **Section 1.5.2** describes the approach that was followed during this study.

1.5.1 Proposed Membrane Technique

Many techniques have been investigated for the desalination of water and separation of salts. The most commonly used is that of RO although other techniques such as thermal desalination and evaporation have been investigated (Kurbiel et al., 1995). The main shortcoming of RO is the need for excessively high pressures at high solute concentrations, as is the case of high saline industrial water such as ash and mine water (Mariah et al., 2006a). This elevated pressure is required in order to overcome the osmotic pressure barrier in concentrate processing. In processes such as thermal evaporation, for example, high temperatures are required in order to achieve evaporation and salt recovery. A need therefore seems to arise for a process which would achieve the recovery of crystalline products and pure water and is capable of operating at high solute concentrations while still maintaining engineering feasibility of *simple* operating conditions.

Membrane distillation (and crystallization) is a technique which potentially leads to an almost complete water recovery and the elimination of the brine disposal problem. Chemical manufacturing complexes frequently have an excess of low-grade heat. This energy can be used to create a temperature gradient across a hydrophobic microporous membrane. The resulting vapour pressure difference produces a flux of water vapour through the membrane thus aqueous brine solutions can be concentrated and crystallised. This process does not have the limitations of processes such as RO and thermal evaporation as this process can operate at high solute concentrations, at low concentration gradients, moderate temperatures and atmospheric pressure (Mariah et al., 2006b). Recent innovative designing of integrated membrane processes have led to process intensification and reduction in pre-treatment costs (Drioli et al., 2002). Integration of various single membrane units might assist in overcoming the shortfalls otherwise experienced if these units operate independently, i.e. many specialised separations as opposed to one big concentration step.

1.5.2 Specific Aims

This thesis is concerned with the technique of membrane distillation for the separation and recovery of salts from concentrated brine effluents. A study into the process of membrane distillation, paying attention to the driving force for the separation process, is examined. This work addresses the problem faced by membrane scientists of the decreasing flux trend by

evaluating the driving force during a batch membrane distillation experiment and examining if this could be correlated with the distillate flux. The following approaches were identified in order to reach the necessary goal:

- Proof of concept – the ability of recovering crystalline salts and pure water from concentrated brine solutions using membrane distillation crystallisation would be investigated. The brine solutions that would be studied consist of single and mixed electrolyte systems of magnesium sulphate and, sodium chloride and magnesium sulphate, respectively. For the mixed salt solutions the objective would be the crystallisation of sodium chloride.

- Vapour pressure modelling – in order to evaluate the driving force during a batch membrane distillation process, the vapour pressure difference across the membrane needs to be measured. However, this is impossible during the experiment itself hence the possibility of modelling these vapour pressures using a geochemical speciation program will be investigated. The accuracy of the computer program will be verified by experimental vapour pressure measurements. These will be performed using a dynamic vapour-liquid equilibrium still.

- Evaluation of driving force - the vapour pressure driving force during the course of the membrane distillation experiments need to be calculated using the geochemical speciation program and correlated with the distillate flux to examine the implications.

An underlying criterion that was necessary for the facilitation of this work was an understanding of high ionic strength electrolyte chemistry. In order to gain this proficiency the initial theoretical work involved an examination of the brine stream used as a feed for a chlor alkali circuit at the Polyfin Umbogintwini (Sasol Polymers) plant (now closed) (Gianadda, 2002). This work has necessitated an understanding of high ionic strength aquatic speciation chemistry and the associated modelling (Mariah et al., 2003).

1.6 THESIS OUTLINE

Chapter 1 provides an introduction to the research work presented in this thesis. The scope of this work is outlined together with the project objectives and the series of methods that would be followed in order to achieve these aims.

Chapter 2 summarises the relevant literature and outlines the important concepts necessary for the development of this work. The review begins with a description of the chemistry of natural waters followed by a discussion of the various techniques of desalination leading to the technique of membrane distillation crystallisation that will be used in this work. The advantages and disadvantages of these methods are specifically discussed.

Chapter 3 presents the results of the membrane distillation of single salt solutions of magnesium sulphate and that of mixed salt systems of sodium chloride and magnesium sulphate in varying mass ratios, chosen in order to crystallise sodium chloride. Details of the experimental procedure are provided together with a discussion of the implication of the results.

Chapter 4 provides a background of the chemistry of high ionic strength solutions and the various models available for the determination of the thermodynamic properties of these solutions. The use of chemical speciation models for the determination of these properties is discussed focussing on the particular model used during this work.

Chapter 5 forms the core results and discussion of this work. This Chapter begins by providing the results obtained from speciation modelling procedures used to determine the vapour pressures of the salt solutions. This is then followed by experimental verification of the computed results. The experimental technique used to obtain the vapour pressures of the salt solutions is described together with the outcome. This research is then drawn together by a correlation of the results obtained from the individual procedures and a discussion thereof.

Chapter 6 brings this work to a close by concluding all major findings and suggesting possibilities for future advancements.

1.7 CHAPTER REFERENCES

ACS (AMERICAN CHEMICAL SOCIETY, 1987). *Cleaning our environment – A chemical perspective.* In: *A report by the committee on environmental improvement.* 2nd edition. Washington, D. C. ISBN 80084758.

ANASTAS PT and WARNER JC (1998). *Green Chemistry, Theory and practice*, Oxford University Press, New York. ISBN: 0-19-850234-8.

ANDREWS LS AND WITTS GM (1993) *An overview of RO concentrate disposal methods.* In *Reverse Osmosis: Membrane Technology, Water Chemistry, and Industrial Applications*, AMJAD Z, ed., Van Nostrand Reinhold, New York. ISBN: 0-442-23964-5. 379-388.

AZZIE BA and FEY MV (2001) *A classification of mine water, reflecting both quality and geochemistry.* In Cidu, R. (ed) 10th International Symposium on Water-Rock Interaction (WRI 10), Villasimius, Italy, Proceedings Volume **1**: 1177-1180.

BCSD (BUSINESS COUNCIL FOR SUSTAINABLE DEVELOPMENT): SOUTH AFRICA (2003) Sustainable development update.

DRIOLI E, CRISUOLI A and CURCIO E (2002) *Integrated membrane operations for seawater desalination.* Desalination **147** 77-81.

DWAF (2005) Water Quality Management in South Africa. Department of Water Affairs and Forestry, South Africa. Accessed on 12 September 2005 at URL http://www-dwaf.pwv.gov.za/Dir_WQM/wqm.htm.

DU PLESSIS M (2005) Draft Terms of Reference for a Solicited WRC Project. Key Strategic Area: *Water use and waste management.* Proceedings of the Workshop to Develop the Terms of Reference for an Investigation of Innovative Approaches to Brine Handling (that will significantly reduce the potential impacts of brines on the water environment). Rietfontein, Pretoria, South Africa, May 19, 2005.

EHSC Note (2002) *Green chemistry.* Environment, Health and Safety Committee, RSC. 1-4.

FAO (2005) *Aquastat: South Africa*. Food and Agricultural Organisation of the United Nations. Accessed on 2nd September 2005 at URL http://www.fao.org/ag/agl/aglw/ aquastat/water_res /south_africa/index.stm.

FREDERICK J (2005) *Green Chemistry and Chemical Engineering*. Accessed on 7 September 2005 at URL http://greenchemistry.jimfred.info.

GIANADDA P (2002) *The development and application of combined water and materials pinch analysis to a chlor-alkali plant*. PhD thesis. Pollution Research Group, University of Natal, South Africa.

GINSTER M, COERTZEN M, ENSLIN W and HUGO DJ (2003). *Preliminary review on alternative brine handling options*. Water and Environmental Research – Sasol Technology R&D.

GINSTER M and JEEVARATNAM EG (2003). *Chemical analysis of sasol brine streams*. Water and Environmental Research – Sasol Technology R&D.

HJERESEN DL, SCHUTT DL and JANET MB (2000) *Green chemistry and education*. J Chem Ed 77 (12) 1543-1547.

JUANICÓ – Environmental Consultants Ltd. International consulting firm on high-tech low-cost low-energy solutions for warm climates. *Salination*. Accessed on 14 September 2005 at URL http://www.juanico.co.il/Main%20frame%20-%20English/Issues/Salination.htm.

KIRKBY J, O'KEEFE P and TIMBERLAKE L (1995). *The earthscan reader in sustainable development*. Earthscan Publications Ltd., London. ISBN: 1-85383-216-2.

KÖHN J, GOWDY J, HINTERBERGER F and VAN DER STRAATEN J (2000). *Sustainability in action: sectoral and regional case studies* in Advances in Ecological Economics. Edward Elgar, UK. ISBN: 1-84064-067-7.

KURBIEL J, BALCERZAK W, RYBICKI MS and ŚWIST K (1995). *Selection of the best desalination technology for highly saline drainage water from coal mines in southern Poland.* Desalination **106** 415-418.

LAWSON KW and LLOYD DR (1997). *Membrane Distillation: Review.* J Membr Sci **124** 1-25.

MANN JG and LIU YA (1999) *Industrial water reuse and wastewater minimization. McGraw-Hill, New York.* ISBN: 0-07-134855-7.

MARIAH L, JEAN R, BUCKLEY CA and JAGANYI D (2003) *Chemical Speciation Modelling of an Industrial Hydroponics system using a Geochemical Equilibrium Speciation Model.* South African Chemical Institute, KwaZulu-Natal Research Colloquim, University of KwaZulu-Natal, Pietermaritzburg, South Africa.

MARIAH L, BUCKLEY CA, JAGANYI D, DRIOLI E and CURCIO E (2004), *The Development of Sustainable Salt Sinks – Evaluation of an Integrated Membrane System for the Recovery and Purification of Magnesium Sulphate and Sodium Chloride from Brine Streams*, The 37th National Convention of the South African Chemical Institute, CSIR International Convention Centre, Pretoria, South Africa, July 4-9.

MARIAH L, BUCKLEY CA, BROUCKAERT CJ, JAGANYI D, CURCIO E and DRIOLIE (2006a). *Membrane Distillation for the Recovery of Crystalline Products from Concentrated Brines*. WISA Biennial Conference, Durban, South Africa, May 21-25.

MARIAH L, BUCKLEY CA, BROUCKAERT CJ, CURCIO E, DRIOLI E, JAGANYI D, and RAMJUGERNATH D (2006b) *Membrane distillation of concentrated brines – role of water activities in the evaluation of driving force.* J Membr Sci. **280** (1-2) 937-947.

NAMEROFF TJ, GARANT RJ and ALBERT MB (2004). *Adoption of green chemistry: an analysis based on US patents*. Research Policy 33 959-974.

PHILLIPS TD and du TOIT FJ (2002). *Water reuse and re-cycling at Sasol*. Proceedings of the 3rd International Conference and Exhibition on Integrated Environmental Management in Southern Africa (CEMSA 2002), Johannesburg, South Africa.

PULLES W, BOER RH and NEL S (2001). *A generic water balance for the South African coal mining industry*. Report to the Water Research Commission on the Project *A generic water balance for the South African coal mining industry*. WRC Report No. 801/1/01. ISBN: 1-86545-777-X.

SANGHI R (2000) *Better living through sustainable green chemistry*. Current Science **79** (12) 1662-1665.

SASOL (2004) *Ash water system: Technical evaluation on salts*. Data Sheet.

SASOL (2005) *Annual Report 2004*. Accessed on 2nd September 2005 at URL http://sasol.quickreport.co.za/sasol_ar_2004/.

TISDELL CA (1991). *Economics of environmental conservation* In: *Economics for environmental and ecological management*. Elsevier, Amsterdam. ISBN 0-444-89075-0.

TUNDO P, ANASTAS P, BLACK D, BREEN J, COLLINS T, MEMOLI S, MIYAMOTO J, POLYAKOFF M and TUMAS W (2000) *Synthetic pathways and processes in green chemistry. Introduction overview*. Pure Appl Chem **72** (7) 1207-1228.

UNITED NATIONS GENERAL ASSEMBLY (1987) Report of the World Commission of Environment and Development (1987) *Our Common Future* (became commonly known as the Brundlandt Report).Official Records of the general Assembly, 42nd Session, Supplement No. 25, (A/42/25). Pg. 24.

U.S. BUREAU OF RECLAMATION and SANDIA NATIONAL LABORATORIES (2003) *Desalination and water purification technology roadmap – A Report of the Executive* Committee. Bureau of Reclamation, Denver Federal Center, Water Treatment Engineering & Research Group, Denver, USA.

Chapter 2

Chapter 2

LITERATURE REVIEW

Salinity is a broad concept and the chemistry of saline waters is complicated. Section 2.1 introduces the concept of salinity; it is followed by a description of the chemistry of brine. A significant amount of research has been performed concerning the desalination of these waters to produce, amongst other components, pure water. Desalination processes and their principle of separation are described in Section 2.2. The operation and evaluation of these membrane processes are described within this Section. As membrane distillation is the subject of this thesis it is described in detail in Section 2.3. Section 2.4 concludes this chapter by demonstrating how these various desalination and separation operations can be brought together to form integrated membrane systems ultimately leading to process intensification.

2.1 SALINITY

The term salinity encompasses a description of a range of waters of differing total dissolved solids (TDS) content. These include fresh water, brackish water, saline water and brine. The TDS content governing the distinction between these terms is < 1 g/ℓ, 1 to 20 g/ℓ, 20 to 50 g/ℓ and > 50 g/ℓ, respectively (Smith, 2000). As described in **Section 1.2**, industrial mine water has a TDS content of more than 20 g/ℓ. These waters are therefore considered saline or brine. The chemistry of brine is complicated and is described in **Section 2.1.1**. However, if this saline water can be desalinated to produce pure salts, **Section 2.1.2** describes how the value of these salts could be exploited.

2.1.1 Brine Chemistry

Brine is a form of water which is significantly more saline than seawater. The chemistry of a brine is determined from the chemistry of the inflow waters (Eugster, 1980). **Section 1.2** outlined the major industrial sources of brine. Natural brines consists of six primary ions, Na^+, Mg^{2+}, Ca^{2+}, Cl^-, SO_4^{2-} and HCO_3^-, although the major contributor to the TDS of mine water is SO_4^{2-} resulting from bacterial and chemical oxidation of pyrites (Juby et al., 1996). The

abundance, diversity and interaction of these ions in solution are complicated and are determined by chemical speciation of the sample. In evaporation ponds, saline waters are concentrated until minerals become saturated. If the saturation index (SI) of a particular mineral is reached, i.e. SI = 0, the mineral will precipitate out of solution and certain elements are removed from the brine while the remaining elements become residually enriched. According to Eugster and Jones (1979) this evaporation and crystallisation process causes all inflow waters of varying chemical composition to tend towards a similar end product. This type of crystallisation is known as fractional crystallisation and implies that the crystallised minerals have no further interaction with the brine (Harvie and Weare, 1980). Equilibrium crystallisation, on the other hand, differs in that the precipitating minerals continue to react with the brine while maintaining equilibrium with the brine. These types of mineral crystallisation are described in more detail in **Section 2.1.1.1** and **Section 2.1.1.2**.

2.1.1.1 Fractional Crystallisation

The Hardie-Eugster model (Figure 2.1) describes how brines evolve through the chemistry of the waters. Mineral precipitation gives rise to *chemical divides* – junctions where the composition of the brine can change course and follow a new path. Based on the general principle: *whenever a binary salt is precipitated during evaporation, and the effective ratio of the two ions in the salt is different from the ratio of the concentrations of these ions in solution, further evaporation will result in an increase in the concentration of the ion present in greater relative concentration in solution and a decrease in the concentration of the ion present in lower relative concentration*, a series of pathways can be followed (Drever, 1997).

Calcite ($CaCO_3$) is typically the first mineral to precipitate and therefore demarks the first chemical divide. The initial pathway is then governed by the ratio of bicarbonate to alkali-earth metals, i.e. whether the calcium concentration ($2m_{Ca^{2+}T}$) is greater or less than the carbonate alkalinity ($m_{HCO_3^-T} + 2m_{CO_3^{2-}T}$), where T signifies total analytical concentration. In a water where solutes are completely obtained from atmospheric CO_2 and dissolution of calcite, the charge balance equation is:

$$2m_{Ca^{2+}} + m_{H^+} = m_{HCO_3^-} + 2m_{CO_3^{2-}} + m_{OH^-} \qquad [2.1]$$

If m_{H^+} and m_{OH^-} are ignored then:

$$2m_{Ca^{2+}} = m_{HCO_3^-} + 2m_{CO_3^{2-}} \quad [2.2]$$

This case defines the balance point of the chemical divide (Drever, 1997). Evaporation of these waters will result in the precipitation of calcite, without the accumulation of Ca^{2+} relative to alkalinity or vice versa. If the conditions of Equation 2.2 are not fulfilled this will result in either the build up of Ca^{2+} or alkalinity following which, one of a series of five pathways may be followed.

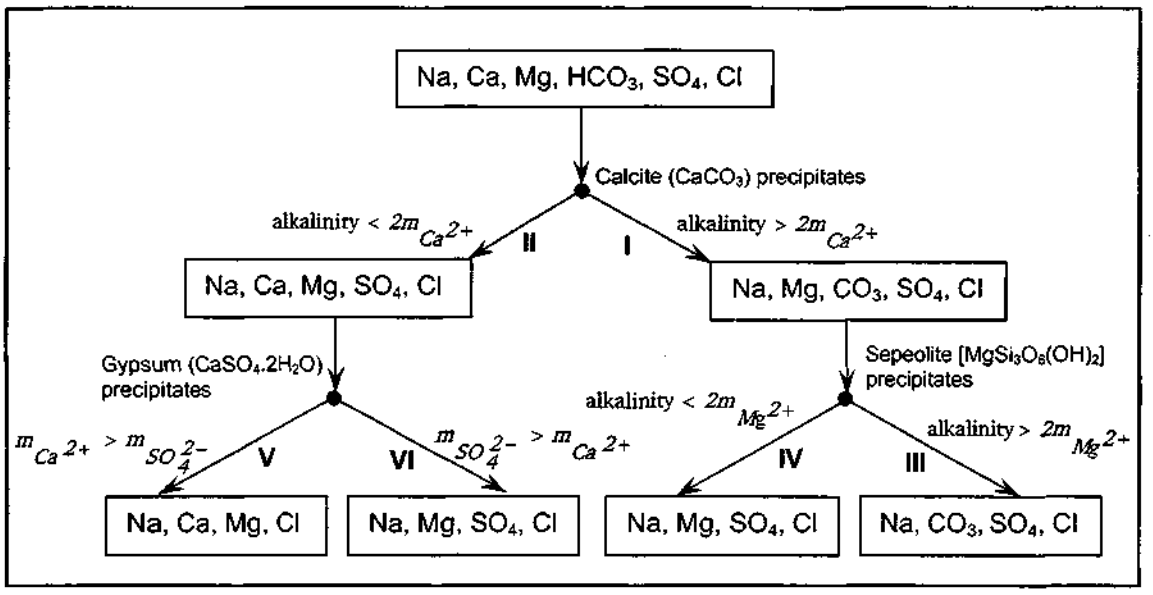

Figure 2.1: *Possible pathways for the model evaporation of natural waters (adapted from Drever, 1997 after Hardie and Eugster, 1970)*

The pathways are described below (Eugster and Jones, 1979 and Drever, 1997):

- **Pathway I**: HCO_3 >> Ca. A low Ca concentration restricts the amount of calcite that can precipitate. During evaporation essentially all the calcium will be removed from solution and the solution will consequently tend toward an alkaline carbonate brine. This ion deficiency results in a brine that is rich in Na-Mg-CO_3-SO_4-Cl. Following this pathway the next mineral to precipitate and cause a chemical divide is sepiolite ($MgSi_3O_6(OH)_2$). This chemical divide involves three species – Mg^{2+}, HCO_3^- and H_4SiO_4. The determinant is whether the Mg concentration is greater or less than the

carbonate alkalinity after calcite precipitation. Depending on this criterion either pathway III or IV will be followed.

- **Pathway II**: $HCO_3 << Ca$. This case is the converse of pathway I. The surplus calcium allows for the formation of gypsum ($CaSO_4.2H_2O$) and the eventual precipitation of this mineral results in a chemical divide. The solution then tends towards a neutral sulphate or chloride path consisting of Na-Ca-Mg-SO_4-Cl. Depending on the calcium concentration after calcite precipitation either pathway V or VI can be followed.

- **Pathway III**: $HCO_3 >> Mg$. If the magnesium concentration, after calcite precipitation, is less than the alkalinity, either gypsum or mirabilite ($Na_2SO_4.10H_2O$) can precipitate and the resulting water will become an alkali carbonate brine consisting of Na-CO_3-SO_4-Cl.

- **Pathway IV**: $HCO_3 << Mg$. If the magnesium concentration, after calcite precipitation, is greater than the alkalinity, the solution will tend toward a carbonate-free sulphate or chloride brine, Na-Mg-SO_4-Cl.

- **Pathway V**: $SO_4 << Ca$. If the calcium concentration, after calcite precipitation, is greater than the sulphate concentration the resulting brine will have chlorides of Na-Ca-Mg as the major solutes.

- **Pathway VI**: $SO_4 >> Ca$. If the calcium concentration, after calcite precipitates is less than the sulphate concentration, the resulting brine will be in the form of Na-Mg-SO_4-Cl.

In summary, the Hardie–Eugster model demonstrates that the composition of the brine could be determined by the composition of the water source from where the brines were derived and should contain relatively few ions as the major species. However, criticism has arisen as to the simplicity of the Hardie–Eugster model and since then more sophisticated models have been developed (Al-Droubi et al., 1980, Drever, 1997 and Harvie et al., 1984).

2.1.1.2 Equilibrium Crystallisation

In this situation both the mineral sequence and quantities of precipitation differ from that of fractional crystallisation. This process can occur, for example, when fresh water flows into a pond with existing water. A process known as back-reaction occurs when the *new* brine begins to equilibrate with the *old* brine or its precipitates. An example is anhydrite ($CaSO_4$) and gypsum back-reacting with the brine to form glauberite ($CaSO_4.Na_2SO_4$) and polyhalite ($2CaSO_4.MgSO_4.K_2SO_4.2H_2O$). The remaining brine composition is changed and new minerals are formed which are often compound salts (Smith, 2000).

The chemistry of brine is complex and suitable chemical speciation methods need to be carried out before the chemical composition of a particular brine can be fully understood. Furthermore, chemical speciation requires the thorough knowledge of thermodynamic properties such as activity coefficients – the modelling of which is rather complex.

2.1.2 *Uses of Salts*

Salt is one of the basic raw materials of all modern industries. The total salt produced in the world in 2002 was 225 million tons, the majority being produced in the United States of America (Salt Institute, 2005). South Africa does not form part of the top ten salt producing countries but contributes a significant proportion to the overall production. Listed in **Sections 2.1.2.1** to **2.1.2.6** are just some of the uses of salt.

2.1.2.1 Industrial Uses

One of the most important uses of salt (NaCl) is as a feedstock to the chlor-alkali industry, used for the manufacture of chlorine and caustic soda and many other industrial and inorganic chemicals, and allied products. Chlorine is an effective disinfectant and bleach. Downstream, vinyl chloride and polyvinyl chloride (PVC) and their derivatives are produced from chlorine. Caustic soda is used in pulp processing, and to make cellulose chemicals and their derivatives. Sodium chlorite is used in the textile industry. Other chemicals manufactured from salt are metallic sodium and sodium chlorate. Salt is used directly by many industries such as in textile dyeing and in industrial uses like curing animal hides whether done commercially or domestically (Salt Institute, 2005). A variety of materials, each of which is used in the

production of many products, are produced by different treatments, or processing of rock salt or salt brine. Some of these include sodium carbonate and sulphate, used in the manufacture of glass, pulp and paper; sodium nitrate, a component of fertilizers and explosives; liquid sodium, used as a coolant or heat exchanger; metallic sodium, used in making brass or bronze and hydrochloric acid, used in making synthetic rubber, amongst other uses. Salt is also significantly useful in the manufacture of soap and glycerine. Fats and oils are saponified using caustic soda while the soap is *salted out* from solution using a strong brine (Hugo, 1974). Saturated brine is used during the drilling of oil wells to preserve the core intact.

2.1.2.2 Water softening

The hardness of water is defined as *the concentration of ions in the water that will react with a sodium soap to precipitate an insoluble residue* (Drever, 1997). Hard water containing excessive magnesium and calcium has become an increasing problem in many parts of the world. Zeolites used for water softening are hydrated aluminosilicates with exchangeable Na or K ions (Grillot, 1956). Therefore, when hard water is passed through a tank containing zeolites, the Ca and Mg are retained by the zeolite in exchange for Na and K. After numerous exchange processes, such that the original sodium zeolite becomes almost completely converted into a Ca and Mg zeolite, the original zeolite may be restored by passing an excess of NaCl through the bed.

2.1.2.3 Human and animal nutrition

Salt is an essential and one of the most demanding components of a human being. Apart from being essential to the nutritional and physiological processes of the body, salt also forms an important flavouring substance in food. Animals have a more well-defined appetite for sodium chloride than any other compound in nature, except water (Salt Institute, 2005). In addition to the basic nutritional requirements in animals, salt functions as a carrier of trace minerals such as iron, copper, zinc, manganese, cobalt, iodine and selenium.

2.1.2.4 Highway de-icing and anti-icing for safety and mobility

When salt is applied to ice and snow it creates a brine that has a lower freezing temperature than the surrounding ice or snow. The use of salt for snow and ice controls was first introduced in the 1930s (Salt Institute, 2005). In the late sixties it increased in popularity facilitating easy

mobility without danger during the winter seasons. Its availability, low-cost, harmless and easily manageable properties makes salt ideal for this purpose.

2.1.2.5 Food Industry

Salt is extensively used in the food industry as an antiseptic and a preservative. It is added to a variety of food products to control the microbial populations therein (Hugo, 1974). Recently, the simultaneous brine thawing / salting operations has been proposed for the processing of frozen meat products which are salted after thawing (Barat et al., 2005). Particularly, Barat and co-workers (2005) showed that the post-salting period is shortened when using the brine salting / thawing method as compared to the tradition pile-salting method, during the production of Spanish cured ham. Salt is also used in aquaculture for example, by fish farmers to keep their product *healthy*. During the canning of vegetables, salts are added to hot blanching water to add tenderness to peas, beans, cucumbers, etc. (Hugo, 1974).

2.1.2.6 Uses of Epsom salt (magnesium sulphate heptahydrate, $MgSO_4.7H_2O$)

Epsomite, $MgSO_4.7H_2O$, is a widely used fertilizer and has other important applications in the medical field such as the administration during cardiac arrest, hypokalaemia, eclampsia and severe asthma. General uses are listed below (Mani Agro Chem, 2005):

- Micro nutrient in agriculture.
- Raw material in soaps and detergents.
- Laxative in medicine.
- Refreshing additive in bath water.
- Raw material in the manufacture of other magnesium compounds.
- Feed supplement in the manufacture of poultry and cattle feed.
- Coagulant in the manufacture of plastics.

The use of these various salts such as sodium chloride, epsomite, caustic soda, etc. in the numerous fields discussed, makes it an indispensable part of many technological processes. The spent solution containing salt, together with several organic matter such as protein or polysaccharides are produced during these processes. Biological methods are traditionally used for wastewater treatment however more stringent government regulations have further lowered the limit of effluent discharge (Gryta et al., 2001). As a result these methods are becoming less

popular as they are unable to meet these new restrictions. However, the demand for freshwater and the increasing value of salts requires processes to be able to desalinate brines with the concomitant production of fresh water and high value chemicals.

2.2 DESALINATION

Desalination can be defined as any process that removes salts from water (Krishna, 2004). This process is used commercially around the world to produce fresh water for many communities and industrial sectors. Desalination processes are divided into (i) thermal methods, in which water is heated to its boiling point to produce water vapour, and (ii) membrane processes, which make use of a relatively permeable membrane for the transport of either water or salt to induce two zones of differing concentrations to produce fresh water (Winter et al., 2001). Descriptions of these desalination processes are given in **Sections 2.2.1** and **2.2.2** that follow. **Section 2.2.3** outlines some of the drawbacks of these desalination processes.

2.2.1 Thermal Desalination Processes

The main thermal method employed for desalination is distillation, where saline water is progressively heated in subsequent vessels at lower pressures and then condensed to produce fresh water. The various distillation processes that are used to produce fresh water are multi-stage flash distillation (MSF), multi-effect distillation (MED) and vapour compression distillation (VCD). In all of these processes conservation of thermal energy is a fundamental objective, therefore distillation involves the production of vapour using low temperatures by reducing the vapour pressure inside the unit thus reducing the boiling point temperature requirement. It therefore appears that the major requirement for these distillation processes is providing the heat for vaporisation to the feedwater.

2.2.1.1 Multi-stage Flash Distillation

MSF is the most widely used desalination method forming 70 % of the total world installation desalination plants (Ismail, 1998). Figure 2.2 provides a schematic representation of the MSF plant setup. In this process saline water is heated in flash chambers to very high temperatures and then passed through vessels of reducing pressure to induce maximum vapour production (Winter, 2001).

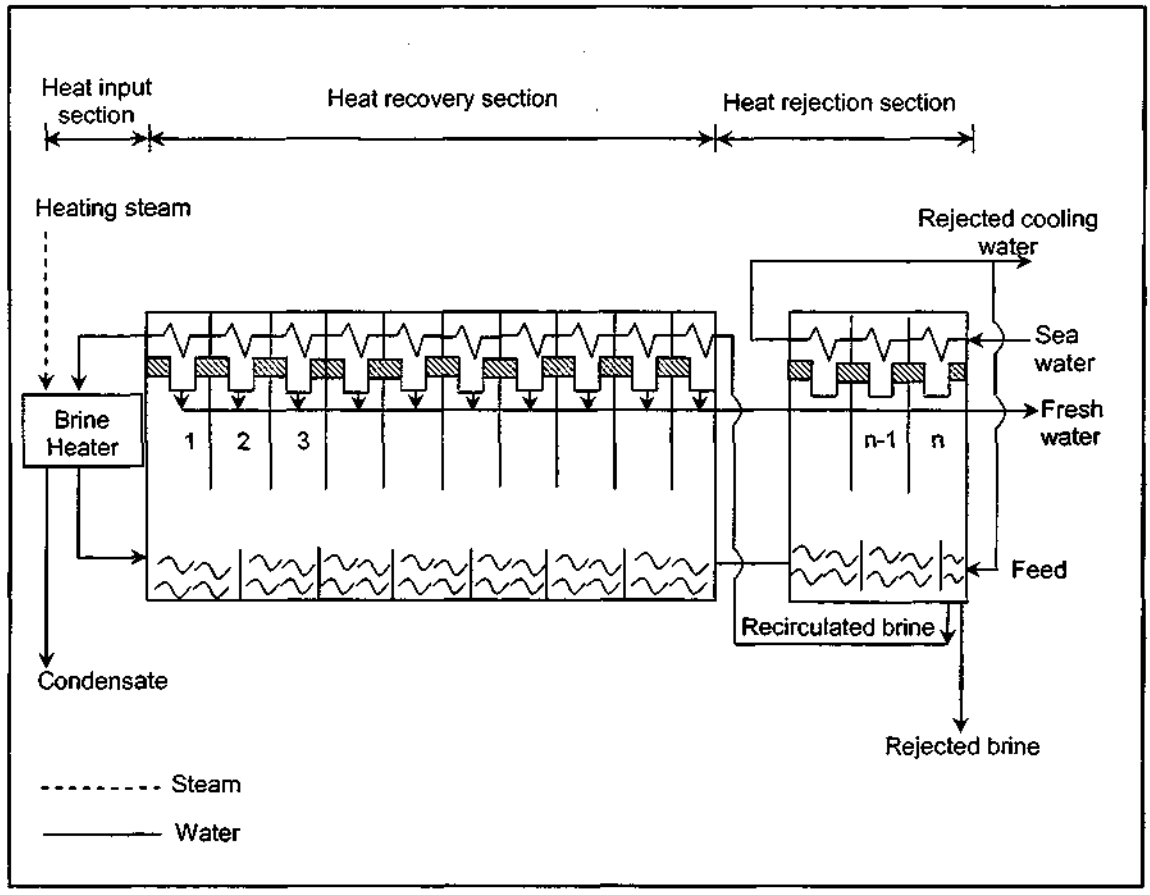

Figure 2.2: *Schematic of multi-stage flash distillation process (adapted from Darwish and El-Dessouky, 1995)*

The vapour pressure in each stage is carefully controlled so that the brine enters each stage at the precise temperature and pressure (each lower than the previous) to ensure instantaneous violent boiling / evaporation (UNEP, 1997). The water vapour is condensed to produce fresh water which is collected at each stage and passed on from stage to stage in conjunction with the brine. The product water is also flash boiled at each stage so that it can be cooled. The surplus heat that is subsequently generated is then recycled and used for preheating the feedwater. The exhausted brine is partially re-circulated to gain a higher water recovery, and partially rejected to the sea in order to maintain a proper brine density in the system (Van der Bruggen, 2003).

The main advantage of MSF distillation is the ease and reliability of the process. Further advantages are listed below (Van der Bruggen and Vandecasteele, 2002):

- There is little or no contact between the heat exchanging surfaces and the brine which avoids problems of corrosion and erosion therefore minimising the likelihood of reduced heat transfer by scaling.
- The precipitation of inorganics within the chambers is a possibility but the occurrence of such may be reduced by applying acid or antiscalants.
- The growth of bacteria may be suppressed by the addition of biocides. Due to the concept of operation of MSF these biocides will not be present in the final product water.
- MSF is insensitive to the initial feed concentration and the presence of suspended particles.
- The product water has a TDS content of less that 50 mg/ℓ which is within the potable water limits of less that 1 000 mg/ℓ (Drever, 1997).

The most important disadvantage of MSF is the low performance ratio which is limited at about 1 ℓ related to a maximum top brine temperature of approximately 110 °C (Van der Bruggen, 2003). Consequently, MSF requires a much higher energy consumption making the process less economic. However, much work is still being carried out with regards to the energy consumption during MSF distillation, and in other studies, modifications to the design of the plants for improved performance with reduced cost factors are being undertaken (Cardona et al., 2003, Farwati, 1997 and Garciá-Rodríguez and Gómez-Camacho, 1999).

2.2.1.2 Multi-effect Distillation

This technique represents one of the oldest techniques of desalination (Al-Shammiri and Safar, 1999). Figure 2.3 provides a schematic representation of a MED setup. The principle of operation of this process is similar to that of MSF only with a lower temperature requirement. As the name suggests, in MED steam is condensed in multiple-effect units on one side of a tube wall while saline water is evaporated on the other side (Krishna, 2004). The steam produced in this way is used for a subsequent step or *effect* which operates at a slightly lower temperature and pressure as with MSF. The heat produced during the condensation of the steam is used as the energy for the evaporation process. The saline water is introduced to the tubes in the form of a thin film. This ensures rapid heat transfer rates and hence evaporation. The process efficiency is proportional to the number of effects that the brine passes through. A typical range is between 8 and 16 effects for MED (Van der Bruggen, 2003).

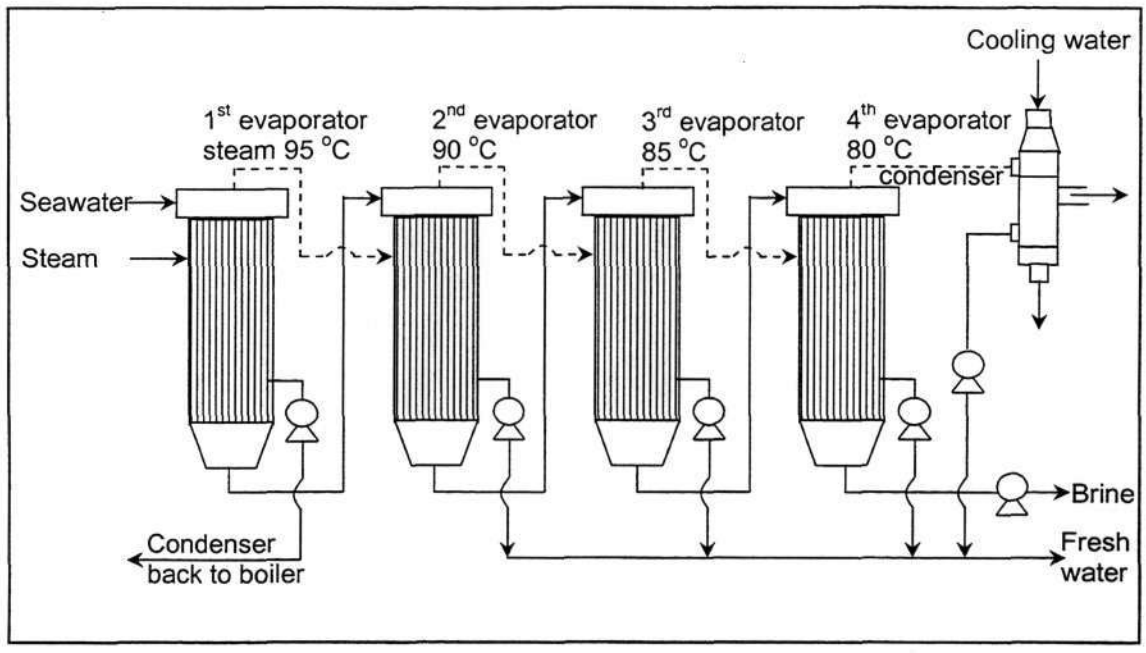

Figure 2.3: *Schematic of multi-effect distillation process (Van der Bruggen and Vandecasteele, 2002)*

MED however, unlike MSF, is more susceptible to corrosion effects due to direct contact between the brine and heat exchange surfaces. Scaling of heat exchangers by oversaturated compounds such as calcium sulphate is more likely to occur in MED. Although MED has been in the market longer than MSF, it has not been as extensively utilised as a primary method of desalination compared to MSF. However, recent developments in MED is threatening technical and economic performances of MSF (Engelien and Skogestad, 2005 and Kumar and Tiwari, 1999).

2.2.1.3 Vapour Compression Distillation

This process is a variation of MED and is normally run in combination with MED, but also operates independently. The difference with VCD is that the heat for evaporating the water comes from the compression of vapour as opposed to condensation of the vapour like in MED and MSF. The subsequent latent heat of the vapour released during the compression is reused in the evaporation process (Figure 2.4).

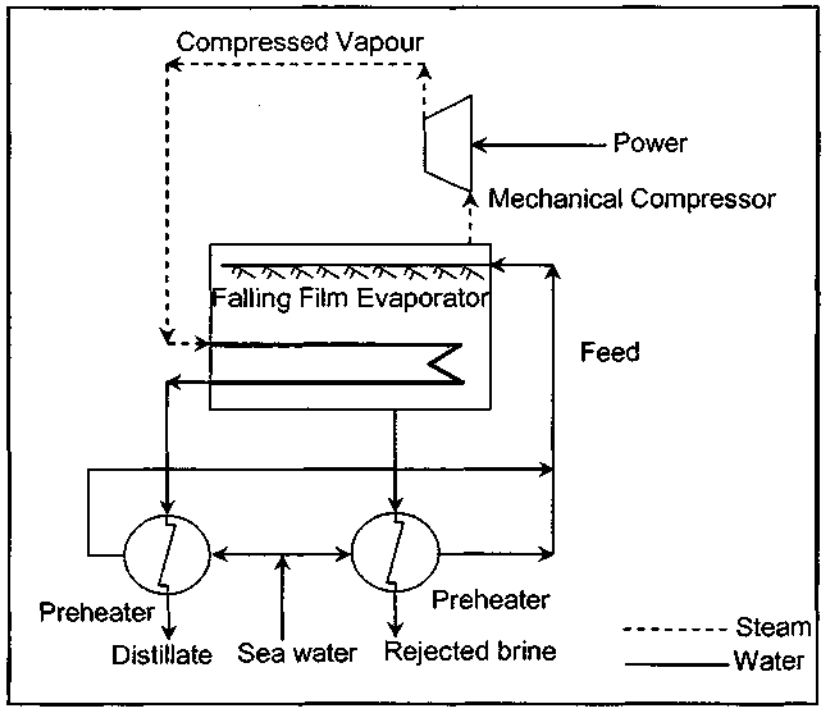

Figure 2.4: *Schematic of mechanical vapour compression distillation system (Darwish and El-Dessouky, 1995)*

Water vapour is drawn from the evaporation chamber by a compressor and, apart from the first stage, is condensed on the outside of tubes in the same chamber as shown in Figure 2.4 (Howe, 1956).

Due to its complex nature, the independent application of VCD is limited to small-scale plants although combination with MED may result in improved process control (Krishna, 2004).

2.2.1.4 Assessment of the Suitability of Distillation Technologies for Desalination

The technical factors affecting the choice of thermal desalination processes can be summarised as follows (Darwish and El-Dessouky, 1995):

- VCD appears to be a better choice of thermal desalination when desalters are directly operated by conventional or waste-heat boilers.
- MED is superior to MSF in terms of thermodynamics and heat transfer efficiency.

- MED can operate at low top brine temperatures to reduce scale formation. However, it is impractical to run MSF at similar temperatures, as a result MSF is more susceptible to scaling and corrosion of the chambers.
- For the same energy consumption VCD uses much smaller heat transfer surfaces than either MSF and MED.

Some of the major advantages and disadvantages of desalination using distillation methods are listed below.

Advantages (UNEP, 1997):

- In comparison to other desalination technologies, distillation was found to have lower operating and maintenance costs associated with the process.
- Usually distillation does not require pre-treatment of the feedwater such as the addition of chemicals or water softening agents.
- Low temperature distillation plants are energy-efficient and economic.
- Due to automation of the distillation plants only a few number of personnel are required for operation and control.
- The impact on the environment by distillation processes is not so harsh, provided that brine disposal is accounted for in the design.
- The technology produces fresh water of high quality with TDS content within the limits of potable water consumption.
- Distillation can be integrated with other processes, for example, coupling of heat energy from an electric power generation plant.

Disadvantages (UNEP, 1997):

- Large distillation plants may not be as economic in terms of energy efficiency.
- The cost factor for running distillation processes, particularly MSF, is very high.
- The design and operation of the distillation process requires significant technical knowledge and aptitude.
- In some instances, the technology may require the use of acids which require precautionary handling and utilisation.

With the development of newer and improved desalination technologies the use of distillation methods for desalination is becoming less popular and is limited to use in countries where cheap energy is available or in resort hotels and high-value-added industries.

2.2.2 Membrane Desalination Processes

Until recently, membrane technologies for desalination were subdivided into two main categories, electrodialysis /electrodialysis reversal (ED/EDR) and reverse osmosis (RO) (nanofiltration (NF) is also included in this category). These are described in the **Sections 2.2.2.1** and **2.2.2.2.**

2.2.2.1 Electrodialysis and Electrodialysis Reversal

ED was first introduced commercially in the 1960s primarily for the desalination of saline, brackish water. In this process, an electric potential is applied across a membrane causing salts to move through the membrane leaving pure water behind. The principle of operation of the process is depicted in Figure 2.5.

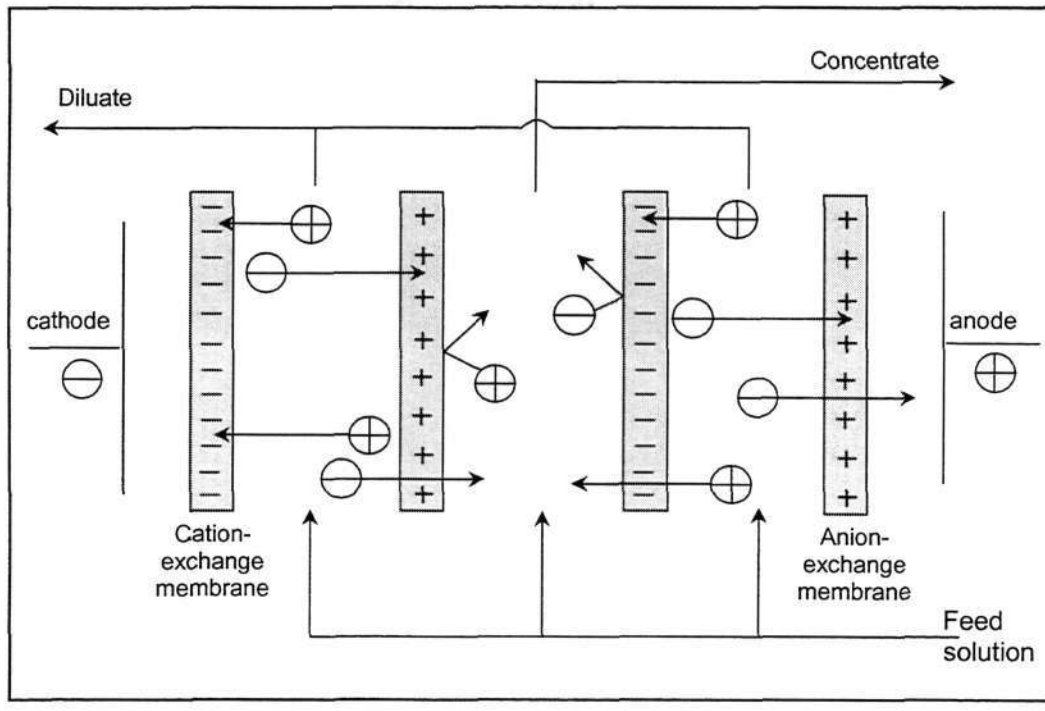

Figure 2.5: *Principle of operation of electrodialysis (Mulder, 1996)*

The process consists of cation- and anion-exchange membranes alternatively placed between a cathode and an anode. The principle of separation is basic. When a saline solution is fed into the system and a current is applied, the positively charged sodium ions (from NaCl) migrate to the cathode and the negative chloride ions migrate to the anode. These ions are unable to permeate the similarly charged membrane and thus a build up of ionic concentration occurs in alternating compartments and a decrease in ionic concentration in the other compartments. As a result, concentrated and dilute solutions are created in the spaces between the membranes.

The production of potable water is one of the most important applications of electrodialysis. One other important application of electrodialysis is the contrary, i.e. the production of salt. In this case the concentrate is the product stream whereas, during the production of potable water, the diluate stream is the product stream (Mulder, 1996). Other applications include the treatment of industrial effluents where ions have to be removed from process streams such as demineralisation of whey, the production of boiler feedwater, the deacidification of fruit juices and the separation of amino acids from each other (Bhattacharyya and Williams, 1992).

2.2.2.2 Reverse Osmosis and Nanofiltration

RO and NF are pressure driven membrane separation processes. As such the production of water is achieved by applying a pressure as the driving force to transport pure water through a semi-permeable membrane. This results in a product water stream and a concentrated brine stream. Both processes have the same basic operational principles (Mulder, 1996). Furthermore, they are both used for desalination of water, NF having a more open structure membrane network, is specific for the retention of multivalent ions such as Ca^{2+} and CO_2^{3-}, therefore suitable only for brackish water desalination whilst RO is particular for the retention of Na^+ and Cl^- and can therefore treat both brackish and seawater. Slight differences arise with regard to the selectivity of the membrane and energy consumption. Whilst RO achieves a finer filtration process it lacks the economic energy reduction of NF (Al-Shammiri and Al-Dawas, 1997).

RO, as the name suggests, is based on the principle of osmosis, only in that an applied pressure provides transport in the reverse direction. Figure 2.6 (I) is an illustration of a RO (or NF) plant that may be used for desalination.

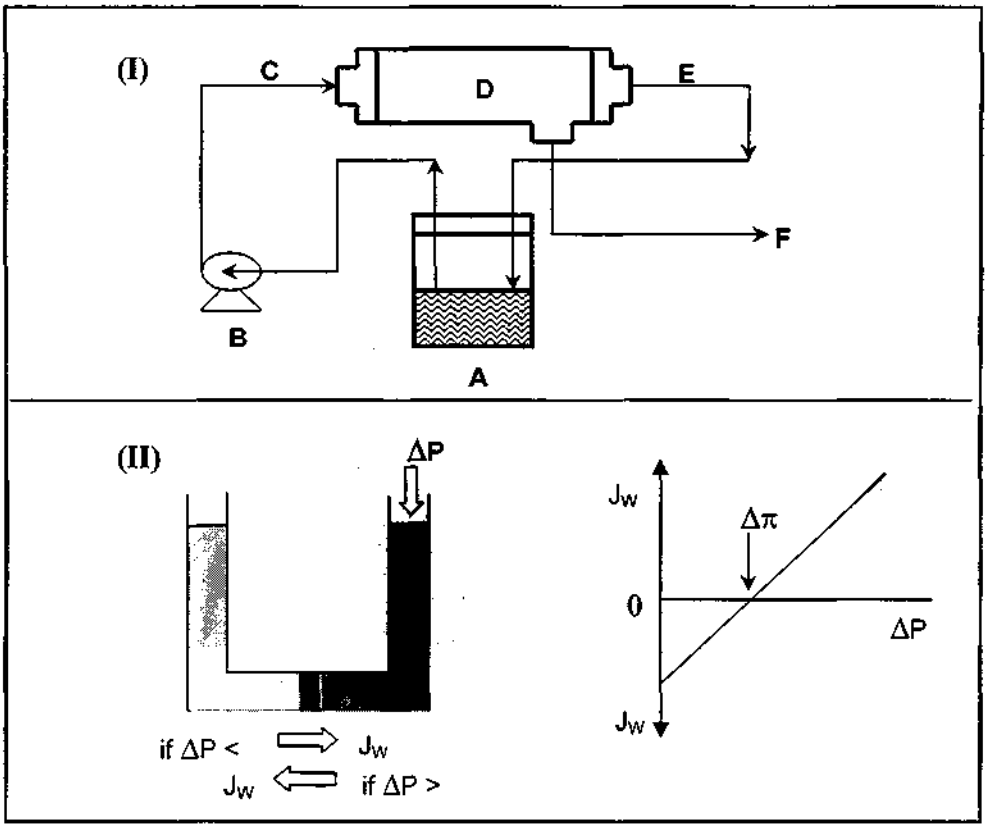

Figure 2.6: *(I) Simplified RO/NF plant setup. A: feed tank, B: pressure pump, C: Feed Stream, D: Membrane module, E: Retentate Stream, F: Permeate Stream (Drioli et al., 2002). (II) Schematic showing mechanism of separation with associated plot of water flow (J_W) as a function of applied pressure (ΔP) (Mulder, 1996)*

The membrane assembly consists of a pressure vessel and a semi-permeable membrane that permits the pure water to pass through it. During passage through the module, the feed inlet stream (C) will split into two streams, i.e. a retentate stream (E) and a permeate stream (F). The membrane is permeable to water but not to the salt. The permeate stream represents the fraction of the feed stream which passes through the membrane whereas the retentate stream is that fraction which is retained. As seen in Figure 2.6 (II), only if the applied pressure overcomes the osmotic pressure, will water pass from the concentrated solution to the dilute solution. This can be represented by Equation 2.3,

$$P_{net} = \Delta P_{appl} - \Delta\pi \qquad [2.3]$$

where the applied pressure (P_{appl}) is necessary to overcome the osmotic pressure (π) and the remaining pressure forms the net pressure (P_{net}) which drives the water through the membrane (Hassan et al., 1998). Until this constraint is overcome the water will flow in the opposite direction. As more and more water passes through the membrane, the retentate stream becomes increasingly concentrated. In NF and RO the applied pressure ranges from 1.5 to 2.5 MPa for brackish water desalination and for seawater desalination using RO, pressures between 4 and 8 MPa are applied (Mulder, 1996).

2.2.2.2 (a) Membrane Configurations for RO and NF

Membranes for RO and NF are available in several different configurations, viz. tubular, hollow-fibre, plate-and-frame, and spiral-wound. The versatility of an individual membrane design depends on the particular application and is affected by factors such as viscosity, concentration of suspended solids, particle size, and temperature. Furthermore, the configuration and material composition of the membrane used is of environmental significance as it represents an important factor in the selection of the method for pre-treatment and chemical conditioning of the feedwater (Morton et al., 1996). The spiral-wound membrane module (Figure 2.7) is one of the more common modules used for NF or RO.

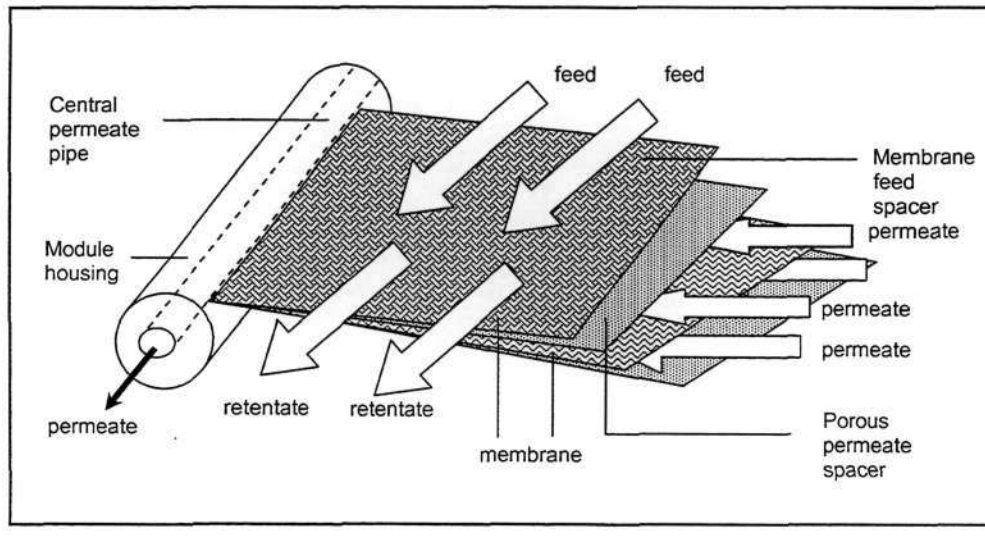

Figure 2.7: *Spiral-wound membrane module commonly used during NF and RO (adapted from Mulder, 1996)*

A spiral-wound module constitutes several *pairs* or *envelopes* of flat sheet membranes wrapped around a central permeate collection tube. The membrane envelopes constitute two flat sheets of membrane with an external active surface, separated by a thin support mesh and glued together along three sides (Rautenbach and Albrecht, 1981).

The open end of the envelope is glued to a perforated collection tube. The pressurised feedwater follows a spiral path along the membrane envelope, and desalinated water is collected in the central tube. The direction of the feed flow is axial to the cylindrical module, parallel along the central pipe, whereas the permeate flows radially toward the central pipe.

The spiral wound membrane configuration offers several attractive advantages for industrial users. These include higher membrane area per unit volume, which allows greater flows, and also spacers between membranes, which promote turbulent flow, an important feature that reduces fouling and extends membrane life (Bhattacharyya and Williams, 1992).

The selectivity of a membrane for a given solute is expressed by the retention coefficient or the rejection coefficient, *R*. The Spiegler-Kedem equation for the rejection is represented in Equation 2.4 (Spiegler and Kedem, 1966):

$$R_{rej} = 1 - \frac{1-\sigma_r}{1-\sigma_r \exp\left[\frac{(\sigma_r - J_w)}{p}\right]} \qquad [2.4]$$

The solute rejection, R_{rej}, is given as a function of the water flux, J_w, and the solute permeability, p. The reflection coefficient, σ_r, of the membrane towards a particular solute, accounts for the fact that in reality the membrane may not be entirely non-permeable to solute and there may be some passage of low molecular weight solutes through the membrane.

Considering that $c_p = \frac{J_s}{J_w}$ where c_p is the solute concentration in the permeate, and the solute flux $J_s = B_s \Delta c_s$, where B_s is the solute permeability coefficient and $\Delta c_s = c_f - c_p$, where c_f is the solute concentration in the feed, Equation 2.4 can then be simplified to Equation 2.5.

$$R_{rej} = \frac{c_f - c_p}{c_f} = 1 - \frac{c_p}{c_f} \qquad [2.5]$$

Equation 2.4 shows that as rejection increases the water flux also increases until the limiting value σ_r (at infinitely high water fluxes) is reached. At this limit, the diffusive flux of the solute transport is negligible, leaving the reflection coefficient σ_r, as a function of the convective transport of the solute alone. A reflection coefficient of 100 % indicates that solute transport through convection is absent, as is the case of RO membranes as these membranes have a denser structure with no pores thereby preventing the convective transport of solutes. However, solute transport may take place by solution-diffusion yielding a reflection coefficient less than 100 %. In the case of NF membranes, the pores on the membranes allow for the passage of small solute molecules yielding a reflection coefficient less than 100 %.

2.2.2.2 (b) Applications of RO and NF

NF and RO have gained popularity mainly due to their application in desalination of waters with a TDS content in the range of brackish and seawater. These processes are also used when low molecular weight solvents have to be separated from solutions. Some examples of these solutes are inorganic salts or small organic molecules such as glucose and sucrose. Furthermore, NF has a high retention for micropollutants or microsolutes such as herbicides, insecticides and pesticides and for other low molecular weight components such as dyes and sugars and is therefore used in the production of potable water from polluted low TDS surface water. NF is also used in water softening, fractionation and demineralisation of effluents and concentration of organic dyes (Garcia-Aleman and Dickson, 2004). It was also found that NF membranes are able to keep their retention selectivity for ions in electrolyte solutions up to concentrations of 200 g/ℓ (Karelin et al., 1996). This feature enables NF membranes to be used for the separation of multicomponent solutions into binary ones, from which the corresponding salts can be recovered by vaporization.

Apart from the desalination of seawater that governs the applicability of RO, this process is also useful in the electronic industry during the production of ultrapure water, in the food industry for the concentration of fruit juice and milk, for the recovering and recycling of valuable products in waste streams from various industries and in the pharmaceutical industry for the clarification and concentration of fermentation broth. RO can be extensively used in the

treatment of industrial effluents such as electroplating process effluents, power station effluents, pulp and paper bleach effluents and mine drainage (Buckley et al., 1993)

2.2.2.2 (c) RO versus Thermal Processes

The 1970s saw the rapid growth and utilisation of thermal desalination, particularly MSF, as the primary desalination process. Following this era, the introduction and advancement of RO as a method of desalination has grown and mostly overcome MSF as the primary desalination technique. RO has almost succeeded thermal desalination processes for the following reasons (Brandt et al., 1993):

- It requires only half the amount of energy as opposed to the energy demand of thermal plants (Espino et al., 2003).
- Ambient temperatures are sufficient and no phase changes are needed for the operations of RO.
- The RO plant is designed using non-corrosive polymeric materials rather than metallic materials, as is the case in thermal operations.
- The RO plant requires a smaller area capacity for installation as opposed to thermal plants.
- Transport and installation of RO plants are more facilitated as the entire plant is built in modular components.
- RO can be easily started up and shut down.
- The operation of RO requires minimal technical skills due to its simplicity.

Overall the choice of RO or thermal processes for desalination depends on economic factors and aptness of the surrounding environment to accommodate the technology.

2.2.3 Problems in the Desalination of Concentrated Salt Solutions

One of the major drawbacks for the use of RO for desalination is the susceptibility of the membrane to scaling, particularly pronounced during the desalination of waters with high TDS content such as seawater. In general, scaling refers to the formation of mineral deposits precipitating from the feed stream on to the surface of the membrane (Van Paassen et al., 1998). The main constituents of scale are the alkaline soft salts $CaCO_3$ and $Mg(OH)_2$ and the non-alkaline hard salt $CaSO_4$ and its derivatives, although $BaSO_4$, $SrSO_4$, CaF_2 and SiO_2 can also

result in membrane scaling (Van de Lisdonk et al., 2000). The formation of non-alkaline hard salts is pronounced at high temperatures as their solubility is inversely related to the temperature. During the production of fresh water by RO, the concentration of dissolved salts increases in the retentate stream inevitably leading to deposition of precipitates on the membrane surface. This scaling phenomenon hinders the maximal operation of the RO unit by half of its full potential (Ohya et al., 2001). Four methods of overcoming this hurdle of membrane scaling are currently in place (Al-Shammiri and Al-Dawas, 1997). The first method is used when the major scale component is calcium carbonate. In this case acid is added for the partial consumption of bicarbonate in the feed for the conversion to carbon dioxide. The second method involves the use of antiscalants such as sodium hexametaphosphate (SHMP). These antiscalants function as inhibitors against the formation and growth of scale-forming components. The third approach is to run RO at lower recovery levels thus remaining under the saturation levels of scaling salts. The final method employs a water softening approach in which lime or soda ash is added to precipitate the carbonates as $CaCO_3$. A novel approach to this problem was described by Juby et al. (1996) for the desalination of calcium sulphate scaling mine water. The membrane desalination technology which is termed SPARRO (slurry precipitation and recycle reverse osmosis) incorporates seeded reverse osmosis (SRO) technology which is based on incorporating a slurry of seed crystals into the feed water to conventional tubular reverse osmosis (O'Neail et al., 1981). During the concentrate processing to produce desalinated water, as the concentration of ions such as Ca^{2+} increases in solution, the seed serves as a growth medium for these ions. Due to preferential growth on the seed, this prevents the precipitation and build-up of scale on the membrane surface itself. Seeded crystallisation may be carried out in one of two forms: (i) seeds of the same material as the crystallising salt can be incorporated in the slurry which leads to the spontaneous growth of the seeds or (ii) seeds of a foreign (heterogeneous) material may be incorporated in the slurry. In the latter case nucleation is still required for crystallisation but the energy barrier for the heterogeneous seeded nucleation is lower that that of the homogenous nucleation resulting in the former occurring at a much lower saturation level (Sluys et al., 1996). The SPARRO process addressed and overcame, to some extent, the shortcomings of other seeded systems concerning energy consumption and recirculation rates, however, this process failed with regards to stability of membrane performance particularly concerning the salt rejection and membrane flux values, which indicated overall membrane fouling and shortened membrane life. This is due to the high concentration of salts or certain ions within the water at which point this process failed.

Another problem during the desalination of waters containing high concentrations of strong electrolytes is that of impurities, macroparticles and macroorganisms, which may lead to membrane fouling. In order to prevent fouling of the RO membrane surface, pre-treatment of the source water must be performed. Large, suspended solids present in the water must first be removed and the water appropriately pre-treated to prevent precipitation of salt or microbial growth on the membrane. Furthermore, apart from high degree of hardness of the water, a high turbidity in the feed lowers the plant performance.

Waters that contain a high TDS content pose a significant economic problem during desalination as considerable amount of pressure is required to overcome the osmotic pressure barrier (Mariah et al., 2006a). This can be explained by considering Equation 2.3 again. The higher the TDS content of the water, the higher the ionic molar concentration resulting in increasing feed osmotic pressure. From Equation 2.3 this consequence implies that a higher applied pressure is required to overcome this osmotic pressure barrier in order to gain a net pressure to transport the water through the membrane. As a result considerable pressure is required during RO concentrate processing and, together with membrane scaling, is the major drawbacks of RO.

2.3 MEMBRANE DISTILLATION-CRYSTALLISATION

Membrane distillation (MD) may be considered as a combination of both of the main categories of desalination processes described in **Section 2.2**, i.e. MD is a *thermally* driven *membrane* desalination / separation process (Mariah et al., 2006b). After a few subtle prefaces to MD in the 1960s under U.S. patents, MD was finally introduced commercially on a small scale in the 1980s (Lawson and Lloyd, 1997). As the name implies, the process combines both the use of membranes and distillation which occurs across the membrane. In the process, saline water is heated to enhance vapour production, and this vapour is exposed to a membrane that can pass vapour but not water. After the vapour passes through the membrane, it is condensed on a cooler surface to produce pure water. In the liquid form, the pure water cannot pass back through the membrane, so it is trapped and collected at the output of the plant. The main advantages of MD lie in its simplicity and the need for only small temperature differentials to operate. One important advantage of MD, which differentiates it from other membrane processes such as RO for example, is the independence of the quality of the permeate from the quality of the feed solution; MD can handle highly concentrated feed solutions without a

significant decay in membrane activity. RO, however, is strongly affected by the osmotic pressure if the feed solution is very concentrated resulting in higher applied pressure requirements furthermore, increasing the susceptibility of the membrane to fouling. **Sections 2.3.1** to **2.3.7** serve to expand the concept of MD describing how a separation is achieved, membrane properties, factors affecting MD and applications of this process.

2.3.1 Process Description

During thermally driven membrane processes, the membrane separates two phases held at different temperatures. Typically this will result in heat flow from the high-temperature side to the low-temperature side (Figure 2.8). Fourier's law governs the heat flux (J_h) according to the thermal or heat conductivity (λ). Fourier's law therefore describes the heat flux through the membrane as:

$$J_h = -\lambda \frac{dT}{dx} \qquad [2.6]$$

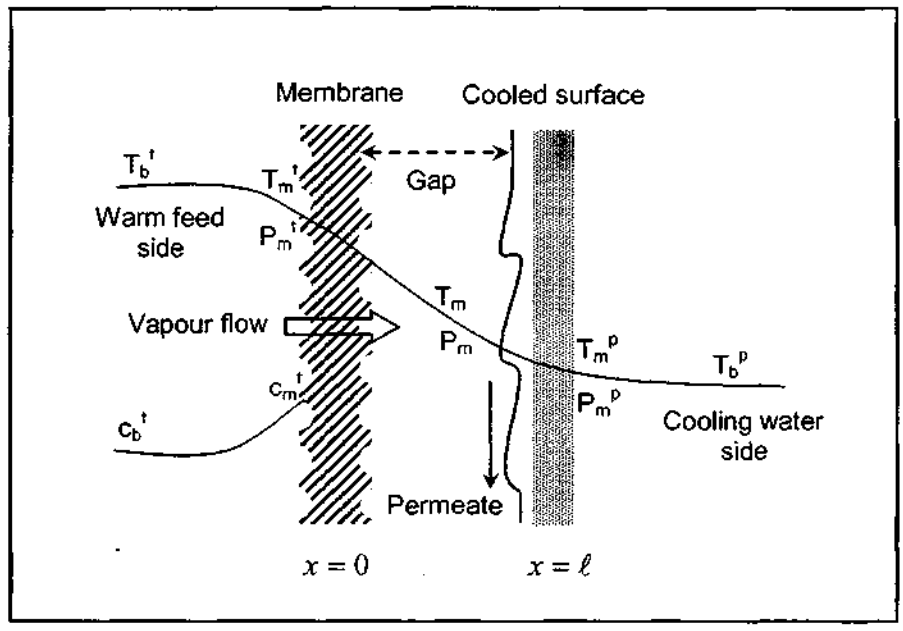

Figure 2.8: *Schematic representation of the air gap MD process showing the flow of vapour and temperature profile across the membrane (Fane et al., 1987, Kimura and Nakao, 1987 and Kurokawa et al., 1990)*

Figure 2.8 is a schematic representation of the transport of vapour molecules across the membrane. This concept is expanded in **Section 2.3.1.2**. During MD a microporous hydrophobic membrane separates a warm aqueous solution from a cold solution. If the liquids do not *wet* the membrane, then pure water vapour is transported from the warm side to the cold side. This process has been described as a sequence of events: (i) the formation of a vapour gap at the warm solution-membrane interface (ii) transport of the vapour phase through the microporous system and (iii) condensation at the cold membrane-solution interface (Drioli and Wu, 1985). The hydrophobicity of the membrane prevents the aqueous solution from entering the pores thus creating a vapour-liquid interface at each of the pore entrances. The driving force for the separation process is therefore the vapour pressure difference arising from the temperature difference across the membrane. The distance between the membrane and the cooling surface is referred to as the diffusion gap and its composition varies according to the membrane configuration that is chosen.

2.3.1.1 Membrane configurations

There are numerous types of methods that can be used to maintain the vapour pressure difference across the membrane to produce an overall solvent flux. MD can be configured as direct contact membrane distillation (DCMD), air-gap membrane distillation (AGMD), vacuum membrane distillation (VMD) and sweeping gas membrane distillation (SGMD). Figure 2.9 provides a schematic illustration of these methods.

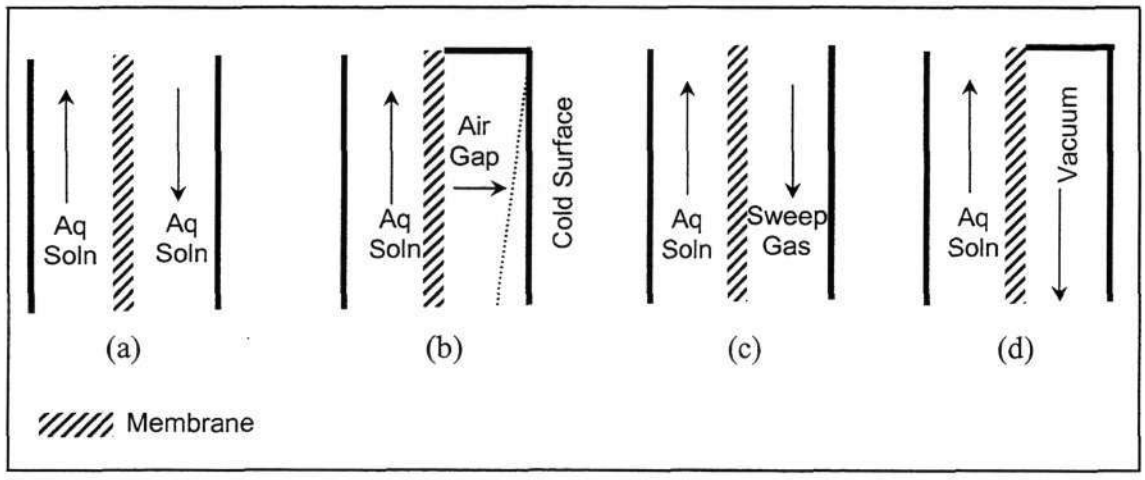

Figure 2.9: *Types of membrane configurations. (a) direct contact membrane distillation, (b) air gap membrane distillation, (c) sweeping gas membrane distillation, (d) vacuum membrane distillation (adapted from Lawson and Lloyd, 1997)*

In the DCMD configuration, two solutions are held at different temperatures in direct contact with the membrane surfaces, while vapour is trapped within the membrane pores. The permeate side contains a cooler solution in direct contact with the membrane. The membrane serves to establish a vapour-liquid interface through which solvent molecules from the warm solution side evaporate, diffuse through the membrane and condense on the cooler side. DCMD is the most frequently applied membrane configuration during MD processes and is most useful for desalination and concentrating aqueous solutions where water is the major permeate component. This method is also most attractive as it requires the least equipment and is easy to operate (Calabro et al., 1991, Fujii et al., 1992, Laganà et al., 2000, Schofield et al., 1990 and Zolotarev et al., 1994).

In AGMD a condensing surface is separated from the membrane by an additional air gap; in VMD a vapour phase is stripped away from the liquid through the membrane and the condensation, if necessary, takes place in a separate vessel and in SGMD a stripping gas is used as a carrier instead of a vacuum (Gostoli and Sarti, 1989). In DCMD and AGMD a diffusive flux of volatile components takes place at the vapour-liquid interface. In VMD the downstream pressure (on the permeate side) is lowered below the equilibrium vapour pressure so that the mass transfer is ruled by the convective transport mechanism (Bandini et al., 1992). The driving force for the process is therefore linked to both the partial pressure gradient and the thermal gradient across the membrane (Cabassud and Wirth, 2002). SGMD and VMD are more suited to applications such as removing volatile organic components such as the removal of ethanol from fermentation broths or when dissolved gases need to be removed from solution (Basini et al., 1987, Cabassud and Wirth, 2003, Saavedra et al., 1992 and Sarti et al., 1993). AGMD covers a much wider spectrum of applications, being useful in almost any type of application (Banat and Simandl, 1993 and Kimura and Nakao, 1987). In particular, the AGMD configuration is very suitable for the desalination of geothermal resources, and the energy demand for pumping is lower (El Amali et al., 2004).

2.3.1.2 Transport across the Membrane

The theory of heat and mass transport has been used to establish a MD theory that is widely used for the description of the MD process. This theory is a combination of heat and mass transfer coefficient functions through both the membrane and the liquid surfaces contacting the membrane on either side. The development of this theory is explained in **Sections 2.3.1.2**

(a) and **2.3.1.2 (b).** Most of the derivations are based on the description of the process as depicted in Figure 2.8.

2.3.1.2 (a) Mass Transfer

Literature provides two models for the description of mass transfer, or the vapour flux across a DCMD membrane. These are the Dusty Gas Model (DGM) and a model proposed by Schofield et al. (1987), albeit, the latter being a combination of different models based on the DGM (Lawson and Lloyd, 1997). Both models are based on the kinetic theory of gas transport to describe the vapour flux through the membrane pores. The choice of an appropriate model depends on the properties of the vapour and the membrane, i.e. the mean free path and mean free pore size (Phattaranawik et al., 2003). Vapour transported through the membrane pores are subjected to two types of molecular resistance: (i) by air trapped in the pores of the membrane and (ii) by the physical structure of the pore (Cath et al., 2004). Figure 2.10 illustrates these mass transfer resistances in MD.

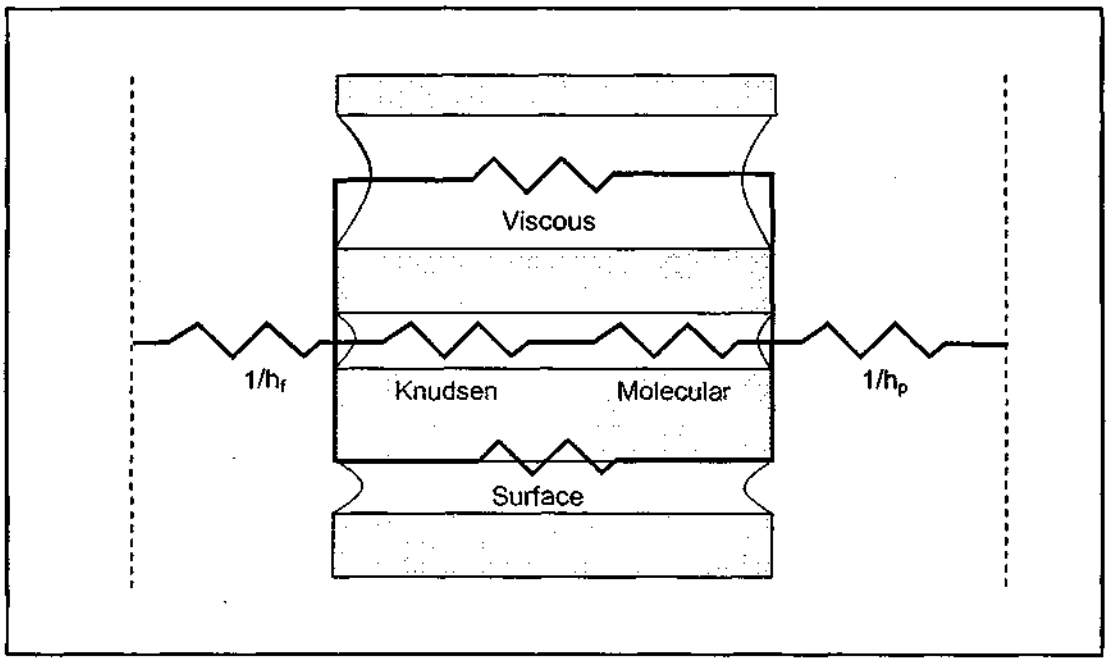

Figure 2.10: *Mass transfer resistances in MD (Lawson and Lloyd, 1997)*

Resistance to mass transfer within the membrane stems from the transfer of momentum to the membrane (viscous or momentum transfer resistance), or Knudsen resistance resulting from the collisions of a diffusing molecule with other molecules (Lawson and Lloyd, 1997). The model proposed by Schofield et al. (1987), to account for the resistances imposed by the membrane structure, assumed that in the transition region between the Knudsen and viscous flows, the permeability of the membrane can be considered as a linear combination of the Knudsen and viscous permeabilities, being described by the Knudsen diffusion and the Poiseuille flow models, respectively. The latter dominates when the membrane pore size is larger than the mean free path of vapour molecules, but as this is not the case in MD, both models were considered (Schofield et al., 1987). The mass flux from the Knudsen diffusion model is expressed according to Equation 2.7.

$$J_K = 1.064\frac{r\varepsilon}{\chi\delta}\left(\frac{M}{RT}\right)^{\frac{1}{2}}\left(P_m^f - P_m^p\right) \qquad [2.7]$$

where r is the pore radius, ε the membrane porosity, χ the pore tortuosity, δ the membrane thickness, M the water molecular weight, R the gas constant, T the temperature and P^f_m and P^p_m the vapour pressures at the membrane surface of the feed and permeate, respectively. However, P^f_m and P^p_m are also dependent on the temperature at the membrane surface of the feed and permeate, respectively; hence the flux dependence on temperature is not simply $T^{-1/2}$.

The mass flux from the Poiseuille flow model is expressed as,

$$J_P = 0.125\frac{r^2\varepsilon}{\chi\delta}\left(\frac{MP_m}{\eta RT}\right)^{\frac{1}{2}}\left(P_m^f - P_m^p\right) \qquad [2.8]$$

where P_m is the water vapour pressure in the membrane and η is the gas viscosity.

To account for the resistance imposed by the air trapped in the membrane pores, the molecular diffusion model was described (Equation 2.9),

$$J_D = \frac{1}{Y_{lm}}\frac{D\varepsilon}{\chi\delta}\frac{M}{RT}\left(P_m^f - P_m^p\right) \qquad [2.9]$$

where Y_{ln} is the mole fraction of air and D the diffusion coefficient.

A common trend is displayed by these three models and as such the linear relationship according to Equation 2.10 can be approximated,

$$J = C\Delta P_m \qquad [2.10]$$

making C a membrane mass transfer coefficient for the system and ΔP the vapour pressure difference across the membrane. C is temperature dependent and dependent on membrane pore geometry or the mole fraction of air within the pores, the discriminating factor being whether convective or diffusive transport is dominant, respectively. Many authors refer to this model, or modifications thereof, when describing vapour flux across the membrane. Furthermore, as the vapour pressure within the membrane is not directly measurable, some authors have found it more convenient to express Equation 2.10 in terms of temperature (Hsu et al., 2002 and Schofield et al., 1987),

$$J = C\left(\frac{dP}{dT}\right)_{T_m}\left(T_m^f - T_m^p\right) \qquad [2.11]$$

where $(T^f_m\text{-}T^p_m)$ is the temperature gradient across the membrane. When $T^f_m\text{-}T^p_m < 15°C$ (dilute solutions), then (dP/dT) can be approximately evaluated using the Clausius-Clapeyron equation,

$$\frac{dP}{dT} = \frac{P\Delta H_{vap}M}{RT_m^{\,2}} \qquad [2.12]$$

where ΔH_{vap} is the molar heat of vaporisation and P can be evaluated from the Antoine equation,

$$\ln P = A_1 + \frac{B_1}{T + C_1} \qquad [2.13]$$

where P is the pressure in Pascal, T is the temperature in Kelvin and A_1, B_1 and C_1 are constants which are substance dependent. Furthermore, it has been shown by Sarti et al. (1985) that Equation 2.11 must be modified before its application to more concentrated solutions, in order

to account for the reduction in vapour pressure caused by dissolved species. Equation 2.11 then becomes,

$$J = C\left(\frac{dP}{dT}\right)\left[\left(T_m^f - T_m^p\right) - \Delta T_{th}\right]\left(1 - x_m\right) \qquad [2.14]$$

where ΔT_{th} is a threshold temperature defined as,

$$\Delta T_{th} = \frac{RT^2}{M\Delta H_{vap}} \frac{x_m^f - x_m^p}{1 - x_m} \qquad [2.15]$$

where x is the mole fraction of dissolved species. If $(T_f - T_0) < \Delta T_{th}$, a negative flux will be observed as a consequence of vapour pressure reduction brought upon by dissolved species in the feed solution.

The second model available in literature for the vapour flux across the DCMD membrane is the Dusty Gas Model (DGM). This model involves three adjustable parameters viz. ordinary, binary and Knudsen diffusivities. When the mean free molecular path of the vapour molecules is approximately equal to the average pore size, surface and ordinary diffusion is neglected and the DGM is found in the Knudsen-viscous transition regime (Figure 2.10) (Imdakm and Matsuura, 2004). In this case, following Schofield et al. (1987), the total pressure drop becomes the sum of the two momentum transfer processes, Knudsen and viscous resistance and the DGM is given by two equations as described by Lawson and Lloyd (1996 and 1997),

$$\frac{J_i^D}{D_{ie}^k} + \sum_{j=1\neq i}^{n} \frac{p_j J_i^D - p_i J_j^D}{D_{ije}^0} = \frac{-1}{RT} \nabla p_i \qquad [2.16]$$

$$J_i^V = \frac{-p_i B_0}{RT\mu} \nabla P \qquad [2.17]$$

where J_i^D is the diffusive flux, J_i^V the viscous flux and a combination of these yields the total flux J_i. ∇P and ∇p_i are the gradient in the total pressure and the partial pressure of the i^{th} component, respectively, μ the fluid viscosity and D the effective diffusivities being defined as,

$$D^{0}_{ije} = K_1 P D_{ij} \text{ and } D^{k}_{ie} = K_0 \left(\frac{8RT}{\pi M_i} \right)^{\frac{1}{2}} \quad [2.18]$$

where D_{ij} is the ordinary diffusion coefficient and M_i is the molecular weight of the i^{th} component and the term $\left(\frac{8RT}{\pi M_i} \right)^{\frac{1}{2}}$ is the mean molecular speed. K_0, K_1 and B_0 are constants depending on the membrane geometry and molecular interactions with the membrane. Evaluation of these parameters have been performed by various authors (Guijt et al., 2000, Lawson and Lloyd, 1996). A combination of the above equations can be re-written to yield a general expression for the DGM (Imdakm and Matsuura, 2004 and Drioli et al., 2004),

$$J_i = \frac{-1}{RT_{avg}} \left[K_0 \left(\frac{8RT_{avg}}{\pi M_i} \right)^{\frac{1}{2}} \nabla p_i + B_0 \frac{p_{i,avg}}{\mu} \nabla P \right] \quad [2.19]$$

Following the work of Schofield et al. (1987) and Lawson and Lloyd (1997) many theories have been developed, some of which are simply modifications of the above (Banat and Simandl, 1993, Ding et al., 2002, Fane et al., 1987, Kurokawa et al., 1990, and Martínez and Florido-Díaz, 2001(a)) or entirely new models on their own (Agashichev and Sivakov, 1993, Bouguecha et al., 2002 and Imdakm and Matsuura, 2004). For example, Burgoyne and Vahdati (1999) used these theories to develop a model to predict permeate fluxes produced at specific operating conditions. Gryta and Tomaszewska (1998) arrived at a heat transfer model with the assumption that the flow of vapour was non-isenthalpic and the temperature distribution was non-linear. These are related to the theories that were developed by Gaeta et al. (1992) for the non-isothermal transport of matter in porous membranes. They then used the temperature at the membrane boundary on the permeate side as the thermodynamic reference temperature in the derivation of their model.

2.3.1.2 (b) Heat Transfer

Simultaneous to mass transport, heat transport occurs across the membrane. This heat transfer occurs by two mechanisms, viz. the latent heat associated with the vapour which directly serves the evaporation process and the heat conducted across the membrane and boundaries of the system (Martínez-Díez et al., 1999). The latter is considered as heat loss as it is no longer

available for use in evaporation. These two forms of heat transfer are described in Equations 2.20 to 2.22.

For dilute solutions the latent heat flux is:

$$Q_L = J\Delta H_{vap} \qquad [2.20]$$

From Equation 2.11, Equation 2.20 becomes,

$$Q_L = C\left(\frac{dP}{dT}\right)_{T_m}\left(T_m^f - T_m^p\right)\Delta H_{vap} \qquad [2.21]$$

And the conductive heat flux is,

$$Q_C = \left(\frac{k_m}{\delta}\right)\left(T_m^f - T_m^p\right) \qquad [2.22]$$

where k_m is the thermal conductivity of the porous membrane.

The total flux is then given by Equation 2.23,

$$\begin{aligned} Q &= Q_L + Q_C \\ &= \left[C\left(\frac{dP}{dT}\right)_{T_m}\Delta H_{vap} + \frac{k_m}{\delta}\right]\left(T_m^f - T_m^p\right) \\ &= J\Delta H_{vap} + \frac{k_m}{\delta}\left(T_m^f - T_m^p\right) \end{aligned} \qquad [2.23]$$

or simply

$$Q = H\Delta T_m$$

where H is the effective heat transfer coefficient. This series of equations is a demonstration of how mass transfer gives rise to heat transfer during the MD process. Much work has been undertaken to explain the flow of heat across the membrane, most of which recognise that heat

transfer and mass transfer are related, the latter giving rise to the former (Bandini et al., 1991, Phataaranawik et al., 2003 and Phataaranawik and Jiraratananon, 2001).

In this work, the average spatial values of inlet parameters will be considered and the local variations (axial and radial) of concentrations, temperatures, flows and partial pressures will not be considered. To describe the variation between inlet and outlet parameters a logarithmic average between the high temperature and low temperature sides of the module will be calculated. The logarithmic mean is considered as the most appropriate average driving force in a counter-current mass or heat transfer device.

2.3.2 Process Parameters

Probably the main criterion of this process is that the membrane must not be *wetted* by the liquid, in other words, the pores of the membrane must only be filled with vapour. Once the liquid wets the membrane, the membrane's pores become immediately filled with the liquid as a result of capillary action. One of the criteria for the prevention of wetting is a low affinity between the liquid and the polymeric material of the membrane. This low affinity was found to occur at contact angles greater than 90° (Peña et al., 1993). The relationship between a membrane's largest allowable pore size and operating conditions is given by Equation 2.24, also known as the Laplace (Cantor) equation.

$$P_{liquid} - P_{vapour} = \Delta P_{interface} < \Delta P_{entry} = \frac{-2B\gamma_L \cos\theta}{r_{max}} \qquad [2.24]$$

Where γ_L is the liquid surface tension, θ is the liquid-solid contact angle, r_{max} is the largest pore radius, and B is a geometric factor determined by pore structure. It is therefore evident that the wettability of the membrane depends on all three of these factors. If $\theta > 90°$ then $\cos\theta < 0$ and $\Delta P > 0$, and the Laplace equation demonstrates that only if a threshold pressure is applied will the liquid penetrate the membrane. Therefore, from Equation 2.24 it can be deduced that in order to avoid wettability of the membrane, the maximum pore size must be small (0.1 to 0.5 μm), the surface tension of the liquid high and the surface energy of the membrane material low (Banat and Simandl, 1993). Membranes fabricated from hydrophobic microporous material such as polypropylene (PP), polytetrafluoroethylene (PTFE), polyethylene (PE) and polyvinylidene fluoride (PVDF) meet these requirements (Wu et al., 1992). The value of

$\gamma_L|\cos\theta|$ is reduced by strong surfactants, therefore care must be exercised to prevent solutions with detergents or other surfactants from coming into contact with the process equipment (Franken et al., 1987). One of the main problems of MD is a possible long-term non-wettability. However, some long term modifications of wettability can indeed occur when adsorption, fouling and membrane ageing occur.

2.3.3 Membrane Modules and Design

Due to the criteria of non-wettability, the surface energy of the polymer of the membrane must be as low as possible. Very hydrophobic materials such as PTFE, PVDF, PE or PP combined with liquids with a high surface tension such as water, provide suitable membrane materials. A variety of membrane modules are available for the MD process. Schematics of typical flat sheet MD modules are shown in Figure 2.11.

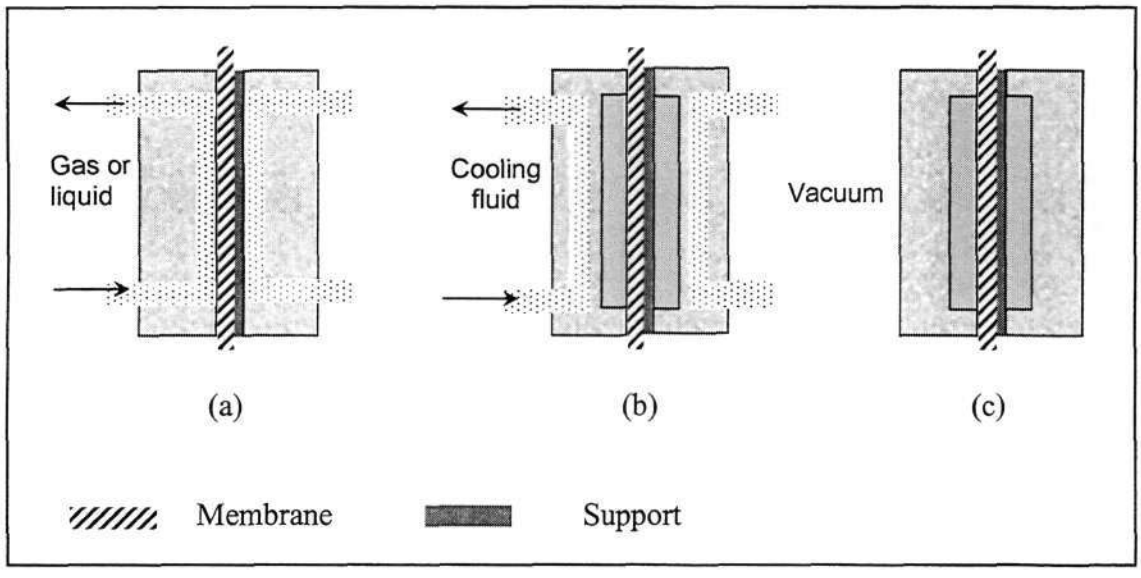

Figure 2.11: *Cells for MD membrane module: (a) direct contact or sweeping gas cell, (b) air gap cell and (b) vacuum cell (adapted from Lawson and Lloyd, 1997)*

Figure 2.11 represents the different types of cells and their orientations with respect to the membrane. In cell (a) the liquid or the sweep gas makes direct contact with the membrane, in (b) the permeate is condensed onto a cool wall, and in (c) permeate is first removed before condensing externally under vacuum. It is also important to choose an appropriate support for

the membrane, one that does not significantly affect the heat and mass transfer resistance, but must be strong enough to prevent deflection or rupture of the membrane.

Characteristics of a well-designed membrane module are one that provides optimum heat and mass transfer between the bulk solution and the solution-membrane interface. Numerous work in this field has demonstrated that DCMD is probably the most simple, economical and efficient configuration to achieve the vapour-liquid equilibria necessary for the operation of the MD process (El Amali et al., 2004, Fane et al., 1987 and Sarti et al., 1985).

2.3.4 Advantages of Membrane Distillation

The main advantages of MD over conventional membrane and distillation processes can be summarised as follows:

Membrane distillation,

- Can be performed at lower operating pressure and lower temperatures than the boiling point of the feed solutions (Andersson et al., 1985, Khayet et al., 2003 and Sarti et al., 1985) and a relatively low temperature difference between the two liquids in contact with the membrane surface gives relatively high fluxes.

- Requires lower vapour space as the vapour-liquid interface is developed by a hydrophobic membrane in MD as opposed to conventional distillation which relies on high vapour velocities to establish a vapour-liquid interface (Jonsson et al., 1985). As such they are very compact and very little equipment space is required. Furthermore, the possibility to overcome corrosion problems by using plastic equipment exists (Banat and Simandl, 1993).

- Is not limited by high osmotic pressure and fouling as the membrane works at atmospheric pressure and is not directly involved in the separation process but acts merely as a support. As such there is reduced chemical interaction between the membrane and process solution (Hsu et al., 2002). Furthermore, due to this characteristic membranes can be fabricated from a variety of chemically resistant polymers (Gekas and Hallstrom, 1987).

- Displays selectivity higher than any other membrane process (Alklaibi and Lior, 2004). MD therefore allows very high separation factors for ions, macromolecules, colloids, cells and other non-volatile solutes in comparison to UF, NF and RO processes (Martínez-Díez and Florida- Díez, 2001(b) and Lawson and Lloyd, 1997).

- Has low sensitivity to feedwater concentrations and has potential applications for concentrating aqueous solutions or producing high-purity water even at very high feedwater concentrations (Alklaibi and Lior, 2004, Kubota et al., 1998, Mariah et al., 2005(a) and (b), Tomaszewska, 1993, and Wu et al., 1991).

- Does not require elevated temperatures therefore the heat can be supplied by solar collectors or other forms of heat such as low-grade waste heat from factories or geothermal energy (Hogan et al., 1991 and Walton et al., 2004).

MD is one of the membrane processes in which the membrane is not directly involved in the separation. The membrane acts only as a support for a vapour-liquid interface and does not contribute to the separation mechanism. Selectivity is determined by the vapour-liquid equilibrium involved. Hence, the component with the highest partial pressure will show the highest permeation rate. For this reason, the separation of NaCl from salted solutions is achieved in very high purity with MD. This is because in water-NaCl mixtures, only water has a vapour pressure (the vapour pressure of NaCl can be neglected), which implies that only water can permeate through the membrane, hence achieving very high selectivities.

2.3.5 Applications of Membrane Distillation

One of the most important applications of MD is in the production of pure water. Studies have shown that a high quality permeate can be obtained during MD. This feature of MD makes this process invaluable in the desalination of seawater, in industry for boiler feedwater and in the semiconductor industry (Mulder, 1996). Other area in which MD is used to treat waste water is in the textile industry (Calabro et al., 1991 and Wu et al., 1991). In the case of a solution containing non-volatile components, e.g. NaCl, only water vapour flows through the membrane, therefore, the retention degree of solutes in MD is close to 100 % (Gryta et al., 2001). This allows the concentration of solutions up to solute saturation (Mariah et al., 2006b). The concentrating process of MD may be exploited in the food industry for the concentration of fruit

juices and milk (Calabro et al., 1994, Kimura and Nakao, 1987 and Laganà et al., 2000). Gostoli and Sarti (1989) and later Sarti et al. (1993) have found VCMD to be very useful for the separation of alcohol-water mixtures such as the extraction of organic components, ethanol and methylterbutyl from aqueous streams. Similarly, Bernado et al. (2003) investigated the potentiality of membrane technologies, including MD, for the substitution of some typical technologies during a traditional ethylene process. Criscuoli et al. (2002) evaluated MD for the treatment of uraemia by employing this process for the purification of human plasma ultrafiltrate and the re-circulation of the purified water to the patients. The feasibility of breaking down azeotropic mixtures by the removal of water has been explored by Udriot et al. (1994). Gryta et al. (2001) used MD for the treatment of NaCl solutions subsequent to use in the food industry. The concept was to produce pure water together with a concentrate containing substances present in the initial solution which could be separated by crystallisation thus facilitating their disposal and potential recycling of the water produced. Based on a similar concept, Tomaszewska (1993) used MD for the concentration of the sulphuric acid solution obtained after the removal of apatite phosphogypsum. This residue contains lanthane compounds which may be recovered by crystallisation after successive concentration steps with MD.

2.3.6 Potential Problems of Membrane Distillation

MD has significant advantages over other processes as described in **Section 2.3.4**. However, some factors that significantly affect the performance of MD do exist. These include concentration phenomena and flux decay, the former leading to the latter. These constraints are discussed in **Sections 2.3.6.1** and **2.3.6.2**.

2.3.6.1 Temperature and Concentration Polarisation

Due to the presence of boundary layers at both sides of the membrane, the transmembrane temperature difference, ΔT_m, is lower than the bulk temperature difference, ΔT_b. This phenomenon is called temperature polarisation and the useful energy for mass transfer of vapours to the total energy input to the process then becomes known as the temperature polarisation coefficient (TPC),τ, (Cath et al., 2004). The value of the TPC is given as the ratio of the temperature difference between the evaporation and condensation surfaces, and the bulk of the feed and permeate (Smolders and Franken, 1989).

$$\tau = \frac{T_m^f - T_m^p}{T_b^f - T_b^p} \qquad [2.25]$$

From Figure 2.8 it is obvious that the differences between T_b^f and T_m^f and between T_m^p and T_b^p will increase as the mass flux increases (i.e. with increasing evaporation rates) and as such the membrane boundary on the feed side has the highest salt concentration (Hsu et al., 2002). This further gives rise to concentration polarisation and the concentration polarisation coefficient (CPC),γ, is defined (Equation 2.26) to measure the increase of solute concentration on the membrane surface with respect to that in the bulk (Martínez, 2004).

$$\gamma = \frac{c_m^f - c_b^f}{c_b^f} \qquad [2.26]$$

T_m^f, T_m^p and c_m^f cannot be measured directly, but many models have been proposed for their approximation (Gostoli and Sarti, 1989, Gryta and Tomaszewska, 1998 and Martínez, 2004). These polarisation phenomena restricts the permeate flux as an increase in the latter tends to induce more severe polarisation (Hsu et al., 2002). Fane et al. (1987) used the model developed by Schofield et al. (1987) of mass and heat transfer to deduce the source of potential inefficiencies due to these transport processes. Three main causes were highlighted: (i) air present in the membrane pores which restricts vapour flow, (ii) heat loss through conduction and (iii) temperature polarisation which results in loss of driving force. Two of these inefficiencies, (i) and (ii) were found to decrease significantly through deaeration which increases the permeate flux seven-fold, however, the consequence of such was a drastic increase in temperature polarisation (Schofield et al., 1990). Schofield et al (1990) found that in order to overcome this, very high film heat transfer coefficients had to be used. Much work has been performed by MD researchers in order to bring the TPC as close to unity as possible. It was found that the dominating factor determining the temperature polarisation coefficient is the thickness of the heat conduction boundary layers on either side of the membrane (Dittscher and Woermann, 1994). The main concept behind the reduction of the TPC was around the improvement of module design and / or operation, such as, using higher flow rates to achieve better mixing and the use of channel spacers to induce turbulent flow (Lawson and Lloyd, 1996, Martínez-Díez and Vázquez-González, 1998 and Ortiz De Zárate et al., 1990 and 1993). More recently, Laganà et al. (2000) found that temperature polarisation is more important than concentration polarisation, during their experiments on the concentration of apple juice. Flux rates were found to be dependent on the TPC and the effect of the CPC was negligible.

Chernyshov et al. (2003) developed a model that was capable of predicting supersaturation fields of sparingly soluble salts such as $BaSO_4$. Their model calculations demonstrated that if the solubility of the salt is an inverse function of temperature, then maximum supersaturation can occur in the bulk of the flow rather than at the membrane surface thus reducing concentration polarisation. Kurokawa et al. (1990) studied the effect of concentration polarisation by using concentrated solutions of LiBr and H_2SO_4. They found that by using concentrated solutions as the feed, this drastically effected the permeate flux due to polarisation phenomena. Accounting for concentration polarisation together with heat and mass transfer, they were able to accurately estimate these permeate fluxes.

2.3.6.2 Flux decay

Although the concentration of the solvent has only a slight effect on the flux the phenomenon of flux decay has still been observed by the majority of MD researchers. The exact explanation as to the cause of this decline is not well understood as very few researchers have performed long term experiments in order to quantify and characterise this phenomenon. Drioli and Wu (1985) are some of the researchers who performed long-term experiments on MD. They observed a decrease in permeate flowrate after the first four days of the experiment, after which the permeate flow rate reached steady-state. They found that transmembrane fluxes increased at constant ΔT with a decrease in the solute concentration of the warm solution and increased with increasing temperature, when the concentration of the warm solution was kept constant. Similar conclusions were also arrived at by other researchers (Li et al., 2003). The work of Drioli and Wu (1985) was expanded by Drioli et al. (1987) when studying the MD of solutions of glucose and NaCl (of maximum feed concentration of 0.5 M). Apart from the above mentioned conclusions, they attributed the flux decline at higher concentration to the increase in solution viscosity, being related to transport phenomena occurring at the membrane-solution interface. This flux decline is therefore expected to increase at higher solute concentrations. Long-term MD experiments were performed by Banat and Simandl (1994) who found that the flux increased during an initial two day period. However, during the course of this period, the flux was only steady during short time intervals (3 h) but could be considered unsteady over the average length of time. After this initial increase period, there was a decline in flux for about seven days before reaching steady state.

Many hypotheses have been proposed for the explanation of this flux decay. Kubota et al. (1988), found that the permeate flux not only depends on the operating temperature and

temperature difference across the membrane, but that the flow rate of the brine and cooling water also play an important role. Franken et al. (1987) explained this phenomenon in terms of membrane wetting. Their theory was that with time during MD, an increasing number of pores became wetted, which result in a back flow of permeate to the feed. They justified their theory experimentally by changing the hydrostatic pressure of the permeate and observed an inverse relationship between the permeate pressure and flux. However, this theory does not hold for the case in which the hydrostatic pressure of the feed is higher than that of the permeate and the pore wetting leads to enhanced flux, but a deterioration in quality. Apart from membrane wetting, another cause of flux decline is membrane fouling. However, this phenomenon is not as pronounced in MD as is in RO or ultrafiltration (UF), for example, due to MD membranes having larger pore sizes therefore being less susceptible to clogging (Alklaibi and Lior, 2004). Despite this advantage, fouling of the membrane in MD still occurs. There are several factors which lead to membrane fouling and subsequently, pore clogging which include, biological fouling through bacterial growth on the membrane surface, scale build-up due to high solute concentrations and the entrapment of particulate or colloid species at the membrane-liquid interface (Lawson and Lloyd, 1997). Gryta et al. (2001) also observed a rapid decline in the flux due to fouling caused by the deposition of organic matter on the membrane surface. Hsu et al. (2002) studied the effect of the type of feed on permeate flux, product water quality and membrane fouling. They found the build-up of scale on the membrane can be suppressed by reducing the degree of polarisation if NaCl solution is used as the feed fluid. However, this is not effective when seawater is the feed. Martínez-Díez and Florido-Díaz (2001) studied the effect of recirculation rate, mean temperature and salt concentration on water fluxes. They found that water flux: (i) increases as the mean temperature in the membrane system increases, (ii) increases with the recirculation rate and (iii) decreases, almost linearly, with the salt concentration of the feed solution. Cath et al. (2004) found that by applying a slightly negative pressure to the permeate stream, reduced temperature polarisation and permeability obstructions in the DCMD salt solutions could be achieved. They showed that fluxes are almost doubled by running the DCMD at reduced pressure as compared to fluxes in the DCMD mode alone. A recent work performed by Tun et al. (2005) looked at the MD of concentrated solutions of sodium chloride and sodium sulphate. They found that a steep decline in the flux occurred beyond the supersaturation point. They attributed this to the growth of crystal deposition on the membrane and loss of membrane permeability.

During these investigations the main drawback was the inability to evaluate the flux and driving force during the distillation operation. This was due to the fact that the vapour pressures cannot

be directly measured during the MD process and, as a result, can only be evaluated by a series of equations derived from the theoretical models described. The direct estimation of the vapour pressure driving force would be an advantage in estimating membrane performance and flux decline.

2.3.7 Membrane Crystallisers

The high value commercial exploitation of inorganic salts requires that crystalline products have the correct quality and structural properties. Crystallisation from solution is a widely used technique to produce large quantities of pure solid product, usually in a single processing step. However, some crystallisation techniques may require large energy inputs and process requirements in order to obtain a good quality product. For example, to produce vacuum evaporated salt with high purity from a natural feedstock, a relatively high volume of mother liquor needs to be purged. These purge streams not only result in a loss of salt but also pose large environmental problems (Samhaber et al., 2001). Recent advances in MD have led to the extension of this process to the crystallisation stage. Membrane crystallisation (MCr) was introduced by Curcio et al. (2001) who undertook investigations to produce high quality crystals from solutions. The advantages of this technique become evident when compared to conventional crystallisation techniques such as the circulating-magma crystalliser. In the latter case solvent evaporation and solute crystallisation occur in the same place. This results in temperature gradients between the surface and the bulk of the body often compromising the suspension uniformity of the crystalline products (Curcio et al., 2001). In MCr however, these two phenomena occur in separate reactors – the solvent evaporation occurs within the MD module whereas the crystallisation takes place in a separate crystalliser. Furthermore, membrane crystallisers functioning under forced solution flow conditions are characterised by an axial flux, in laminar regime of the crystallising solution through the membrane fibres (Curcio et al., 2005). This apparently induces a well-organised orientation of the particles thus resulting in crystals with improved quality and size distribution which is important when crystals need to undergo further treatment or reactions (Curcio et al., 2005).

In the MCr unit (Figure 2.12) the warm brine (retentate) flows counter current to the cold distillate (pure water). The two streams are separated by a microporous hydrophobic membrane in the form of capillary tubes. Continual removal of water from the retentate increases the concentration in the mother liquor. Nucleation and crystal growth is initialised in the crystalliser. The crystallisation process must be controlled in order avoid crystal deposition on

the membrane thus blocking the membrane pores. Therefore, a suitable heating system must exist which would ensure that the solution flowing through the membrane is always at an appropriately high temperature in order to maintain under saturation conditions, while the crystallisation tank should be at a temperature that would favour crystal formation.

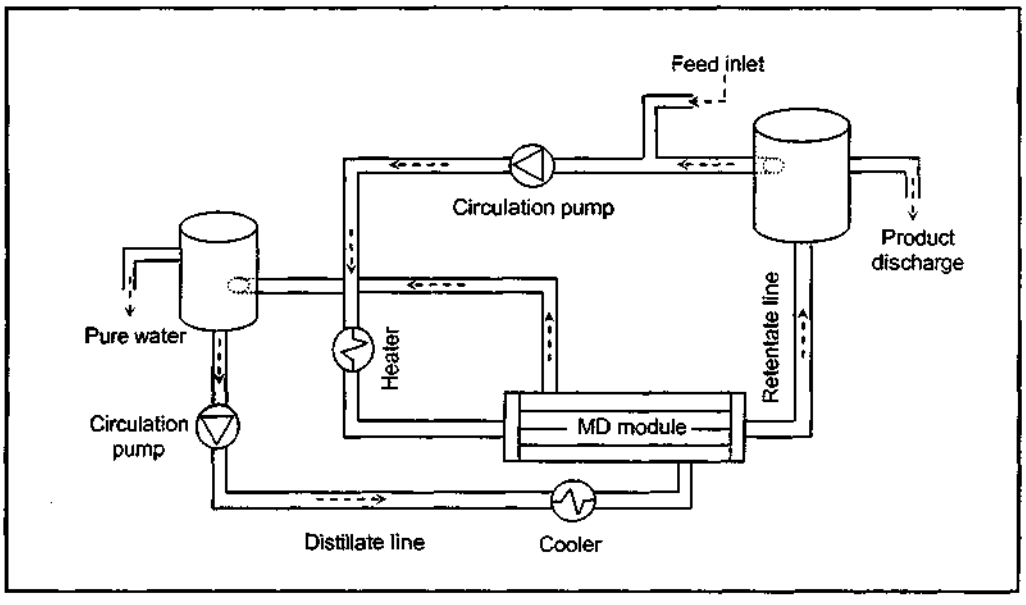

Figure 2.12: *Schematic of a membrane crystalliser unit (Curcio et al., 2001)*

A significant feature of membrane crystallisers is that the membrane does not merely serve as a support for the vapour-liquid interface, but it also induces heterogeneous nucleation due to the low supersaturation ratios (Curcio et al., 2005). The crystals obtained show improved quality and size distribution which is important for the quality of the final product and in turn influences the performance of downstream processes, crystals separation from mother liquor, drying and storage (Drioli et al., 2004).

Recently, Curcio et al. (2003) used this technique in the field of protein science for the crystallisation of lysozyme from supersaturated solutions. Another recent study performed by Drioli et al. (2004) used the membrane crystalliser to obtain epsomite ($MgSO_4.7H_2O$) and sodium chloride as solid products from NF retentate streams. The kinetics of crystallisation for sodium chloride were studied in this and an earlier investigation by Curcio et al., 2001. Preliminary data concerning the growth rate and morphological quality of magnesium sulphate crystals has been evaluated for low ionic strength solutions (Drioli et al., 2004).

2.4 INTEGRATED DESALINATION AND SEPARATION TECHNOLOGIES

In order to address some of the shortcomings of membrane processes such as RO, UF and NF, integrated membrane operations have gained much popularity within recent years. Integrated operations involve the combination of various membrane processes to achieve *process intensification* – a concept with a strategic approach towards major improvements in processing, reduction in equipment size / production-capacity ratio, reduced energy consumption, waste production, raw and hazardous materials utilisation, and recycling waste materials, resulting in more economic and sustainable technologies (Stankiewicz and Moulijn, 2002). Furthermore, the unified effect of the integration of various single membrane units might assist in overcoming the shortfalls otherwise experienced if these units operate independently. Various pre-treatment stages have been studied in order to treat the feedwater, prior to exposure to the RO membrane, in order to remove hardness, turbidity and microorganisms which ultimately lead to higher water recovery levels coupled with a reduction in energy consumption. **Section 2.4.1** describes some of the more common pre-treatment operations such as NF, UF and microfiltration (MF) integrated with further water recovery processes such as RO, and **Section 2.4.2** describes how MD and MCr can be incorporated into integrated membrane systems.

2.4.1 Pre-treatment with Pressure Driven Membrane Operations

One method of reducing fouling phenomena and prolonging the lifetime of RO membranes is by using pressure driven membrane processes, such as MF and UF for pre-treatment. The principle of separation in these techniques is based on a sieving mechanism using microporous hydrophobic membranes. The pore size for MF and UF membranes range between 10 and 0.05 μm and 0.05 μm to 1 nm, respectively (Mulder, 1996). This therefore makes these processes suitable for the retention of suspensions and emulsions or macromolecules and colloids, depending on their respective size range. Research has shown that when MF or UF is used as a pre-treatment to RO a 39 % reduction in operating and maintenance costs of water treatment for potable water production is achieved together with a reduction in RO capital costs (Drioli et al., 2002). In another study performed by Cassano et al. (2003) UF was placed ahead of RO followed by osmotic distillation (OD) in order to clarify and concentrate citrus and carrot juices. UF functioned to clarify the raw juice while RO acted on the UF permeate by pre-concentrating it before entering the OD stage for the final concentration. The advantages of concentrating fruit juices using membrane technology as opposed to conventional thermal

concentration are that the juices retain their colour and a large part of their aroma which is otherwise lost in conventional processes. Hsu et al. (2002) studied the effect of product water quality and permeate flux using different feed solutions. They found that in the case were the raw water was pre-treated by MF, the permeate flux increased by about 25 %. It is now a common practice to use MF and UF as pre-treatment to RO and has become the industry standard for the treatment of municipal wastewater in indirect potable reuse projects including aquifer recharge, industrial uses and irrigation (Durham et al., 2001 and Schaefer, 2001).

Another pretreatment option considered by Kedem and Zalmon (1997) includes the use of compact accelerated precipitation softening (CAPS) as a pre-treatment for membrane desalination. This process achieves the rapid precipitation of calcium carbonate by cake filtration through a fast equilibration. This pretreatment step reduces potential scaling effects thereby increasing the recovery ratio in membrane desalination. Pretreatment by CAPS also acts as an effective filtration step reducing the turbidity and the silt density index consequently reducing the potential for membrane fouling. In another study performed by Turek (2002), an integrated membrane system which couples ED-MSF-crystallisation stages has been described for the simultaneous production of desalinated water and valuable products.

Together with MF and UF, the removal and recovery of scale components from seawater by NF ahead of RO units is increasing in reliability. Based on this premise, investigations on NF membranes are underway, as pretreatment systems in order to remove hardness, to reduce TDS and decrease turbidity thus achieving recovery factors near to 70 % coupled to a reduction of energy consumption by about 25-30 % (Drioli, 2002). Hassan et al. (1998) have investigated the first NF-RO, NF-MSF and NF-RO_{reject}-MSF fully integrated systems for seawater desalination. They reported that when NF is placed ahead of RO, the NF unit reduced turbidity and microorganisms, removed hardness ions of Ca^{2+}, Mg^{2+}, SO_4^{2-}, HCO_3^- and total hardness by 89.6 %, 94 %, 97.8 %, 76.6 % and 93.3 %, respectively. Furthermore, the system also effected a reduction of monovalent ions of Cl^-, Na^+, K^+ and an overall TDS reduction of 57.7 %. This led to the added benefit of being able to run a MSF plant at top brine temperatures of 120 °C without the risk of added antiscalant or acid formation. This integrated system also fulfilled many of the principles of green chemistry including lower thermal load with reduced chemical consumption thereby making the process less hazardous to the environment. An earlier study performed by Turek and Gonet (1996) demonstrated how pre-treatment of coal-mine brines by NF decreases the concentration of divalent ions in the permeate with almost no changes in the

NaCl concentration. This pre-treatment then facilitated subsequent concentration in evaporation processes such as MSF, using lower energy, as there was no risk of gypsum crystallisation.

From their work on energetic and exergetic analyses of an integrated system, Criscuoli and Drioli (1999) showed that by operating a RO unit without NF pre-treatment, the quality and quantity of freshwater produced is reduced and the energy consumption remains high. Figure 2.13 represents an integrated system of MF-NF-RO proposed by Drioli et al. (2002) for the desalination of seawater.

Water recovery from the individual pressure-driven membrane units, MF, NF and RO was found to be 94.7 %, 75.3 % and 50.5 % respectively through this integrated system (Drioli et al., 2002).

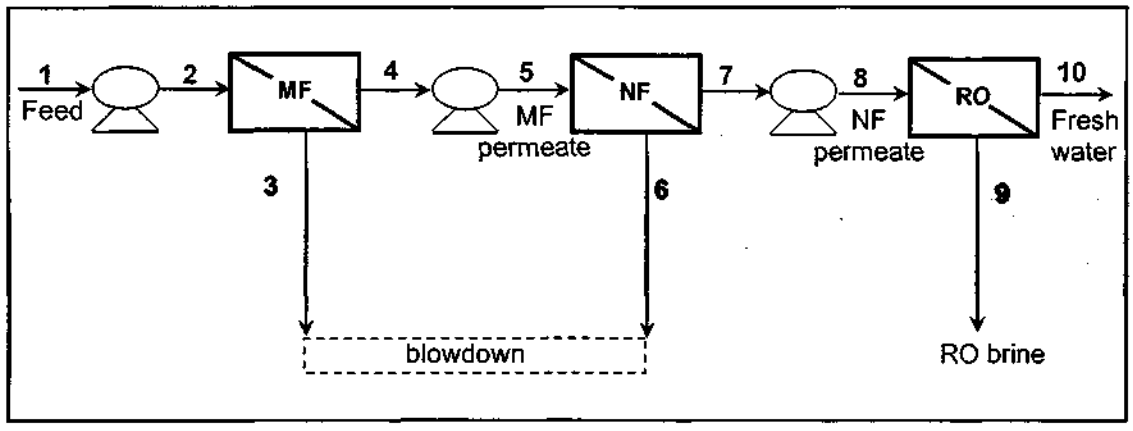

Figure 2.13: *An integrated MF-NF-RO system for seawater desalination (adapted from Curcio et al., 2005 and Drioli et al., 1999)*

2.4.2 Integrated MF/UF-NF-RO-MCr/MD System

Following the integration of the membrane units represented in Figure 2.13, Drioli et al. (1999) extended this system to incorporate a MD unit to process the RO brine and proposed an ideal high-recovery process for the desalination of seawater (Figure 2.14). The integrated system proposed a *pre-treatment* stage which included MF/UF-NF-MC and a *processing* stage consisting of RO-MD. The pre-treatment stage included a gas-liquid membrane contactor unit (MC). This MC operation serves to reduce the amount of dissolved gases such as CO_2 and O_2

that are present in the feed solution, if deemed necessary. The MC operation is simply a distillation across a microporous hydrophobic membrane. These membranes serve as an interface for the mass transfer between phases of the adsorption stage. An energetic and exergetic analysis of this integrated membrane system indicated that the recovery factor of the MD unit was 77 % and the RO unit alone yielded a recovery factor of 40 %. However, by coupling these two membrane units the global recovery factor was a high of 87.6 % (Criscuoli and Drioli, 1999).

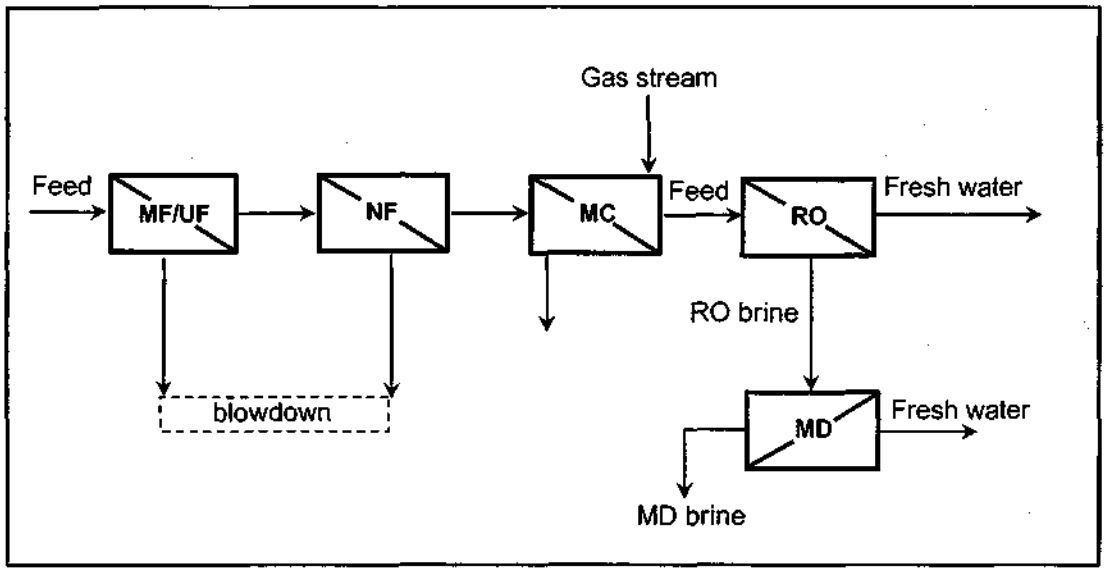

Figure 2.14: *Proposed ideal integrated membrane system for seawater desalination (Drioli et al, 1999)*

Later, Drioli et al. (2004) exploited this CO_2 removal by MC for the reactive transfer into sodium hydroxide solutions for the production of $NaHCO_3$ / Na_2CO_3 salts. These carbonate solutions were necessary for the precipitation of Ca^{2+} ions as carbonates. The aim was to lower the Ca^{2+} ion content in solution as this led to the formation of $CaSO_4$ which is one of the major scale-forming components. Furthermore Drioli et al. (2004) aimed at the crystallisation of $MgSO_4.7H_2O$ (epsomite), as one of the salts, from solution and the formation of the soluble $CaSO_4$ ion pair hindered the formation and precipitation of epsomite by harbouring SO_4^{2-} ions.

Further conclusions were drawn from the exergetic and energetic analysis by Criscuoli and Drioli (1999) on the systems similar to the ones described above. From their analyses it was

found that by placing NF ahead of RO the osmotic pressure of the feed solution is lowered and hence a lower applied pressure is required to move water through the membrane. The added electrical energy that is required to run NF as a pre-treatment to RO can be offset by using the NF concentrate to pre-pressurise the feedwater thus reducing the RO electrical energy requirements. For the coupling of RO with MD a higher thermal demand arises due to the MD process. However, when these two units are further coupled with NF it was found that this energy demand is lowered. In summary, the NF-RO-MD integrated system operates at the highest performance level, and is particularly appropriate if excess low-grade thermal energy is available.

Other integrated MD operations proposed by Wang et al. (2001) consisted of the integration of MD and OD to form the overall process which they termed membrane osmotic distillation (MOD). Furthermore, their experimental system involved the circulation of brine in the cold side of the MD. They found that with the integration of these systems, and with brine circulated on the cold side, the water flux increased through the membrane due to a decrease in the water vapour pressure in the brine side. Furthermore, the integrated MOD process resulted in higher heat efficiencies.

Following the proposal of the ideal integrated system of Figure 2.14, a further investigation by Drioli et al. (2002) incorporated a membrane crystalliser to form the NF-RO-MCr integrated system. The membrane crystalliser achieves the complete recovery of desalted water and solid salts. Feeding the MD unit with RO retentate allows the production of sodium chloride crystals. Although this system represents a higher thermal energy requirement, it does, however, eliminate the environmental problems related to brine disposal and if there is excess low-grade thermal energy available within the plant, it could be used making the overall energy requirement then comparable to an NF-RO coupled system (Drioli et al., 2002).

Van der Bruggen et al. (2004), proposed an integrated membrane system which leads to process intensification in the textile finishing industry. This system consisted of MF as a pre-treatment to used finishing baths, followed by a dual NF unit. Furthermore, the concentrate stream from the first NF unit is fed to a MD unit, making advantageous use of the high temperature for further concentration, and the concentrate from the second NF unit is fed to a membrane crystalliser for salt recovery and reuse for new finishing baths. Although their concept needs experimental verification they nonetheless proposed an overall waste minimisation and reduction in energy and water losses thus fulfilling the concept of process intensification.

Curcio et al. (2005) extended the work of Drioli et al. (2004) by performing an energetic, exergetic and cost analysis on the systems MF-NF-RO and NF-MC-RO-MCr. In one instance, the NF retentate from the integrated system represented in Figure 2.14 was mixed with Na_2CO_3, produced from the reactive adsorption of CO_2 via MC, for the removal of Ca^{2+} ions as $CaCO_3$, before entering the MCr unit. In the second instance the RO brine was subjected to $CaCO_3$ precipitation before reaching the crystalliser. In the former case a global recovery factor of water of up to 58.6 % was achieved and in the latter case a 70.1 % global water recovery was achieved. Although the membrane crystalliser requires additional energy for its operation, in addition to drinking water this system allows for the recovery of solid salts of NaCl and $MgSO_4.7H_2O$. Proceeds arising from the sale of these salts could counterbalance the high unit cost of water production. A further advantage of completing this integrated system with a crystalliser stage is that both the cost and environmental impacts of brine disposal operations are considerably reduced thus favouring the concepts of green chemistry and moving towards sustainable industrial growth.

2.5 CHAPTER REFERENCES

AGASHICHEV SP and SIVAKOV AV (1993) *Modeling and calculation of temperature-concentration polarisation in the membrane distillation process (MD).* Desalination **93** 245-258.

AL-DROUBI A, FRITZ B, GAC J-Y and TARDY Y (1980) *Generalised residual alkalinity concept; application to prediction of natural waters by evaporation.* Am J Sci **280** 560-572.

ALKLAIBI AM and LIOR N (2004) *Membrane-distillation desalination: status and potential.* Desalination **171** 111-131.

AL-SHAMMIRI M and AL-DAWAS M (1997) *Maximum recovery from seawater reverse osmosis plants in Kuwait.* Desalination **110** 37-48.

AL-SHAMMIRI M and SAFAR M (1999) *Multi-effect distillation plants: state of the art.* Desalination **126** 45-59.

ANDERSSON SI, KJELLANDER N and RODESJO B (1985) *Design and field tests of a new membrane distillation desalination process*. Desalination **56** 345-354.

BANAT FA and SIMANDL J (1993) *Theoretical and experimental study in membrane distillation*. Desalination **95** 39-52.

BANDINI S, GOSTOLI C and SARTI GC (1991) *Role of heat and mass transfer in membrane distillation process*. Desalination **184** 91-106.

BANDINI S, GOSTOLI C and SARTI GC (1992) *Separation efficiency in vacuum membrane distillation*. J Membr Sci **73** 217-229.

BARAT JM, GRAU R, IBÁÑEZ JB and FITO P (2005) *Post-salting studies in Spanish cured ham manufacturing. Time reduction using brine thawing-salting*. Meat Science **69** 201-208.

BASINI L, ANGELO GD, GOBBI M, SARTI GC and GOSTOLI C (1987) *A desalination process through seeping gas membrane distillation* Desalination **64** 245-257.

BHATTACHARYYA D and WILLIAMS ME (1992) Chapter 21. *Reverse Osmosis. Introduction and Definitions*. In *Membrane Handbook*, WINSTON HO WS and SIRKAR KK, Van Nostrand Reinhold, pg. 265.

BERNARDO P, CRISCUOLI A, CLARIZIA G, BARBIERI G, DRIOLI E, FLERES G and PICCIOTTI M (2003) *Applications of membrane unit operations in ethylene process*. Clean Technologies and Environmental Policy, Springer-Verlag, DOI 10.1007/s10098-003-0225-8.

BOUGUECHA S, CHOUIKH R and DHAHBI M (2002) *Numerical study of the coupled heat and mass transfer in membrane distillation*. Desalination **152** 245-252.

BRANDT DC, LEITNER GF and LEITNER WE (1993) *Reverse osmosis membranes: State of the art*. In *Reverse Osmosis: Membrane Technology, Water Chemistry, and Industrial Applications*, AMJAD Z, ed., Van Nostrand Reinhold, New York, ISBN: 0-442-23964-5, pg. 1.

BURGOYNE A and VAHDATI MM (1999) *Permeate flux modelling of membrane distillation.* Filtration and Separation 49-53.

BUCKLEY CA, BROUCKAERT CJ and KERR CA (1993) RO application in brackish water desalination and in the treatment of industrial effluents. In *Reverse Osmosis: Membrane Technology, Water Chemistry, and Industrial Applications*, AMJAD Z, ed., Van Nostrand Reinhold, New York. ISBN: 0-442-23964-5. pg. 275.

CABASSUD C and WIRTH D (2002) *Water desalination using membrane distillation: comparison between inside/out and outside/in permaeation* Desalination **147** 139-145.

CABASSUD C and WIRTH D (2003) *Membrane distillation for water desalination: how to chose an appropriate membrane?* Desalination **157** 307-314.

CALABRO V, DRIOLI E and MATERA F (1991) *Membrane distillation in the textile wastewater treatment.* Desalination **83** 209-224.

CALABRO V, JIAO BL and DRIOLI E (1994) *Theoretical and experimental study on membrane distillation in the concentration of fruit juice.* Ind Eng Chem Res **33** 1803-1808.

CARDONA E, CULOTTA S and PIACENTINO A (2003) *Energy saving with MSF-RO series desalination plants.* Desalination, **153** 167-171

CASSANO A, DRIOLI E, GALAVERNA G, MARCHELLI R, DI SILVESTRO G and CAGNASSO P (2003) *Clarification and concentration of citrus and carrot juices by integrated membrane processes.* Journal of Food Engineering **57** 153-163.

CATH TY, ADAMS VD and CHILDRESS AE (2004) *Experimental study of desalination using direct contact membrane distillation: a new approach to flux enhancement.* J Membr Sci **228** 5-16.

CHERNYSHOV MN, MEINDERSMA GW and de HAAN AB (2003) *Modelling temperature and salt concentration distribution in membrane distillation feed channel.* Desalination **157** 315-324.

CRISCUOLI A and DRIOLI E (1999) *Energetic and exergetic analysis of an integrated membrane desalination system*. Desalination **124** 243-249.

CRISCUOLI A, DRIOLI E, CAPUANO A, MEMOLI B and ANDREUCCI VE (2002) *Human plasma ultrafiltrate purification by membrane distillation: process optimization and evaluation of its possible application on-line*. Desalination **147** 147-148.

CURCIO E, CRISCUOLI A and DRIOLI E (2001) *Membrane crystallizers*. Ind Eng Chem Res **40** 2679-2684.

CURCIO E, DI PROFIO G and DRIOLI E (2003) *A new membrane-based crystallization technique: tests on lysozyme*. J Crystal Growth **247** 166-176.

CURCIO E, DI PROFIO G, MARIAH L and DRIOLI E (2005) *A fully integrated membrane operation for sea water and brackish water desalination*. Proceedings of the World Conference for Chemical Engineers, Glascow, 2005.

DARWISH MA and EL-DESSOUKY H (1995) *The heat recovery thermal vapour-compression desalting system: A comparison with other thermal desalination processes*. Applied Thermal Engineering **16** (6) 523-537.

DING Z, MA R and FANE AG (2002) *A new model for mass transfer in direct contact membrane distillation*. Desalination **151** 217-227.

DITTSCHER U and WOERMANN D (1994) *Temperature polarization in membrane distillation of water using a porous hydrophobic membrane*. Ber Bunsenges Phys Chem **98**(8) 1056-1061.

DREVER, JI (1997). *The Geochemistry of Natural Waters: Surface and Groundwater Environments* 3rd edition. Prentice-Hall, New Jersey. ISBN: 0-13-272790-0.

DRIOLI E, CRISCUOLI A and CURCIO E (2002) *Integrated membrane operations for seawater desalination*. Desalination **147** 77-81.

DRIOLI E, CURCIO E, CRISCUOLI A and DI PROFIO G (2004) *Integrated system for recovery of $CaCO_3$, NaCl and $MgSO_4.7H_2O$ from nanofiltration retentate.* J Membr Sci **239** 27-38.

DRIOLI E, LAGANÁ F, CRISCUOLI A and BARBIERI G (1999) *Integrated membrane operations in desalination processes.* Desalination **122** 141-145.

DRIOLI E and WU Y (1985) *Membrane distillation: an experimental study.* Desalination **53** 339-346.

DRIOLI E, WU Y and CALABRO V (1987) *Membrane distillation in the treatment of aqueous solutions.* J Membr Sci **33** 277-284.

DURHAM B, BOURBIGOT MM and PANKRATZ T (2001) *Membranes as pre-treatment to desalination in wastewater reuse: operating experience in the municipal and industrial sectors.* Desalination **138** 83-90.

EL AMALI A, BOUGUECHA S and MAALEJ M (2004) *Experimental study of air gap and direct contact membrane distillation configurations: application to geothermal and seawater desalination.* Desalination **168** 357.

ENGELIEN HK and SKOGESTAD S (2005) *Multi-effect distillation applied to an industrial case study.* Chemical Engineering and Processing **44**(8) 819-826.

ESPINO T, PEÑATE B, PIERNAVIEJA G, HEROLD D and NESKAKIS A (2003) *Optimised desalination of seawater by a PV powered reverse osmosis plant for a decentralised coastal water supply.* Desalination **156** 349-350.

EUGSTER H.P (1980) *Geochemistry of evaporitic lacustrine deposits.* Ann Rev Earth Planet Sci **8** 35-63.

EUGSTER HP and JONES BF (1979) *Behaviour of major solutes during closed-basin brine evolution.* American Journal of Science **279** 609-631.

FANE AG, SCHOFIELD RW and FELL CJD (1987) *The efficient use of energy in membrane distillation*. Desalination **64** 234-243.

FARWATI MA (1997) *Theoretical study of a multi-stage flash distillation using solar energy*. Desalination **22** 1-5.

FRANKEN ACM, NOLTEN JAM, MULDER MHV, BARGEMAN D and SMOLDERS CA (1987) *Wetting criteria for the applicability of membrane distillation*. J Membr Sci **33** 315-328.

FUJII Y, KIGOSHI S, IWATANI H and AOYAMA M (1992) *Selectivity and characteristics of direct contact membrane distillation type experiment. I. Permeability and selectivity through fried hydrophobic fine porous membranes*. J Membr Sci **72** 53-72.

GAETA FS, ASCOLESE E, BENCIVENGA U, ORTIZ de ZÁRATE, PAGLIUCA N, PERNA G, ROSSI S and MITA DG (1992) *Theories and experiments on nonisothermal matter transport in porous membranes*. J Phys Chem **96** 6342-6354.

GARCIA-ALEMAN J and DICKSON JM (2004) *Mathematical modelling of nanofiltration membranes with mixed electrolyte solutions*. J Membr Sci **235** 1-13.

GARCIÁ-RODRÍGUEZ L and GÓMEZ-CAMACHO C (1999) *Conditions for economical benefits of the use of solar energy in multi-stage flash distillation*. Desalination **125** 133-138.

GEKAS V and HALLISTROM B (1987) *Mass transfer in the membrane concentration polarization layer under turbulent cross flow. I. Critical literature review and adaptation of existing Sherwood correlations to membrane operations*. J Membr Sci **30** 153-170.

GOSTOLI C and SARTI GC (1989) *Separation of liquid mixtures by membrane distillation*. J Membr Sci **41** 211-224.

GRILLOT G (1956) *The biological and agricultural problems presented by plants tolerant of saline or brackish water and the employment of such water for irrigation*. In *Utilization of saline water, Reviews of research*, 2nd edition, UNESCO, France, 9.

GRYTA M and TOMASZEWSKA M (1998) *Heat transport in the membrane distillation process*. J Membr Sci **144** 211-222.

GRYTA M, TOMASZEWSKA M, GRZECHULSKA J and MORAWSKI AW (2001) Short Communication. *Membrane distillation of NaCl solution containing natural organic matter*. J Membr Sci **181** 179-187.

GUIJT CM, RÁCZ IG, REITH T and de HAAN AB (2000) *Determination of membrane properties for use in the modeling of a membrane distillation module*. Proceedings of the Conference on Membranes in Drinking and Industrial Water Production, Volume 2, Desalination Publications L'Aquila, Italy 511-517 ISBN 0-86689-060-2.

HARDIE LA and EUGSTER HP (1970) *The evolution of closed-basin brines*. Mineralogical Soc Am Spec Publ **3** 273-290.

HARVIE CE and WEARE JH (1980) *The prediction of mineral solubilities in natural waters: the Na-K-Mg-Ca-Cl-SO_4-H_2O system from zero to high concentration at 25°C*. Geochimica et Cosmochimica Acta **44** 981-997.

HARVIE, C.E., MØLLER, N. and WEARE, J.H. (1984). *The prediction of mineral solubilities in natural waters: The Na-K-Mg-Ca-H-Cl-SO_4-OH-HCO_3-CO_3-CO_2-H_2O system to high ionic strengths at 25°C*. Geochimica et Cosmochimica Acta **48** 723-751.

HASSAN AM, AL-SOFI AK, AL-AMOUDI AS, JAMALUDDIN ATM, FAROOQUE AM, ROWAILI A, DALVI AGI, KITHER NM, MUSTAFA GM and AL-TISAN IAR (1998) *A new approach to membrane and thermal seawater desalination processes using nanofiltration membranes (Part 1)*. Desalination **118** 35-51.

HOGAN PA, SUDJITO, FANE AG and MORRISON GL (1991) *Desalination by solar heated membrane distillation*. Desalination **81** 81-90.

HOWE DE (1956) Utilisation of seawater. In *Utilization of saline water, Reviews of research*, 2nd edition, UNESCO, France, 73.

HSU ST, CHENG KT and CHIOU JS (2002) *Seawater desalination by direct contact membrane distillation*. Desalination. **143** 279-287.

HUGO PJ (1974) Salt in the Republic of South Africa. Department of mines Geological Survey, Memoir 65, The Government Printer, Pretoria.

IMDAKM AO and MATSUURA T (2004) *A Monte Carlo simulation model for membrane distillation processes: direct contact (MD)*. J Membr Sci **237** 51-59.

ISMAIL A (1998) *Control of multi-stage flash desalination plants: A survey*. Desalination **116** 145-156.

JONSSON AS, WIMMERSTEDT R and HARRYSON AC (1985) *Membrane distillation – a theoretical study of evaporation through microporous membranes*. Desalination **56** 237-249.

JUBY GJG, SCHUTTE CF and VAN LEEUWEN J (1996) *Desalination of calcium sulphate scaling mine water: Design and operation of the SPARRO process*. Water SA **22** (2) 161-171.

KARELIN FN, ASKERNIYA AA, GRIL ML and PARILOVA OF (1996) *Salt concentration and recovery from aqueous solutions using pressure-driven membrane processes*. Desalination **104** 69-74.

KEDEM O and ZALMON G (1997) *Compact accelerated precipitation softening (CAPS) as a pre-treatment for membrane desalination 1. Softening by NaOH*. Desalination **113** 65-71.

KHAYET M, GODINO MP and MENGUAL JI (2003) *Theoretical and experimental studies on desalination using the sweeping gas membrane distillation method*. Desalination **157** 297-305.

KIMURA S and NAKAO S-I (1987) *Transport phenomena in membrane distillation*. J Membr Sci **33** 285-298.

KRISHNA HJ (2004) *Introduction to desalination technologies*. TWDB Volume 2: Technical papers, case studies and desalination technology resources. Accessed on 05 September 2005 at URL http://www.twdb.state.tx.us/Desalination/The%20Future%20of%20 Desalination %20in%20Texas%20-%20Volume%202/documents/C1.pdf#search='vapor% 20 compression%20distillation %20for%20desalination'.

KUBOTA A, OHTA K, HAYANO I, HIRAI M, KIKUCHI K and MURAYAMA Y (1988) *Experiments on seawater desalination by membrane distillation*. Desalination **69** 19-26.

KUMAR S and TIWARI GN (1999) *Optimization of design parameters for multi-effect active distillation systems using the Runge-Kutta method*. Desalination **121** 87-96.

KUROKAWA H, EBARA K, KURODA O and TAKAHASHI S (1990) *Vapor permeate characteristics of membrane distillation*. Sep Sci & Technol **25**(13-15) 1349-1359.

LAGANÁ F, BARBIERI G and DRIOLI E (2000) *Direct contact membrane distillation: modeling and concentration experiments*. J Membr Sci **166** 1-11.

LAWSON KW and LLOYD DR (1996) *Membrane distillation. II. Direct contact MD*. J Membr Sci **120** 123-133.

LAWSON KW and LLOYD DR (1997) Review. *Membrane distillation*. J Membr Sci **124** 1-25.

LI J-M, XU Z-K, LIU Z-M, YUAN W-F, XIANG H, WANG S-Y and XU Y-Y (2003) *Microporous polypropylene and polyethylene hollow fiber membranes. Part 3. Experimental studies on membrane distillation for desalination*. Desalination **155** 153-156.

MANI AGRO CHEM (2005). *Magnesium sulphate heptahydrate ($MgSO_4.7H_2O$)*. Accessed on 02 November 2005 at URL http://www.indiamart.com/maniagrochem/#magnesium-sulphate-hepta-hydrate.

MARIAH L, BUCKLEY CA, BROUCKAERT CJ, JAGANYI D, CURCIO E and DRIOLI E (2006a) *Membrane distillation for the recovery of crystalline products from concentrated brines*. WISA Biennial Conference, Durban, South Africa, 21-25 May.

MARIAH L, BUCKLEY CA, BROUCKAERT CJ, CURCIO E, DRIOLI E, JAGANYI D, and RAMJUGERNATH D (2006b) *Membrane distillation of concentrated brines – role of water activities in the evaluation of driving force.* J Membr Sci. **280** (1-2) 937-947.

MARIAH L, BUCKLEY CA, JAGANYI D, DRIOLI E and CURCIO E (2005a), *The Development of Sustainable Salt Sinks – Evaluation of an Integrated Membrane System for the Recovery and Purification of Magnesium Sulphate and Sodium Chloride from Brine Streams,* 6th WISA MTD Workshop, Membrane Technical Division (MTD). Eastern Cape, 14-15 March.

MARIAH L, BUCKLEY CA, BROUCKAERT CJ, RAMJUGERNATH D, JAGANYI D, CURCIO E and DRIOLI E (2005b), *The role of water activities in membrane distillation of concentrated brines for recovery of crystalline products from brine effluents.* IWA-WISA, Sandton Convention Centre, Johannesburg, South Africa, 9-12 August.

MARTÍNEZ L (2004) *Comparison of membrane distillation performance using different feeds.* Desalination **168** 359-365.

MARTÍNEZ L and FLORIDO-DÍAZ FJ (2001a) *Theoretical and experimental studies on desalination using membrane distillation.* Desalination **139** 373-379.

MARTÍNEZ-DÍEZ L and FLORIDO-DÍAZ FJ (2001b) *Desalination of brines by membrane distillation.* Desalination **137** 267-273.

MARTÍNEZ-DÍEZ L, FLORIDO-DÍAZ FJ and VÁZQUEZ-GONZÁLEZ MI (1999) *Study of evaporation efficiency in membrane distillation.* Desalination **126** 193-198.

MARTÍNEZ-DÍEZ L and VÁZQUEZ-GONZÁLEZ MI (1998) *Study of membrane distillation using channel spacers* J Membr Sci **144** 45-56.

MORTON AJ, CALLISTER IK and WADE NM (1996) *Environmental impacts of seawater distillation and reverse osmosis processes.* Desalination **108** 1-10.

MULDER M (1996) *Basic principles of membrane technology.* Kluwer Academic Press, The Netherlands. ISBN: 0-7923-4248-8.

OHYA H, SUZUKI T and NAKAO S (2001) *Integrated system for complete usage of components in seawater. A proposal of inorganic chemical combinat on seawater.* Desalination **134** 29-36.

ORTIZ DE ZÁRATE, GARCÍA-LÓPEZ and MENGUAL JI (1990) *Temperature polarization in non-isothermal mass transport through membranes.* J Chem Soc Faraday Trans **86**(16) 2891-2896.

ORTIZ DE ZÁRATE JM, VELAZQUEZ A, PENA L and MEGUAL JI (1993) *Influence of temperature polarization on separation by membrane distillation.* Sep Sci & Technol **28**(7) 1421-1436.

O'NEAIL TM, KIRCHNER OE and DAY WJ (1981) *Achieving high recovery from brackish water with seeded reverse osmosis systems.* Proceedings of the 42nd Annu Meeting, Int Water Conf, Pittsburgh, Pennsylvania, October.

PEÑA L, ORTIZ DE ZARATE JM and MENGUAL JI (1993) *Steady states in membrane distillation: Influence of membrane wetting.* J Chem Soc Faraday Trans **89**(24) 4333-4338.

PHATTARANAWIK J and JIRARATANANON R (2001) Rapid Communication. *Direct contact membrane distillation: effect of mass transfer on heat transfer.* J Membr Sci **188** 137-143.

PHATTARANAWIK J, JIRARATANANON R and FANE AG (2003) *Heat transport and membrane distillation coefficients in direct contact membrane distillation.* J Membr Sci **212** 177-193.

RAUTENBACH R and ALBRECHT R (1981) *Membrane processes.* John Wiley & Sons, Switzerland. ISBN 0-471-91110-0.

SAAVEDRA A, BANDINI S and SARTI GC (1992) *Separation of v. o. c. from aqueous streams through vacuum membrane distillation*, Proc. Of the Euromembrane Conf., Paris, France,119-204.

SALT INSTITUTE (2005) *What is salt used for?* Accessed on 4 October 2005 at URL http://www.saltinstitute.org/30.html.

SAMHABER WM, KRENN K and SCHWAIGER H (2001) *Field test results of nanofiltration for separating almost saturated brine solutions of the vacuum salt production.* ECCE, Nürnberg 26.

SARTI GC, GOSTOLI C and BANDINI S (1993) *Extraction of organic components from aqueous streams by vacuum membrane distillation.* J Membr Sci **80** 21-33.

SARTI GC, GOSTOLI C and MATULLI S (1985) *Low energy cost desalination processes using hydrophobic membranes.* Desalination **56** 277-286.

SCHAEFER J (2001) *Reliable water supply by reusing wastewater after membrane treatment.* Desalination **138** 91.

SCHOFIELD RW, FANE AG and FELL CJD (1987) *Heat and mass transfer in membrane distillation.* J Membr Sci **33** 299-313.

SCHOFIELD RW, FANE AG and FELL CJD (1990) *Gas and vapour transport through microporous membranes. II. Membrane Distillation.* J Membr Sci **53** 173-185.

SLUYS JTM, VERDOES D and HANEMAAIJER JH (1996) *Water treatment in a Membrane-Assisted Crystallizer (MAC).* Desalination **104** 135-139.

SMITH M (2000) *A geochemical investigation of the Darling and Ysterfontein saline pans, Western Cape, South Africa.* MSc Thesis. University of Cape Town, South Africa.

SMOLDERS K and FRANKEN ACM (1989) *Terminology for membrane distillation.* Desalination **72** 249-262.

SPIEGLER KS and KEDEM O (1966) *Thermodynamics of hyperfiltration, criteria for efficient membranes* Desalination **1** 311-326.

STANKIEWICZ A and MOULIJN JA (2002) *Process intensification.* Ind Eng Chem Res **41** (8) 1920.

TOMASZEWSKA M (1993) *Concentration of the extraction fluid from sulfuric acid treatment of phosphogypsum by membrane distill*ation. J Membr Sci **78** 277-282.

TUN CM, FANE AG, MATHEICKAL JT and SHEIKHOLESLAMI R (2005) *Membrane distillation crystallization of concentrated salts – flux and crystal formation.* J Membr Sci **257** 144-155.

TUREK M (2002) *Dual-purpose desalination-salt production electrodialysis.* Desalination **153** 377-381.

TUREK M and GONET M (1996) *Nanofiltration in the utilization of coal-mine brines.* Desalination **108** 171-177.

UDRIOT H, ARAQUE A and von STOCKAR U (1994) *Azeotropic mixtures may be broken by membrane distillation.* The Chemical Engineering Journal **54** 87-93.

UNEP (1997) *Source book of alternative technologies for freshwater augmentation in Latin America and the Caribbean.* International Environmental Technology Centre, United Nations Environmental Programme. Accessed on 05 September 2005 at URL http://www.oas.org/osde/publications/Unit/oea59e/begin.htm#Contents.

VAN DER BRUGGEN B (2003) *Desalination by distillation and by reverse osmosis – trends towards the future.* Membrane Technology Feature 6-9.

VAN DER BRUGGEN B, CURCIO E and DRIOLI E (2004) *Process intensification in the textile industry: the role of membrane technology.* Journal of Environmental Management **73** 267-274.

VAN DER BRUGGEN B and VANDECASTEELE C (2002) *Distillation vs. membrane filtration: overview of process evolutions in seawater desalination.* Desalination **143** 207-218.

VAN DE LISDONK CAC, VAN PAASSEN JAM and SCHIPPERS JC (2000) *Monitoring scaling in naofiltration and reverse osmosis membrane systems*. Desalination **132** 101-108.

VAN PAASSEN JAM, KRUITHOF JC, BAKKER SM and KEGEL FS (1998) *Integrated multi-objective membrane systems for surface water treatment: pre-treatment of nanofiltration by riverbank filtration and conventional groundwater treatment*. Desalination **118** 239-248.

WALTON J, LU H, TURNER C, SOLIS S and HEIN H (2004) *Solar and waste heat desalination by membrane distillation*. Desalination and Water Purification Research and Development Program Report No. 81. Agreement No. 98-FC-81-0048. U.S. Department of Interior, Bureau of Reclamation, Denver Federal Center, USA.

WANG Z, ZHENG F and WANG S (2001) *Experimental study of membrane distillation with brine circulated in the cold side*. J Membr Sci **183** 171-179.

WINTER T, PANNELL DJ and McCANN L (2001) *The economics of desalination and its potential application in Australia*. SEA News Issue No. 9. Sustainability and Economics in Agriculture (SEA) GRDC Project UWA251.

WU Y, KONG Y, LIN X, LUI W and XU J (1992) *Surface-modified hydrophilic membranes in membrane distillation*. J Membr Sci **72** 189-196.

WU Y, KONG Y, LIU J, ZHANG J and XU J (1991) *An experimental study on membrane distillation – crystallization for treating waste water in Turine production*. Desalination **80** 235-242.

ZOLOTAREV PP, UGROZOV VV, VOLKINA IB and NIKULIN VN (1994) *Treatment of waste water for removing heavy metals by membrane distillation*. J. Membr. Sci. **37** 77-82.

CHAPTER 3

Chapter 3

MDC OF CONCENTRATED BRINES

Having studied the various desalination processes and their advantages and disadvantages, it appears that membrane distillation forms a very attractive approach to the production of pure water and recovery of crystalline products, from concentrated salt solutions. This chapter therefore forms the first in the series of methods outlined in Section 1.4 for providing a proof of the concept of membrane distillation crystallisation for the recovery of solid products from concentrated salt solutions. The experimental equipment design and operational characteristics are described in Section 3.1. Section 3.2 provides and discusses the results for two series of experiments that were identified, i.e. single electrolyte and mixed electrolyte systems. The important findings from this experimental work are then summarised in Section 3.3.

3.1 EXPERIMENTAL

The experimental plant design that was used during these series of membrane distillation and crystallisation (MDC) experiments is shown in Figure 3.1. The MD equipment was operated in a batch concentration mode where the recirculating permeate stream, consisting of deionized water, and the retentate stream flowed countercurrent through the membrane module. The membrane module, MD 020CP-2N, supplied by Microdyn, contained 40 hydrophobic polypropylene capillary fibres of 0.1 m^2 total interfacial area and 45 cm in length. The nominal pore size of the polypropylene membranes was 0.2 μm and the internal and shell diameters of the fibres were 1.8 mm and 21 mm, respectively. The thickness of the membrane was 120 μm with a packing density of 70 %.

During the process the solution in the retentate line was heated. A vapour-liquid interface was established at the membrane surface and water vapour molecules from the retentate stream diffuse across the membrane and condenses in the permeate stream.

The performance of the membrane was evaluated by calculating the water flux or permeation rate (Equation 3.1).

$$\text{Flux} = \frac{\text{mass of water extracted (g)}}{\text{unit area (m}^2\text{)} \times \text{time interval (h)}} \qquad [3.1]$$

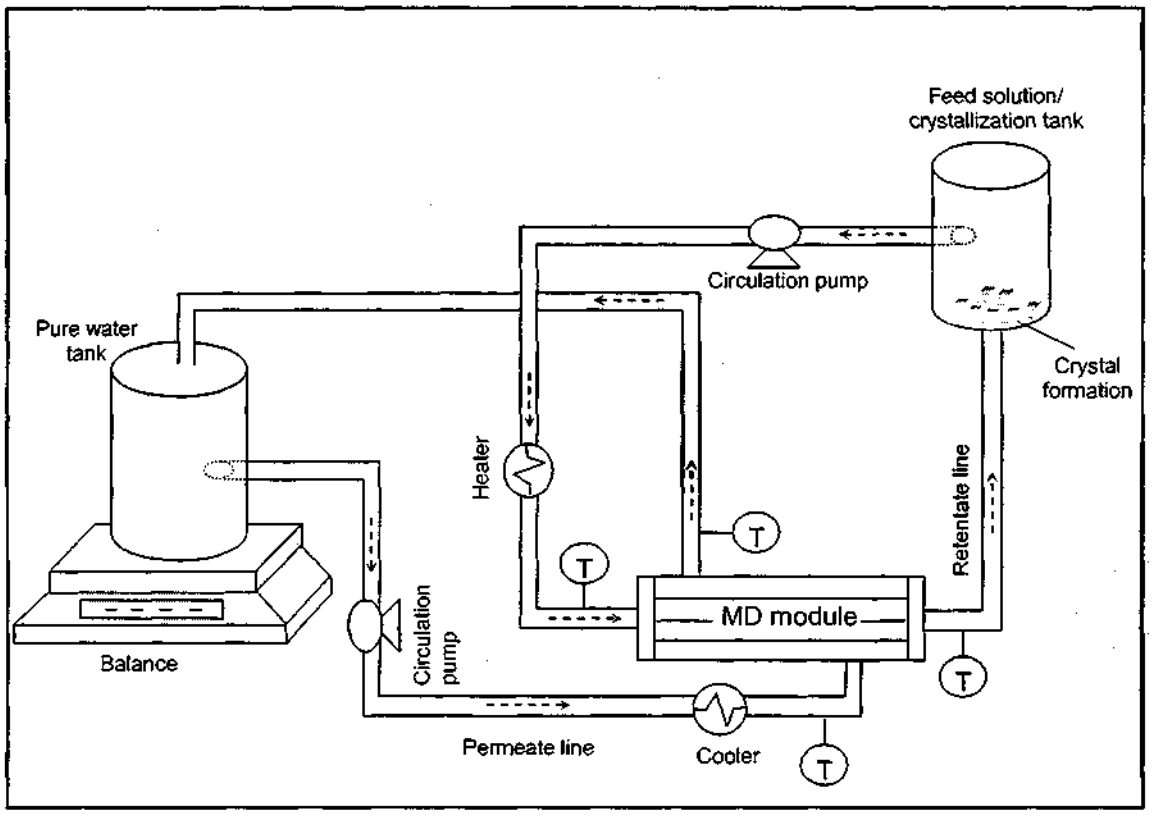

Figure 3.1: *Experimental setup for membrane distillation crystallisation of concentrated salts*

Continual removal of pure water from the retentate leads to the concentration of the remaining solution resulting in a mother liquor in which nucleation and crystal growth is initialised. Crystallisation occurs in a separate vessel from which a centrifugal pump (Caster Pump mono-phase 0.25 CV, 2780 rpm) circulates the mother liquor through the membrane module. Both the feed and crystallisation tanks were plastic containers of approximately 3 ℓ in volume. The temperature was measured at module inlet and outlet for both the retentate and permeate lines as shown in Figure 3.1 and the precision was estimated to be ±0.1 °C. The pipes that were used to circulate the solution were plastic pipes of approximately 20 mm in diameter. The flowrate was

of the order of 100 ℓ/h. Samples were routinely withdrawn from the crystallisation tank and visually examined and photographed using a video-camera, (Axiovert 25), equipped with optical head 25 X, to determine the crystal size distribution. Nucleation rate has been evaluated by microscopic visualization, i.e. monitoring the evolution in time of the crystal size distribution.

3.2 RESULTS AND DISCUSSION

For the series of MDC experiments, two types of systems were investigated. Although some work has been done concerning the MDC of magnesium sulphate for the recovery of crystalline product (Drioli et al., 2004), solutions of high concentration (close to saturation) have not been performed. Therefore, the first part of this work investigated the MDC of concentrated solutions of magnesium sulphate for the crystallisation of epsomite. This was then followed by the MDC of concentrated solutions of a mixture of sodium chloride and magnesium sulphate, in varying ratios, aimed at the crystallisation of sodium chloride.

3.2.1 Single Electrolyte System

For this purpose, concentrated solutions of magnesium sulphate of 375 g/ℓ (1.93 m) and 625 g/ℓ (3.98 m) were prepared by dissolving the appropriate amount of solid magnesium sulphate heptahydrate ($MgSO_4.7H_2O$) in demineralised water. The solution was fed into the membrane distillation equipment which operated in the manner described in **Section 3.1**. The temperature was set to an approximate value for the feed solution and the solution gradually heated before starting the MDC process. Once the appropriate temperature was reached the permeate cooler, circulating pumps and weighing balance were switched on. However, the temperature did fluctuate during the initial stages of the process as the temperature difference across the membrane was established. The average temperatures at module inlet on retentate and distillate sides were 29.8 ± 1.6 °C and 17.6 ± 4.4 °C, respectively. (the effect of temperature polarisation, cf. **Section 2.3.6.1**, was beyond the scope of this work, but could be a useful parameter to evaluate). The water flux was evaluated by measuring the amount of water extracted at time intervals during the course of the experiment according to Equation 3.1. The permeate conductivity was measured at random time intervals to ensure that there was no salt passing through the membrane, thus implying membrane wetting. The approximate Reynolds number

on the tube and shell sides were 448 and 2389, respectively, corresponding to calm and regular laminar flow.

3.2.1.1 Crystallisation of Epsomite

For the solution containing 375 g/ℓ of epsomite, the first visual appearance of crystals was observed after approximately 15 h of operation of the distillation plant. The crystals were sampled and immediately photographed (Figure 3.2) and it was seen that the salt crystallised in the typical orthorhombic geometry characteristic of epsomite crystals, at a concentration of 1.34 kg/ℓ. Figure 3.2 represents the crystal samples that were withdrawn at the indicated times after the first appearance of crystals together with the average length of the crystals in each sample. The crystal size distribution (CSD) was determined by evaluating the coefficient of variation, CV, for each crystal sample withdrawn. This parameter, which governs the shape of CSD, is defined in Equation 3.2.

$$CV = \frac{F_{80\%} - F_{20\%}}{2F_{50\%}} \times 100 \qquad [3.2]$$

where F is the cumulative crystal size distribution. Analysis of the experimental cumulative size distribution functions enabled CV values to be calculated and was found to be in the range of 10 – 30 %.

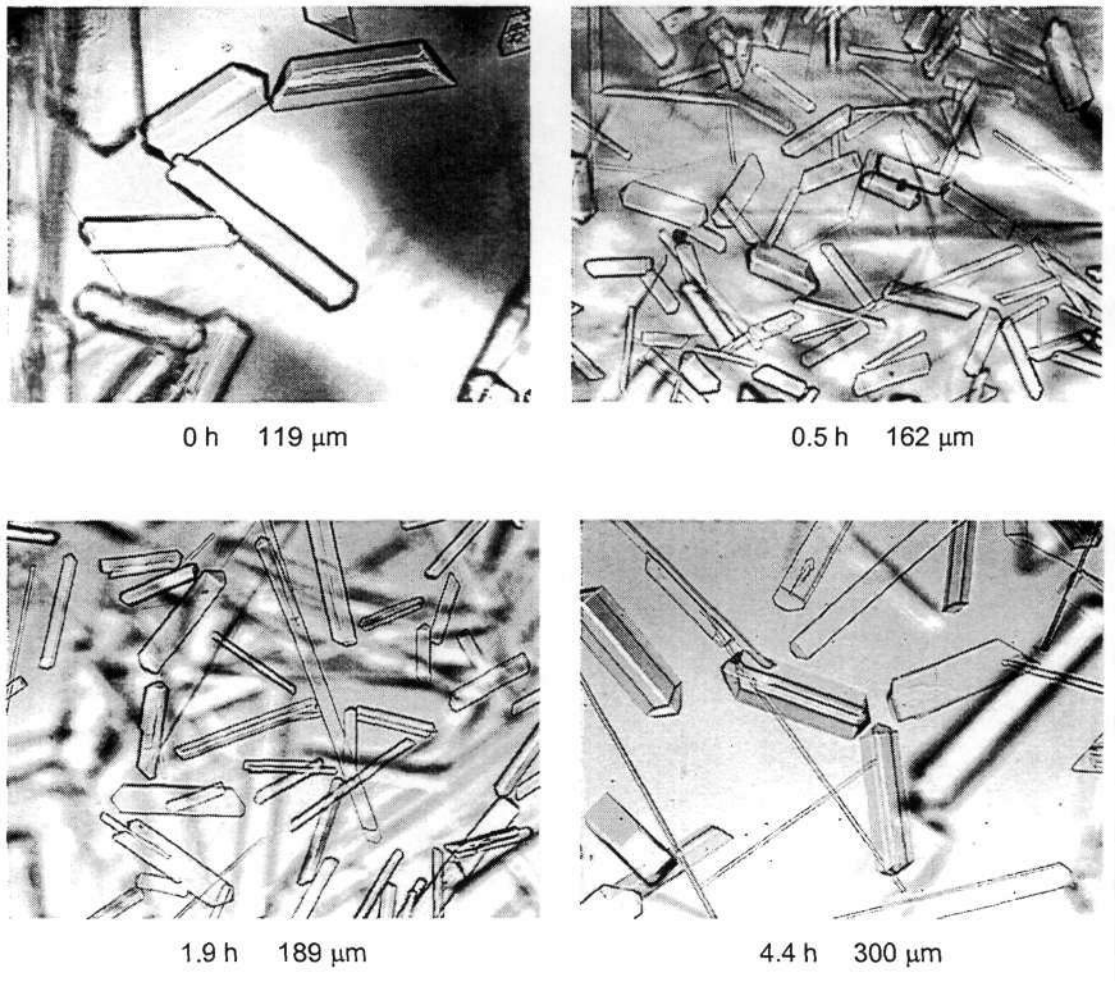

Figure 3.2: *Epsomite crystals obtained from the MDC of a single salt solution of initial concentration 375 g/ℓ, first sampled approximately 17 h from the start of the MD process. Concentration of magnesium sulphate at precipitation was 1.34 kg/ℓ. The average crystal size per sample is indicated. The indicated times refer to the sampling times after the first visual appearance of crystals*

The CSD for the crystallisation of epsomite (Figure 3.3) shows that the initial peak of the CSD progressively migrates towards increasing crystal size due to the crystal growth process. The indicated times (t) refer to the time intervals at which the crystals were sampled after the first visual appearance of crystals.

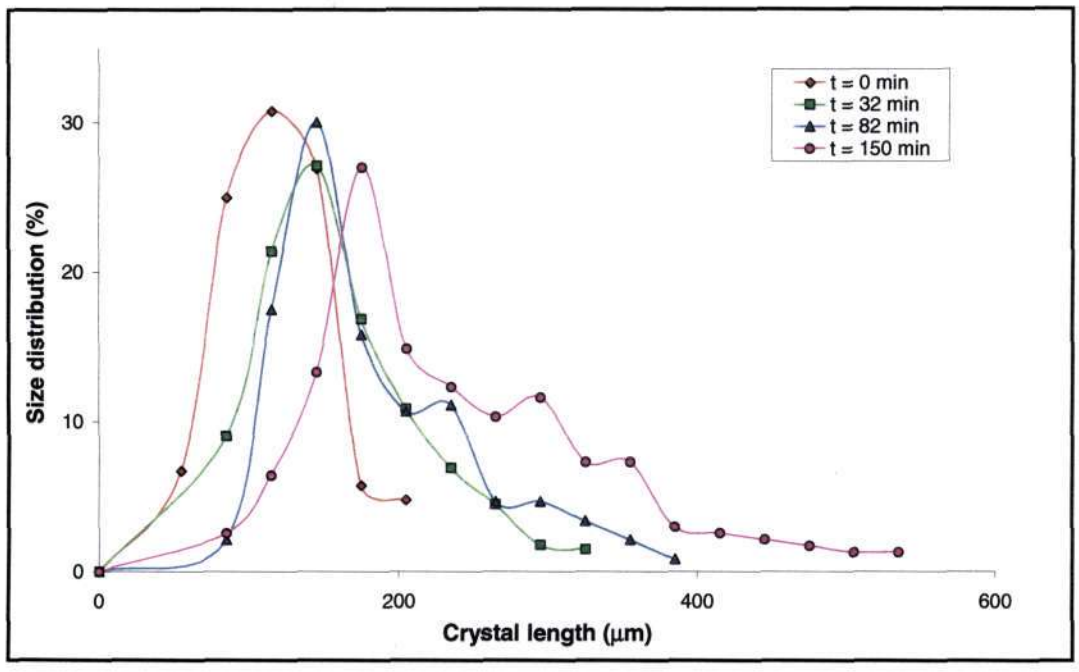

Figure 3.3: *Crystal size distribution for the crystallisation of a concentrated solution of magnesium sulphate of 375 g/ℓ using MDC. The indicated times refer to the experimental sampling times after the first visual appearance of crystals.*

From a plot of the average crystal length per sample against the sampling time, the crystal growth rate can be determined from the linear regression (Figure 3.4). A crystal growth rate of 38.8 $\mu mh^{-1} \equiv 1.08 \times 10^{-8}$ ms^{-1} was found for the crystallisation of epsomite. Furthermore, Figure 3.4 also indicates that the initial crystallisation occurred more than 3 h before the first crystals were detected. Al-Jibbouri et al. (2002) reported a growth rate of 2.82×10^{-7} ms^{-1} for the crystallisation of epsomite at 24 °C at a supersaturation of 0.64 g epsomite/100g H_2O. Ramalingom et al. (2003) showed that epsomite, in the presence of urea, crystallised at a rate of 1.85×10^{-8} ms^{-1} through seeded crystallisation. Drioli et al. (2004) reported a growth rate of 5×10^{-7} ms^{-1} of epsomite at 25 °C from a solution containing a mixture of salts representing that of seawater.

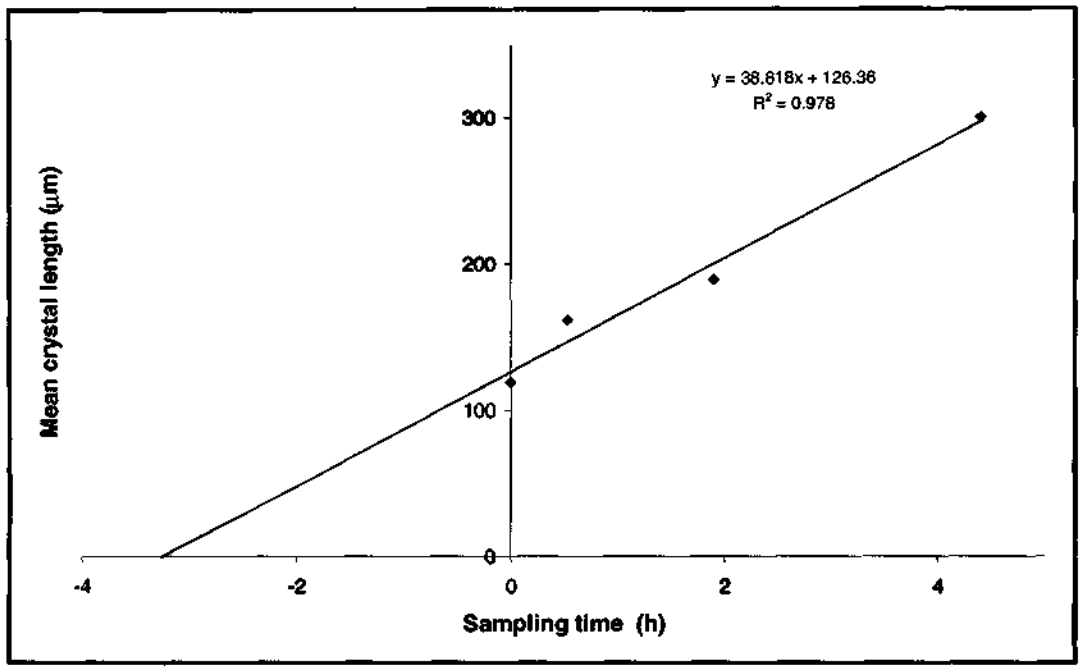

Figure 3.4: *Average length of crystals in sample at time of sampling from the start of crystallisation, to determine the crystal growth rate*

Apart from the highly concentrated solutions used in this work, the techniques and experimental conditions under which the mentioned crystallisations were performed differ from those used in this work. Therefore, the diminished growth rate observed in this work could be attributed to the fact that kinetics of crystallisation as well as crystal morphology is strongly related to the different components present in the crystallising solution, degree of supersaturation, temperature and hydrodynamic conditions. However, it is difficult to draw any meaningful conclusions from the comparison between the crystallisation rate observed in this study and those from the literature, because of the different composition of the solutions. For example, Al-Jibbouri et al. (2002) showed that the presence of NaCl in the crystallising solution tends to increase the growth rate of epsomite which explains the increased growth rate observed by Drioli et al. (2004) for the crystallisation of epsomite from a solution in which NaCl was present in an appreciable amount, as opposed to that observed in this experiment where epsomite existed alone in solution.

The flux for the distillation was evaluated and plotted as a function of elapsed time during the MD process (Figure 3.5). However, the flux trend could not be adequately evaluated as seen by the *gap* in the graph from 2 to 12 h of the MD process. The reason for this was that the

distillation was performed overnight, hence only a few data points were recorded during the first stages of the distillation and the majority of the data points were recorded during the final stages, just before and during the crystallisation.

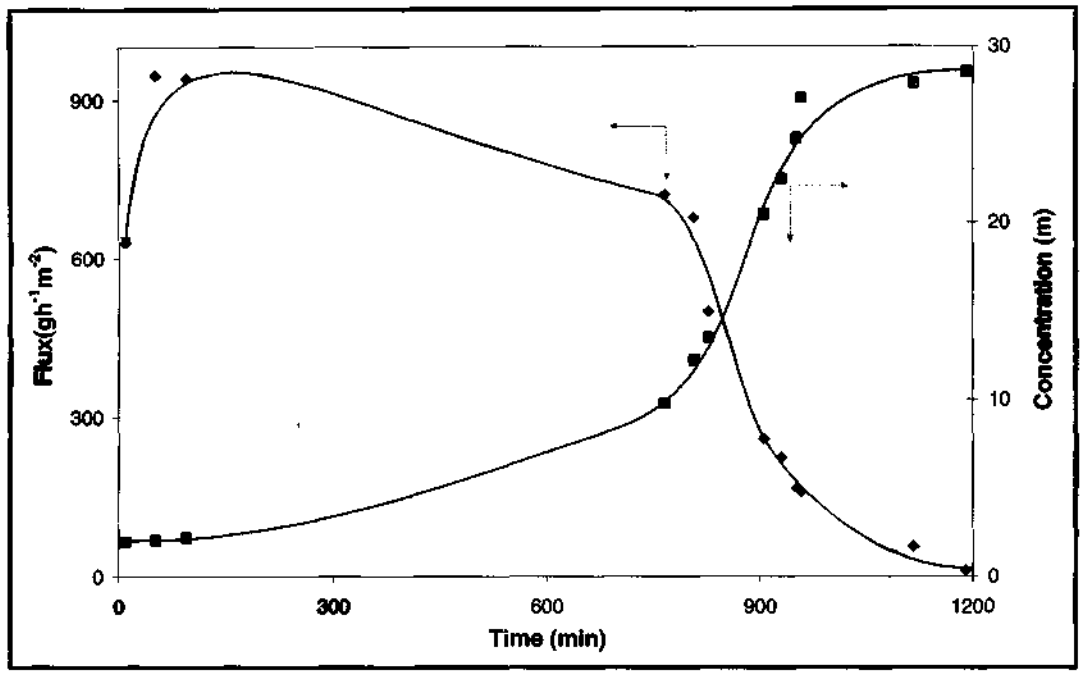

Figure 3.5: *Transmembrane flux and electrolyte concentration during MDC of magnesium sulphate of initial concentration 375 g/ℓ*

Nevertheless, the overall decrease in transmembrane flux with a concomitant rise in the electrolyte concentration until supersaturation and crystallisation is evident. The continual concentration of the solution through the extraction of water resulted in a decrease in the solution activity coefficient and hence a decrease in the vapour pressure of the solution. As a result the transmembrane flux, which is governed by the vapour pressure difference across the membrane, decreased during the process. This effect is more severe when one deals with solutions of high concentration (Sarti et al., 1985).

A second set of experiments was performed on a solution of epsomite of initial concentration of 625 g/ℓ. The operating conditions of the equipment were not changed. For this distillation process the transmembrane flux was evaluated, paying particular attention to the first portion of the experiment in order to *fill the gap* in Figure 3.5 and improve the understanding of the behaviour of the transmembrane flux before the onset of supersaturation and crystallisation.

The corresponding trend in transmembrane flux and electrolyte concentration with time is featured in Figure 3.6.

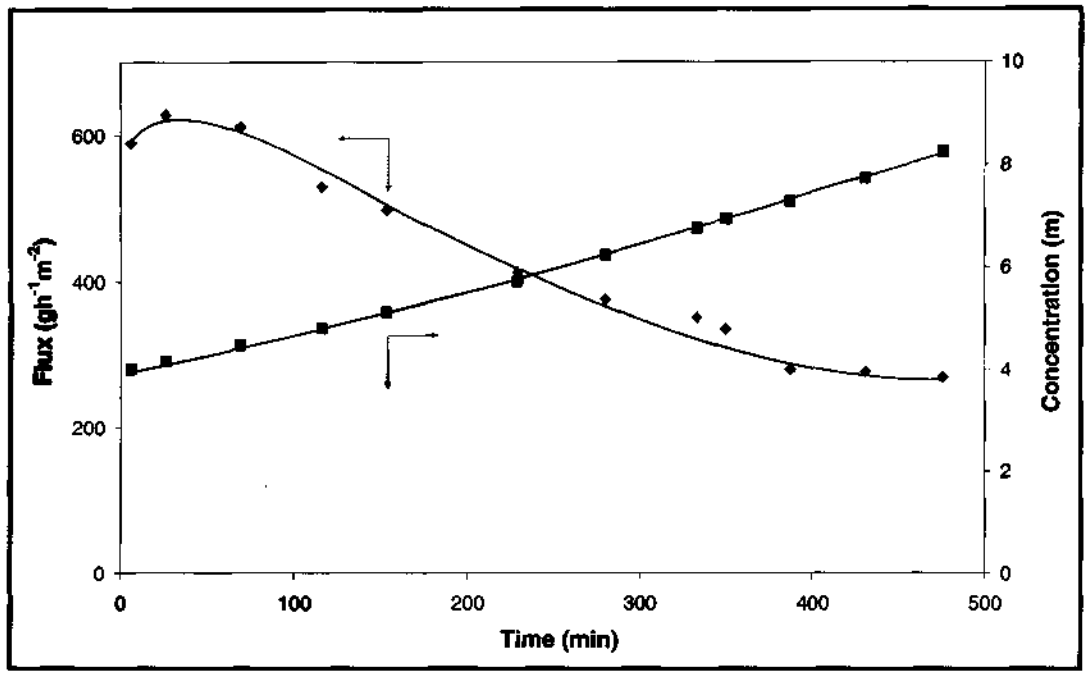

Figure 3.6: *Trend of transmembrane flux and concentration of magnesium sulphate during the first half of the MDC of a concentrated solution of magnesium sulphate of 625 g/ℓ*

The experiments were performed in a closed (non-continuous) membrane system evolving with time. At the beginning of the experimental run depicted in Figure 3.6 (and Figure 3.5), the brine heater, the permeate cooler and the circulating pumps for both streams were switched on. There was an initial rise in flux as the temperature difference across the membrane was established. Thereafter the flux declined as the brine concentration increased. Thus the initial rise in the flux that is observed in Figures 3.5 and 3.6 (and Figures 3.9, 3.11 and 3.12 below) is due to the stabilisation of concentration and temperature profiles as well as fluid dynamic conditions inside the membrane module. In Figure 3.6 from an initial value of approximately 600 $gh^{-1}m^{-2}$, the water flux progressively decreased in accordance with the increase of solution concentration and the consequent decrease of the solution activity coefficient. After the solution had been concentrated to supersaturation, i.e. once a metastable phase had been formed, the global reduction in transmembrane flux was evaluated at approximately 52 %. Furthermore, the salinity increase displays a linear increase at a rate of 39.1 g/ℓ/h. As exhibited by Figure 3.6,

after this metastable stage and crystal disengagement, the transmembrane flux decreases rapidly reaching a zero value as observed in Figure 3.5. In general, it is typical that when a crystallisation run is carried out in a batch concentration mode i.e. the retentate line is not continuously replenished with fresh feed solution, the flux will decrease with time (once the system has stabilised) as the solution becomes more concentrated (Crisuoli and Drioli, 1999 and Drioli et al., 2004). This has been variously attributed to the growth of crystals on the membrane thus blocking the membrane pores (Tun et al., 2005) and to the reduction of the vapour pressure gradient due to the increase of the concentration of salts in the solution (Drioli et al., 2004). Knowledge of the vapour pressures of the salt solutions, and hence the driving force during the distillation process, will highly facilitate a deeper and more rigorous understanding of the latter postulation. Furthermore, some crystal deposition was seen to form within the pipes (and suspected to form on the membrane surface as well) after crystal disengagement began as the crystals were re-circulated to the membrane module. This is thought to be an added factor to flux decline as established by Tun et al. (2005).

3.2.2 Mixed Electrolyte System

During the series of mixed electrolyte system experiments, solutions of magnesium sulphate and sodium chloride were prepared and subject to MDC, which aimed at the crystallisation of only sodium chloride. Aqueous solutions of analytical grade magnesium sulphate heptahydrate ($MgSO_4.7H_2O$) and sodium chloride were prepared in mass ratios of 1:1, 1:2 and 1:3, respectively, with initial concentrations of 225 g/ℓ of $MgSO_4$ and NaCl for the 1:1 mix (i.e. 1.16 and 4.89 m, respectively); 138 g/ℓ and 275 g/ℓ of $MgSO_4$ and NaCl (i.e. 0.686 and 5.78 m), respectively, for the 1:2 mix; and 93 g/ℓ and 280 g/ℓ of $MgSO_4$ and NaCl (i.e. 0.451 and 5.72 m), respectively for the 1:3 mix. These were fed into the distillation plant, the conditions of which, and characteristics of the membrane module, being the same as that described in **Section 3.1**. The average temperatures at module inlet on retentate and distillate sides for the 1:1 mix was 32.6 ± 1.7 °C and 16.0 ± 0.5 °C, respectively; for the 1:2 mix 32.6 ± 1.2 °C and 16.8 ± 0.4 °C, respectively; and for the 1:3 mix 33.6 ± 2.6 °C and 14.8 ± 0.5 °C, respectively. The average temperatures at module outlet on retentate and distillate sides for the 1:1 mix was 29.3 ± 1.4 °C and 16.9 ± 0.7 °C, respectively; for the 1:2 mix 30.5 ± 1.0 °C and 17.4 ± 0.7 °C, respectively; and for the 1:3 mix 27.6 ± 1.0 °C and 16.1 ± 0.6 °C, respectively. The water flux was evaluated and samples were routinely withdrawn from the crystallisation tank and visually examined and photographed.

3.2.2.1 Crystallisation of Sodium Chloride

For the 1:1, 1:2 and 1:3 mixes, the first visual appearance of crystals was observed after approximately 8, 13 and 17 h of operation of the membrane distillation equipment, respectively. The crystals were sampled and photographed as shown in Figure 3.7. Although, the general trend in the crystal geometry seems to follow the characteristic cubic geometry typically displayed by sodium chloride crystals, there does, however, in some instances seem to appear a distortion of the crystal geometry exemplified by an elongation of the crystal shape.

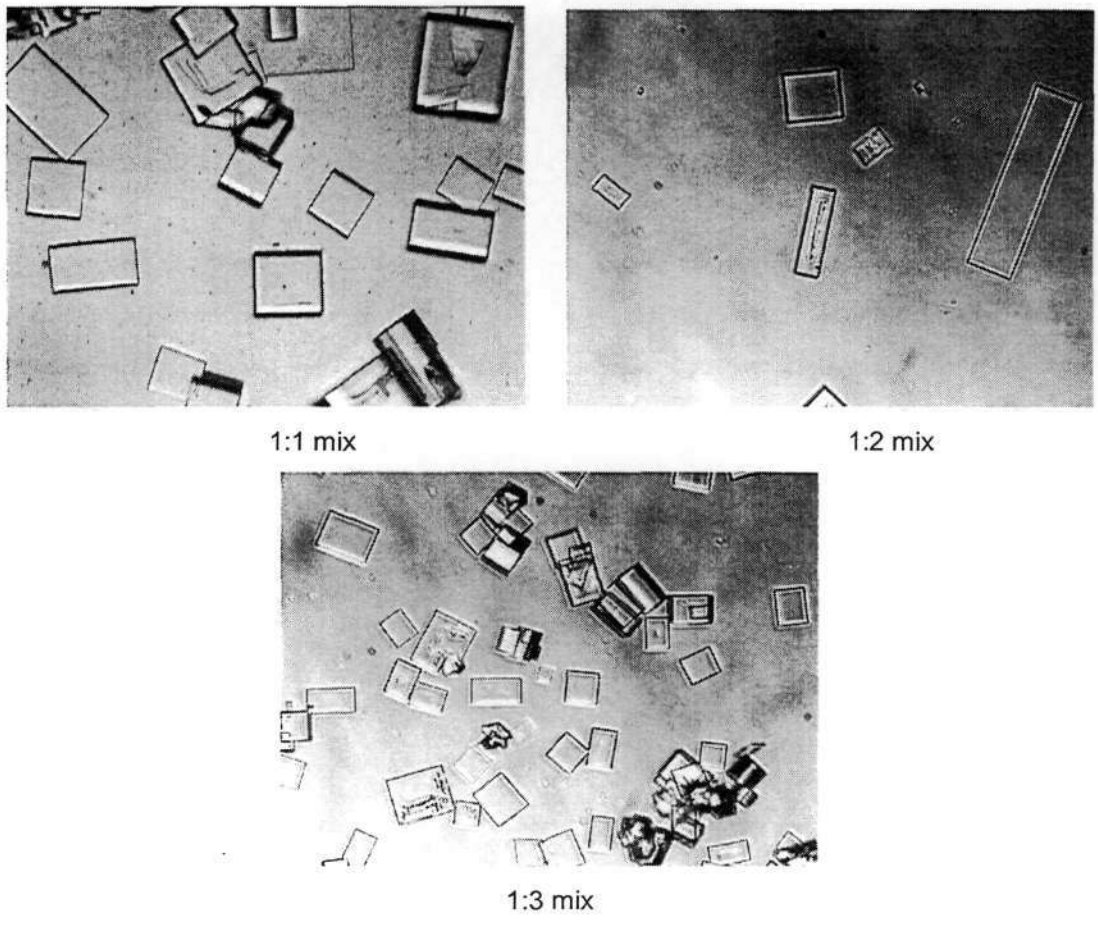

Figure 3.7: *Sodium chloride crystals obtained from a mixed salt system of varying ratios of sodium chloride and magnesium sulphate as indicated* (25 X)

It was noted that this effect is more intense for the 1:2 mix whereas the 1:3 mix shows less distortion of crystal geometry. The 1:1 mix, however, lies in the middle of these two extremes as can be seen from the crystal size distribution of samples taken approximately 1 h from the start of crystallisation of each of the mixes (Figure 3.8).

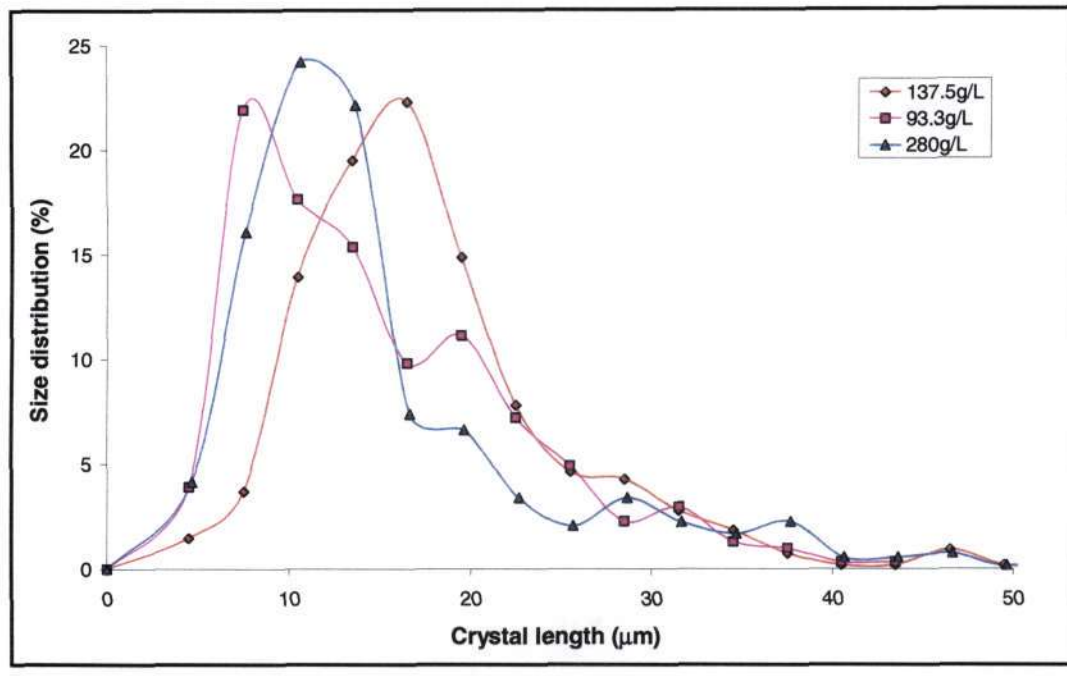

Figure 3.8: *Evolution of crystal size distribution for the crystallisation of sodium chloride with increasing amounts of magnesium sulphate in solution.*

Again, as described in **Section 3.2.1.1,** this change in morphology of the crystal structure is attributed to the fact that crystal kinetics and morphology is strongly affected by other components present in the crystallising solution (Al-Jibbouri and Ulrich, 2001 and 2002). The authors studied the effect of $MgCl_2$ on the crystallisation kinetics of sodium chloride in a fluidised bed crystalliser. They found that the solubility of NaCl is reduced with increasing amount of $MgCl_2$ in the solution. Furthermore, the growth rate of the NaCl crystals is also inhibited; being more pronounced at high $MgCl_2$ concentrations. This offers a plausible explanation of the increase in times of solution supersaturation and onset of crystallisation of NaCl as the concentration of magnesium sulphate in the solution is increased, i.e. as we move from the 1:1 mix to the 1:3 mix the time of the first visual appearance of crystals is lengthened. The authors did not specify the effect of *impurities* on the morphology of the NaCl crystals. However, it is known that significant changes in ionic strength could effect the growth of the

crystal and its morphology (Davey and Garside, 2000). Furthermore, this change in crystal shape could merely be just a change in *external* shape but not necessarily a change in the *crystal lattice*, i.e. the crystal still displays cubic geometry with the same space group. This can only be verified by performing a crystal structure analysis of each of the crystals either by Xray crystallography or powder diffraction to examine the crystal lattice and point group of these *different* crystal shapes.

The fluxes for each of the runs were evaluated and are shown, together with the concentration of the salts, in molality units, for the three mixes in Figures 3.9, 3.11 and 3.12. The overall trend of an initial rise in the flux, followed by gradual decline, is generally observed in Figures 3.9, 3.11 and 3.12.

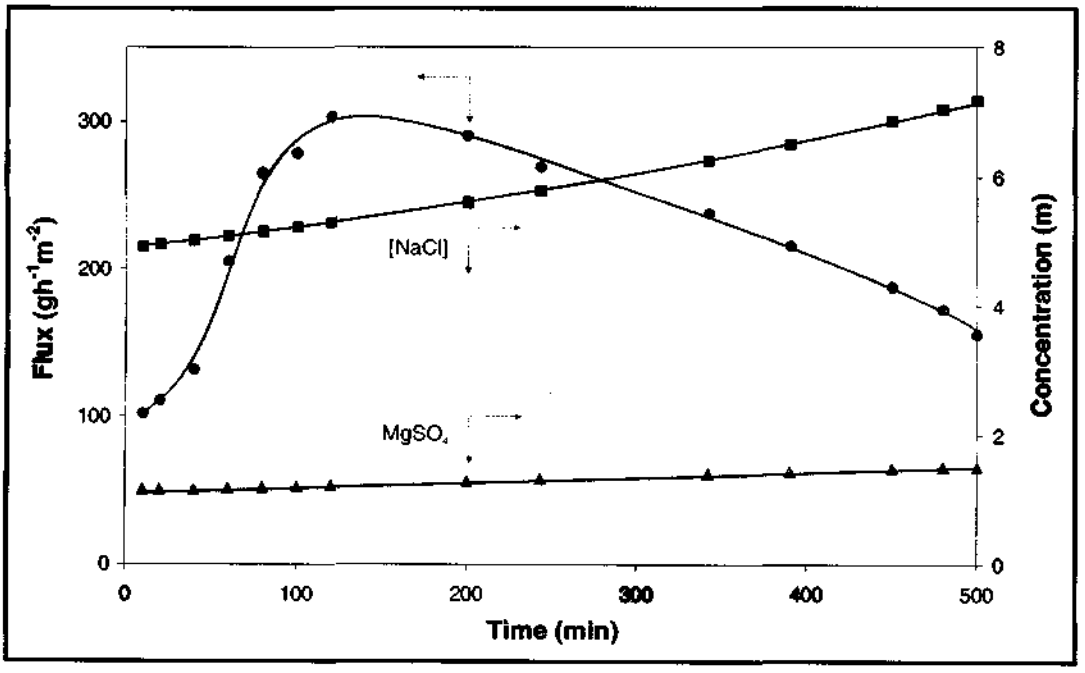

Figure 3.9: *Trend of transmembrane flux and concentration of salts during the course of the MDC of the 1:1 mix*

The initial rise is again due to the stabilisation of the temperature and concentration profiles at the beginning of the experiment as described above. Figure 3.10 shows the temperature profile for the distillation run for the 1:1 mix. As can be seen, there is a slight increase in the temperature at the beginning of the distillation therefore causing a rise in the transmembrane flux, where after it begins to plateau off.

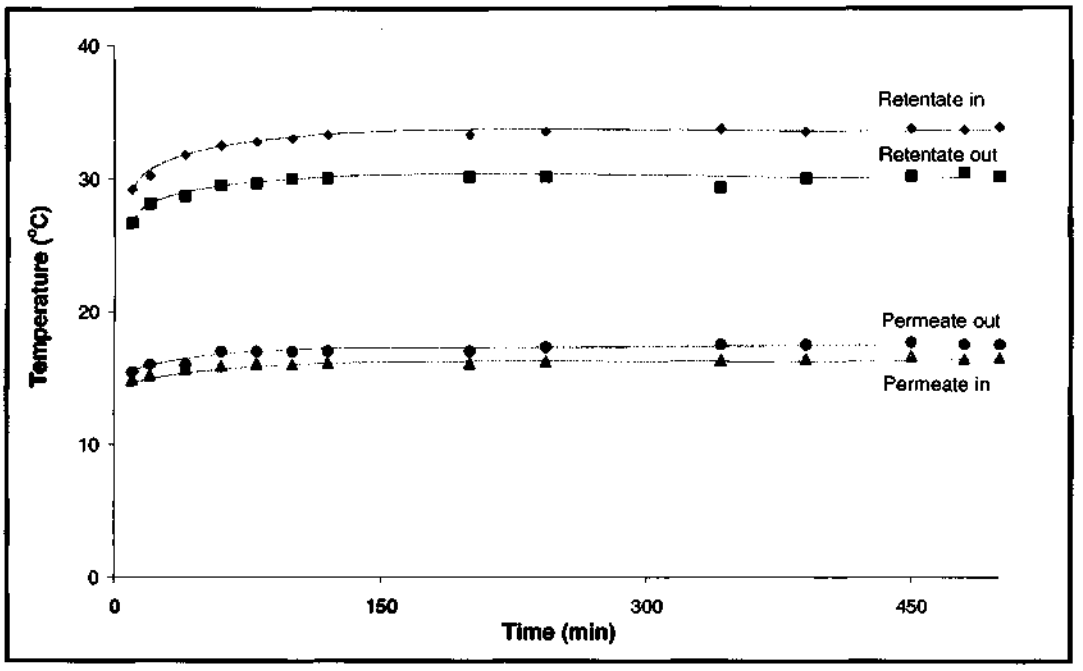

Figure 3.10: *Temperature profile for the 1:1 mix during the MD process*

The reduction in transmembrane flux for the 1:1 mix, from the highest flux of 303 $gh^{-1}m^{-2}$ that was reached after 2 h of operation, is approximately 49 %. The rate of salinity increase for each salt displayed a linear trend, up to the metastable state, of 0.26 kg of NaCl/kg of H_2O/h and 0.19 kg of $MgSO_4.7H_2O$/kg of H_2O/h.

For the 1:2 mix (Figure 3.11), the reduction in transmembrane flux, from the highest flux of 315 $gh^{-1}m^{-2}$ that was reached after 1.7 h of operation of the distillation plant was approximately 30 %. The salinity increases were calculated as 0.24 kg of NaCl/kg of H_2O/h and 0.11 kg of $MgSO_4.7H_2O$/kg of H_2O/h.

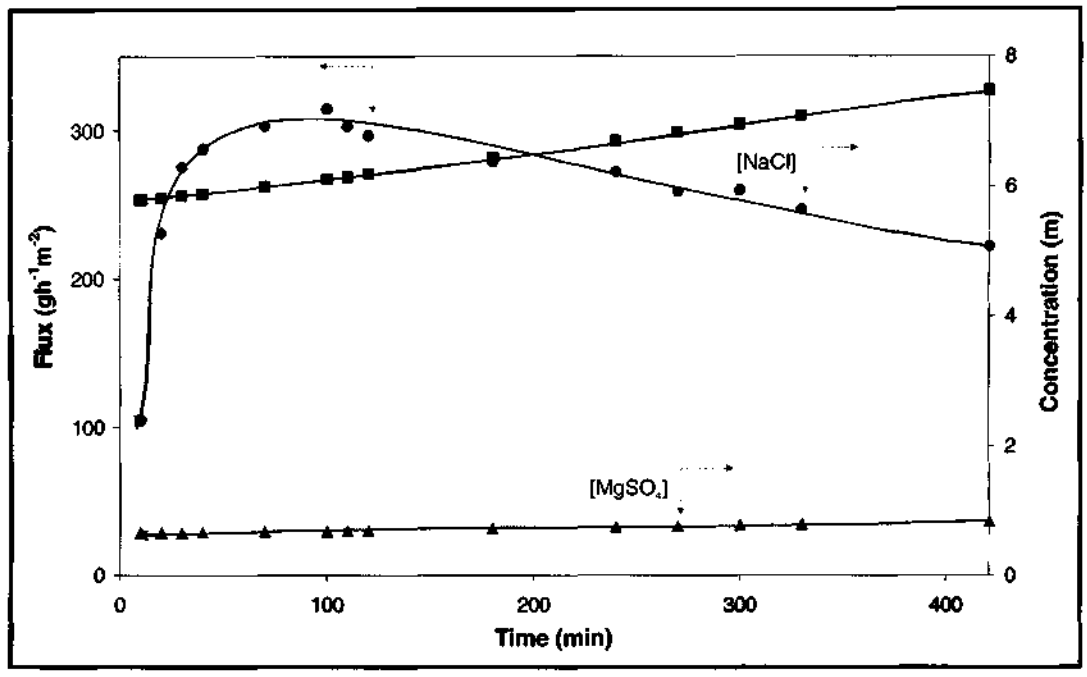

Figure 3.11: *Trend of transmembrane flux and concentration of salts during the course of the MDC of the 1:2 mix*

The transmembrane flux for the 1:3 mix (Figure 3.12) was reduced by 60 % from its highest value of 278 $gh^{-1}m^{-2}$ that was reached after 3 h of operation of the distillation plant. The salinity increases were of the order 0.12 kg of NaCl/kg of H_2O/h and 0.04 kg of $MgSO_4.7H_2O$/kg of H_2O/h.

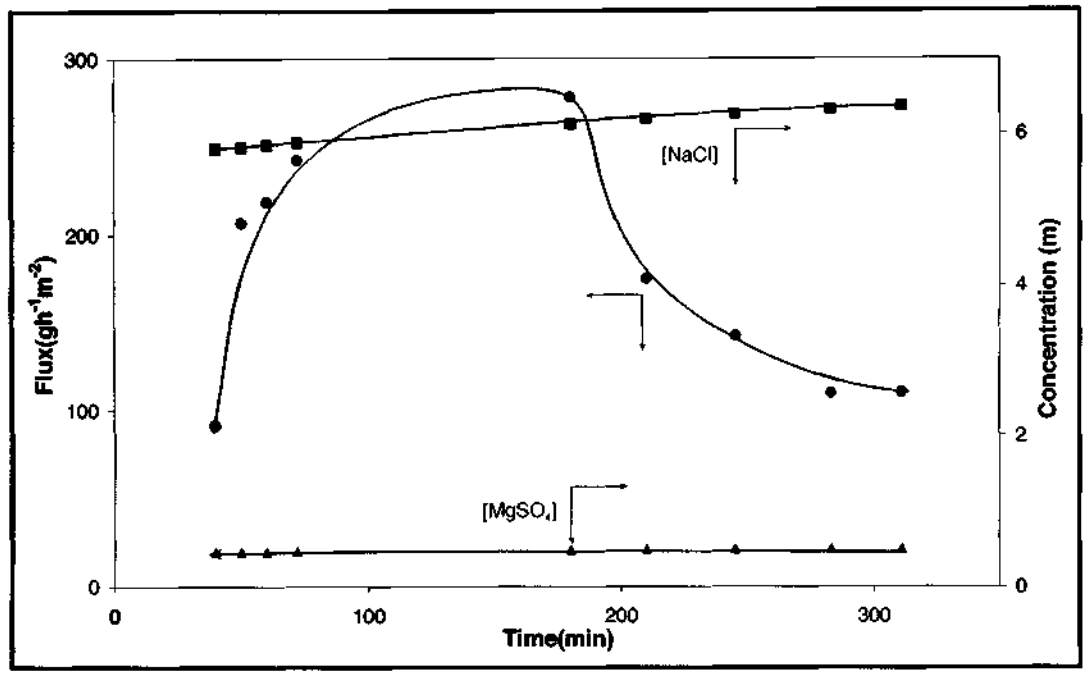

Figure 3.12: *Trend of transmembrane flux and concentration of salts during the course of the MDC of the 1:3 mix*

The characteristic trend of decreasing transmembrane flux will be investigated by examining the vapour pressure driving force for the MD process to see if these two relationships could be correlated. This is discussed in Chapter 5 of this thesis.

3.3 CONCLUSIONS

The MDC technique has proved successful for the recovery of solid products from concentrated salt solutions. Due to the characteristics described in Chapter 2, this process overcomes many shortcomings of conventional purification and crystallisation processes. A maximum temperature of only 33 °C on the retentate line and a minimum of approximately 17 °C on the distillate line was necessary to afford a significant vapour pressure difference and hence driving force for the separation. Furthermore, pure water was produced with the recovery of crystalline product without the need for additional applied pressure or elevated temperature gradients. However, one of the main shortcomings of this process as seen above, is the rapid decline in flux that is observed after the metastable phase, when crystallisation occurs. This flux decline prevents the concentration process from proceeding after the initial crystallisation has commenced. The flux could be more accurately evaluated if knowledge of the vapour pressures

of the solutions was possible. This would enable the assessment of the process on the basis of the driving force and improve the predictability of the separation. Therefore it becomes crucial to be able to evaluate the vapour pressures of the solutions. However, this determination cannot be performed during the experiment itself. Furthermore, the chemistry of strong electrolytes is complicated and the evaluation of the activity coefficient of these systems leads one to encountering a series of complex thermodynamic models.

3.4 CHAPTER REFERENCES

AL-JIBBOURI S and ULRICH J (2001) *The influence of impurities on crystallisation kinetics of sodium chloride.* Cryst Res Technol **234** (12) 1365-1375.

AL-JIBBOURI S and ULRICH J (2002) *The growth and dissolution of sodium chloride in a fluidized bed crystallizer.* J Cryst Growth **234** 237-246.

AL-JIBBOURI S, STREGE C and ULRICH J (2002) *Crystallization kinetics of epsomite influenced by pH-value and impurities.* J Cryst Growth **236** 400-406.

CRISCUOLI A and DRIOLI E (1999) *Energetic and exergetic analysis of an integrated membrane desalination system.* Desalination **124** 243-249.

DAVEY RJ and GARSIDE J (2000) *From molecules to crystallisers.* Oxford University Press Inc., New York. ISBN: 0 19 850489 6.

DRIOLI E, CURCIO E, CRISCUOLI A and DI PROFIO G (2004) *Integrated system for recovery of $CaCO_3$, NaCl and $MgSO_4.7H_2O$ from nanofiltration retentate.* J Membr Sci **239** 27-38.

RAMALINGOM S, PODDER J, NARAYANA S and BOCELLI G (2003) *Habit modification of epsomite in the presence of urea.* J Cryst Growth **247** 523-530.

SARTI GC, GOSTOLI C and MATULLI S (1985) *Low energy cost desalination processes using hydrophobic membranes.* Desalination **56** 277-286.

TUN CM, FANE AG, MATHIECKAL JT and SHEIKHOLESLAMI R (2005) *Membrane distillation crystallization of concentrated salts – flux and crystal formation.* J Membr Sci **257** 144-147.

CHAPTER 4

Chapter 4

HIGH IONIC STRENGTH ELECTROLYTE MODELLING

Knowledge of the thermodynamic properties, such as activity and osmotic coefficients, of the components in a system is essential in any chemically related field. This chapter therefore provides an overview of the methods that are available for the modelling of electrolytes systems, particularly focussing on high ionic strength electrolyte systems. In Section 4.1 the theoretical equations concerning the calculation of osmotic and activity coefficients of high ionic strength solutions are described together with an evaluation of the shortcomings of certain models and suitability of others for modelling these systems. The Pitzer approach appears to be the most suitable for modelling of high ionic strength electrolyte systems. Section 4.2 describes the geochemical equilibrium computer model known as PHRQPITZ which uses the Pitzer virial coefficient approach for calculation of activity coefficients in brines and other related systems. The features and ability of this program for modelling high ionic strength systems are described.

4.1 THERMODYNAMICS OF HIGH IONIC STRENGTH SOLUTIONS

In subjects such as sea water desalination, solution crystallisation, extractive distillation, geothermal energy recovery, chemical oceanography, pulp and paper chemistry and prediction of vapour-liquid equilibrium data in systems containing salts, knowledge on the solubility of the electrolytes is essential (Anderko et al., 2002, Das, 2003 and Hu and Guo, 1999). In order to ascertain these solubility predictions, thorough knowledge of the principle thermodynamic properties, such as the chemical speciation and osmotic and activity coefficients, is mandatory. Failure to do so could lead to large errors when predicting the solubility in aqueous multicomponent ionic solutions of high ionic strength, irrespective if only a few chemical species are present in the solution. For this purpose, there is a growing interest in the determination of activity coefficients and solubility data of electrolytes in solutions.

There have been extensive experimental and theoretical investigations into the thermodynamic properties of aqueous electrolytes. Literature provides various models for the determination of these thermodynamic properties (Anderko et al., 2002, Bromley, 1973, Davies, 1938, Guggenheim and Turgeon, 1954, Hu and Guo, 1999, Meissner et al., 1972, Meissner and Kusik, 1972, Meissner and Tester, 1972, Pitzer, 1973 and Wang et al., 2002 and 2004). Most of these models are based on work performed by Debye and Hückel (1923) on the thermodynamic properties of electrolyte solutions. The formulae derived by Debye and Hückel were based on the model of rigid ions, all of which were assumed to have equal diameters. The Debye-Hückel Limiting Law calculates the mean activity coefficient, $\gamma_{\pm}$, according to Equation 4.1,

$$\log_{10}\gamma_{\pm} = -z_{+}\,|\,z_{-}\,|\,B_{I}\sqrt{I} \qquad [4.1]$$

where, B_I is a quantity that depends on properties such as molar absorptivity and temperature, z is the charge on the ion and I is the ionic strength of the solution and is described according to Equation 4.2,

$$I = \frac{1}{2}\sum_{i} c_i z_i^2 \qquad [4.2]$$

where c_i is the molar concentration of the ions of type i (Laidler and Meiser, 1999). The limiting law depends only on the valences of the ions, the temperature and dielectric constant of the solvent. However, in concentrated solutions the sizes of the ions and their effects on the dielectric constants must be taken into accounted (Scatchard, 1936). If the theory is modified to account for the space occupied by the ions by assuming that the ions are restricted to a distance a between them, then Equation 4.1 is modified to Equation 4.3,

$$\log_{10}\gamma_{\pm} = -\frac{z_{+}\,|\,z_{-}\,|\,B_{I}\sqrt{I}}{1+aB_{I}'\sqrt{I}} \qquad [4.3]$$

where B_I' is the new constant. Furthermore one needs to take into account the orientation of solvent molecules by the ionic atmosphere (Equation 4.4),

$$\log_{10}\gamma_{\pm} = -\frac{z_{+}\,|\,z_{-}\,|\,B_{I}\sqrt{I}}{1+aB_{I}'\sqrt{I}} + C_{I}I \qquad [4.4]$$

where C_I is a constant and the term $C_I I$, known as the *salting-out* term, which dominates at high ionic strengths thus accounting for the lowered solubility of salts under these concentrations (Laidler and Meiser, 1999). Equation 4.4 is known as the extended Debye-Hückel formula. The application of the extended Debye-Hückel equation to binary systems (e.g. NaCl in H_2O) has been well studied by Robinson (1965). They found reasonable agreement to ionic strengths of up to 1 m. However, the use of this model for more complex systems of higher ionic strength has been found to be inadequate (Harvie and Weare, 1980). For this reason numerous attempts were made in order to establish equations to fit the high ionic strength behaviour of brines. One of the most primitive attempts for mixed electrolyte systems was the Brönsted-Guggenheim specific interaction model. This approach, proposed by Guggenheim (1935) based on Brönsted's (1922) principle of specific interaction, appears to be theoretically and experimentally consistent, and is an extension of the Debye-Hückel limiting law for mixed electrolytes by using a second virial expansion of the activity coefficient. In the Brönsted-Guggenheim model the second virial coefficient was included to account for the short range forces that are experienced by pairs of ions of opposite charge as well as the solvent structure (Harvie and Weare, 1980). The general form for the activity coefficient, γ_{MX}, and the osmotic coefficient, ϕ, for a mixed electrolyte is shown in Equations 4.5.

$$\ln \gamma_{MX} = -\frac{A_\gamma \mid z_M z_X \mid I^{\frac{3}{2}}}{1+I^{\frac{1}{2}}} + \frac{2\nu_M}{\nu_M+\nu_X}\sum_a m_a \beta_{Ma} + \frac{2\nu_X}{\nu_M+\nu_X}\sum_c m_c \beta_{cX} \qquad [4.5a]$$

$$\phi - 1 = \left(\sum_c m_c + \sum_a m_a\right)^{-1}\left[-2A_\phi I^{\frac{3}{2}}\sigma\left(I^{\frac{1}{2}}\right)\right] + \sum_c\sum_a m_c m_a \beta_{ca} \qquad [4.5b]$$

where ν_M and ν_X are the numbers of ions in the formula, m is the conventional molality and the sums cover all cations c and all anions a. The function $\sigma(x)$ and the Debye-Hückel parameters A_γ and A_ϕ, have the form shown in Equations 4.6.

$$\sigma(x) = \left(\frac{3}{x^3}\right)\left\{1 + x - \left[\frac{1}{(1+x)}\right] - 2\ln(1+x)\right\} \qquad [4.6a]$$

$$A_\phi = \frac{1}{3}\left(\frac{2\pi N_0 d_w}{1000}\right)^{\frac{1}{2}} l^{\frac{3}{2}}$$

$$\text{where } l = \frac{e^2}{D_w kT} \qquad [4.6b]$$

$$A_\gamma = 3A_\phi$$

A_γ and A_ϕ are the Debye-Hückel coefficients for the activity and osmotic functions, respectively, N_0 Avagadro's number and d_w and D_w are the density and dielectric constant of water at 25 °C, respectively. ℓ is a parameter which expresses the distance at which the electrostatic energy for singly charged ions in the dielectric just equals thermal energy (Pitzer, 1973). The parameters β are constants at a given temperature.

For single 1-1 electrolytes, Equations 4.5 takes the form of Equations 4.7 below.

$$\ln\gamma = -\left[\frac{A_\gamma m^{\frac{1}{2}}}{1+m^{\frac{1}{2}}}\right] + 2\beta_{MX} m \qquad [4.7a]$$

$$\phi - 1 = -A_\phi m^{\frac{1}{2}} \sigma\left(m^{\frac{1}{2}}\right) + \beta_{MX} m \qquad [4.7b]$$

Guggenheim and Turgeon (1954) demonstrated that Equations 4.7 were in good agreement with experiment data up to concentrations of 0.1 m for 1-1 electrolytes in water at 0 °C and room temperature. However, above these concentrations considerable discrepancies occur. For mixed electrolyte systems, the work of Whitfield (1973 and 1974) confirmed that this theory is accurate for concentrations up to 4 m. However, for concentrations above 4 m Scatchard (1968), Scatchard et al. (1970) and Pitzer (1973) demonstrated that third or higher order virial coefficients must be included to account for the short range potential between like-charged ions and solvent structure which become important at significantly high concentrations. Mayer (1950) suggested that the virial expansion will result in Equation 4.4 taking the form of,

$$\ln\gamma_i = \ln\gamma_{DH} + \sum_j B_{ij}(I) m_j + \sum_{jk} C_{ijk}(I) m_j m_k + \ldots \qquad [4.8]$$

where $B_{ij}(I)$ and $C_{ijk}(I)$ are the second and third virial coefficients respectively, and $ln\gamma_{DH}$ is the Debye-Hückel coefficient from Equation 4.4. Harvie and Weare (1980) demonstrated that second and third virial coefficients are essential to predict mineral solubilities and thermodynamically stable paragenesis. For this reason the Pitzer equation seems to be the most appropriate choice to model high ionic strength electrolyte systems.

The Pitzer approach begins with a virial expansion of the excess free energy and takes the form of Equation 4.6. This approach is used because, in order to predict mineral solubilities knowledge of the osmotic and activity coefficients is required. However, these quantities are not independent and must be consistent with the laws of thermodynamics (Harvie and Weare, 1980). The excess free energy, G_{ex}, is the difference in the actual free energy and the free energy of an ideal solution of the same composition.

$$\frac{G_{ex}}{RT} = n_w\left[f(I) + \sum_i \sum_j \lambda_{ij}(I) m_i m_j + \sum_i \sum_j \sum_k \mu_{ijk} m_i m_j m_k \right] \quad [4.9]$$

where n_w is the mass of water, m_i and m_j the molality of species i and j, respectively, $f(I)$ is the Debye-Hückel type term and $\lambda_{ij}(I)$ and μ_{ijk} are the second and third virial coefficients respectively. $\lambda_{ij}(I)$ represents short-range interaction in the presence of the solvent between solute particles i and j. This second virial coefficient parameter, for ions, depends on ionic strength, the type of solute species i and j, and the temperature and pressure. For neutral species however, there is no composition dependence (Pitzer, 1991). The third virial coefficient parameter μ_{ijk}, in principle should be ionic strength dependent, but there is no experimental verification for this observation (Pitzer, 1991). The derivative of Equation 4.9, with respect to the number of moles of each component, results in expressions for the osmotic and activity coefficients. Since the functionality $\lambda_{ij}(I)$ cannot be determined experimentally, but sums and differences of λ's are measurable, Equation 4.9 is re-written in terms of the sums and differences of the measurable quantities λ's and μ's. Therefore in the Pitzer ion interaction model the fundamental equations for the osmotic coefficient, ϕ and activity coefficients, γ_M and γ_X, for cations and anions respectively, in a mixed electrolyte system, are given in Equations 4.10 (Harvie and Weare, 1980, Pitzer, 1973, Pitzer, 1991 and Plummer et al., 1988). The equations considered below are for those in mixtures of strong electrolytes, as is the case of this work.

$$(\phi-1)=\frac{2}{\left(\sum_i m_i\right)}\left\{\begin{array}{l}-\dfrac{A^{\phi}I^{3/2}}{1+bI^{1/2}}+\sum_c\sum_a m_c m_a\left(B^{\phi}_{ca}+ZC_{ca}\right)+\\ \sum_{c<c'}\sum m_c m_{c'}\left(\Phi^{\phi}_{cc'}+\sum_a m_a\psi_{cc'a}\right)+\\ \sum_{a<a'}\sum m_a m_{a'}\left(\Phi^{\phi}_{aa'}+\sum_c m_c\psi_{aa'c}\right)\end{array}\right\} \qquad [4.10a]$$

$$\ln\gamma_M = z_M^2F+\sum_a m_a\left(2B_{Ma}+ZC_{Ma}\right)+\sum_c m_c\left(2\Phi_{Mc}+\sum_a m_a\psi_{Mca}\right)+\sum_{a<a'}\sum m_a m_{a'}\psi_{aa'M}+ |z_M|\sum_c\sum_a m_c m_a C_{ca} \qquad [4.10b]$$

$$\ln\gamma_X = z_X^2F+\sum_c m_c\left(2B_{cX}+ZC_{cX}\right)+\sum_a m_a\left(2\Phi_{Xa}+\sum_c m_c\psi_{Xac}\right)+\sum_{c<c'}\sum m_c m_{c'}\psi_{cc'X}+ |z_X|\sum_c\sum_a m_c m_a C_{ca} \qquad [4.10c]$$

where m_c is the molality of cation c with charge z_c. The subscripts M, c and c' refer to cations and X, a and a' anions. The summation index c refers to the sum over all cations and the double summation index $c<c'$ the sum over all distinguishable pairs of dissimilar cations; similarly, for the anions. The other quantities have the form as shown in Equations 4.11 to 4.13.

The quantity F includes the Debye-Hückel terms amongst others as shown by Equation 4.11a.

$$F=-A^{\phi}\left[\frac{\sqrt{I}}{1+b\sqrt{I}}+\frac{2}{b}\ln\left(1+b\sqrt{I}\right)\right]+\sum_c\sum_a m_c m_a B'_{ca}+\sum_{c<c'}\sum m_c m_{c'}\Phi'_{cc'}+\sum_{a<a'}\sum m_a m_{a'}\Phi'_{aa'} \qquad [4.11a]$$

and A^{ϕ} has been defined in Equation 4.6b. A^{ϕ} is 0.392 for water and b is a universal empirical parameter assigned to be 1.2 at 25 °C.

The coefficients B_{MX} are functions of ionic strength and are defined as,

$$\begin{aligned} B^{\phi}_{MX} &= \beta^{(0)}_{MX} + \beta^{(1)}_{MX} e^{-\alpha\sqrt{I}} \\ B_{MX} &= \beta^{(0)}_{MX} + \beta^{(1)}_{MX} g\left(\alpha\sqrt{I}\right) \\ B'_{MX} &= \beta^{(1)}_{MX} g'\left(\alpha\sqrt{I}\right)/I \end{aligned} \qquad [4.11b]$$

where g and g' are,

$$\begin{aligned} g(x) &= \frac{2\left[1-(1+x)e^{-x}\right]}{x^2} \\ g'(x) &= \frac{-2\left[1-\left(1+x+\frac{1}{2}x^2\right)e^{-x}\right]}{x^2} \end{aligned} \qquad [4.11c]$$

and $x = \alpha\sqrt{I}$.

The remaining terms in Equations 4.10 contain either single electrolyte third virial coefficients, C_{MX}, or mixed electrolyte coefficients, Φ_{ij} and ψ_{ijk}. The latter two terms account for interactions of like sign. Z is a concentration dependence function.

$$Z = \sum_i m_i |z_i| \qquad [4.12]$$

The parameters Φ_{ij} and ψ_{ijk} are determined from aqueous mixtures of two salts. Φ_{ij} accounts for like-charge interactions, cation-cation and anion-anion, while ψ_{ijk} accounts for interactions of the form cation-cation-anion and anion-anion-cation. Values of Φ_{ij} are given in Equation 4.13.

$$\begin{aligned} \Phi^{\phi}_{ij} &= \theta_{ij} + {}^{E}\theta_{ij}(I) + I\,{}^{E}\theta'_{ij}(I) \\ \Phi_{ij} &= \theta_{ij} + {}^{E}\theta_{ij}(I) \\ \Phi'_{ij} &= {}^{E}\theta'_{ij}(I) \end{aligned} \qquad [4.13]$$

θ_{ij} is a single parameter for each pair of anions or cations and the terms ${}^{E}\theta_{ij}(I)$ and ${}^{E}\theta'_{ij}(I)$ account for electrostatic unsymmetric mixing effects of cation-cation and anion-anion pairs.

The main characteristics of models of Pitzer and similar ion interaction models, take into account interactions between pairs of ions of like sign and also triplets of ions. This consideration enables calculations to be performed for multicomponent solutions at high concentrations (Pitzer, 1991). Pitzer's model has gained much popularity since the 1990s especially within the geochemical field. Perhaps the most extensive geochemical application of the Pitzer model is for the studies of mineral solubilities in brines (Pitzer, 1986). These are widespread and include the calculation of gypsum and halite solubility, study of evaporate sequences, alkaline earth sulphate solubilities in deep brines, scale mineral formation in oilfield brines and equilibria in acid mine drainage waters (Fürst and Renon, 1982 and Pitzer, 1991). The model has also been extended to include neutral species and incorporated into geochemical computer models such as PHRQPITZ (Plummer et al., 1988).

4.2 GEOCHEMICAL EQUILIBRIUM MODELLING

The origin and evolution of natural systems has been described by numerous geochemical models based on thermodynamics from as early as 1912 after Van't Hoff's first interpretation to clarify field observations (Harvie and Weare, 1980 and Harvie et al., 1984). Reviews of Nordstrom et al. (1979), Kerrisk (1981) and Bethke (1996) exemplifies the extent of work that has been performed on thermodynamic equilibrium modelling of natural saline brines. A number of mathematical models encompassing years of research is now available for the modelling of geochemical systems. These include programs such as PHREEQE, PHREEQC, MINTEQA2 and WATEQ, amongst others. For the representation of the behaviour of mixed electrolyte systems up to high concentrations, a specific model based on virial expansion with ionic strength dependent virial coefficients is required (Harvie et al., 1984). For this reason the models mentioned above are inappropriate as the activity coefficient calculations are mainly based on equations such as the Debye-Hückel and Davies equations. As such these models are limited to calculations in systems of low ionic strength. For systems of high ionic strength the Pitzer virial coefficient approach for calculating osmotic and activity coefficients therefore seems to fit the above requirements aptly.

4.2.1 PHRQPITZ

The computer program, PHRQPITZ, is able to perform geochemical calculations in brines and other electrolyte systems to high concentrations (Plummer et al., 1988). This is possible as the main code of this program uses the Pitzer virial coefficient approach for activity coefficient corrections according to the works of Harvie (1980) and Harvie et al. (1984) for the prediction of mineral solubilities in natural waters for the Na-K-Mg-Ca-H-Cl-SO_4-OH-HCO_3-CO_3-CO_2-H_2O system to high ionic strengths. PHRQPITZ is an adaptation of the original program called PHREEQE in that the aqueous model of the latter has been replaced with the Pitzer virial coefficient approach, in order to extend the modelling capability range in terms of ionic strength (Parkhurst, 1995). This approach is described mainly in the equations presented in **Section 4.1**. The activity of water, a_{H2O}, is computed from the osmotic coefficient, ϕ, given in Equation 4.10a, according to Equation 4.14.

$$\ln a_{H_2O} = -\frac{\phi \sum_i m_i}{55.50837} \qquad [4.14]$$

where m_i is the molality of the i^{th} ion in solution and there are 55.0837 moles of water per kilogram of water.

The main input parameters into the program include the total analytical content of the system as well as information such as pH and temperature. However, the number and type of input parameters that the program would require varies according to the reaction being modelled (Appendix A gives a detailed description of the input and output files from PHRQPITZ). Some of the main reaction modelling potentials of PHRQPITZ includes (Plummer et al., 1988):

- Aqueous speciation and mineral-saturation index.
- Mineral solubility.
- Mixing or titrations of aqueous solutions.
- Irreversible reactions and mineral-water mass transfer.
- Reaction path.

The general types of reactions that can be simulated in PHRQPITZ are as follows:

- Mixing of two solutions.
- Titrating one solution with a second solution.
- Adding or subtracting a net stoichiometric reaction (changing total concentrations of elements in proportion to a given stoichiometry).
- Adding a net stoichiometric reaction until the phase boundary of a specified mineral is reached.
- Equilibrating with mineral phases. Any condition which can be written in the form

$$\log(K_p) = \sum_i c_{p,i} \log(a_i) \qquad [4.15]$$

where a_i is the activity of the i^{th} aqueous species, $c_{p,i}$ is the stoichiometric coefficient of the i^{th} aqueous species in the p^{th} phase, and K_p is the equilibrium constant for the p^{th} phase, is considered a mineral phase.

- Changing temperature.

The output of the calculations performed with PHRQPITZ includes the osmotic coefficient, water activity, mineral saturation indices, mean-activity coefficients, total-activity coefficients, and scale-dependent values of pH, individual ion activities and individual ion activity coefficients.

4.2.1.1 Precautions and Limitations of PHRQPITZ

Although the program can be applied to a wide range of hydrogeochemical environments, there does exist some limitations to the use of this program for modelling. Of the precautions and limitations described by Parkhurst (1995) and Plummer et al. (1988) a few of the more possibly applicable ones to the modelling performed in this work are described below:

- The temperature range for the equilibria in the PHRQPITZ database is variable and is from 0 to 60 °C, if ΔH_r is known. However, the values in the database for the NaCl system are valid to a temperature of approximately 350 °C, and those for the carbonate system are consistent to approximately 100 °C. The precaution in terms of temperature limitations is provided, as the solubility of the minerals in the PHRQPITZ database is not precisely known and could lead to large errors if calculations are made outside these

temperature ranges for these solids. Furthermore, PHRQPITZ provides a (nonfatal) warning when the temperature is outside the interval 0 to 55 °C.

- PHRQPITZ is based on the Na-K-Mg-Ca-H-Cl-SO_4-OH-HCO_3-CO_3-CO_2-H_2O system of Harvie et al. (1984). The mineral database is therefore limited to these mineral precipitates. Other minerals such as Fe^{2+}, Mn^{2+}, Sr^{2+}, Ba^{2+}, Li^{+} and Br^{-} have been manually included, however, this extension to the database has not been validated.

- As the individual ion activities and activity coefficients are not independently measurable quantities, Equations 4.10b and 4.10c are only valid when individual ion activity coefficients are combined to define properties of neutral combinations of ions, e.g. in the calculation of mean activity coefficients, saturation indices and solubility. As such, the individual ion activities and activity coefficients are only meaningful on a relative scale. Therefore, the individual values of these parameters would depend on the choice of scale convention. PHRQPITZ provides a choice of two scale conventions, viz. no scaling which results in Equations 4.10b and 4.10c being used to calculate the individual ion activity coefficients, or scaling using the MacInnes convention. In the latter case the activity coefficient of Cl is defined to be equivalent to the mean activity coefficient of KCl in a KCl solution of equal ionic strength, i.e. $\gamma_{Cl(Mac)} \equiv \gamma_{\pm KCl}$. A problem may arise when the *measured* pH is introduced in geochemical calculations and may lead to erroneous calculations of mean activities and saturation indices. This is because the measured pH is unlikely to be on the same activity coefficient scale as the aqueous model as the buffers used to define pH are conventional (Plummer et al., 1988). Furthermore, it has been observed that even if the measured pH is on the same scale as the aqueous model, uncertainties in the calibration of pH in brines, like those due to liquid-junction potentials, will introduce inconsistencies in activity coefficient computations (Bates, 1973 and Wescott 1978). Therefore, when using measured pH values of brines, it is important to recognise the magnitude of error that can accompany the evaluation of mean activity and saturation indices due to the differences in the scale of activity coefficients. This problem of pH is particularly important when performing calculations in carbonate systems of high ionic strength brines.

4.2.1.2 How to Solve a Problem with PHRQPITZ

Like in any analyses, one is initially faced with a problem relating to real world situations (Figure 4.1). The first step therefore, is the conversion of a *real* problem into *chemical* terms. Ideal components necessary to formulate the problem must be considered together with possible separations (if necessary). Once the problem has been formulated, it then needs to be input into the computer program.

There are certain limitations considering the use of a program for modeling and these must be considered before commencing with the problem solution. Restrictions such as the available species in the thermodynamic database and ionic strength limitations must be taken into account. The application of a geochemical equilibrium model to an environmental problem involves four basic steps (Allison et al., 1991 and Wadley and Buckley, 1997):

i) Formulate one or more precise and relevant chemical questions that can be answered if one knows the equilibrium composition of the system. The formulation of the chemical questions must respect the inherent limitations in the site-specific data such as incomplete sampling or incomplete chemical analyses of samples.
ii) Pose the chemical questions to the model in terms of those symbols and formats appropriate to the computer program and from which the program may interpret a mathematical problem.
iii) Cause the program, i.e. the geochemical equilibrium model, to solve the mathematical problem.
iv) Interpret the output from the model in terms of the original environmental problem.

PHRQPITZ is designed to carry out a series of simulations in a single computer run. Each simulation consists of two separate problems – processing of an initial solution and / or modelling of a reaction (Plummer et al., 1988). The first step is almost always the most difficult – the ability to do this well improves with each application of the program. The input file for the program is PITZINPT and is designed to perform step (ii) by asking questions about the chemical system to be modelled and building the appropriate input file from the answers (this is described in detail in **Appendix A**). Step (iii), the actual execution of the calculations is automatic once initiated. In some instances computational problems may occur during execution which would require the user to modify the input file accordingly.

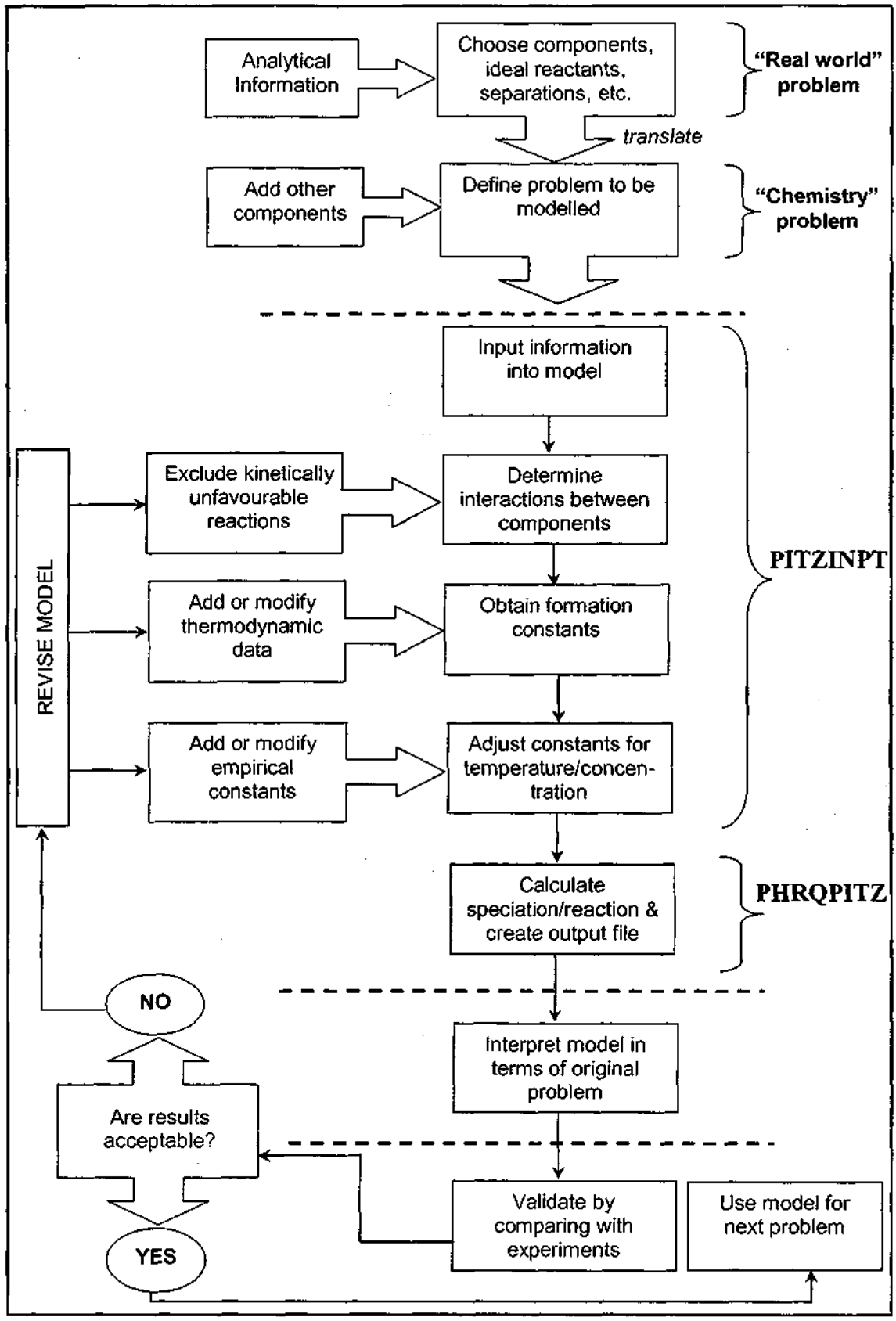

Figure 4.1: *Sequence of solving a problem in PHRQPITZ (adaptation of Allison et al., 1991 and Wadley and Buckley, 1997)*

Step (iv) is executed by the user by examining the PHRQPITZ output file and relating the results to the initial problem. This is then followed by validation of the results. This can only be performed physically by the necessary experiments and comparison with the appropriate literature.

4.3 CHAPTER REFERENCES

ALLISON JD, BROWN DS and NOVO-GRADAC KJ (1991) *MINTEQA2/PRODEFA2, A geochemical assessment model for environmental systems: Version 3.0 User's Manual*, EPA/600/3-91/021, Environmental Research Laboratory, Office of Research and Development, US Environmental Protection Agency, Athens, Georgia.

ANDERKO A, WANG P and RAFAL M (2002) *Electrolyte solutions: from thermodynamic and transport property models to the simulation of industrial processes*. Fluid Phase Equilibria **194-197** 123-142.

BATES RG (1973) *Determination of pH, Theory and Practice*, 2nd edition, John Wiley and Sons, New York. ISBN: 0-471-05647-2.

BETHKE CM (1996) *Geochemical Reaction Modeling: Concepts and applications*, Oxford University Press, New York. ISBN: 0 19 509475 1.

BROMLEY LA (1973) *Thermodynamic properties of strong electrolytes in aqueous solutions*. AIChE Journal **19**(2) 313-320.

BRÖNSTED JN (1922) *Studies on solubility. IV. The principle of the specific interaction of ions*. J Am Chem Soc **44**(5) 877-898.

DAS B (2003) *Pitzer ion interaction parameters of single aqueous electrolytes at 25°C*. J Soln Chem **33**(1) 33-45.

DAVIES CW (1938) *The extent of dissociation of salts in water. Part VIII. An equation for the mean ionic activity coefficient of an electrolyte in water, and a revision of the dissociation constants of some sulphates*. J Chem Soc 2093-2098.

DEBYE and HÜCKEL (1923) *Zur theorie der electrolyte.* Phys Z **24** 185-208.

FÜRST W and RENON H (1982) *Effect of the various parameters in the application of Pitzer's model to solid-liquid equilibrium. Preliminary study for strong 1-1 electrolytes.* Ind Eng Chem Process Des Develop **21** 396-400.

GUGGENHEIM EA (1935) *The specific thermodynamic properties of aqueous solutions of strong electrolytes.* Philos Mag **19** 588-643.

GUGGENHEIM EA and TURGEON JC (1954) *Specific interaction of ions.* Trans Faraday Soc **51** 747-761.

HARVIE CE, MØLLER N and WEARE JH (1984) *The prediction of mineral solubilities in natural waters: The Na-K-Mg-Ca-H-Cl-SO_4-OH-HCO_3-CO_3-CO_2-H_2O system to high ionic strengths at 25 °C.* Geochimica et Cosmochimica Acta **48** 723-751.

HARVIE CE and WEARE JH (1980) *The prediction of mineral solubilities in natural waters: the Na-K-Mg-Ca-Cl-SO_4-H_2O system from zero to high concentration at 25 °C.* Geochimica et Cosmochimica Acta **44** 981-997.

HU Y-F and GUO T-M (1999) *Thermodynamics of electrolytes in aqueous systems containing both ionic and non-ionic solutes. Application of the Pitzer-Simonson-Clegg equations to activity coefficients and solubilities of 1:1 electrolytes in four electrolyte-non-electrolyte-H_2O ternary systems at 298.15 K.* Phys Chem Chem Phys **1** 3303-3308.

KERRISK JF (1981) *Chemical equilibrium calculations for aqueous geothermal brines.* Los Alamos Sci Lab Report LA-8851-MS., Los Alamos, N.M. 87545.

LAIDLER KJ and MEISER JH (1999) *Physical Chemistry*, 3rd edition, Houghton Mifflin Company, New York. ISBN 0-395-91848-0.

MAYER JE (1950) *The theory of ionic solutions.* J Chem Phys **18** 1426-1436.

MEISSNER HP and KUSIK CL (1972) *Activity coefficients of strong electrolytes in multicomponent aqueous solutions.* AIChE Journal **18**(2) 294-298.

MEISSNER HP, KUSIK CL and TESTER JW (1972) *Activity coefficients of strong electrolytes in aqueous solution-effect of temperature.* AIChE Journal **18**(3) 661-662.

MEISSNER HP and TESTER JW (1972) *Activity coefficients of strong electrolytes in aqueous solutions.* Ind Eng Chem Process Des Develop **11**(1) 128-133.

NORDSTROM PK, PLUMMER LN, WIGLEY TM, WOLERY TJ, BALL JW, JENNE EA, BASSET RL, CRERAR DA, FLORENCE TM, FRITZ B, HOFFMAN M, HOLDREN GR.Jr., LAFON GM, MATTIGOD SV, McDUFF RE, MOREL F, REDDY MM, SPOSITO G and THRAILKILL J (1979) *A comparison of computerized chemical models for equilibrium calculation in aqueous systems.* ACS Symposium Series No. 93, 857-892.

PARKHURST DL (1995) *User's guide to PHREEQC – A computer program for speciation, reaction-path, advective-transport and inverse geochemical calculations*, US Geological Survey, Water-Resources Investigations Report 95-4227, Lakewood, Colorado.

PITZER KS (1973) *Thermodynamics of electrolytes I: Theoretical basis and general equations.* J Phys Chem **77** 268-277.

PITZER KS (1986) *Theoretical considerations of solubility with emphasis on mixed aqueous electrolytes.* Pure Appl Chem **58** 1599 1612.

PITZER KS (1991) Chapter 3. *Theory: Ion Interaction Approach.* In *Activity coefficients in electrolyte solutions*, PYTKOWICZ RM, ed., Boca Raton Fla: CRC , London. ISBN: 0-8493-5411-0, 77.

PLUMMER LN, PARKHURST DL, FLEMING GW and DUNKLE SA (1988) *A computer program incorporating Pitzer's equations for calculation of geochemical reactions in brines*, US Geological Survey, Water-Resources Investigations Report 88-4153, Reston, Virginia.

ROBINSON RA and SROKES RH (1965) *Electrolyte Solutions*, Butterworths, London.

SCATCHARD G (1936) *Concentrated solutions of strong electrolytes*. Chem Rev **19** 309 -327.

SCATCHARD G (1968) *The excess free energy and related properties of solutions containing electrolytes*. J Am Chem Soc **90** 3124-3127.

SCATCHARD G, RUSH RM and JOHNSON JS (1970) *Osmotic and activity coefficients for binary mixtures of sodium chloride, sodium sulphate, magnesium sulphate and magnesium chloride in water at 25 °C. III: Treatment with the ions as components*. J Phys Chem **74** 3786-3796.

WADLEY S and BUCKLEY CA (1997) *Chemical speciation self-study work manual*, WRC Project No. K8/208, Pollution Research Group, Department of Chemical Engineering, Durban, South Africa.

WANG P, ANDERKO A and YOUNG RD (2002) *A speciation-based model for mixed-solvent electrolyte systems*. Fluid Phase Equilibria **203** 141-176.

WANG P, SPRINGER RD, ANDERKO A and YOUNG RD (2004) *Modeling phase equilibria and speciation in mixed-solvent electrolyte systems*. Fluid Phase Equilibria **222-223** 11-17.

WESCOTT CC (1978) *pH measurements*, Academic Press, New York. ISBN: 0-12-745150-1

WHITFIELD M (1973) *A chemical model for the major electrolyte components of seawater based on Brönsted-Guggenheim hypothesis*. Mar Chem **1** 251-266.

WHITFIELD M (1974) *An improved specific interaction model for seawater at 25 °C and 1 atmosphere total pressure*. Mar Chem **3** 197-213.

CHAPTER 5

Chapter 5

VAPOUR PRESSURE MODELLING AND EXPERIMENTS

This Chapter forms the second and final approaches in the series of methods described in Chapter 1, i.e. the determination of vapour pressures and evaluation of driving force. The decline in transmembrane flux experienced during the MD experiments described in Chapter 3 is addressed by evaluating the vapour pressures of the solution and hence driving force of the MD process which will indicate the nature of the flux decline. Section 5.1.1 illustrates the use of the computer program PHRQPITZ to model vapour pressures. The suitability of the program to accurately model vapour pressures was validated by vapour-liquid equilibrium experiments performed using the dynamic vapour-liquid equilibrium still which is described in Section 5.1.2. The results obtained are described in Section 5.2 - the results of the VLE experiments are discussed in Section 5.2.1 while the comparison between the experimental data and those modelled are shown in Section 5.2.2. PHRQPITZ was then used to model the vapour pressures of the solutions throughout the MD process which led to the evaluation of the driving force. Section 5.2.3 compares and discusses the trend displayed between the flux and driving force. Section 5.3 demonstrates the potential of PHRQPITZ to predict and thus possibly enable finer control of the MD process. This chapter ends with a summary in Section 5.4.

5.1 DETERMINATION OF VAPOUR PRESSURES

The initial purpose of this stage of the research stems from the work that was performed with MD as described in Chapter 3. The problem of the decline in transmembrane flux that was observed during the batch MD of concentrated salt solutions is an inhibiting factor to the prolonged functioning of the process. Our aim is to establish why the flux declines, in accordance with the process description. The only way in which this transmembrane flux could be evaluated is by measuring the actual driving force for the process, i.e. the vapour pressures of the solutions which give rise to the driving force for the flux and transport. Since this cannot be

performed during the experiment itself, one needs a means of evaluating the vapour pressures. Being able to computationally model the performance of the system outside to the process itself is an excellent and valuable means of predicting the outcome of the process. The computer program PHRQPITZ described in Chapter 4 seems to contain the necessary modelling capabilities for the purposes of this work. Therefore, this program was used in order to determine the vapour pressures of the solutions that were subject to MD and the results are described in **Section 5.1.1**. Before this program could be used further to evaluate the flux decline during MD, its suitability and accuracy for modelling vapour pressures was validated by experimental vapour-liquid equilibrium measurements, described in **Section 5.1.2**.

5.1.1 PHRQPITZ modelling

The program PHRQPITZ is designed to execute a series of simulations in a single computer run by solving two separate problems: (i) processing of an initial solution/s and (or) (ii) modelling of a reaction (Plummer, 1988). There are a variety of reactions that can be modelled but in each type of reaction the initial solutions must be specified. The total concentrations of species as well as information such as pH and temperature are input into a specific solution which is assigned a unique number. Any further reactions or mineral equilibria are then performed on this solution. The output of the calculations performed with PHRQPITZ includes the osmotic coefficient, water activity, mineral saturation indices, mean-activity coefficients, total-activity coefficients, and scale-dependent values of pH, individual ion activities and individual ion activity coefficients. For the purposes of this work, the activity of water was the crucial output required from PHRQPITZ which was then used to obtain the solution vapour pressures directly (Equation 5.1), of the three mixes of salt solutions over a range of temperatures. The effective vapour pressure of a solution (P_{soln}) is defined as the product of the vapour pressure of pure water (P_{H2O}) at the same temperature as the solution and the activity of water (α_{H2O}) in the solution.

$$P_{soln} = P_{H_2O}\alpha_{H_2O} \qquad [5.1]$$

An example of a section of a typical output file, containing the necessary information required for the purposes of this work, is shown in Table 5.1 with the key information highlighted. The initial information that was fed to the program was the concentration of the solutions, as shown under "TOTAL MOLALITIES OF ELEMENTS" and the temperature of the solution. The aim was to

obtain the activity of water of this solution from which the corresponding vapour pressure was calculated. Further details of the modelling procedure are explained in **Appendix A.**

Table 5.1: *Example of a section of an output file from PHRQPITZ*

```
MD process for retentate temperatures
 0000020000 0 0          0.00000
 SOLUTION 1
 time=0
  4  0 0      7.00       4.00       27.3       1.00
    5  1.163D+00  16  1.163D+00    6  4.895D+00  14  4.895D+00
1SOLUTION NUMBER 1

                        TOTAL MOLALITIES OF ELEMENTS
                        ----- ---------- -- --------
                ELEMENT          MOLALITY          LOG MOLALITY

                MG              1.163000D+00           0.0656
                NA              4.895000D+00           0.6898
                CL              4.895000D+00           0.6898
                S               1.163000D+00           0.0656

                      ----DESCRIPTION OF SOLUTION----
                                        PH =   7.0000
                                ACTIVITY H2O =   0.7391
                           OSMOTIC COEFFICIENT =   1.3853
                                IONIC STRENGTH =   9.5469
                                   TEMPERATURE =  27.3000
                                      PRESSURE =   1.0000 ATM
                                DENSITY OF H2O =   0.9964 G/CC
                             ELECTRICAL BALANCE =  -7.0283D-05
                               TOTAL ALKALINITY =   7.0567D-05
                                     ITERATIONS =   1

                                 -----------------------
                                 DISTRIBUTION OF SPECIES
                                 -----------------------
                                                          UNSCALED              UNSCALED
  I  SPECIES   Z    MOLALITY   LOG MOLAL   ACTIVITY   LOG ACT    GAMMA    LOGGAM

  1  H+       1.0  3.005E-08   -7.522   1.000E-07   -7.000  3.327E+00   0.522
  3  H2O      0.0  7.391E-01   -0.131   7.391E-01   -0.131  1.000E+00   0.000
  5  MG+2     2.0  1.163E+00    0.066   1.179E+00    0.072  1.014E+00   0.006
  6  NA+      1.0  4.895E+00    0.690   3.882E+00    0.589  7.930E-01  -0.101
 14  CL-     -1.0  4.895E+00    0.690   8.073E+00    0.907  1.649E+00   0.217
 16  SO4-2   -2.0  1.163E+00    0.066   2.982E-02   -1.526  2.564E-02  -1.591
 31  OH-     -1.0  2.526E-07   -6.598   8.822E-08   -7.054  3.493E-01  -0.457
 40  HSO4-   -1.0  2.539E-07   -6.595   3.029E-07   -6.519  1.193E+00   0.077
 85  MGOH+    1.0  7.031E-05   -4.153   1.651E-05   -4.782  2.348E-01  -0.629
```

Initially PHRQPITZ was used to gain the activity of water for mixtures of the compositions of the salt mixes that were used during MD, i.e. 1:1 mix (225 g/ℓ NaCl and $MgSO_4$, i.e. 4.89 and

1.16 m, respectively), 1:2 mix (275 g/ℓ NaCl and 137.5 g/ℓ $MgSO_4$, i.e. 5.78 and 0.686 m, respectively) and 1:3 mix (280 g/ℓ NaCl and 93.3 g/ℓ $MgSO_4$, i.e. 5.72 and 0.451 m, respectively) as described in **Section 3.2.2**, with arbitrarily chosen temperatures ranging from 303 to 373 K in order to test the applicability of PHRQPITZ to model vapour pressures. Figures 5.1 and 5.2 show the vapour pressure curves that were obtained for each of the salt mixes together with that of pure water for comparison.

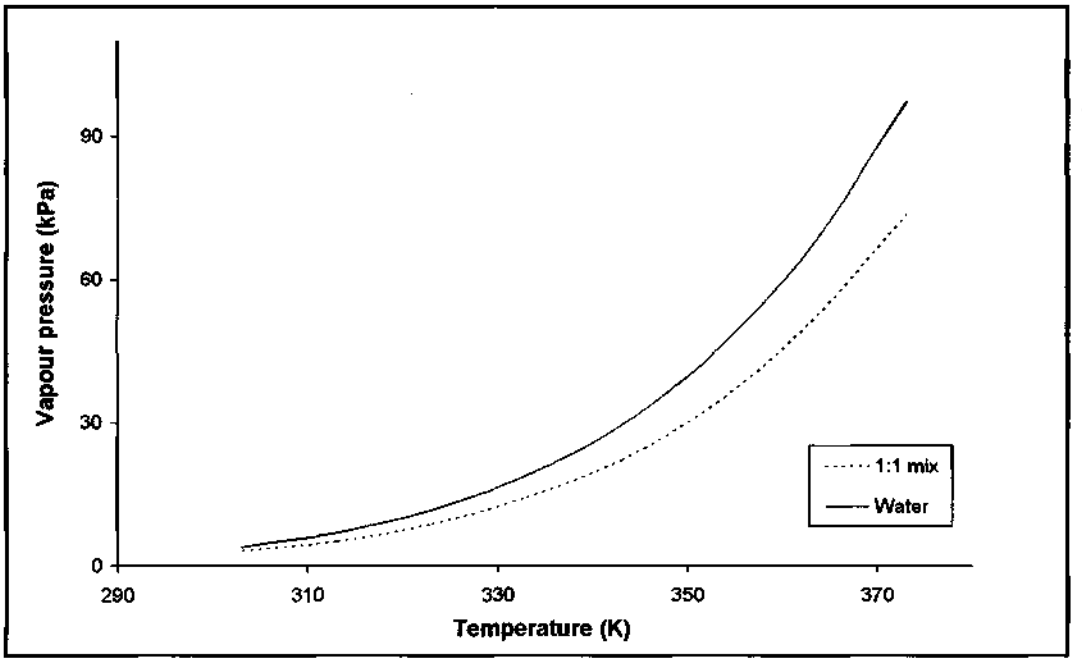

Figure 5.1: *Vapour pressure curve for the 1:1 mix predicted through PHRQPITZ modelling; pure water vapour pressure curve shown for comparison.*

The vapour pressure of pure water is higher than that of the hot brine (1:1 mix) at a particular temperature. It is this difference in vapour pressure that drives the separation during the MD process as described in **Section 2.3.1**. The same is true for the other salt concentrations shown in Figure 5.2 below.

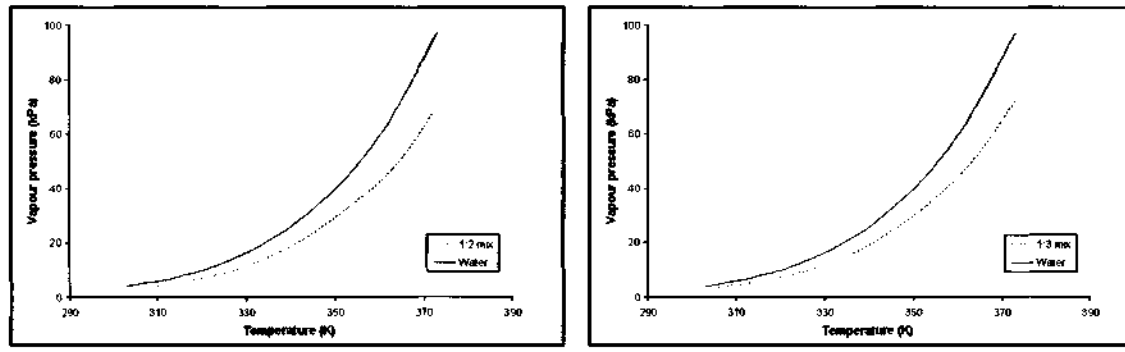

Figure 5.2: *Vapour pressure curves for the 1:2 and 1:3 mixes predicted through PHRQPITZ modelling; pure water vapour pressure curve shown for comparison.*

Before proceeding with any further calculations concerning the actual MD process and the actual temperature and concentration changes occurring during the process, as described in **Section 4.2.1.2,** the next stage, in any modelling procedure, is the validation of the vapour pressure predictions. This can be performed by physically conducting the necessary experiments or by comparison with the literature.

5.1.2 Vapour-liquid equilibrium measurements

Apart from the purposes of our measurements, which are to obtain the vapour pressure of inorganic salt solutions, vapour-liquid equilibrium (VLE) data are required in the design of chemical processes as well as mass transfer equipment such as distillation and absorption columns (Şeker and Somer, 1993). However, the acquisition of VLE data is not a straightforward task. Accurate theoretical determination of VLE data is often less feasible due to the uncertainties in the properties of liquid mixtures. These include parameters such as fugacity and activity coefficients that cannot merely be estimated by simple theoretical approaches as they are dependent on the chemical structure and compositions of the compounds. Furthermore, the majority of theoretical approaches are based on dilute solutions which are not always appropriate in real situations such as concentration and precipitation. Therefore, experimental methods for the measurement of VLE data in non-ideal solutions become mandatory. Various methods exist for the direct measurement of VLE data.

They are grouped according to the following (Şeker and Somer, 1993):

- Distillation methods.
- Circulation method – mechanical circulation of vapour.
- Static method.
- Dew and bubble point method.

Each of these methods has their characteristic operational parameters and advantages and disadvantages associated with them (Raal and Mühlbauer, 1998). In the present work the apparatus known as the vapour-liquid equilibrium still was used to measure the vapour pressures of solutions of mixtures of inorganic salts, sodium chloride and magnesium sulphate, as a function of temperature.

5.1.2.1 The vapour-liquid equilibrium still

The particular VLE still developed by Raal and Mühlbauer (1998) has two essential parts: (i) vaporiser and (ii) equilibrium chamber (Figure 5.3). The binary liquid mixture is placed in the boiling chamber where it is vaporized by an electrical heating coil within the chamber and a further external heater which permits rapid boiling of the mixture. The mixture in the boiling chamber is stirred which ensures that the returning equilibrium mixture is thoroughly mixed with the original mixture before further evaporation – this prevents flashing. The vapour-liquid mixture is then forced up the Cottrell tube into the equilibrium chamber. The mixture then flows downwards through the packing which consists of stainless steel wire mesh cylinders of 3 mm dimension. Close contact between the liquid and vapour in this packed section allows rapid attainment of equilibrium (Joseph et al., 2001). The temperature in the chamber is recorded by the thermometer (Pt-100) which extends well inside the equilibrium chamber. The resulting equilibrium mixture leaves the chamber through the drain holes perforated at the bottom of the chamber. The released equilibrium liquid then flows down over the stainless steel mixing spiral before a portion of the liquid is caught in the liquid trap for sampling, whilst the remainder is returned to the boiling chamber.

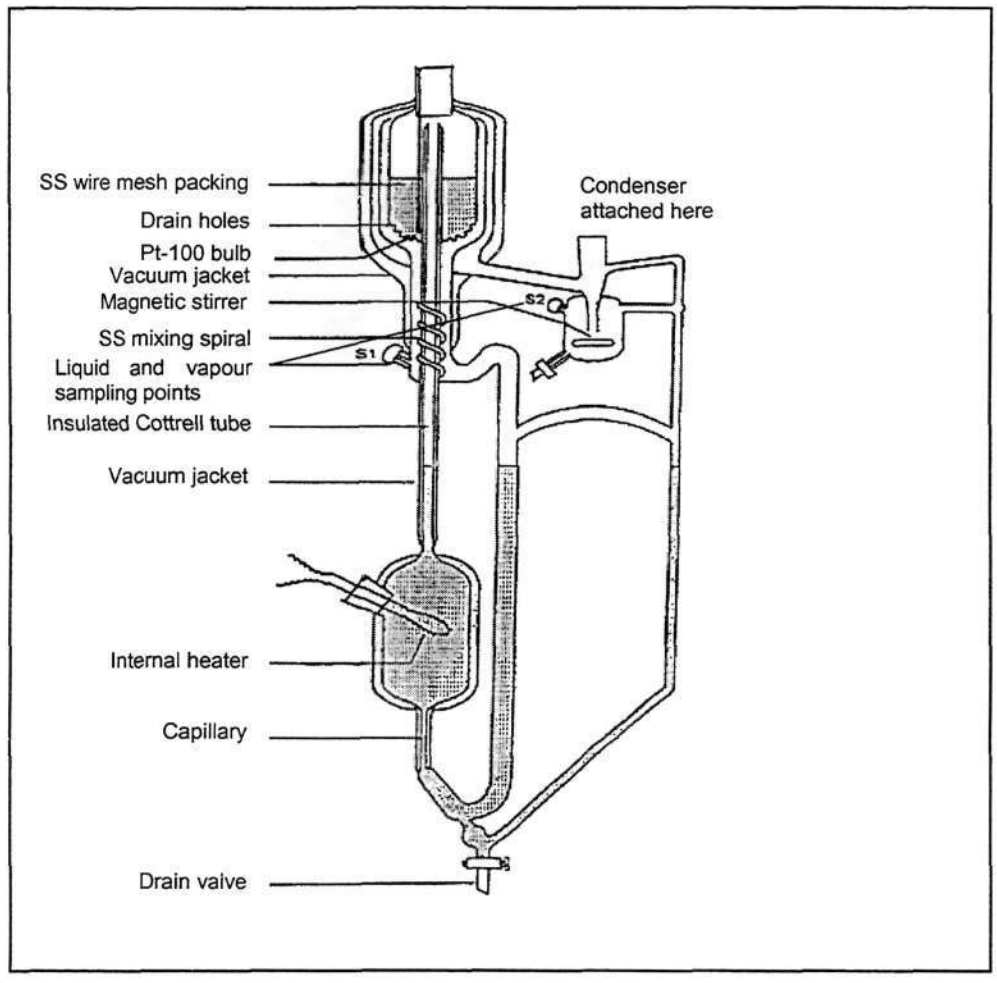

Figure 5.3: *Schematic diagram of the vapour-liquid equilibrium still (Joseph et al., 2001).*

The discharged vapour, on the other hand, flows upward forming a thermal lagging around the equilibrium chamber and, together with the vacuum jacket that insulates the upper portion of the still, provides an adiabatic environment for the operation of the equilibrium chamber. The vapour then flows through the condenser where it is cooled and condensed into the condensate receiver where it can be sampled before returning to the boiling chamber. The condensate receiver is equipped with a magnetic stirrer which prevents the possibility of temperature and concentration gradients which enables sample concentrations to be reproduced accurately.

The VLE still is incorporated in an environment where the temperature and pressure is monitored and controlled. A block diagram of the VLE measurement system is shown in Figure 5.4.

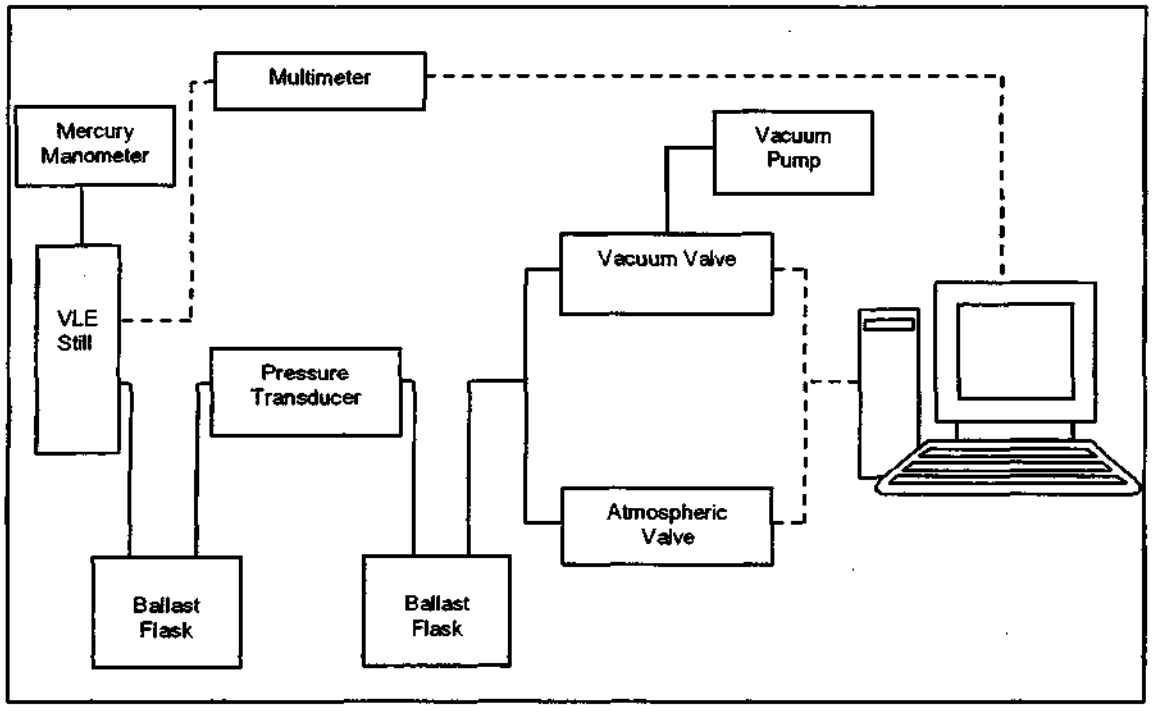

Figure 5.4: *Block diagram of VLE system (Joseph et al., 2001)*

The central component of the system consists of the VLE still whilst secondary components which enable pressure and temperature to be controlled consist of a 6.5 digit multimeter, a Sensotec Super TJ pressure transducer, two solenoid valves, a vacuum pump, differential mercury manometer, two ballasts flasks and a computer. The multimeter functioned to record the temperature of the Pt-100 temperature sensor; the pressure transducer serving the purpose of monitoring the pressure. The two solenoid valves together with the computer are used in a method based on pulse-width modulation which controls the temperature within a range of 0.01 to 0.05 K, depending on the composition of the mixture (Joseph et al., 2001).

5.1.2.2 Experimental

The VLE still was used to measure the vapour pressure of the solutions of sodium chloride and magnesium sulphate of a similar range in compositions to those used in the MD experiments.

The still was initially calibrated in order to determine the correction factors that needed to be applied to the temperature and pressure that were recorded by the computer. The calibrations led to the corrections taking the form of Equations 5.2 and 5.3 for temperature and pressure, respectively.

$$T_{(^{\circ}C)} = 2.5881R_{(ohm)} - 259.61 \qquad [5.2]$$

$$P_{(kPa)} = 0.9945P_{disp} - 0.3267 \qquad [5.3]$$

Where R_{ohm} is the resistance in ohms measured by the multimeter and P_{disp} is the pressure displayed by the computer.

The composition and concentration of the mixed electrolyte solutions are the same as those described in **Section 3.2.2** of this thesis. However, before these measurements took place, the performance and suitability of the still to measure vapour pressures of inorganic salt solutions were tested by performing measurements on solutions of known concentrations of sodium chloride and comparing the experimental results to those reported in literature. For this purpose concentrated solutions of analytical grade sodium chloride were prepared in concentrations of 20 g/ℓ, 200 g/ℓ and 280 g/ℓ and the vapour pressure of these solutions were measured as a function of temperature between 298 and 373 K. The temperature and pressure in the still were computer controlled and the accuracies were estimated to be ±0.02 K and ±0.03 kPa, respectively. The desired temperature was set and once vapour-liquid equilibrium was established, the corresponding pressure was recorded.

5.2 RESULTS AND DISCUSSION

Section 5.2.1 provides the results that were obtained from the VLE experiments on pure and mixed salt solutions, the former being performed to test the applicability of the VLE still for measuring the vapour pressures of inorganic salts, by comparison to literature. The vapour pressures measured for the solutions of mixed salts at different temperatures were then compared to those modelled using PHRQPITZ. This comparison is illustrated in **Section 5.2.2.** **Section 5.2.3** then shows how PHRQPITZ was used to measure the vapour pressure of the solution throughout the MD process and, when compared to the transmembrane flux, demonstrates the importance of taking into account the activities of water when calculating the driving force for the MD process.

5.2.1 Vapour pressure measurements using the VLE still

Section 5.2.1.1 describes the results that were obtained from the measurements of pure solutions of sodium chloride that were used as a verification of the VLE method. The results were compared to two literature sources. Once the suitability of the method was verified, measurements concerning the mixed salt solutions were undertaken. These results are described in **Section 5.2.1.2.**

5.2.1.1 Verification of VLE method

Figure 5.5 represents the vapour pressure curves that were obtained for each sodium chloride solution followed by the vapour pressure locus curve in Figure 5.6. The Antoine equation (Equation 2.13) was fitted to the experimental vapour pressure data by using a regression procedure to determine the parameters. The constants A, B and C in the Antoine equation that were obtained from the regression procedure are given in **Appendix B**.

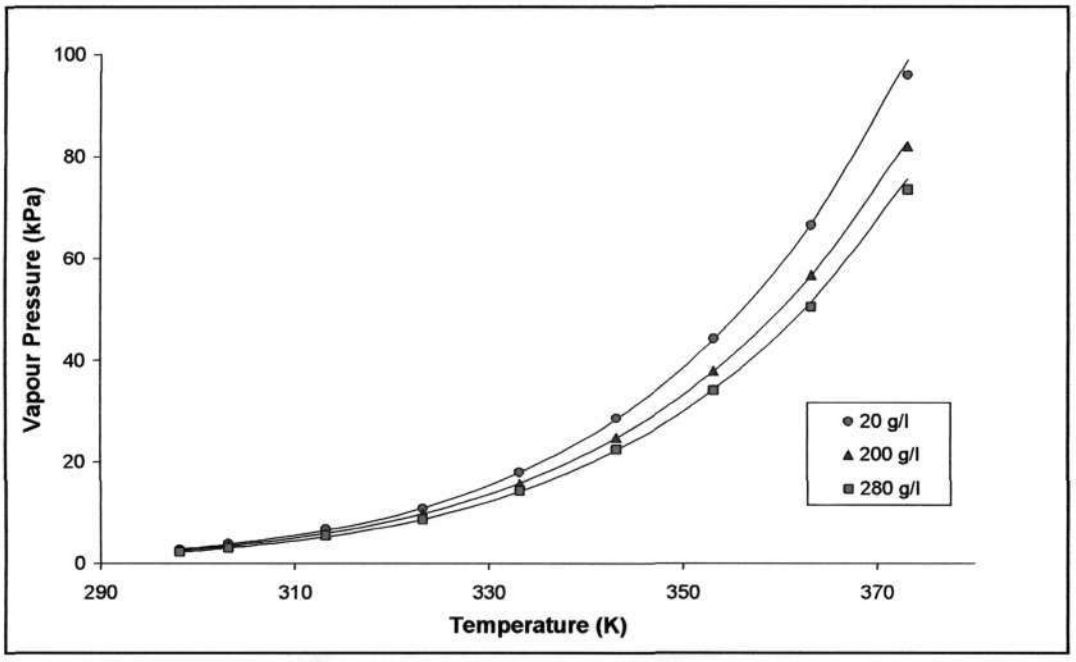

Figure 5.5: *Vapour pressure curves together with the fitted Antoine curves for solutions of sodium chloride in varying concentrations*

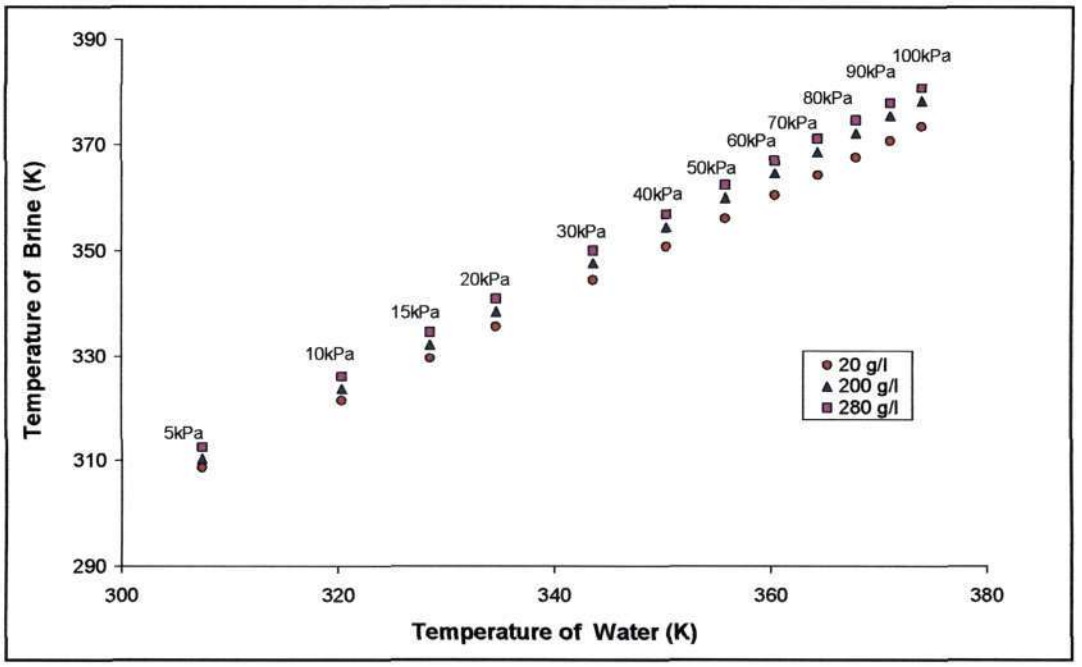

Figure 5.6: *Vapour pressure locus curve for sodium chloride solutions*

The experimental vapour pressure data were compared to two literature sources. Liu and Lindsay (1972) performed vapour pressure lowering experiments on concentrated solutions of sodium chloride (from 4 m to saturation) and at temperatures from 348 K to 573 K. The vapour pressure measurements performed in this work on the concentrated sodium chloride solutions were performed at temperatures from 298 K to 373 K. As no literature data were found containing measurements which fall within these precise concentrations *and* temperature ranges, graphs of vapour pressures against concentration at each of the temperature ranges studied by Lui and Lindsay were plotted (**Appendix B**) from which the vapour pressures at the concentrations used in this work were extrapolated and plotted against the temperatures studied by Lui and Lindsay. The Antoine equation was then fitted to these points and then extrapolated to the temperatures studied in this work. The plots of Antoine's regressions to Lui and Lindsay's data are shown in Figure 5.7.

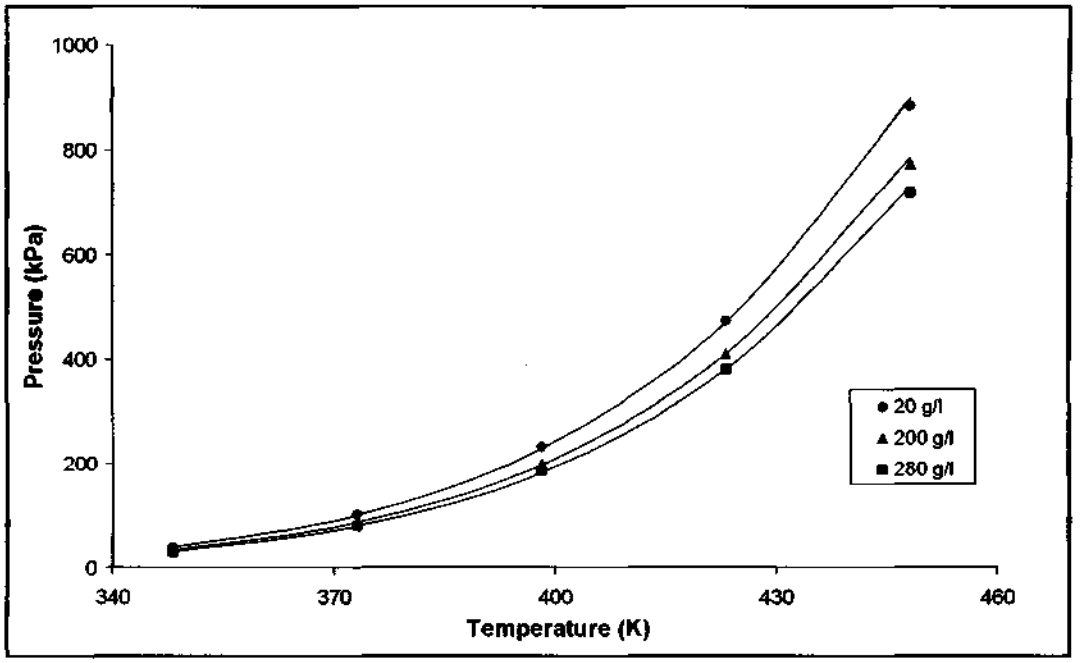

Figure 5.7: *Antoine fit to the data of Lui and Lindsay (1972) for each concentration of sodium chloride at the corresponding temperature*

The sum of the square of the residuals for the fit of the Antoine regression to the experimental data of Lui and Lindsay were 6.202×10^{-4}, 6.787×10^{-4} and 6.249×10^{-4} kPa^2 for the 20, 200 and 280 g/ℓ sodium chloride solutions, respectively. A comparison between the experimental data obtained from the VLE measurements performed in this work and that of Lui and Lindsay for each concentration studied is shown in Figure 5.8.

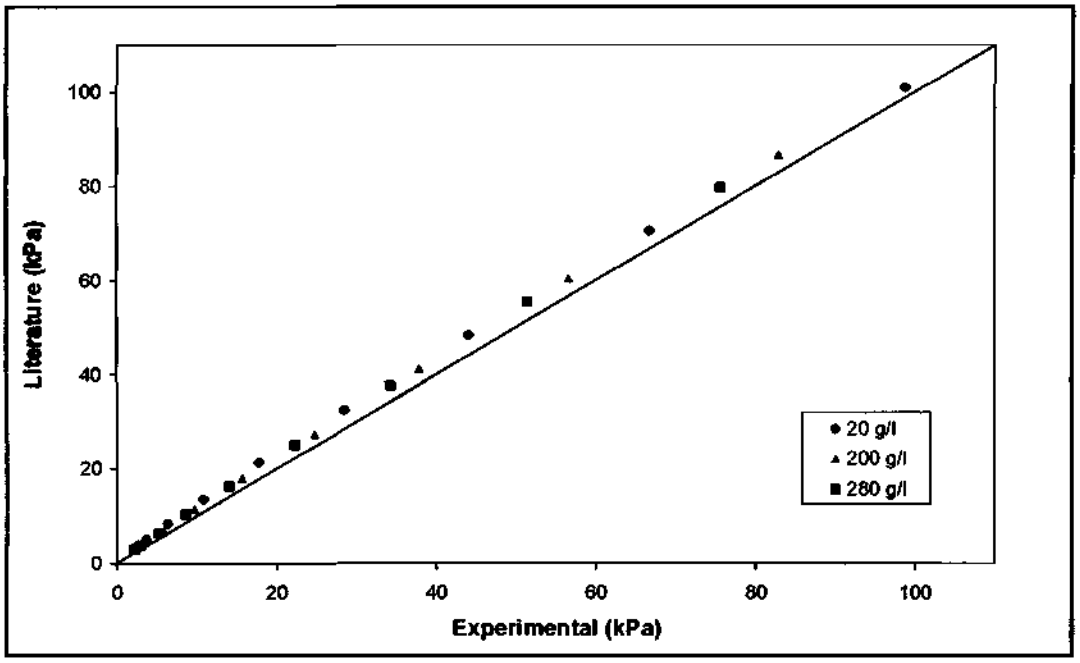

Figure 5.8: *Comparison between literature (Lui and Lindsay, 1972) and measured vapour pressures for each concentration of sodium chloride solution*

The relative error between the VLE experimental data and those extrapolated from literature, range between -0.030 to -0.19 for the 20 g/ℓ solution, -0.057 to -0.19 for the 200 g/ℓ solution and -0.065 to -0.18 for the 280 g/ℓ solution. Considering the accumulated error that would have occurred during the extrapolation procedures, it can be concluded that there is good agreement between the experimental and literature data.

The empirical equations presented by Sparrow (2003) for thermodynamic properties of aqueous NaCl were used as a second comparison with the data obtained from these VLE experiments. The empirical equations of Sparrow are functions of temperature and concentration and are useful for estimating the solubility, density, vapour pressure, specific enthalpy and entropy of aqueous sodium chloride for temperatures from 273 to 573 K, and concentrations extending to saturation (Sparrow, 2003). The equation derived by Sparrow for the evaluation of vapour pressures is shown in Equation 5.4 with the explanations following.

$$P_{VAP} = A + BT + CT^2 + DT^3 + ET^4 \qquad [5.4]$$

when $273.15K \le T \le 423.15K$

$$A = \left(0.9083 - 0.569X + 0.1945X^2 - 3.736X^3 + 2.82X^4\right)10^{-3}$$

$$B = \left(-0.0669 + 0.0582X - 0.1668X^2 + 0.676X^3 - 2.091X^4\right)10^{-3}$$

$$C = \left(7.541 - 5.143X + 6.482X^2 - 52.62X^3 + 115.7X^4\right)10^{-6}$$

$$D = \left(-0.0922 + 0.0649X - 0.1313X^2 + 0.8024X^3 - 1.986X^4\right)10^{-6}$$

$$E = \left(1.237 - 0.753X + 0.1448X^2 - 6.964X^3 + 14.61X^4\right)10^{-9}$$

where X is the salt mass fraction of a solution and is related to the molality of the salt according to Equation 5.5.

$$X = \frac{mM_{NaCl}}{\left(1000 + mM_{NaCl}\right)} \qquad [5.5]$$

The comparison between the experimental vapour pressure measurements and those calculated from the empirical equations of Sparrow are shown in Figure 5.9.

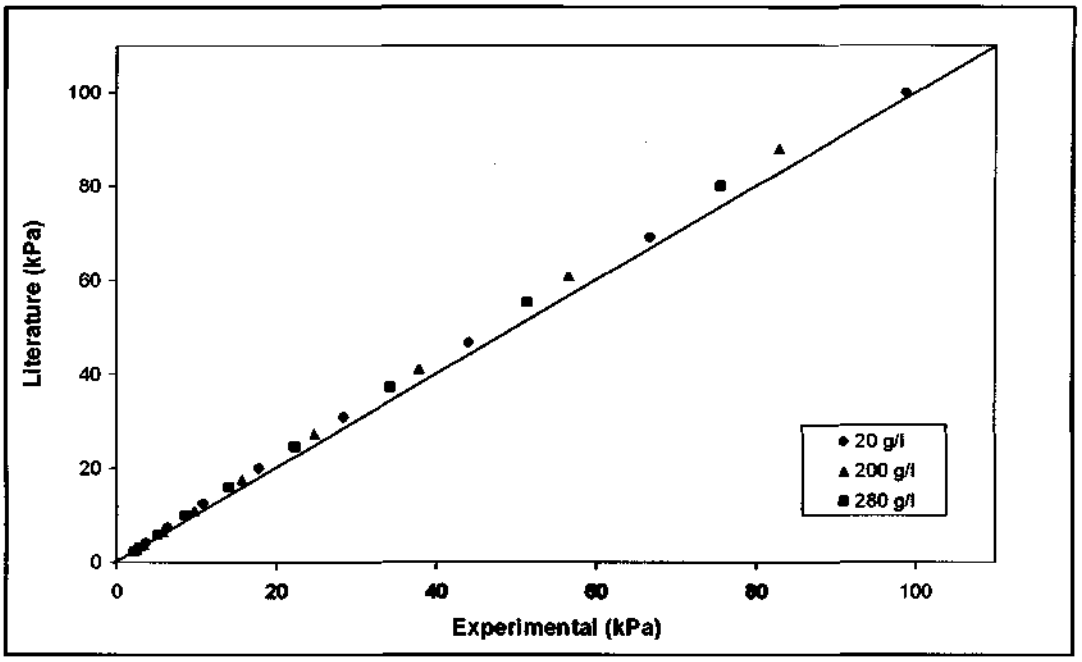

Figure 5.9: *Comparison between literature (Sparrow, 2003) and measured vapour pressures for each concentration of sodium chloride solution*

The relative error between the VLE experimental data and those calculated from the empirical equations of Sparrow range between -0.021 to -0.11 for the 20 g/ℓ solution, 0.0030 to -0.11 for the 200 g/ℓ solution and -0.035 to -0.10 for the 280 g/ℓ solution. There is therefore good agreement between the measured vapour pressures and those calculated from literature.

From the above work, the agreement between literature and the measured vapour pressures for each of the sodium chloride solutions was substantial to acknowledge VLE as a suitably accurate apparatus for obtaining the vapour pressures of inorganic salt solutions. This apparatus was then used to measure the vapour pressures of the solutions of the mixed salts.

5.2.1.2 Measurement of vapour pressures of the mixed salt solutions using VLE

The temperatures and concentrations that were used during the modelling using PHRQPITZ were adhered to for comparison. The vapour pressure curves that were obtained for these salt mixes are shown in Figures 5.10 to 5.12 together with the Antoine fit to the experimental data. The regression constants for the Antoine fit are featured in **Appendix B.**

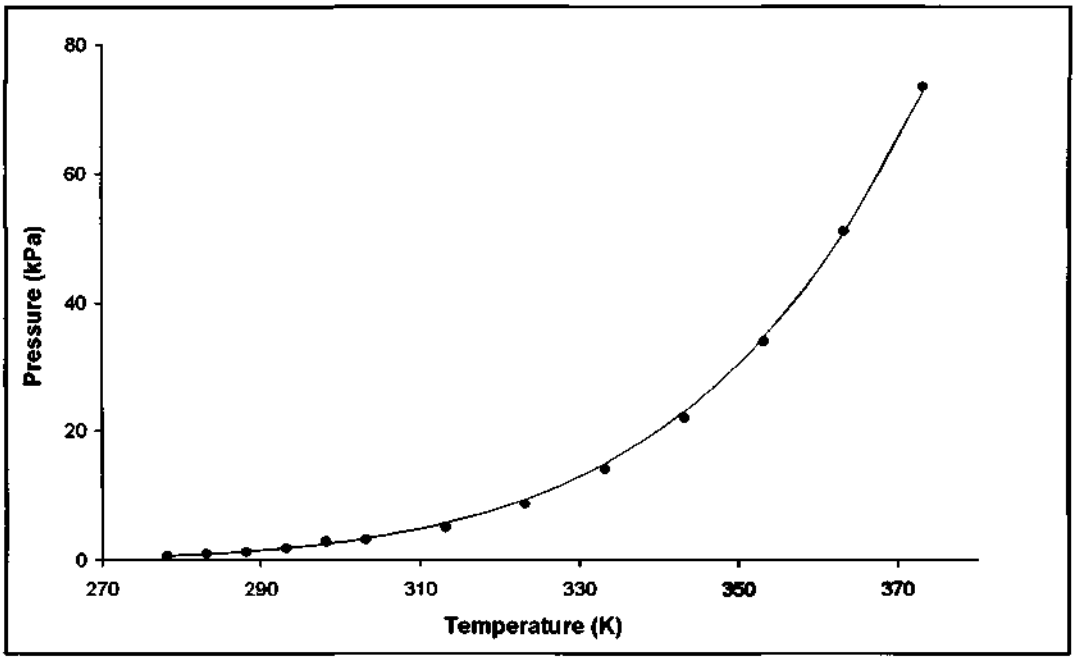

Figure 5.10: *Experimental vapour pressure curve obtained from VLE measurements for the 1:1 mix together with the fitted Antoine curve*

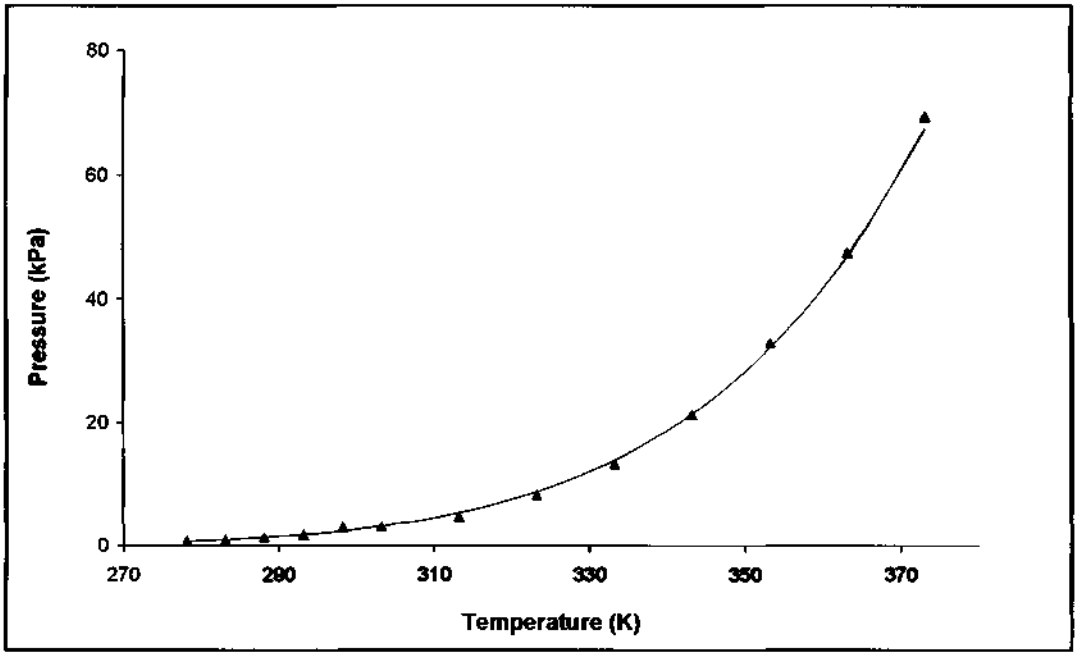

Figure 5.11: *Experimental vapour pressure curve obtained from VLE measurements for the 1:2 mix together with the fitted Antoine curve*

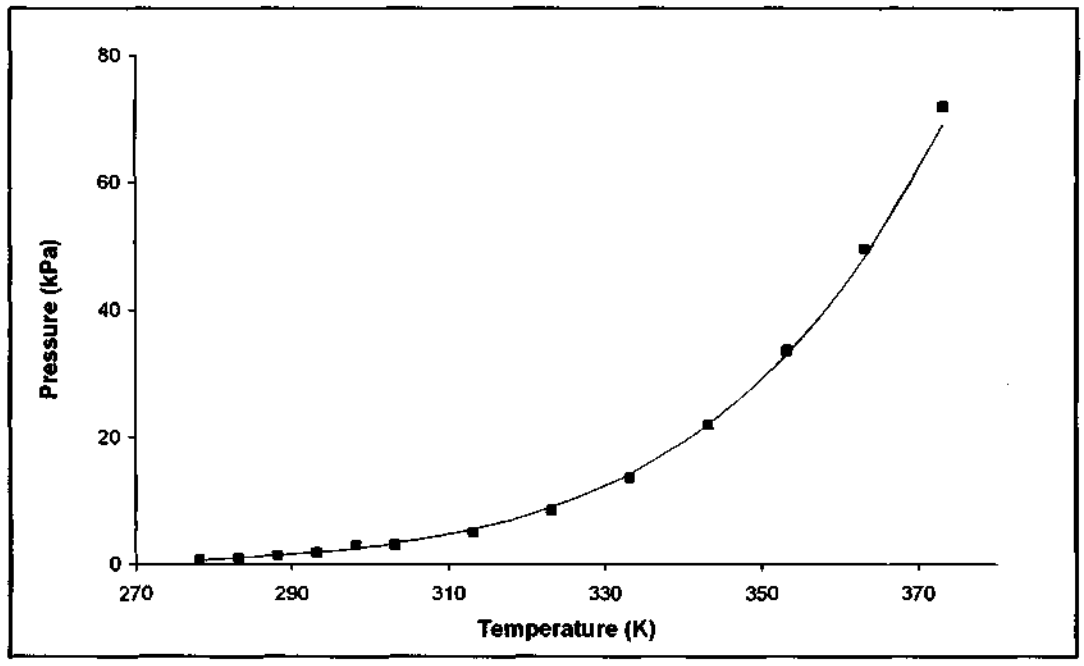

Figure 5.12: *Experimental vapour pressure curve obtained from VLE measurements for the 1:3 mix together with the fitted Antoine curve*

5.2.2 Comparison between modelled and experimental vapour pressures

Having successfully measured experimentally the vapour pressures of the salt solutions, these data were compared to the modelled data in order to ascertain whether the modelling procedure is accurate. The comparison between the experimental VLE data and that modelled using PHRQPITZ is shown in Figure 5.13 for each of the salt mixes.

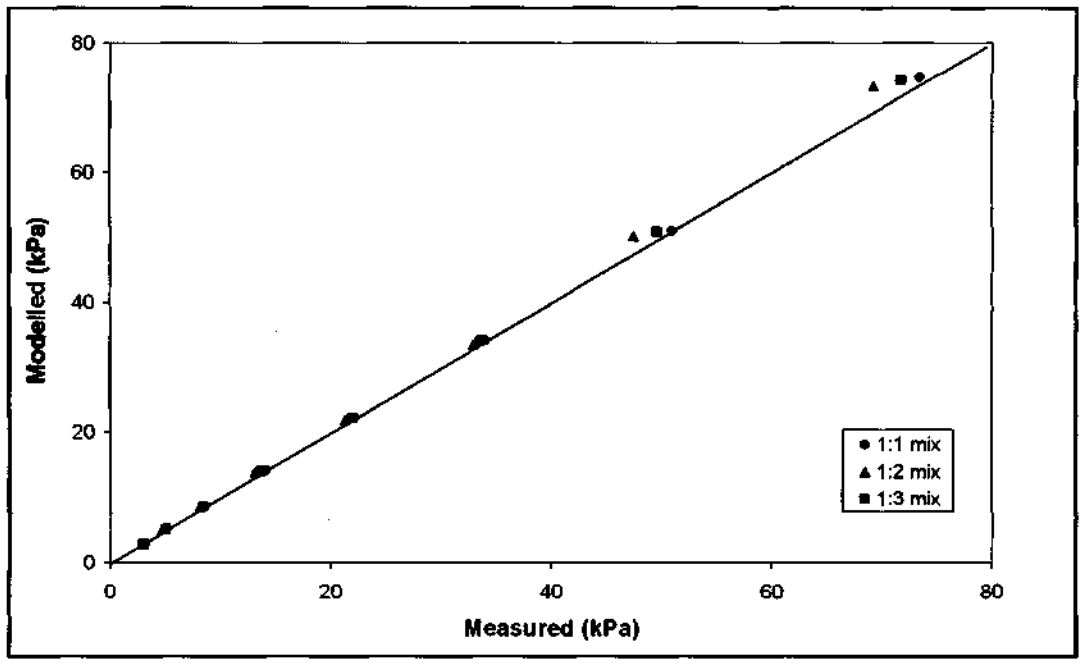

Figure 5.13: *Comparison between modelled and measured vapour pressures for each of the salt mixes*

The relative errors between the vapour pressures modelled and those obtained experimentally range between -0.0014 to 0.096 for the 1:1 mix, -0.019 to -0.058 for the 1:2 mix and -0.014 to -0.033 for the 1:3 mix. There is therefore excellent agreement between the modelled data and those obtained experimentally through VLE measurements. The larger deviations are those at higher vapour pressures. This is due to the limitation of the input data to PHRQPITZ, with regards to the uncertainty in PHRQPITZ calculations above 60°C (cf. **Section 4.2.1.1**). This uncertainty, however, does not affect the outcome of the results in this study as the maximum retentate temperature did not exceed 33 °C and it is seldom that MD, in general, would operate at temperatures above 60 °C. It therefore appears that the vapour pressures of concentrated mixed salt solutions of sodium chloride and magnesium sulphate can be sufficiently accurately modelled using PHRQPITZ.

5.2.3 Evaluation of driving force using PHRQPITZ

Knowing the temperature and concentration of the inlet and outlet retentate and distillate streams during the course of a batch concentration run, the vapour pressures of these streams were calculated at each time interval (water recovery level) during the MD process.

Figures 5.14 and 5.15 show the variation of the vapour pressures of each of the streams as indicated in the legend for the 1:1 and 1:2 mixes[1]. The pure retentate stream refers to the pure hot water that enters the module, i.e. the activity of water at the temperature of the brine at module inlet and outlet. The retentate stream on the other hand, refers to the activity of the brine according to its temperature when entering and leaving the module. The permeate streams refer to the cooling pure water streams at module inlet and outlet.

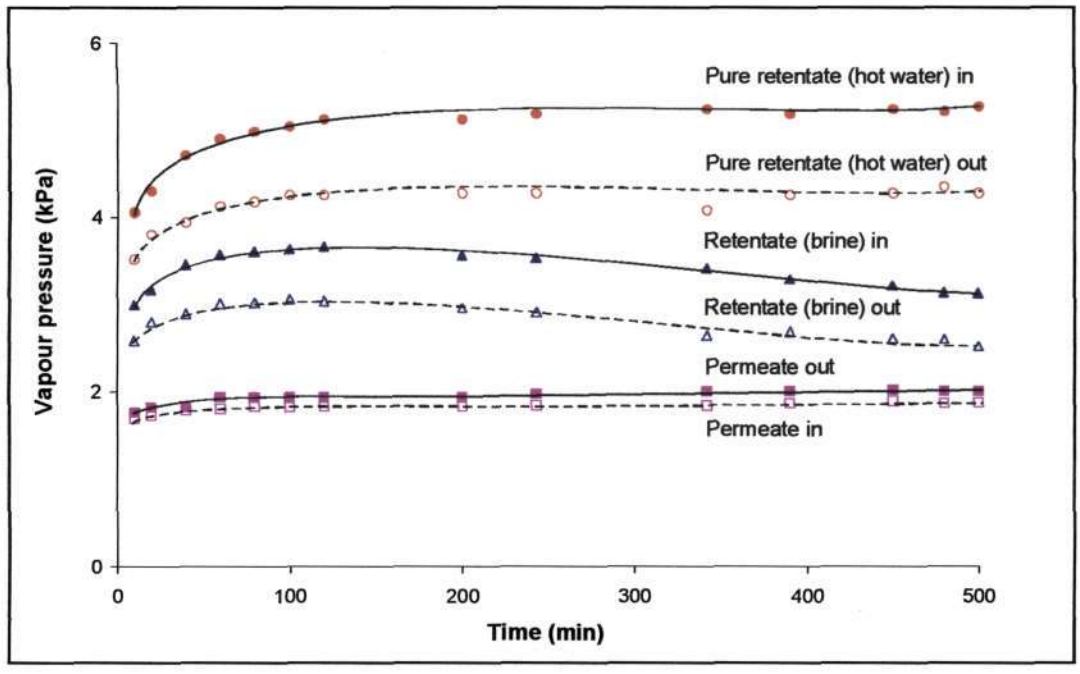

Figure 5.14: *Vapour pressures of respective streams in membrane distillation of a 1:1 mix, emphasising the significant change in activities of the pure water retentate streams at outlet and inlet of the membrane module. The curves labelled "pure retentate (hot water)" are calculated for pure water at the same temperatures as the brine at that point in the run.*

[1] *The vapour pressures for each stream for the 1:3 mix could not be completely evaluated as data were unavailable for the temperatures at the module outlet for the retentate and distillate streams due to some experimental difficulty. The calculations therefore performed for the evaluation of flux and driving force included the 1:1 and 1:2 mixes only.*

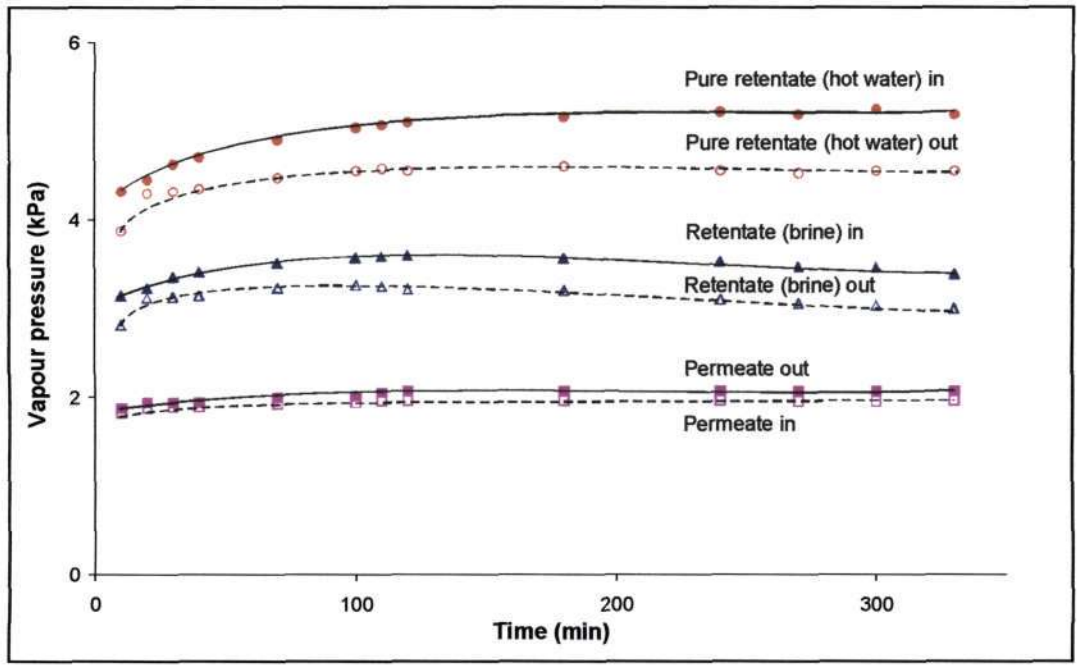

Figure 5.15: *Vapour pressures of respective streams in membrane distillation of a 1:2 mix*

The most salient feature of these plots is the significant difference in vapour pressures over time between the pure retentate streams at module inlet and outlet contrasted to the negligible difference between the pure water vapour pressures for the distillate at the module inlet and outlet (the gradual increase at the beginning of the distillation process up to approximately 100 mins, is again due the instability in temperature during the start of the process, cf. **Section 3.2.1.1**). It then follows that when determining the driving force for the process it becomes mandatory to take into account these changes in water activities of the pure rentetate streams. For this reason the logarithmic mean vapour pressure (ΔP_{lm}) differences between the high temperature and low temperature sides of the module were calculated when evaluating the driving force for the process (Equation 5.6).

$$\frac{(\text{Retentate in - distillate out}) - (\text{Retentate out - distillate in})}{\ln \dfrac{(\text{Retentate in - distillate out})}{(\text{Retentate out - distillate in})}} \qquad [5.6]$$

The logarithmic mean is generally considered as the most appropriate average driving force in a counter-current mass or heat transfer device. The log mean vapour pressure difference is plotted together with the transmembrane flux time relationships in Figures 5.16 and 5.17 for the 1:1 and 1:2 mixes, respectively.

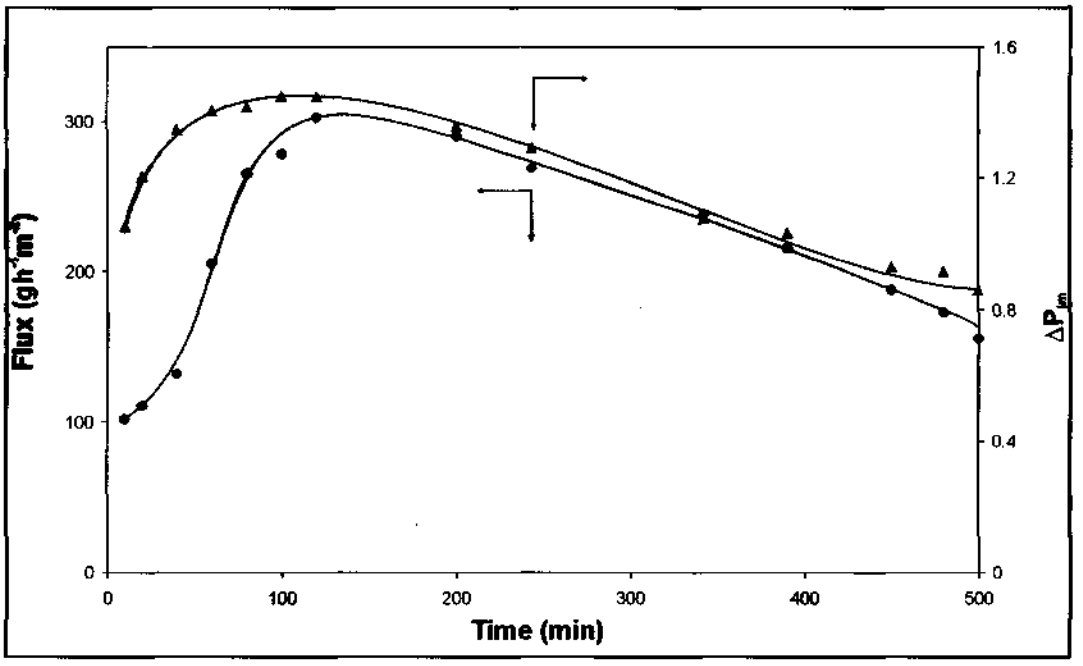

Figure 5.16: *Variation of transmembrane flux and the log mean vapour pressure driving force as a function of time for the 1:1 mix, indicating that the flux decline is due to a decline in driving force as seen from the similarity in these trends*

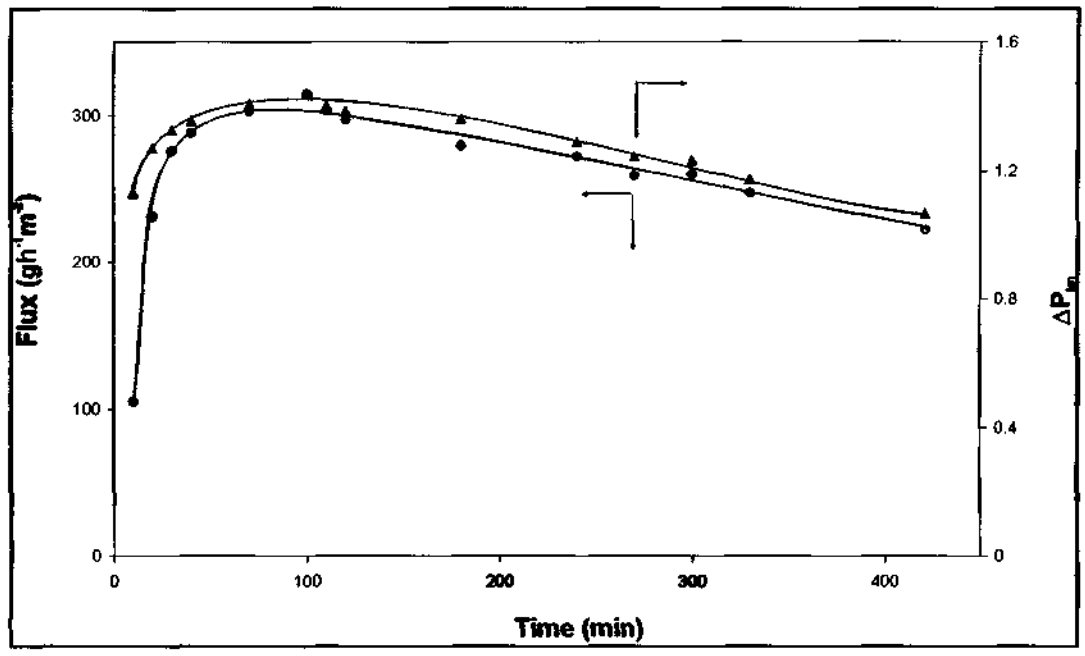

Figure 5.17: *Variation of transmembrane flux and the log mean driving force as a function of time for the 1:2 mix indicating the similarity in these trends*

Figures 5.16 and 5.17 reveal a marked similarity between the transmembrane flux and driving force for the process. The flux and driving force show a constant rise after which it slightly plateaus before rapidly declining. As previously described, the initial rise in flux is due to the stabilisation of concentration and temperature profiles as well as fluid dynamic conditions inside the membrane module. However, Figure 5.17 also demonstrates that a simultaneous rise in the driving force occurs during this period hence the relationship between flux and driving force also holds during this phase. As the initial solute content of the 1:2 mix (275 g/ℓ NaCl and 138 g/ℓ $MgSO_4$) is lower than that of the 1:1 mix (225 g/ℓ NaCl and 225 g/ℓ $MgSO_4$), the flux decline is less profound for the former as opposed to the latter as can be seen from their corresponding plots (Figures 5.16 and 5.17). From the relationships above, it can be deduced that one of the reasons for the decline in the transmembrane flux is due to a decline or loss of driving force for the process. This has been revealed by accounting for the activity of water at module inlet and outlet which seems to play an important role, particularly concerning concentrated salt solutions.

In Figure 5.18 the data are re-plotted to show the relationship between flux and vapour pressure driving force.

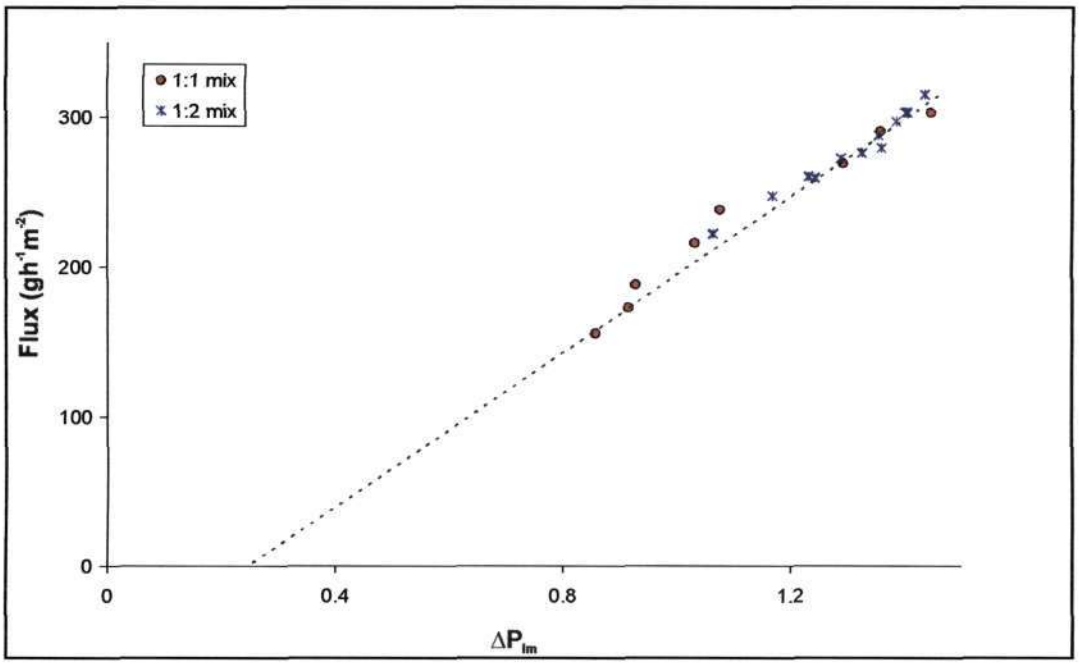

Figure 5.18: *Transmembrane flux as a function of log mean driving force during the distillation of 1:1 and 1:2 magnesium sulphate and sodium chloride solutions. The graph displays a non-zero intercept*

The initial steep rising parts of the curves in Figures 5.16 and 5.17 have been excluded in the construction of Figure 5.18 as it is believed that, because the temperatures were changing too rapidly to record an accurate measurement of the corresponding fluxes, this resulted in a lag in the measurement of flux relative to the measurement of temperature. A notable feature of the plot in Figure 5.18 is the non-zero intercept where the flux is zero, although the apparent vapour pressure driving force is positive. This can be explained as an interaction between the transmembrane concentration and temperature differences, conductive heat transfer and temperature polarization (Mariah et al., 2006a). In the case where the pure water and brine streams are at the same temperature, the brine vapour pressure is depressed by the salt concentration, causing a reverse flux of water across the membrane - i.e. from the pure water side to the brine side. As the brine temperature is raised, its vapour pressure is raised, counteracting the concentration effect. At the point where the temperature effect balances the concentration effect exactly, the flux is zero, which is the intercept point on the graph. Because there is no mass flux at this point, there is no concentration polarisation; however the temperature difference across the membrane causes a conductive heat flux across the

membrane, so there is temperature polarisation. This means that the difference between the bulk temperatures of the brine and water streams is greater than the difference between the temperatures at the membrane surfaces. Hence the apparent vapour pressure driving force, calculated from the bulk stream temperatures, is greater than the true driving force based on the membrane surface temperatures. This effect is usually negligible for dilute solutions, but has been observed in concentrated solutions by other investigators (Walton et al., 2004).

5.3 PREDICTION OF HIGH WATER RECOVERIES

Having obtained a way to accurately estimate the vapour pressures, it becomes possible to predict the course of a batch MD by accounting for the continual concentration of salts in the solution, which subsequently decreases the vapour pressure and hence the driving force. In Figure 5.19 the starting solution is that of the 1:1 mix with a brine temperature of 55 °C and a pure water temperature of 20 °C. The solution is modelled so as to calculate the saturation index (SI) of the salts at each water recovery level according to the experimental findings. Once crystallisation of sodium chloride begins, i.e. $SI_{NaCl} = 0$, the system is modelled so as to keep the SI of sodium chloride at 0 (by continual removal of the crystals) while the concentration of magnesium sulphate increases. The saturation index (SI) of a salt is defined as the logarithm of the ratio of the ion activity product (IAP) and the solubility product (K_{sp}), Equation 5.7.

$$SI = \log \frac{IAP}{K_{sp}T} \qquad [5.7]$$

If the crystals are continually removed from the re-circulating solution, Figure 5.19 illustrates how the initial rapid decline in driving force is changed to a subtle decline once crystal disengagement begins at a concentration factor of approximately 1.2. Previously, when the crystals were not removed from the re-circulating solution, part of the crystals was re-circulated back to the membrane module causing the flux to rapidly fall to zero once crystallisation began and bringing the process to a halt. Figure 5.19 shows that the continuous removal of the crystallised salt enables the process to proceed for an extended period of time.

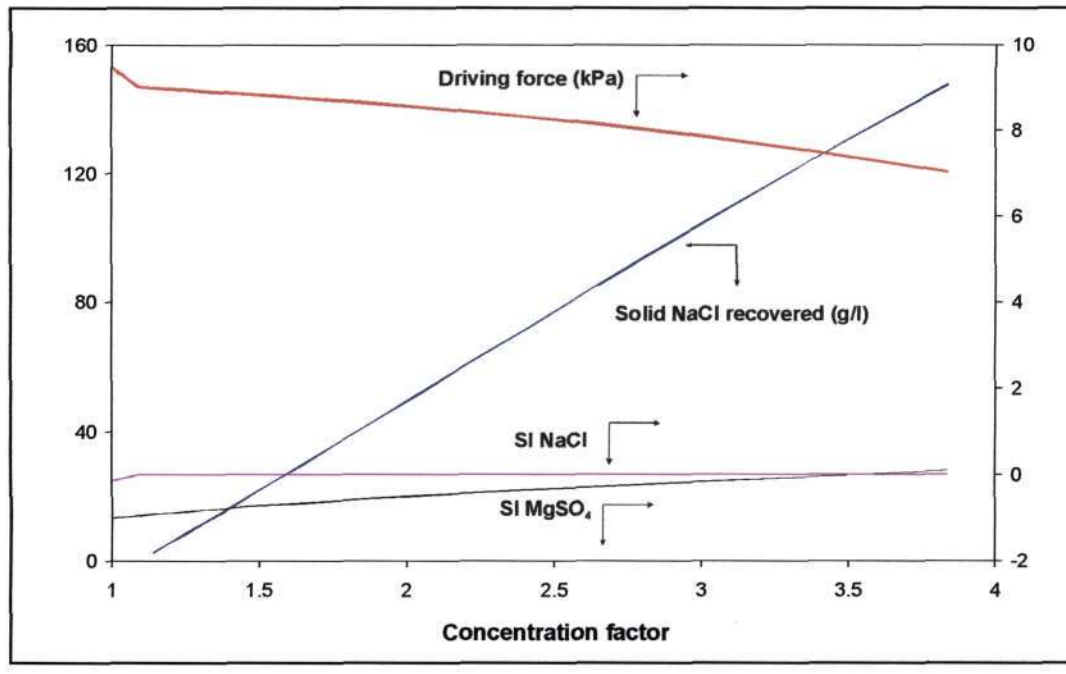

Figure 5.19: *Evolution of flux with the saturation index of epsomite and sodium chloride for the 1:1 mix obtained from modelling using PHRQPITZ*

It can be seen that MD can concentrate the solution up to the point of sodium chloride crystallisation and beyond with approximately 150 g/L of pure crystalline sodium chloride being recovered and a 74 % water recovery being achieved before epsomite would start to precipitate, while still maintaining an existent vapour pressure driving force. It was calculated that in order for RO to produce a positive driving force at these concentrations, a minimum pressure of approximately 44 MPa has to be applied before the osmotic pressure barrier is overcome, to obtain a resultant driving force (Mariah et al., 2006b).

5.4 CONCLUSIONS

The investigations performed in this Chapter have revealed one of the mechanisms of the flux decline that occurs during the MD of concentrated salt solutions described in Chapter 3 - the key aspect being the difference in the water activities at module inlet and outlet which must be accounted for when evaluating the driving force for the process. The complexity of performing thermodynamic calculations such as activity and vapour pressure evaluations on solutions of strong electrolytes is alleviated by the use of a speciation program incorporating the algorithm

for these calculations within the program code. This program therefore provides a means of calculating the fundamental solution parameters for the MD process, i.e. the vapour pressure, which otherwise cannot be performed during the process itself. PHRQPITZ can model and predict changes in the MD process.

5.5 CHAPTER REFERENCES

JOSEPH MA, RAAL JD and RAMJUGERNATH D (2001) *Phase equilibrium properties of binary systems with diacetyl from a computer controlled vapour-liquid equilibrium still.* Fluid Phase Equilibria **182** 157-176.

LIU C and LINDSAY WT (1972) *Thermodynamics of sodium chloride solutions at high temperatures.* J Soln Chem **1** 45-69.

MARIAH L, BUCKLEY CA, BROUCKAERT CJ, CURCIO E, DRIOLI E, JAGANYI D, and RAMJUGERNATH D (2006a) *Membrane distillation of concentrated brines – role of water activities in the evaluation of driving force.* J Membr Sci. **280** (1-2) 937-947.

MARIAH L, BUCKLEY CA, BROUCKAERT CJ, JAGANYI D, CURCIO E and DRIOLI E (2006b) *Membrane distillation for the recovery of crystalline products from concentrated brines.* WISA Biennial Conference, Durban, South Africa, 21-25 May.

PLUMMER LN, PARKHURST DL, FLEMING GW and DUNKLE SA (1988) *A computer program incorporating Pitzer's equations for calculation of geochemical reactions in brines,* US Geological Survey, Water-Resources Investigations Report 88-4153, Reston, Virginia.

RAAL JD and MÜHLBAUER AL (1998) *Phase equilibria: measurement and computation.* Taylor and Francis, Washington DC. ISBN: 1-560-32550-X.

ŞEKER E and SOMER TG (1993) *Vapour-liquid equilibrium still – a new design.* Meas Sci Technol **4** 776-779.

SPARROW BS (2003) *Empirical equations for the thermodynamic properties of aqueous sodium chloride.* Desalination **159** 161-170.

WALTON J, LU H, TURNER C, SOLIS S and HEIN H (2004) *Solar and waste heat desalination by membrane distillation*. Desalination and Water Purification Research and Development Program Report No. 81. Agreement No. 98-FC-81-0048. U.S. Department of Interior, Bureau of Reclamation, Denver Federal Center, USA.

Chapter 6

Chapter 6

CONCLUSIONS

6.1 CONCLUDING REMARKS

The investigations performed in this work dealt with the batch membrane distillation of concentrated mixed brines for the recovery of crystalline products. The main focus of this study was to evaluate the driving force during the experiments in order to determine whether this correlated with the declining flux that is experienced during a batch membrane distillation experiment. Furthermore, as the measurement of vapour pressures during the membrane distillation experiment is not a readily accomplishable task, a method to evaluate vapour pressures and hence driving forces during MD would be invaluable to the membrane researcher. In terms of the original objectives of this study described in Chapter 1, the following conclusions can be drawn:

- The membrane distillation of concentrated solutions of single and mixed salts is possible. MD was capable of producing water and solid crystalline products from high ionic strength (exceeding 5 m) solutions and at average feed and distillate temperatures of 33 °C and 17 °C, respectively and at atmospheric pressure. At these high ionic strengths the osmostic pressure would be approximately 44 MPa and hence a minimum applied pressure of this order and over would be required to obtain a resultant flux during reverse osmosis processes (Mariah et al., 2006).

- Using a geochemical speciation program specific for modelling high ionic strength electrolyte solutions, the vapour pressures of the concentrated salt solutions subject to MD can be suitably accurately modelled. The current database for this computer program is limited to a temperature range of 0 to 60 °C which is sufficient for our system, and MD in general, as seldom an operating temperature of 40 °C is exceeded.

- The trend of driving force is similar to the distillate flux during a typical batch MD experiment. We can therefore conclude that one of the reasons for the MD flux decline is due to the decline in the vapour pressure driving force. Furthermore, it has been found that for concentrated solutions the activities of water at outlet and inlet of the membrane module must be accounted for when attempting to evaluate the driving force for the process. The magnitude of the ionic strength of the solutions also plays an important role when correlating the distillate flux with the driving force in that the graph of the latter displays a non-zero intercept due to the effects of simultaneous heat and mass transfer. This causes the temperatures and vapour pressures at the membrane surface to be different from those in the bulk thus giving rise to temperature polarisation. Because of the conductive heat transfer through the membrane, this discrepancy occurs even when there is no flux of vapour through the membrane, which accounts for the non-zero intercept. This effect is usually negligible for dilute solutions, but for concentrated solutions is more pronounced.

The ability to model vapour pressures and hence driving forces during a MD experiment enables predictions of changes during the MD process and of water and salt recoveries. Preliminary modelling have revealed that, if the crystallising salt is continuously removed from the recirculating solution, the driving force for the process can be extend up to very high water and salt recoveries. Furthermore, these recoveries can be performed by retentate and distillate temperatures of 55 and 20°C, respectively and, as is the case in many industries, an excess of low-grade thermal energy could be used for this energy requirement thus making MD a more economic process as opposed to processes such as RO which would require exceptionally high applied pressures in order to overcome the osmotic pressure barriers when concentrating solutions with the same magnitude of ionic strength. Therefore MD fulfils the major concepts of green chemistry by not making use of hazardous starting materials or reagents, being an energy conserving process and furthermore, the crystalliser stage enables the recovery of crystalline products as such both the cost and environmental impacts of brine disposal can be considerably reduced (as valuable end products could be made from these purified salts or used as a substitute for raw material process streams) thus moving towards sustainable industrial growth.

6.2 RECOMMENDATIONS FOR FUTURE WORK

An evaluation of the kinetics of crystallisation of the salts is necessary to complete the understanding of the process. These need to be well understood as the process must avoid crystallisation in the membrane module (which is another proposed mechanism of flux decline, Tun et al., 2005) while producing a high quality final product which influences the performance of downstream processes (solid-liquid separation steps, drying and storage).

6.3 CHAPTER REFERENCES

MARIAH L, BUCKLEY CA, BROUCKAERT CJ, JAGANYI D, CURCIO E and DRIOLI E (2006) *Membrane distillation for the recovery of crystalline products from brines*, WISA Biennial Conference, Durban, South Africa, 21-25 May 2006.

TUN CM, FANE AG, MATHEICKAL JT and SHEIKHOLESLAMI R (2005) *Membrane distillation crystallization of concentrated salts – flux and crystal formation*. J Membr Sci **257** 144-155.

Appendix A

Appendix A

MODELLING

This Appendix provides a summary of the PHRQPITZ computer programming procedures. Obtaining the program is described, followed by a description of options that are available for modelling in the PHRQPITZ database and choice of appropriate options according to the desired output. Examples of input and output files are provided together with an explanation of the important results and how PHRQPITZ could be used for solving specific geochemical-related problems.

A.1 OBTAINING PHRQPITZ

PHRQPITZ can be downloaded from the USGS website at the following URLs:

http://wwwbrr.cr.usgs.gov/projects/GWC_coupled/phrqpitz/

http://wwwbrr.cr.usgs.gov/projects/GWC_coupled/phreeqc/index.html[1]

Part of the PHRQPITZ software is an application called PITZINP.exe which allows easy creation of input files for PHRQPITZ. The following sections serve as an explanation of the various options available for modelling using PHRQPITZ.

A.2 CREATING AN INPUT FILE IN PITZINPT

The PITZINPT file can be run from Windows Explorer. The program offers a number of options for data input. It is best to read through the following questions first and decide which options are appropriate before running the program, as there is no way to *undo* and the program has to be rerun from the beginning if one makes a mistake. Italics indicate text shown by the program.

[1] *The PHRQPITZ program itself has become obsolete during the time of writing this thesis as the original PHREEQC program has been modified to include the Pitzer activity coefficient model in the pitzer.dat database, eliminating the need for a separate program. New users are directed to PHREEQC version 2.12.*

Name of PHRQINPT database file? Default: pitzinpt.dat

Unless there is a reason to change the database file, hit return.

Name of PHRQPITZ database file? Default: phrqpitz.dat

Unless there is a reason to change the database file, hit return.

Enter name of output file (input to PHRQPITZ). Default: phrqpitz.inp

This is the name of the file that PITZINPT will generate and which can be used as an input file for PHRQPITZ. If you reject to type in a new file name, the existing one will be overwritten.

Enter reference file name: <hit <cr> to omit>

This option allows you to call up a previous file to use as a reference. Hitting return with no file name will pass this option.

Input the title

A title which will be displayed on the output file.

The next section covers the various options for modelling:

Input IOPT(1)

Options are:

0 No print of thermodynamic data or coefficients of aqueous species.

1 Print the aqueous model data (which are stored on disk) once during the entire computer run.

Input IOPT(2)

Options are:

0 Initial solutions are not to be charge balanced. Reaction solutions maintain the initial charge imbalance.

1 pH is adjusted in initial solutions to obtain charge balance.

2 The total concentration of one of the elements (except H or O) is adjusted to obtain electrical balance. Neutral input is required.

Input IOPT(3)

Options are:

0 No reactions modelled. Only the initial solutions are solved.

1 Solution 1 is mixed (a hypothetical constant volume process) with solution 2 in specified reaction steps. **Steps** input and a value for *nsteps* are required. Minerals input may be included.

2 Solution 1 is titrated with solution 2 in specific reaction steps. **Steps** input, a value for *nsteps* and a value for *V0* are required. Minerals input may be included.

3 A stoichiometric reaction is added in specified reaction steps. **Reaction** input, **Steps** input, a value for *nsteps* and a value for *ncomps* are required. Minerals input may be included.

4 A net stoichiometric reaction is added in *nsteps* equal increments. **Reaction** input, **Steps** input, a value for *nsteps* and a value for *ncomps* are required. Minerals input may be included. Only one value for the total reaction is read in **Steps.**

5 Solution 1 is equilibrated with mineral phases only. No other reaction is performed. **Minerals** input is required.

6 A reaction is added to solution 1 until equilibrium is attained with the first phase in mineral input (equilibrium with other minerals is maintained throughout the reaction). **Reaction** input, a value for *ncomps*, and **Minerals** input are required. No **Steps** input is required. Note: there should be a common element in the reaction and the first phase in **Minerals** input.

Input IOPT(4)

Options are:

0 The temperature of the reaction solution is: (a): the same as the initial solution if adding a reaction, or (b): calculated linearly from the end members if mixing or titrating. No **Temp** input is required.

1 The temperature is constant during the reaction steps and differs from that of the initial solution(s). One value is read in **Temp** input.

2 The temperature is varied from T(0) to T(F) in *nsteps* equal increments, during the reaction steps.

3 The temperature of each reaction step is specified in **Temp** input, in order. *Nsteps* values are needed.

IOPT(5)

This option is automatically set and does not appear but its explanation is as below.

0 The pe of the initial solution (defined to be 4.0 if PITZINPT is used to construct input sets) is held constant during all the reaction steps for the simulation. Redox reactions are currently not considered.

IOPT(6)

This option is also automatic.

2 Activity coefficients are calculated according to the Pitzer model. No other options are available.

Input IOPT(7)

Options are:

0 Do not save the aqueous phase composition at the end of a reaction for additional simulations.

1 Save the final reaction solution in solution number 1.

2 Save the final reaction solution in solution number 2.

Input IOPT(8)

Options are:

0 The debugging print routine is not called.

1 A long printout is output at each iteration in each problem. This print is to be used only if there are convergence problems with the program (see subroutine Pbug).

Input IOPT(9)

Options are:

0 No printout of each array inverted.

1 A long printout occurs of the entire array to be inverted at each iteration. This print is to be used only if there are convergence problems (see subroutine SLNQ).

Input IOPT(10)

Options are:

0 No convention for activity coefficient is used.

1 MacInnes convention is used.

Input nsteps

Number of steps. A value is required if **IOPT(3)** = 1, 2, 3 or 4 or if **IOPT(4)** = 2 or 3.

Input V0

Initial volume of solution 1 when modelling a titration. This unit of *V0* must be the same as that of *nstep* (see **Steps** input) if IOPT(3) = 2. Otherwise *V0* is not required.

Input ncomps

The number of constituents in a net stoichiometric reaction. A constituent may be any element with an index number between 4 and 30 inclusive. No aqueous species with index numbers >30 may be included as reaction constituents except H_2 and O_2. Any constituent with index number greater than 30 is assumed to be either H_2 or O_2 and has the effect of raising or lowering the redox state of the solution depending on the assigned valence (*thmean*). A value for *ncomps* is required if **IOPT(3)** = 3, 4 or 6.

Keyword data blocks

There are 11 keywords which can be used to design the modelling input. These are described below.

ELEMENTS

Defines a name and index of all elements in the aqueous model database.

Input tname

Alphanumeric name of element. Type **LIST** to bring up a list of the elements currently in the database (Table A.1).

Input NELT

Index number assigned to element. Number must be between 4 and 30 inclusive.

Input TGFW

GFW of species used to report analytical data. If solution data is to include alkalinity, *TGFW* for element C must be the equivalent weight of the reported alkalinity species.

Table A.1: *Elements in the PHRQPITZ database*

Elements	Index number	Gram formula weight (GFW)	Input formula corresponding to GFW	Master species	OPV
*****	1	0	*****	*****	+0.00
*****	2	0	*****	*****	+0.00
*****	3	18.0152	*****	*****	+0.00
Ca	4	40.0800	Ca^{2+}	Ca^{2+}	+0.00
Mg	5	24.3050	Mg^{2+}	Mg^{2+}	+0.00
Na	6	22.9898	Na^{+}	Na^{+}	+0.00
K	7	39.0983	K^{+}	K^{+}	+0.00
Fe	8	55.8470	Fe^{2+}	Fe^{2+}	+2.00
Mn	9	54.9380	Mn^{2+}	Mn^{2+}	+2.00
Ba	11	137.330	Ba^{2+}	Ba^{2+}	+0.00
Sr	12	87.6200	Sr^{2+}	Sr^{2+}	+0.00
Cl	14	35.4530	Cl^{-}	Cl^{-}	+0.00
C	15	44.0098	CO_2	CO_3^{2-}	+4.00
S	16	96.0600	SO_4^{2-}	SO_4^{2-}	+6.00
B	18	10.8100	B	$B(OH)_3$	+0.00
Li	21	6.9410	Li^{+}	Li^{+}	+0.00
Br	22	79.9040	Br^{-}	Br^{-}	+0.00

SPECIES

Defines names, index numbers and composition of all aqueous species in the aqueous model data base.

Input I

Index number assigned to aqueous species. Numbers 4 through 30 are reserved for master species. 250 is the maximum index number for an aqueous species.

Input SNAME

Alphanumeric species name

Input NSP

Total number of master species in the association reaction that forms this species. Do not count the species itself unless the species is a master species.

Input KFLAG

Options are:

0 Van't Hoff expression is used to calculate temperature dependence of the association constant for this species.

1 An analytical expression is used to calculate temperature dependence of the association constant.

Input GFLAG

Options are:

0 The extended Debye-Hückel or Davis expression (according to **IOPT(6)**) is used to calculate the activity coefficient for this species.

1 The Wateq-Debye-Hückel expression is used to calculate the activity coefficient for this species (regardless of the value of **IOPT(6)**).

Input ZSP

Charge on this aqueous species.

Input DHA

The extended Debye-Hückel A-0 term.

Input ALKSP

The alkalinity assigned to this aqueous species.

Input LKTOSP

Log K at 25°C where $\log K = A1 + A2(T) + A3/T + (A4 * \log(T)) + A5/T^2$

Input DHSP

Standard enthalpy of association reaction at 25°C (H(R), in kcal/mol).

SOLUTION

Used to define starting solution.

Input solution number

A number, either 1 or 2, indicating the solution number of the following data.

Input solution heading

Title or comments about the solution.

Input NTOTS

The number of total concentrations to be read from card input, for example, if the starting solution is $MgCl_2$-$NaHCO_3$ solution, *NTOTS* = 4 (for Mg, Cl, Na and C).

Input IALK

Flag which indicates whether total C or total alkalinity is to be input.

0 indicates total concentration of C (not alkalinity) is input in the units specified by *IUNITS*.

N 4<N<30 where N is the index number for the element C (in PHRQPITZ.DATA, N = 15), indicates total alkalinity is being entered. **Elements** input may be required. The units of alkalinity are specified by *IUNITS* and if *IUNITS* > 0, the GFW of the element C is critically important. The GFW in the case of alkalinity must be the gram equivalent weight (g/equivalent) of the chemical species in which alkalinity is being reported. The following is a list of species commonly used for reporting alkalinity and their corresponding equivalent weight:

$CaCO_3$ = 50.0446 g/eq

HCO_3^- = 61.0171 g/eq

CO_3^{2-} = 30.0046 g/eq

In PHRQPITZ.DATA, 44.010 is the GFW of C which is suitable for entering C as total CO_2. This GFW must be changed via **Elements** input if alkalinity is to be entered as mg/l or ppm (*IUNITS* = 2 or 3). If *IUNITS* = 0, alkalinity must be input as eq/kg H_2O and in this case the GFW need not be changed since no conversion is necessary.

Input IUNITS

Flag describing units of input concentrations. The program makes all of its calculations in terms of molality and any other allowed concentration units (mmol/ℓ, mg/ℓ, ppm or mmol/kg) must be converted to molality before calculation may begin. To make the conversions it is necessary to know the GFW in g/mole of the chemical formula in which elemental analyses are reported. The GFW is an input parameter under **Elements** input and must be in agreement with the analytical units for each solution dataset. (If the units are molality, no conversion is necessary and the GFW's are not used). Note: All elements must have the same units. It is not possible to enter mg/l of one element and molality of another.

0 concentration of elements entered as molality of each element, or for alkalinity, equivalents/kg H_2O.

1 concentration of elements entered as mmol/ℓ of each element, or for alkalinity meq/ℓ.

2 concentration of elements entered as mg/ℓ of the species which has a GFW given in **Elements** input (**Elements** input may be required).

3 concentration of elements entered as ppm of the species which has a GFW given in **Elements** input (**Elements** input may be required).

4 concentration of elements entered as mmol/kg solution.

Input pH

The pH of the solution (estimate if *IOPT(2)* = 1)

Input PE (automatic)

Automatically set at 4.0 as PHRQPITZ does not currently treat redox reactions.

Input Temp

Temperature of solution in °C.

Input LT(NTOTS)

LT = index number of element N

Input DTOT(NTOTS)

Total concentration of the element in molality, mmols/kg, mg/ℓ or ppm according to *Iunits*.

MINERALS

Defines phases which will be maintained at equilibrium with each of the reaction solutions. *Pre-constructed mineral data are available. Do you wish to have any of them?* (see Table A.2).

Table A.2: *Minerals in the PHRQPITZ database*

1. Anhydrite	2. Aragonite	3. Arcanite	4. Bischofite	5. Bloedite
6. Brucite	7. Burkeite	8. Calcite	9. Carnallite	10. Dolomite
11. Epsomite	12. Gaylussite	13. Glaserite	14. Glauberite	15. Gypsum
16. Halite	17.Hexahydrite	18. Kainite	19. Kalcinite	20. Kieserite
21. Labile S	22. Leonhardite	23. Leonite	24. Magnesite	25. Mirabilite
26. Misenite	27. Nahcolite	28. Natron	29. Nesquehonite	30. P_{CO2}
31. Pentahydrite	32. Pirssonite	33. Polyhalite	34. Portlandite	35. Schoenite
36. Sylvite	37. Syngenite	38. Trona	39. Borax	40. B-Acid, S
41. KB5O84W	42. K2B4O74W	43. NABO24W	44. NAB5O85W	45. Teepleite

More minerals to be typed in from the terminal?

Input MNAME

Alphanumeric name of mineral

Input NMINO

Number of different species in the mineral dissociation reaction (including H^+, e^-, and H_2O). *NMINO* must be ≤ 10.

Input LKTOM

Log of the equilibrium constant at 25°C for reaction

Input DHMIN

Delta H_r° (Kcal/mol) for the Van't Hoff expression

Input MFLAG

0 The Van't Hoff expression is used to calculate the temperature dependence of the equilibrium constant.

1 The analytical expression is used to calculate the temperature dependence of the equilibrium constant.

Input SIMIN

Saturation index (log IAP/K_{sp}) desired in the final solution. *SIMIN* = 0.0 would result in equilibrium with the mineral while 1.0 would produce a solution 10 times supersaturated (SI = 1.0). This variable is useful in specifying the partial pressure of a gas. The Henry's Law constant for the gas would be entered using the Van't Hoff (*LKTOM*) or analytical expression (*AMIN*) and the log of the partial pressure would be entered for *SIMIN*.

Input LMIN(NMINO)

Index number of species (not necessarily master species) in the dissociation reaction for this mineral.

Input CMIN(NMINO)

Stoichiometric coefficient of species in dissociation reaction.

LOOKMIN

Provides information on the saturation state of aqueous phases with respect to desired minerals. Minerals in this block of input do not affect calculations of initial solution or any of the reaction solutions. Never mandatory.

Do you want to delete all old minerals?

Input variables as for **Minerals** keyword block.

TEMP

Varies temperature during reaction steps. It is not required when IOPT(4) = 0.

Input XTEMP(NSTEP)

Temperature in degrees C.

STEPS

Defines steps of reaction process. Not required when IOPT(3) = 0, 5 or 6.

Input XSTEP(NSTEP)

The value of XSTEP will vary depending on IOPT(3).

1 The fraction of solution 1 to be mixed with solution 2

2 Volume of solution 2 to be titrated into solution 1. Units must be the same as V0

3 The moles of reaction to be added to solution 1.

4 Total number of moles of reaction to be added in *NSTEPS* steps. *NSTEPS* reaction solutions will be calculated. The i^{th} solution will have *I XSTEP/NSTEPS* moles of reaction added to solution 1.

REACTION

Describes the stoichiometry and valence of elements to be added as reaction.

Input LREAC(1)

Index number of element for the reaction. *LREAC* must be between 4 and 30 inclusive. If *LREAC*>30 the program considers this constituent to be H_2 or O_2 and only uses *CREAC* and *THMEAN* to change the oxidation state of the reaction solution.

Input CREAC(1)

Stoichiometric coefficient of element in reaction.

NEUTRAL

Thus input defines elements to be used to adjust the initial solutions to electrical neutrality (i.e. IOPT(2) =2).

Input LPOS

Index number of an element with a cation master species.

Input LNEG

Index number of an element with an anion master species.

SUMS

Sums the molalities of aqueous species which are then printed in the output of reaction. These sums do not affect the calculations in any way and are never mandatory.

Do you want to delete all old sums?

Input SUNAME

Alphanumeric name to be printed to identify reaction.

Input NSUM

The number of index numbers to be read (<50)

Input LSUM(NSUM)

Index numbers of species in sum.

END

Terminates input operations for a single simulation. Any computer run has at least one end line.

More simulations?

If yes...

Do you wish to define the previous output as your new reference?

Enter reference file name? Etc, etc.....

A.3 EXAMPLE OF PHRQPITZ INPUT FILE

Table A.3 shows a typical input file for a basic speciation of a solution of magnesium sulphate and sodium chloride. Below is an explanation of each line.

Table A.3: *Input file for PITZINPT*

```
MD process for retentate temperatures
0000020000 0 0        0.0
SOLUTION 1
time=0
 4   0 0    7.          4.0       29.2        1.0
   5 1.164        16 1.164          6 4.926        14 4.926
END
```

Where: Line(1): Title

Line(2): Iopt(1); Iopt(2); Iopt(3); Iopt(4), Iopt(5), Iopt(6), Iopt(7), Iopt(8), Iopt(9), Iopt(10), Nsteps; Ncomps V.O.

Line(3): Keyword "Solution" plus solution number

Line(4): Solution heading

Line(5): Ntots; Ialk; Iunits; pH; pe; Temp; Solution number

Line(6): Concentration input in format: Index number of element (from Table A1); Total concentration of element in units according to *Iunits*

Table A.4 lists the corresponding output file associated with this run followed by an explanation.

Table A.4: *Output file from PHRQPITZ*

```
DATA READ FROM DISK

 ELEMENTS
 SPECIES
 LOOK MIN
 MEAN GAM
1MD process for retentate temperatures
 0000020000 0 0          0.00000
 SOLUTION 1
 time=0
  4   0 0      7.00       4.00       29.2       1.00
    5  1.164D+00  16  1.164D+00   6  4.926D+00  14  4.926D+00
1SOLUTION NUMBER 1
 time=0
                        TOTAL MOLALITIES OF ELEMENTS
                        ----- ---------- -- --------

                ELEMENT          MOLALITY         LOG MOLALITY

                MG             1.164000D+00           0.0660
                NA             4.926000D+00           0.6925
                CL             4.926000D+00           0.6925
                S              1.164000D+00           0.0660


                      ----DESCRIPTION OF SOLUTION----

                                        PH =    7.0000
                              ACTIVITY H2O =    0.7379
                         OSMOTIC COEFFICIENT =  1.3853
                              IONIC STRENGTH =  9.5819
                                 TEMPERATURE = 29.2000
                                    PRESSURE =  1.0000 ATM
                                DENSITY OF H2O =  0.9959 G/CC
                            ELECTRICAL BALANCE = -8.2610D-05
                              TOTAL ALKALINITY =  8.2911D-05
                                   ITERATIONS =  1


                                 -----------------------
                                 DISTRIBUTION OF SPECIES
                                 -----------------------
                                                          UNSCALED          UNSCALED
  I  SPECIES   Z    MOLALITY   LOG MOLAL ACTIVITY  LOG ACT  GAMMA      LOG GAM

  1  H+       1.0  3.000E-08   -7.523   1.000E-07  -7.000  3.334E+00   0.523
  3  H2O      0.0  7.379E-01   -0.132   7.379E-01  -0.132  1.000E+00   0.000
  5  MG+2     2.0  1.164E+00    0.066   1.164E+00   0.066  1.000E+00   0.000
  6  NA+      1.0  4.926E+00    0.692   3.934E+00   0.595  7.985E-01  -0.098
 14  CL-     -1.0  4.926E+00    0.692   8.118E+00   0.909  1.648E+00   0.217
 16  SO4-2   -2.0  1.164E+00    0.066   2.985E-02  -1.525  2.565E-02  -1.591
```

31 OH-	-1.0	2.926E-07	-6.534	1.014E-07	-6.994	3.464E-01	-0.460
40 HSO4-	-1.0	2.707E-07	-6.568	3.199E-07	-6.495	1.182E+00	0.072
85 MGOH+	1.0	8.262E-05	-4.083	1.914E-05	-4.718	2.317E-01	-0.635

SPECIES	TOTAL MOL	UNSCALED ACTIVITY	UNSCALED TOTAL GAMMA
H+	3.0069D-07	1.0000D-07	3.3257D-01
MG+2	1.1640D+00	1.1641D+00	1.0001D+00
NA+	4.9260D+00	3.9336D+00	7.9855D-01
CL-	4.9260D+00	8.1182D+00	1.6480D+00
SO4-2	1.1640D+00	2.9851D-02	2.5645D-02
OH-	8.2911D-05	1.0136D-07	1.2225D-03

---- MEAN ACTIVITY COEFFICIENT ----

FORMULA	MEAN GAMMA
MGCL2	1.3953D+00
MGSO4	1.6015D-01
MG(OH)2	1.1434D-02
NACL	1.1472D+00
NA2SO4	2.5383D-01
NAOH	3.1245D-02
HCL	7.4032D-01
H2SO4	1.4155D-01

---- LOOK MIN IAP ----

PHASE	LOG IAP	LOG KT	LOG IAP/KT
BISCHOFI	1.0929	4.4421	-3.3493
BLOEDITE	-2.3225	-2.3470	0.0245
BRUCITE	-13.9223	-10.8753	-3.0469
EPSOMITE	-2.3831	-1.8309	-0.5523
HALITE	1.5043	1.5759	-0.0717
HEXAHYDR	-2.2511	-1.5850	-0.6662
KIESERIT	-1.5911	-0.1230	-1.4681
LEONHARD	-1.9871	-0.8870	-1.1001
MIRABIL	-1.6556	-1.0286	-0.6270
PENTAHYD	-2.1191	-1.2850	-0.8341

The first four keywords that appear, ELEMENTS, SPECIES, LOOK MIN and MEAN GAM were printed as appropriate data from the PHRQPITZ.DATA were read. The computed output begins with a print of the total molalities of all elements in Solution 1 followed by a description of the solution and distribution of species. Computed variables under the heading "Description of Solution" include the activity of water, osmotic coefficient, ionic strength, pressure (in atmosphere) together with the vapour pressure line of pure water (if the temperature is greater than 100 °C), the density of pure water at the given temperature and pressure, the electrical imbalance (in equivalents per kilogram H_2O), and the total concentration of inorganic carbon (moles per kg H_2O). The "Distribution of species" lists the molality, activity, and activity

coefficient (and log values) of all aqueous species in the PHRQPITZ.DATA file for which an input concentration was given. This output is followed by tables of total molalities, activities, activity coefficients, mean activity coefficients and saturation indices. The saturation indices are given under the heading LOOK MIN IAP as log(IAP/KT).

A.4 EVAPORATION MODELLING IN PHRQPITZ

PHRQPITZ can be used to determine the amount of water that needs to be extracted from a given starting solution in order to reach a stipulated mineral phase boundary (in this example the mineral phase is halite). For our series of experiments it is useful to know at what stage or exactly how much of water needs to be removed (by MD) before the crystallisation will begin. In PHRQPITZ evaporation of the solution is achieved by setting IOPT(3) = 6, *i.e.* specifying that a reaction will be added until the first mineral of MINERALS input is just saturated, and defining the reaction under REACTION input as water (LREAC(1) = 3 and CREAC (1) = 1.0). PHRQPITZ identifies this combination of input as the special case of evaporation (or dilution, if the starting solution is oversaturated with the first mineral of MINERALS input) and additional output is provided as seen in Table A.5 for the evaporation of a solution of magnesium sulphate and sodium chloride until the halite phase boundary is reached.

Table A.5: *Output from PHRQPITZ for the evaporation of a solution of NaCl and $MgSO_4$ until the halite phase boundary is reached*

```
DATA READ FROM DISK

 ELEMENTS
 SPECIES
 LOOK MIN
 MEAN GAM
1evaporation with halite saturation of 1:1 mix, 225g/l
 0060020000 0 1          0.00000
 SOLUTION 1
 MgSO4:NaCl, 1:1
  4  0 0      7.00       4.00       33.0       1.00
    5  1.869D+00  16  1.869D+00   6  3.850D+00  14  3.850D+00

 MINERALS
 HALITE      2      0.00        1.6       0.00          1              0.000
    6   1.00       14   1.00
  -7.1346E+02 -1.2012E-01  3.7302E+04  2.6246E+02 -2.1069E+06
            0      0.00       0.00       0.00          0              0.000
 REACTION
    3   1.000    0.000
1SOLUTION NUMBER 1
 MgSO4:NaCl, 1:1
```

TOTAL MOLALITIES OF ELEMENTS

ELEMENT	MOLALITY	LOG MOLALITY
MG	1.869000D+00	0.2716
NA	3.850000D+00	0.5855
CL	3.850000D+00	0.5855
S	1.869000D+00	0.2716

----DESCRIPTION OF SOLUTION----

PH =	7.0000
ACTIVITY H2O =	0.7488
OSMOTIC COEFFICIENT =	1.4037
IONIC STRENGTH =	11.3258
TEMPERATURE =	33.0000
PRESSURE =	1.0000 ATM
DENSITY OF H2O =	0.9947 G/CC
ELECTRICAL BALANCE =	-1.1625D-04
TOTAL ALKALINITY =	1.1668D-04
ITERATIONS =	1

DISTRIBUTION OF SPECIES

I	SPECIES	Z	MOLALITY	LOG MOLAL	UNSCALED ACTIVITY	LOG ACT	UNSCALED GAMMA	LOG GAM
1	H+	1.0	3.839E-08	-7.416	1.000E-07	-7.000	2.605E+00	0.416
3	H2O	0.0	7.488E-01	-0.126	7.488E-01	-0.126	1.000E+00	0.000
5	MG+2	2.0	1.869E+00	0.272	1.021E+00	0.009	5.463E-01	-0.263
6	NA+	1.0	3.850E+00	0.585	2.635E+00	0.421	6.845E-01	-0.165
14	CL-	-1.0	3.850E+00	0.585	8.217E+00	0.915	2.134E+00	0.329
16	SO4-2	-2.0	1.869E+00	0.272	5.995E-02	-1.222	3.208E-02	-1.494
31	OH-	-1.0	4.973E-07	-6.303	1.355E-07	-6.868	2.725E-01	-0.565
40	HSO4-	-1.0	3.935E-07	-6.405	7.155E-07	-6.145	1.818E+00	0.260
85	MGOH+	1.0	1.162E-04	-3.935	2.343E-05	-4.630	2.017E-01	-0.695

SPECIES	TOTAL MOL	UNSCALED ACTIVITY	UNSCALED TOTAL GAMMA
H+	4.3189D-07	1.0000D-07	2.3154D-01
MG+2	1.8690D+00	1.0210D+00	5.4629D-01
NA+	3.8500D+00	2.6354D+00	6.8451D-01
CL-	3.8500D+00	8.2172D+00	2.1343D+00
SO4-2	1.8690D+00	5.9951D-02	3.2076D-02
OH-	1.1668D-04	1.3552D-07	1.1614D-03

---- MEAN ACTIVITY COEFFICIENT ----

FORMULA	MEAN GAMMA
MGCL2	1.3551D+00
MGSO4	1.3237D-01
MG(OH)2	9.0325D-03
NACL	1.2087D+00
NA2SO4	2.4678D-01
NAOH	2.8196D-02
HCL	7.0299D-01
H2SO4	1.1981D-01

---- LOOK MIN IAP ----

PHASE	LOG IAP	LOG KT	LOG IAP/KT
BISCHOFI	1.0848	4.4307	-3.3460
BLOEDITE	-2.0962	-2.3470	0.2508
BRUCITE	-13.7270	-10.8677	-2.8593
EPSOMITE	-2.0925	-1.7868	-0.3057
HALITE	1.3356	1.5803	-0.2448
HEXAHYDR	-1.9669	-1.5396	-0.4273
KIESERIT	-1.3388	-0.1230	-1.2158
LEONHARD	-1.7157	-0.8870	-0.8287
MIRABIL	-1.6367	-0.8721	-0.7646
PENTAHYD	-1.8413	-1.2850	-0.5563

1STEP NUMBER 1
0----------

TOTAL MOLALITIES OF ELEMENTS

ELEMENT	MOLALITY	LOG MOLALITY
MG	1.869000D+00	0.2716
NA	3.850000D+00	0.5855
CL	3.850000D+00	0.5855
S	1.869000D+00	0.2716

----PHASE BOUNDARIES----

MASS PRECIPITATED/DISSOLVED FROM INITIAL KILOGRAM WATER

PHASE	DELTA PHASE*	LOG IAP	LOG KT	LOG IAP/KT
HALITE	0.000000D+00	1.5803	1.5803	0.0000

+ **

* NEGATIVE DELTA PHASE INDICATES PRECIPITATION
AND POSITIVE DELTA PHASE INDICATES DISSOLUTION.

** 1.138248D+00 IS THE EVAPORATION FACTOR NECESSARY TO REACH THE HALITE PHASE BOUNDARY.

MOLES OF ELEMENTS REMAINING AFTER REACTION

ELEMENT	MOLES	LOG MOLES
MG	1.869000D+00	0.2716
NA	3.850000D+00	0.5855
CL	3.850000D+00	0.5855
S	1.869000D+00	0.2716

8.785435D-01 KILOGRAMS OF WATER REMAINING

---- LOOK MIN IAP ----

PHASE	LOG IAP	LOG KT	LOG IAP/KT
BISCHOFI	1.4534	4.4307	-2.9773
BLOEDITE	-1.6348	-2.3470	0.7122
BRUCITE	-14.0297	-10.8677	-3.1620
EPSOMITE	-1.9815	-1.7868	-0.1946
HALITE	1.5803	1.5803	0.0000
HEXAHYDR	-1.8262	-1.5396	-0.2866
KIESERIT	-1.0501	-0.1230	-0.9271
LEONHARD	-1.5158	-0.8870	-0.6288
MIRABIL	-1.6712	-0.8721	-0.7991
PENTAHYD	-1.6710	-1.2850	-0.3860

TOTAL MOLALITIES OF ELEMENTS

ELEMENT	MOLALITY	LOG MOLALITY
MG	2.127385D+00	0.3278
NA	4.382253D+00	0.6417
CL	4.382253D+00	0.6417
S	2.127385D+00	0.3278

----DESCRIPTION OF SOLUTION----

PH =	6.7613
ACTIVITY H2O =	0.6995
OSMOTIC COEFFICIENT =	1.5238
IONIC STRENGTH =	12.8916
TEMPERATURE =	33.0000
PRESSURE =	1.0000 ATM
DENSITY OF H2O =	0.9947 G/CC
ELECTRICAL BALANCE =	-1.1625D-04
TOTAL ALKALINITY =	1.1700D-04
ITERATIONS =	5

DISTRIBUTION OF SPECIES

I	SPECIES	Z	MOLALITY	LOG MOLAL	UNSCALED ACTIVITY	UNSCALED LOG ACT	UNSCALED GAMMA	UNSCALED LOG GAM
1	H+	1.0	4.671E-08	-7.331	1.733E-07	-6.761	3.709E+00	0.569
3	H2O	0.0	6.995E-01	-0.155	6.995E-01	-0.155	1.000E+00	0.000
5	MG+2	2.0	2.127E+00	0.328	1.750E+00	0.243	8.226E-01	-0.085
6	NA+	1.0	4.382E+00	0.642	3.232E+00	0.509	7.375E-01	-0.132
14	CL-	-1.0	4.382E+00	0.642	1.177E+01	1.071	2.686E+00	0.429
16	SO4-2	-2.0	2.127E+00	0.328	7.279E-02	-1.138	3.422E-02	-1.466
31	OH-	-1.0	2.738E-07	-6.563	7.306E-08	-7.136	2.669E-01	-0.574
40	HSO4-	-1.0	7.057E-07	-6.151	1.505E-06	-5.822	2.133E+00	0.329
85	MGOH+	1.0	1.167E-04	-3.933	2.165E-05	-4.665	1.854E-01	-0.732

SPECIES	TOTAL MOL	UNSCALED ACTIVITY	UNSCALED TOTAL GAMMA
H+	7.5242D-07	1.7327D-07	2.3029D-01
MG+2	2.1274D+00	1.7498D+00	8.2253D-01
NA+	4.3823D+00	3.2319D+00	7.3750D-01
CL-	4.3823D+00	1.1772D+01	2.6864D+00
SO4-2	2.1274D+00	7.2793D-02	3.4217D-02
OH-	1.1700D-04	7.3056D-08	6.2441D-04

---- MEAN ACTIVITY COEFFICIENT ----

FORMULA	MEAN GAMMA
MGCL2	1.8106D+00
MGSO4	1.6776D-01
MG(OH)2	6.8449D-03
NACL	1.4076D+00
NA2SO4	2.6501D-01
NAOH	2.1459D-02
HCL	7.8655D-01
H2SO4	1.2197D-01

The first paragraph in the initial section of the output (which actually is a portion of the input file) is the same as described above. The difference occurs in the second paragraph as a MINERALS input has been included. These lines described the characteristics of the mineral that has been defined. A REACTION has also been specified as described above and this is shown in the last few lines of the first section of the output file. PHRQPITZ performs the usual calculations on the initial solution and is described in the output under the various headings as before. However, in this case, the saturation step with halite appears under the heading "step number 1". After the print of mass transfer under the heading "phase boundaries", PHRQPITZ prints the evaporation factor necessary to reach saturation with the first mineral in the MINERALS input (halite). In this case the evaporation factor is 1.138 which means that the concentration of an inert component in the initial solution would increase by a factor of 1.138 upon evaporation to the phase boundary. PHRQPITZ also furnishes the output with the total moles of elements remaining with regards to the initial solution defined in solution 1 together with the amount of water remaining. The output is completed with a full description of the resulting solution.

APPENDIX B

Appendix B

DATA

This appendix provides the raw data that were used to process the results featured in Chapter 3 and Chapter 5 of this thesis. The data recorded during the MD of the salt mixes are presented first followed by that of the experiments performed using the VLE still. The method of linear regression using Antoine's equation to fit the experimental vapour pressure data is shown, together with the comparisons between literature and measured vapour pressures. Data used during the evaluation of the flux and driving force are also listed.

B.1 MEMBRANE DISTILLATION DATA

Table B.1 to B.5 provide the data that were collected during the membrane distillation of the individual and mixed salt solutions.

Table B.1: *MD of a 375 g/ℓ magnesium sulphate solution (initial solution volume = 3 ℓ)*

Time (h)	H_2O removed (g)	Ret. in temp. (°C)	Dist. in temp. (°C)	Flux (g/hm^2)	$[MgSO_4]$ (g/ℓ)
0.15	18.9	28.8	8.9	630.0	377.4
0.85	151.4	28.8	14.1	946.4	395.0
1.58	289.6	31.9	17.4	942.3	415.1
12.77	1900.2	30.3	20.6	720.1	1022.9
13.45	1992.7	31.2	20.5	676.8	1116.9
13.80	2027.6	31.1	20.3	498.6	1156.9
15.08	2163.2	30.0	20.0	259.6	1344.4
15.50	2181.9	30.0	19.8	224.4	1375.1
15.85	2202.6	30.2	19.7	166.7	1410.8
15.97	2206.3	30.1	19.7	158.6	1417.4
18.60	2194.0	17.6	13.0	56.1	1395.8
19.83	2196.8	17.9	11.2	11.4	1400.7

Table B.2: *MD of a 625 g/ℓ magnesium sulphate solution (initial solution volume = 2 ℓ)*

Time (h)	H_2O removed (g)	Ret. in temp. (°C)	Dist. Out temp. (°C)	Flux (g/hm^2)	$[MgSO_4]$ (g/ℓ)
0.10	11.8	38.2	16.0	590.0	628.7
0.43	53.7	47.2	17.7	628.5	642.2
1.15	141.4	44.3	20.6	611.9	672.6
1.93	224.4	44.3	22.1	529.8	704.0
2.55	285.9	44.4	22.9	498.6	729.3
3.82	390.5	44.6	23.0	412.9	776.6
4.67	463.5	44.3	24.0	376.4	813.5
5.55	525.6	44.2	24.1	351.5	847.8
5.83	544.6	44.1	24.2	335.3	858.9
6.45	579.1	44.1	24.1	279.7	879.7
7.18	619.7	44.0	23.8	276.8	905.6
7.93	660.0	44.1	23.6	268.7	932.8

Table B.3: *Data from the MD of a 1:1 salt mix*

Time (min)	H_2O removed (g)	Ret.in temp. (°C)	Ret.out temp. (°C)	Dist.in temp. (°C)	Dist.out temp. (°C)	Flux (g/hm^2)	[NaCl] (m)	$[MgSO_4]$ (m)
10	3.6	29.2	26.7	14.9	15.5	102.0	4.93	1.16
20	7.3	30.2	28.1	15.2	16.0	111.0	4.96	1.17
40	13.4	31.8	28.7	15.7	16.0	132.0	5.02	1.17
60	27.1	32.5	29.5	15.9	17.0	205.5	5.09	1.18
80	44.8	32.8	29.7	16.1	17.0	265.5	5.16	1.20
100	63.4	33.0	30.0	16.0	17.0	279.0	5.23	1.21
120	83.6	33.3	30.0	16.1	17.0	303.0	5.30	1.23
200	157.7	33.3	30.1	16.1	17.0	290.6	5.61	1.29
243	196.3	33.5	30.1	16.2	17.3	269.3	5.79	1.33
342	274.9	33.7	29.3	16.3	17.5	238.2	6.25	1.41
390	309.6	33.5	30.0	16.4	17.5	216.0	6.51	1.45
450	346.3	33.7	30.1	16.6	17.7	188.0	6.86	1.49
480	363.6	33.6	30.4	16.4	17.5	173.0	7.04	1.51
500	374.8	33.8	30.1	16.5	17.5	156.0	7.17	1.52

Table B.4: *Data from the MD of a 1:2 salt mix*

Time (min)	H_2O removed (g)	Ret.in temp. (°C)	Ret.out temp. (°C)	Dist.in temp. (°C)	Dist.out temp. (°C)	Flux (g/hm^2)	[NaCl] (m)	[$MgSO_4$] (m)
10	5.0	30.3	28.4	16.0	16.5	105.0	5.80	0.64
20	12.7	30.8	29.1	16.2	16.5	231.0	5.83	0.64
30	21.9	31.5	29.6	16.3	16.5	276.0	5.86	0.65
40	31.5	31.8	30.0	16.5	17.0	288.0	5.89	0.65
70	59.5	32.5	30.4	16.6	17.0	303.0	6.00	0.66
100	89.3	33.0	30.9	16.9	17.5	315.0	6.12	0.68
110	99.4	33.1	30.8	17.0	17.5	303.0	6.16	0.68
120	109.3	33.2	31.0	17.1	17.5	297.0	6.20	0.68
180	167.8	33.4	31.3	17.2	17.9	279.5	6.44	0.71
240	224.1	33.6	31.3	17.4	18.0	272.3	6.70	0.74
270	250.0	33.5	31.4	17.2	18.0	259.0	6.83	0.75
300	276.0	33.7	31.4	17.5	18.5	260.0	6.96	0.77
330	300.7	33.5	31.2	17.2	18.0	247.0	7.09	0.78
421	369.2	33.4	31.0	17.1	18.0	221.8	7.48	0.83

Table B.5: *Data from the MD of a 1:3 salt mix*

Time (h)	H_2O removed (g)	Ret. in temp. (°C)	Dist. in temp. (°C)	Flux (g/hm^2)	[NaCl] (m)	[$MgSO_4$] (m)
10	11.8	28.7	13.7	138.00	5.742	0.450
20	**18.1**	30.6	13.9	189.00	5.758	0.451
50	**31.1**	31.0	14.2	207.00	5.780	0.453
60	**38.4**	32.7	14.6	219.00	5.826	0.456
72	48.1	32.7	14.7	242.50	5.852	0.458
180	113.1	33.2	14.9	278.18	5.887	0.461
210	130.6	34.9	15.3	175.00	6.132	0.480
245	147.2	35.3	15.4	142.29	6.201	0.485
283	161.1	36.2	15.4	109.74	6.269	0.491
311	171.4	37.7	15.2	110.36	6.326	0.495

B.1.1 Crystal Size Distribution

The data sets that were used in order to obtain the CSD for the MD and crystallisation of a 375 g/ℓ magnesium sulphate solution are listed in Tables B6a to B6d. This data was used according to Equation 3.2 and the general approach of characterisation of size distribution, in order to obtain the overall CSD as shown in Figure 3.3.

Table B.6a: *CSD for sample 1 for the MD of a 375 g/ℓ magnesium sulphate solution*

Length (cm)	Range	N (cm)	% distribution
0	0.1-0.4	0	0
5.5	0.4-0.7	7	6.73
8.5	0.7-1.0	26	25.00
11.5	1.0-1.3	32	30.77
14.5	1.3-1.6	28	26.92
17.5	1.6-1.9	**6**	**5.77**
20.5	1.9-2.2	**5**	**4.81**
SUM		**104**	
MEDIAN	**11.9**		

Table B.6b: *CSD for sample 2 for the MD of a 375 g/ℓ magnesium sulphate solution*

Length (cm)	Range	N (cm)	% distribution
0	0.4-0.7	0	0
8.5	0.7-1.0	30	9.04
11.5	1.0-1.3	71	21.39
14.5	1.3-1.6	90	27.11
17.5	1.6-1.9	56	16.87
20.5	1.9-2.2	36	10.84
23.5	2.2-2.5	23	6.93
26.5	2.5-2.8	15	4.52
29.5	2.8-3.1	6	**1.81**
32.5	3.1-3.4	5	1.51
SUM		**332**	
MEDIAN	**16.2**		

Table B.6c: *CSD for sample 3 for the MD of a 375 g/ℓ magnesium sulphate solution*

Length (cm)	Range	N (cm)	% distribution
0	0.4-0.7	0	0
8.5	0.7-1.0	5	2.14
11.5	1.0-1.3	41	17.52
14.5	1.3-1.6	63	30.00
17.5	1.6-1.9	37	15.81
20.5	1.9-2.2	25	10.68
23.5	2.2-2.5	26	11.11
26.5	2.5-2.8	11	4.70
29.5	2.8-3.1	11	4.70
32.5	3.1-3.4	8	3.42
35.5	3.4-3.7	5	2.14
38.5	3.7-4.0	2	0.85
SUM		**234**	
MEDIAN	**19.0**		

Table B.6d: *CSD for sample 4 for the MD of a 375 g/ℓ magnesium sulphate solution*

Length (cm)	Range	N (cm)	% distribution
0	0.4-0.7	0	0
8.5	0.7-1.0	6	2.58
11.5	1.0-1.3	15	6.44
14.5	1.3-1.6	31	13.30
17.5	1.6-1.9	21	27.00
20.5	1.9-2.2	23	14.87
23.5	2.2-2.5	24	12.30
26.5	2.5-2.8	24	10.30
29.5	2.8-3.1	27	11.59
32.5	3.1-3.4	17	7.30
35.5	3.4-3.7	17	7.30
38.5	3.7-4.0	7	3.00
41.5	4.0-4.3	6	2.58
44.5	4.3-4.6	5	2.15
47.5	4.6-4.9	4	1.72
50.5	4.9-5.2	3	1.29
53.5	5.2-5.5	3	1.29
SUM		**233**	
MEDIAN	**30.0**		

B.2 VAPOUR PRESSURES OBTAINED USING PHRQPITZ

The modelling of vapour pressures performed using the PHRQPITZ computer program for each of the streams during the MD of the 1:1 and 1:2 salt mixes are listed in Table B.7 and 8. The log mean vapour pressures (ΔP_{lm}), calculated from the difference between the inlet and outlet retentate and distillate streams, are also shown.

Table B.7: *Vapour pressures of various streams during MD of 1:1 mix together with calculated log mean vapour pressure*

Ret. in (kPa)	Ret. out (kPa)	Pure Ret. in (kPa)	Pure Ret. out (kPa)	Dist. In (kPa)	Dist. Out (kPa)	ΔP_1 (kPa)	ΔP_2 (kPa)	ΔP_{lm} (-)
2.99	2.59	4.06	3.51	1.70	1.76	1.23	0.89	1.05
3.16	2.80	4.30	3.81	1.73	1.82	1.34	1.07	1.20
3.45	2.88	4.71	3.94	1.78	1.82	1.63	1.10	1.35
3.57	3.01	4.90	4.13	1.81	1.94	1.63	1.20	1.40
3.61	3.02	4.98	4.17	1.83	1.94	1.67	1.19	1.42
3.63	3.05	5.04	4.25	1.82	1.94	1.69	1.23	1.45
3.66	3.03	5.12	4.25	1.83	1.94	1.72	1.20	1.45
3.55	2.96	5.12	4.27	1.83	1.94	1.62	1.13	1.36
3.53	2.90	5.18	4.27	1.84	1.98	1.55	1.06	1.29
3.41	2.64	5.24	4.08	1.84	2.00	1.41	0.80	1.08
3.28	2.68	5.18	4.25	1.87	2.00	1.28	0.82	1.03
3.21	2.60	5.24	4.27	1.89	2.03	1.18	0.71	0.93
3.13	2.60	5.21	4.35	1.87	2.00	1.13	0.73	0.92
3.12	2.52	5.27	4.27	1.88	2.00	1.12	0.64	0.86

Table B.8: *Vapour pressures of various streams during MD of 1:2 mix together with calculated log mean vapour pressure*

Ret. in (kPa)	Ret. out (kPa)	Pure Ret. in (kPa)	Pure Ret. out (kPa)	Dist. In (kPa)	Dist. Out (kPa)	ΔP_1 (kPa)	ΔP_2 (kPa)	ΔP_{lm} (-)
3.15	2.82	4.32	3.87	1.82	1.88	1.27	1.00	1.13
3.23	3.12	4.45	4.30	1.88	1.94	1.29	1.24	1.27
3.35	3.13	4.63	4.32	1.89	1.94	1.42	1.24	1.33
3.40	3.14	4.71	4.35	1.89	1.94	1.47	1.25	1.36
3.51	3.23	4.90	4.47	1.93	2.00	1.51	1.31	1.41
3.57	3.26	5.04	4.55	1.94	2.01	1.56	1.32	1.44
3.58	3.24	5.06	4.57	1.96	2.05	1.53	1.28	1.40
3.59	3.22	5.09	4.55	1.96	2.07	1.53	1.25	1.39
3.56	3.20	5.15	4.60	1.96	2.07	1.50	1.23	1.36
3.52	3.10	5.21	4.55	1.96	2.07	1.46	1.14	1.29
3.46	3.05	5.18	4.52	1.95	2.07	1.40	1.10	1.24
3.46	3.04	5.24	4.55	1.95	2.07	1.39	1.08	1.23
3.38	3.00	5.18	4.55	1.96	2.07	1.32	1.03	1.17
3.24	2.91	5.15	4.50	1.95	2.07	1.17	0.96	1.07

B.3 VLE EXPERIMENTS

The experimental VLE data are listed below. The non-linear regressions for fitting Antoine's constants to the experimental data are also shown. **Section B3.1** lists the results obtained for the pure sodium chloride solutions that were investigated as a test of the suitability of the VLE still to measure vapour pressures of inorganic salts. This is confirmed by a comparison of the experimental vapour pressures to those obtained from literature. **Section B.3.2** then lists the vapour pressures that were measured for each of the salt mixes.

B.3.1 Suitability of VLE to measure vapour pressures of inorganic salts

Table B.9 to B.11 lists the measured vapour pressures for three sodium chloride solutions that were studied together with the Antoine's regression that was used to fit the experimental points.

Table B.9: *Non-linear regression for fitting Antoine's constants to experimental VLE data for 20 g/ℓ NaCl solution*

		A	B	C	$\sum r_i^2$
		18.6	5139	-6.00	7.13×10^{-3}
Temp. (K)	**P_{expt} (kPa)**	**P_{calc} (kPa)**	**$\ln P_{expt}$**	**$\ln P_{calc}$**	**r**
298	2.64	2.72	0.970	1.00	8.69×10^{-4}
303	3.77	3.65	1.33	1.30	1.03×10^{-3}
313	6.75	6.41	1.91	1.86	2.70×10^{-3}
323	10.7	10.9	2.37	2.39	1.82×10^{-4}
333	17.9	17.8	2.89	2.88	2.41×10^{-5}
343	28.6	28.4	3.36	3.34	6.12×10^{-5}
353	44.3	44.1	3.79	3.79	2.01×10^{-5}
363	66.6	66.7	4.20	4.20	3.32×10^{-6}
373	96.0	98.8	4.56	4.59	8.25×10^{-4}

Table B.10: *Non-linear regression for fitting Antoine's constants to experimental VLE data for 200 g/ℓ NaCl solution*

		A	B	C	$\sum r_i^2$
		18.0	4958	-7.21	3.91×10^{-3}
Temp. (K)	**P_{expt} (kPa)**	**P_{calc} (kPa)**	**$\ln P_{expt}$**	**$\ln P_{calc}$**	**r**
298	2.637	2.520	0.970	0.924	2.06×10^{-3}
303	3.400	3.361	1.224	1.212	1.36×10^{-4}
313	5.750	5.811	1.749	1.760	1.11×10^{-4}
323	9.648	9.705	2.267	2.273	3.41×10^{-5}
333	15.645	15.706	2.750	2.754	1.53×10^{-5}
343	24.745	24.701	3.209	3.207	3.13×10^{-6}
353	37.932	37.843	3.636	3.633	5.47×10^{-6}
363	56.817	56.604	4.040	4.036	1.41×10^{-5}
373	81.968	82.824	4.406	4.417	1.08×10^{-4}

Table B.11: *Non-linear regression for fitting Antoine's constants to experimental VLE data for 280 g/ℓ NaCl solution*

		A	B	C	$\sum r_i^2$
		18.0	4996	-7.87	1.33×10^{-2}
Temp. (K)	**P_{expt} (kPa)**	**P_{calc} (kPa)**	**$\ln P_{expt}$**	**$\ln P_{calc}$**	**r**
298	2.24	2.21	0.806	0.791	2.41×10^{-4}
303	2.97	2.95	1.09	1.08	2.41×10^{-5}
313	5.38	5.14	1.68	1.64	2.18×10^{-3}
323	8.71	8.63	2.17	2.16	8.96×10^{-5}
333	14.3	14.1	2.66	2.64	2.71×10^{-4}
343	22.5	22.2	3.11	3.10	1.50×10^{-4}
353	34.0	34.2	3.53	3.53	2.46×10^{-5}
363	50.5	51.4	3.92	3.94	2.96×10^{-4}
373	73.5	75.5	4.30	4.33	7.18×10^{-4}

The experimental vapour pressures were compared to those calculated using the empirical equations derived by Sparrow (2003) for the calculation of thermodynamic properties of aqueous sodium chloride solutions. The results obtained using Equation 5.4 are listed in Tables B.12 to B.14 for each sodium chloride concentration.

Table B.12: *Calculation of vapour pressures from Sparrows (2003) equations for comparison to experimental VLE data for 20 g/ℓ NaCl solution*

Temperature (K)	Constants		Pressure (kPa)
298	0	**A**	2.96
303	-6.58×10^{-5}	**B**	**4.15**
313	7.44×10^{-6}	**C**	**7.48**
323	-9.09×10^{-8}	**D**	**12.5**
333	1.22×10^{-9}	**E**	**19.9**
343			30.9
353			46.7
363			69.1
373			100

Table B.13: *Calculation of vapour pressures from Sparrows (2003) equations for comparison to experimental VLE data for 200 g/ℓ NaCl solution*

Temperature (K)	Constants		Pressure (kPa)
298	7.93×10^{-4}	**A**	2.59
303	-6.01×10^{-5}	**B**	3.65
313	6.64×10^{-6}	**C**	6.58
323	-8.22×10^{-8}	**D**	11.0
333	1.08×10^{-9}	**E**	17.6
343			27.2
353			41.2
363			60.9
373			88.1

Table B.14: *Calculation of vapour pressures from Sparrows (2003) equations for comparison to experimental VLE data for 280 g/ℓ NaCl solution*

Temperature (K)	Constants		Pressure (kPa)
298	7.41×10^{-4}	**A**	**2.35**
303	-6.01×10^{-5}	**B**	**3.31**
313	6.34×10^{-6}	**C**	**5.98**
323	-7.97×10^{-8}	**D**	**9.97**
333	1.02×10^{-9}	**E**	**15.9**
343			24.7
353			**37.3**
363			55.3
373			80.1

The second set of comparisons of was to the data of Lui and Lindsay (1972). However, their data had first to be extrapolated to the appropriate concentrations and temperatures of our experiments. These were performed by calculating Antoine's constants for their data and extrapolating for the values used in this work. The data are listed in Tables B.15 to B.17.

Table B.15: *Non-linear regression for fitting Antoine's constants to literature data for 20 g/ℓ NaCl solution (Lui and Lindsay, 1972)*

		A	B	C	$\sum r_i^2$
		17.8	4999	5.50	6.20×10^{-4}
Temp. (K)	**P_{expt} (kPa)**	**P_{calc} (kPa)**	**$\ln P_{expt}$**	**$\ln P_{calc}$**	**r**
348	39.2	39.69	3.67	3.68	1.48×10^{-4}
373	101.8	100.9	4.62	4.62	7.79×10^{-5}
398	231.6	228.7	5.45	5.43	1.62×10^{-4}
423	473.2	470.9	6.16	6.16	2.47×10^{-5}
448	882.7	895.5	6.78	6.80	2.07×10^{-4}

Table B.16: *Non-linear regression for fitting Antoine's constants to literature data for 200 g/ℓ NaCl solution (Lui and Lindsay, 1972)*

		A	B	C	$\sum r_i^2$
		17.7	4996	3.50	6.79×10^{-4}
Temp. (K)	**P_{expt} (kPa)**	**P_{calc} (kPa)**	**$\ln P_{expt}$**	**$\ln P_{calc}$**	**r**
348	33.3	33.7	3.51	3.52	1.75×10^{-4}
373	87.6	86.6	4.47	4.46	1.09×10^{-4}
398	200.5	197.8	5.30	5.29	1.75×10^{-4}
423	411.6	410.0	6.02	6.02	1.49×10^{-5}
448	772.8	783.9	6.65	6.67	2.05×10^{-4}

Table B.17: *Non-linear regression for fitting Antoine's constants to literature data for 280 g/ℓ NaCl solution (Lui and Lindsay, 1972)*

		A	B	C	$\sum r_i^2$
		17.7	4996	2.55	6.25×10^{-4}
Temp. (K)	**P_{expt} (kPa)**	**P_{calc} (kPa)**	**$\ln P_{expt}$**	**$\ln P_{calc}$**	**r**
348	30.5	30.9	3.42	3.43	1.61×10^{-4}
373	80.5	79.7	4.39	4.38	9.74×10^{-5}
398	185.1	182.7	5.22	5.21	1.69×10^{-4}
423	381.2	379.9	5.94	5.94	1.17×10^{-5}
448	718.5	728.4	6.58	6.59	1.86×10^{-4}

Figure B.1 shows the plots of vapour pressure against concentration for each of the temperatures studied by Lui and Lindsay from which our conditions were extrapolated using Antoines constants. The data are showed in Table B.18.

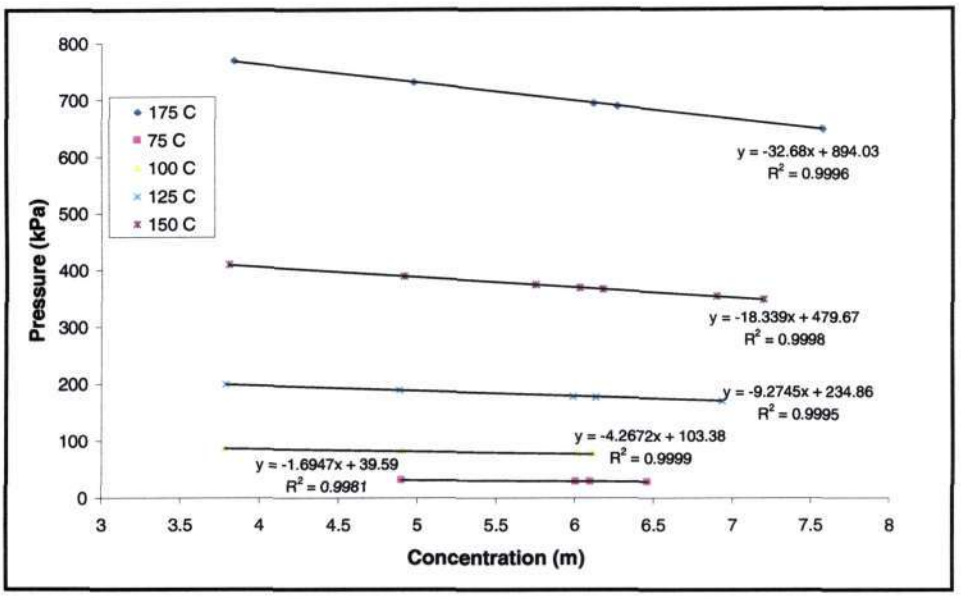

Figure B.1: *Standard plots of Lui and Lindsays concentrations at varying temperatures used to extrapolate our concentrations*

Table B.18: *Extrapolated literature values for vapour pressures of NaCl solutions*

	NaCl concentration (g/ℓ)		
Temperature (K)	**20**	**200**	**280**
298	3.87	3.20	2.89
303	5.05	4.20	3.79
313	8.40	7.02	6.36
323	13.5	11.4	10.3
333	21.2	18.0	16.3
343	32.4	27.5	25.1
353	48.3	41.2	37.7
363	70.6	60.3	55.4
373	100.9	86.6	79.7

B.3.2 Experimental vapour pressures of salt mixes

Tables B.19 to B.21 lists the vapour pressures that were measured for each of the salt mixes using the VLE still.

Table B.19: *Non-linear regression for fitting Antoine's constants to experimental VLE data for 1:1 mix*

		A	B	C	$\sum r_i^2$
		16.1	3987	-34.5	7.97×10^{-2}
Temp. (K)	**P_{expt} (kPa)**	**P_{calc} (kPa)**	**$\ln P_{expt}$**	**$\ln P_{calc}$**	**r**
298	2.94	2.55	1.19	0.936	6.36×10^{-2}
303	3.17	3.38	1.26	1.22	1.72×10^{-3}
313	5.06	5.75	1.69	1.75	3.55×10^{-3}
323	8.65	9.44	2.20	2.25	2.01×10^{-3}
333	14.2	15.0	2.68	2.71	8.74×10-^{4}
343	22.1	23.1	3.12	3.14	6.29×10^{-4}
353	34.0	34.7	3.54	3.55	2.90×10^{-5}
363	51.0	50.7	3.94	3.93	2.90×10^{-4}
373	73.5	72.6	4.31	4.29	4.80×10^{-4}

Table B.20: *Non-linear regression for fitting Antoine's constants to experimental VLE data for 1:2 mix*

		A	B	C	$\sum r_i^2$
		16.0	4002	-34.3	7.06×10^{-2}
Temp. (K)	**P_{expt} (kPa)**	**P_{calc} (kPa)**	**$\ln P_{expt}$**	**$\ln P_{calc}$**	**r**
298	2.90	2.34	1.06	0.851	4.51×10^{-2}
303	3.01	3.11	1.10	1.13	1.07×10^{-3}
313	4.73	5.30	1.55	1.67	1.30×10^{-2}
323	8.19	8.70	2.10	2.16	3.76×10^{-3}
333	13.1	13.8	2.58	2.63	2.61×10^{-3}
343	21.3	21.4	3.06	3.06	1.66×10^{-5}
353	32.9	32.1	3.50	3.47	6.57×10^{-4}
363	47.4	47.0	3.86	3.85	9.18×10^{-5}
373	69.3	67.3	4.24	4.21	8.92×10^{-4}

Table B.21: *Non-linear regression for fitting Antoine's constants to experimental VLE data for 1:3 mix*

		A	B	C	$\sum r_i^2$
		16.0	3987	-34.3	5.41×10^{-2}
Temp. (K)	**P_{expt} (kPa)**	**P_{calc} (kPa)**	**$\ln P_{expt}$**	**$\ln P_{calc}$**	**r**
298	2.91	2.43	1.07	0.888	3.18×10^{-2}
303	3.00	3.22	1.10	1.17	5.24×10^{-3}
313	5.02	5.48	1.61	1.70	7.56×10^{-3}
323	8.48	8.99	2.14	2.20	3.48×10^{-3}
333	13.7	14.3	2.62	2.66	1.73×10^{-3}
343	21.9	22.0	3.09	3.09	1.12×10^{-5}
353	33.5	32.9	3.51	3.50	3.32×10^{-4}
363	49.5	48.2	3.90	3.88	7.63×10^{-4}
373	71.8	69.0	4.27	4.23	1.66×10^{-3}

B.4 COMPARISON BETWEEN MEASURED AND MODELLED VAPOUR PRESSURES

Tables B.22 to B.24 list the experimental and modelled vapour pressures obtained from VLE experiments and PHRQPITZ modelling, respectively, for each of the salt mixes.

Table B.22: *Measured and modelled vapour pressures to test accuracy of modelling for 1:1 mix*

Temperature (K)	Expt. P_{soln} (kPa)	Expt. α_{H2O}	Modelled P_{soln} (kPa)	Modelled α_{H2O}	$P_{measured}/P_{modelled}$
303	3.17	0.811	2.90	0.740	1.096
313	5.06	0.739	5.09	0.743	0.994
323	8.65	0.750	8.61	0.747	1.01
333	14.2	0.756	14.1	0.751	1.01
343	22.1	0.750	22.2	0.755	0.994
353	34.0	0.755	34.1	0.759	0.995
363	51.0	0.762	51.1	0.763	0.999
373	73.5	0.756	74.6	0.768	0.984

Table B.23: *Measured and modelled vapour pressures to test accuracy of modelling for 1:2 mix*

Temperature (K)	Expt. P_{soln} (kPa)	Expt. α_{H2O}	Modelled P_{soln} (kPa)	Modelled α_{H2O}	$P_{measured}/P_{modelled}$
303	3.00	0.768	2.85	0.729	1.05
313	4.73	0.690	5.01	0.732	0.942
323	8.19	0.710	8.47	0.735	0.966
333	13.2	0.702	13.8	0.738	0.951
343	21.3	0.722	21.8	0.742	0.974
353	32.9	0.731	33.5	0.746	0.981
363	47.4	0.709	50.2	0.750	0.945
373	69.3	0.713	73.3	0.754	0.946

Table B.24: *Measured and modelled vapour pressures to test accuracy of modelling for 1:3 mix*

Temperature (K)	Expt. P_{soln} (kPa)	Expt. α_{H2O}	Modelled P_{soln} (kPa)	Modelled α_{H2O}	$P_{measured}/P_{modelled}$
303	2.99	0.765	2.91	0.745	1.03
313	5.02	0.733	5.12	0.747	0.982
323	8.47	0.735	8.63	0.749	0.982
333	13.7	0.731	14.1	0.751	0.973
343	21.9	0.744	22.2	0.754	0.986
353	33.6	0.746	34.1	0.757	0.985
363	49.5	0.740	50.9	0.760	0.974
373	71.8	0.738	74.2	0.764	0.967

B.5 APPENDIX REFERENCES

LIU C and LINDSAY WT (1972) *Thermodynamics of sodium chloride solutions at high temperatures*. J Soln Chem **1** 45-69.

SPARROW BS (2003) *Empirical equations for the thermodynamic properties of aqueous sodium chloride*. Desalination **159** 161-170.

Appendix C

Appendix C

PAPERS

This Appendix is comprised of four papers:

(i) Mariah L, Buckley CA, Brouckaert CJ, Ramjugernath D, Jaganyi D, Curcio E and Drioli E, *The role of water activities in the membrane distillation of concentrated brines for the recovery of crystalline products from brine effluents*, IWA/WISA Conference: Management of Residues Emanating from Water and Wastewater Treatment, Sandton Conference Centre, Johannesburg, South Africa, 9-12 August 2005.

(ii) Curcio E, Di Profio G, Mariah L and Drioli E, *A fully integrated membrane operation for sea water and brackish water desalination*. Proceedings of the World Conference for Chemical Engineers, Glascow, 2005.

(iii) Mariah L, Buckley CA, Brouckaert CJ, Curcio E, Drioli E, Jaganyi D and Ramjugernath D (2006) *Membrane distillation of concentrated brines – role of water activities in the evaluation of driving force.* J Membr Sci. **280** (1-2) 937-947.

(iv) Mariah L, Buckley CA, Brouckaert CJ, Jaganyi D, Curcio E and Drioli E, *Membrane distillation for the recovery of crystalline products from concentrated brines*. WISA Biennial Conference, Durban, South Africa, 21-25 May 2006.

PAPER 1

The role of water activities in membrane distillation of concentrated brines for recovery of crystalline products from brine effluents

L. Mariah*, C. A. Buckley*, C. J. Brouckaert*, D. Ramjugernath*, D. Jaganyi**, E. Curcio*** and E. Drioli***

* School of Chemical Engineering, University of KwaZulu-Natal, Durban, 4041, South Africa.
(E-mail: 992215708@ukzn.ac.za; buckley@ukzn.ac.za; brouckae@ukzn.ac.za, Ramjuger@ukzn.ac.za)
** School of Chemistry, Private Bag X01, University of KwaZulu-Natal, Scottsville, 3209, South Africa
(E-mail: jaganyi@ukzn.ac.za)
*** Institute on Membrane Technology (ITM-CNR), Via P. Bucci 17/C, c/o University of Calabria, 87030, Rende (CS), Italy
(E-mail: e.drioli@itm.cnr.it; e.curcio@itm.cnr.it)

Abstract
Membrane distillation for the desalination of sea water and purification of other effluent streams has been explored to quite an extent over the last years. Many theories have been postulated to account for the decline in flux that is experienced during a batch membrane distillation run, the majority of which are with respect to low concentration solutions. This paper demonstrates the importance of taking into account the activities of water during the membrane distillation of concentrated solutions of mixed electrolytes, which, in the case of dilute solutions, are often neglected. The geochemical equilibrium speciation program, PHRQPITZ, provides a means of accurately modeling these activities. The suitability of the program for this application was verified by experiments performed with the aid of a dynamic vapour liquid equilibrium (VLE) still. This accountability of water activities showed how the trend of decreasing flux fitted with that of the driving force for the distillation process. These effects are particularly important in the membrane distillation of concentrated brines for the recovery of crystalline products from brine effluents.

Keywords
Brines, membrane distillation/crystallization, desalination, activities, vapour pressure

INTRODUCTION

Salinity is one of South Africa's most critical environmental problems, threatening economic and social consequences. Industries such as Sasol and Eskom currently have reverse osmosis (RO) plants producing waste brine, but brine disposal is a problem. If there is no intervention, the completed mining operations will produce saline aqueous effluents for hundreds of years. Exploiting the fact that inorganic concentrates can be separated into high value chemicals and reusable water, membrane distillation (and crystallization) is a technique which potentially leads to a 100 % water recovery and the elimination of the brine disposal problem. This is achieved by the production of pure water by concentrating aqueous solutions through the existence of a vapour pressure difference induced by a transmembrane temperature gradient resulting in highly concentrated mother liquors in which nucleation and crystal growth occurs (Lawson and Lloyd, 1997; Curcio *et al*, 2001). This process does not have the limitations of processes such as reverse osmosis and thermal evaporation as this process can operate at higher concentrations, at low concentration gradients, moderate temperatures and atmospheric pressure. Despite the fact that much work has been performed in the field of membrane distillation over the last years, this work still suffers from inadequate or speculative accounting for the subsequent decrease in transmembrane flux observed during a typical membrane distillation run. Some authors (Franken *et al*, 1987; Calabro *et al*, 1994; Hsu *et al*, 2002; Tzahi *et al*, 2004) have attributed the decrease to membrane wettability or membrane fouling. These accounts, however, dealt with solutions of low concentrations, or at least not up to concentrations at saturation levels. When considering such solutions, it becomes necessary to take into account the activities of water on either side of the

membrane. It is not possible to measure the transmembrane vapour pressures directly during a membrane distillation process. Hence the aim of this work is to provide a means of accurately evaluating activity changes during the membrane distillation of concentrated mixed brines, and to show how these activities contribute to the overall trend of decreasing flux.

METHODS

A series of methods was used to achieve the overall goal.

- Membrane distillation was used to evaluate the production of sodium chloride and magnesium sulphate from an aqueous solution of these salts.
- Vapour pressure measurements on brines with compositions similar to those used in the membrane experiments were conducted using a dynamic vapour liquid equilibrium (VLE) still and these data were compared to those calculated using the thermodynamic geochemical speciation program in order to test its accuracy.
- The vapour pressure driving force during the membrane distillation experiments was calculated and correlated with the distillate flux.

Membrane distillation

Figure 1 is a schematic diagram of the membrane distillation plant and crystalliser used during these series of experiments. In the process, saline water is heated to induce vapour production (retentate line), and this vapour is exposed to a membrane that can typically pass vapour but not water. After the vapour passes through the membrane, it is condensed in the cooler distillate stream, producing pure water. In the fluid phase, the fresh water cannot return through the membrane, so it is trapped and collected at the output of the plant.

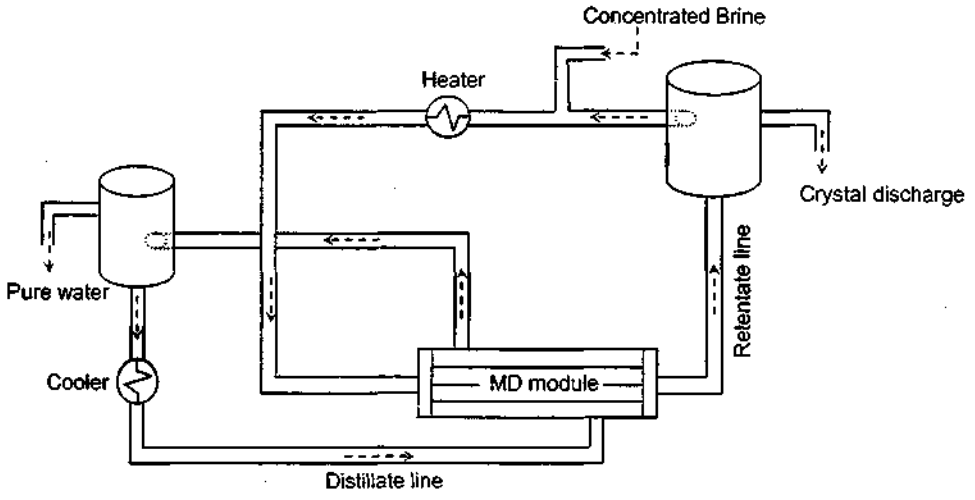

Figure 1: Schematic representation of the membrane distillation and crystallisation process

The performance of the membrane was evaluated by calculating the water flux or permeation rate. This is defined as the mass flowing through the membrane per unit area per unit time interval,

$$\text{Flux} = \frac{\text{mass of water extracted (g)}}{\text{unit area (m}^2\text{)} \times \text{time interval (h)}} \qquad [1]$$

Experimental. Aqueous solutions of analytical grade magnesium sulphate and sodium chloride were prepared in mass ratios of 1:1 and 1:2, respectively, with initial concentrations of 22.5 g and 27.5 g of NaCl /100 g of H_2O and the corresponding ratio of magnesium sulphate, respectively (hereafter referred to as 1:1 mix and 1:2 mix). These were fed into the distillation plant

which was operated in a batch concentration mode where the recirculating permeate stream, consisting of deionized water, and the retentate stream flowed countercurrent through the membrane module. The membrane module, MD020CP-2N, supplied by Microdyn, contains 40 hydrophobic polypropylene hollow fibres of 0.1 m^2 total interfacial area. The nominal pore size of the polypropylene membranes was 0.2 μm and the external diameter was 1.8 mm. The crystallisation vessel operated at 25 °C and atmospheric pressure. The average temperatures at module inlet on retentate and distillate sides were 33 ± 2 °C and 17 ± 1 °C, respectively. The water flux was evaluated by measuring the amount of water extracted at time intervals during the course of the experiment.

Vapour liquid equilibrium still

The vapour liquid equilibrium (VLE) still developed by Raal and Mühlbauer (1998) was used to measure the vapour pressures as a function of the temperature of aqueous solutions of pure sodium chloride and solutions of mixtures of sodium chloride and magnesium sulphate corresponding to the range of compositions of those used during the distillation process. The design and operation of the still is described by Joseph *et al* (2001). The vapour pressures are related to temperature by the Antoine equation.

$$\ln P = A - \frac{B}{T + C} \qquad [2]$$

where P is the pressure in pascal, T is the temperature in Kelvin and A, B and C are constants which vary from substance to substance. The Antoine equation was used in a regression procedure to determine parameters to fit the experimental vapour pressure data.

Experimental. The preparation of the solutions followed the same procedure as that used for membrane distillation. Varying concentrations of aqueous solutions of pure sodium chloride were prepared in order to gain data for comparison with literature to substantiate the progression of investigations into our systems. The temperature and pressure in the still were computer controlled. The desired temperature was set and once vapour-liquid equilibrium was established, the corresponding pressure was recorded.

Geochemical equilibrium speciation program, PHRQPITZ

PHRQPITZ is a computer program which enables geochemical calculations in brines and other electrolyte solutions at high concentrations by making use of the Pitzer-virial coefficient approach for activity coefficient corrections (Plummer *et al*, 1988). In addition to being able to calculate the activity coefficients for the above solutions with temperature, the program is also able to model mineral solubility thus predicting the evaporation factor needed in order to reach supersaturation and crystallisation. For the purposes of this paper, this program was used to test its applicability for modeling vapour pressures by comparison to the data obtained from the VLE experiments. The effective vapour pressure of a solution is the product of the vapour pressure of pure water at the same temperature as the solution and the activity of water in the solution.

There does, however, exist some limitations concerning the use of this code for modeling purposes. One which applies to our system is that the temperature range for equilibria in the PHRQPITZ database is variable and is within the range 0 to 60 °C but the sodium chloride system is valid up to approximately 350 °C.

RESULTS AND DISCUSSION

Membrane Distillation

The performance of the membrane distillation was evaluated by examining the water flux trend as illustrated in Figure 2. This trend represents that of a solution containing equal amounts of each salt per 100 g H_2O (1:1 mix).

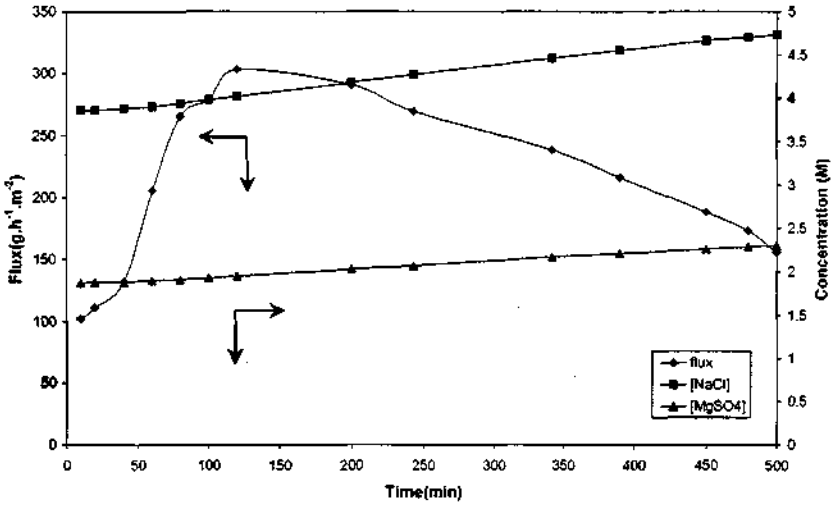

Figure 2: Trends of the water transmembrane flux and the concentration of magnesium sulphate and sodium chloride with time for a solution containing equal masses of each salt per 100 gram of water

Typically, if a crystallisation run is carried out in a batch concentration mode i.e. the retentate line is not continuously replenished with fresh feed solution, the flux will decrease with time as the solution becomes more concentrated. A similar trend was obtained for the 1:2 $MgSO_4$:NaCl solution.

Vapour-liquid equilibrium still

In order to test the performance of the still the vapour pressure of aqueous solutions of pure sodium chloride was measured as a function of temperature and was found to be in good agreement with those of previous authors (Lui and Lindsay, 1971; Sparrow, 2003). The vapour pressures obtained for the subsequent mixes of salt solutions, in addition to that of pure water are shown in Figure 3. It can be clearly seen that the difference in vapour pressure between the hot (brine) and cold (pure water) sides drives the separation process.

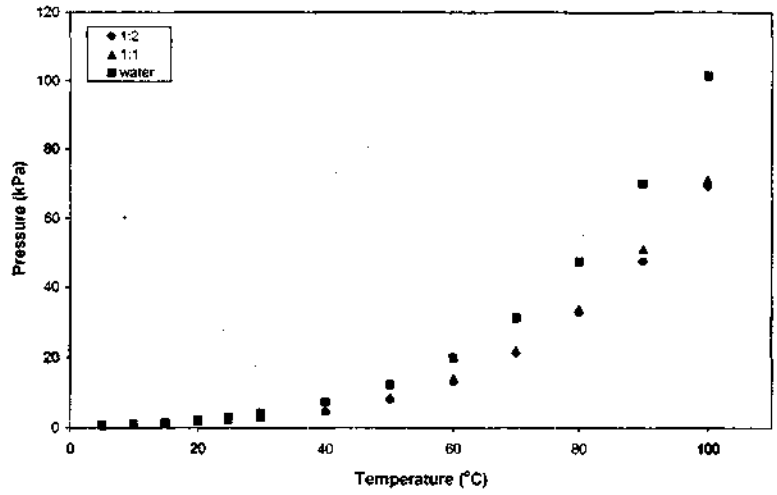

Figure 3: Vapour pressures of salt mixes containing magnesium sulphate and sodium chloride 1:1 solution, 1:2 solution and pure water

PHRQPITZ

PHRQPITZ was used to obtain the activity coefficients, hence the vapour pressures, of the two mixes of salt solutions at the range of temperatures used during the VLE experiments. Figure 4 shows the comparison of the vapour pressure trend obtained from both methods and Figure 5 compares the activities calculated in both cases. The slight deviation of the experimental results from those of PHRQPITZ at increasing temperatures in Figure 5 is attributed to the uncertainty in PHRQPITZ calculations above 60 °C. This uncertainty, however, does not effect the outcome of the results in this study as the membrane distillation plant operates at an average retentate temperature of 33 °C. It therefore appears that the vapour pressure can be sufficiently accurately modeled using PHRQPITZ for the analysis of the experimental membrane distillation results.

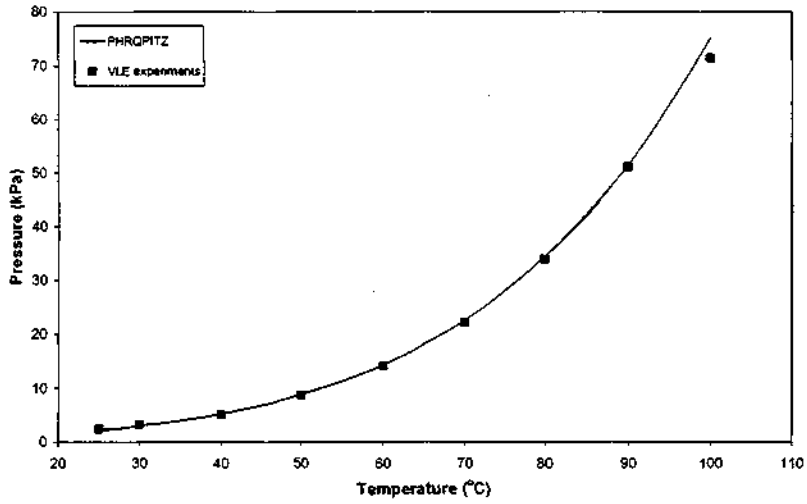

Figure 4: Vapour pressures obtained for 1:1 salt mix from PHRQPITZ calculations and VLE experiments.

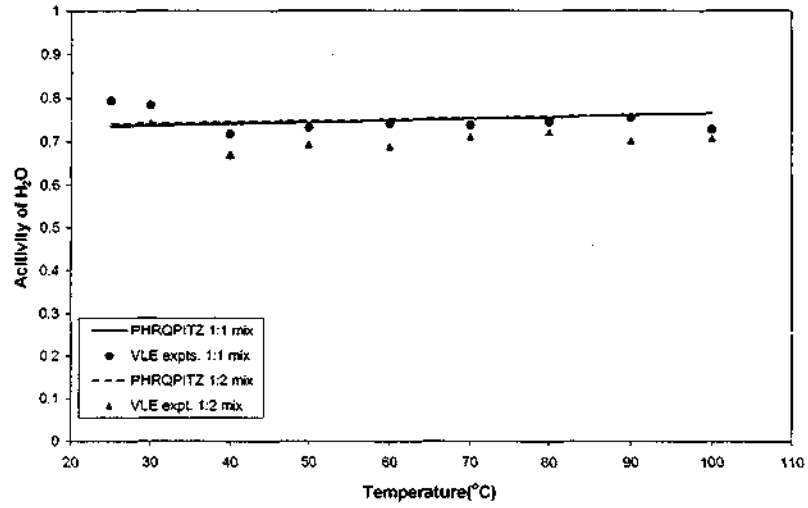

Figure 5: Comparison of activities calculated from PHRQPITZ and VLE experiments for each of the salt mixes

This then led to a further investigation into the decline of flux experienced during the membrane distillation run. The speciation program was used to calculate the activities from the temperature of the retentate and distillate streams and concentration of the solutions at time intervals during the separation process. Appropriate treatment of these data yielded the driving force at these time intervals. Figure 6 shows the variation of the vapour pressures of each of the streams as indicated in the legend. It emphasises the significant change in activities between the inlet and outlet retentate and permeate streams and the negligible change in the pure water vapour pressure between the inlet and outlet streams.

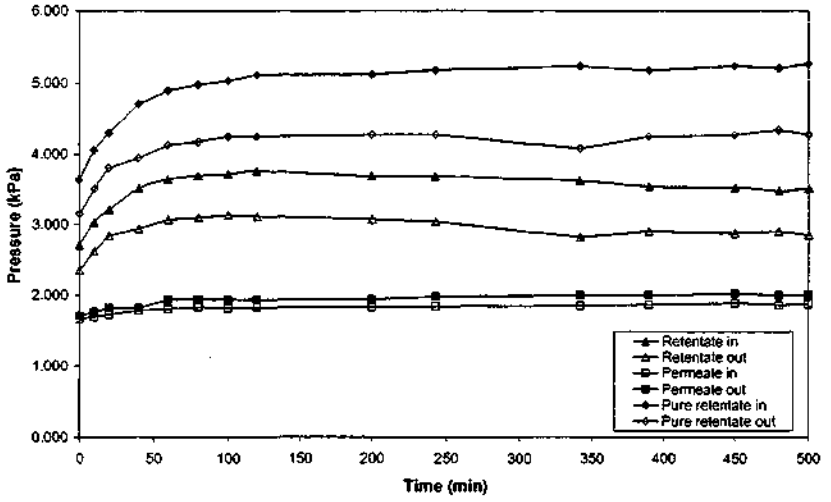

Figure 6: Vapour pressures of respective streams in membrane distillation of a 1:1 mix

The driving force, expressed as the log mean vapour pressures differences (ΔP_{lm}), where calculated and plotted on the same graph as the transmembrane flux time relationship. Figure 7 demonstrates the similarity in trend between the driving force and transmembrane flux for the distillation of the 1:1 mix revealed by accounting for the change in water activities at either ends of the membrane.

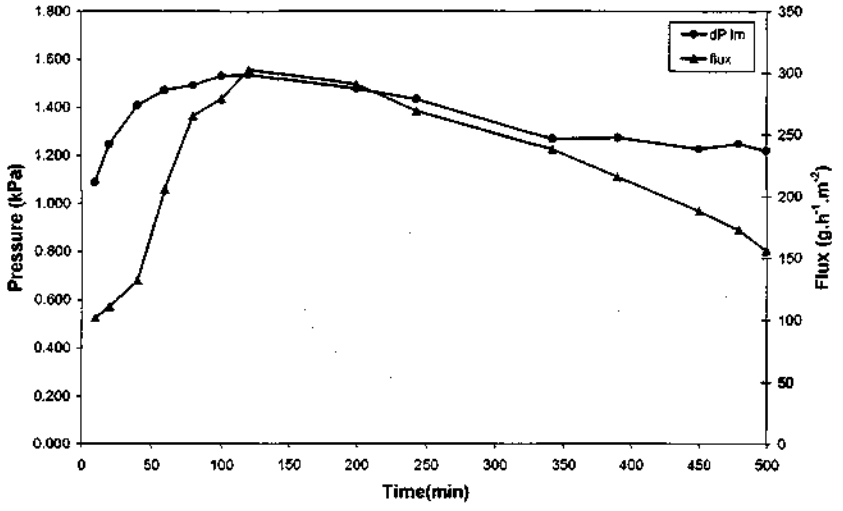

Figure 7: Variation of transmembrane flux with the driving force as a function of time for the 1:1 mix

In Figure 8 the data are replotted to show the relationship between flux and vapour pressure driving force. A notable feature of this plot is the non-zero intercept, which can be explained in terms of the simultaneous heat and mass transfer through the membrane, which causes the temperatures and vapour pressures at the membrane surfaces to be different from those in the bulk liquid. Because of the conductive heat transfer through the membrane, this discrepancy occurs even when there is no flux of vapour through the membrane, which accounts for the observed non-zero intercept. This effect is usually negligible for dilute solutions, but has been observed elsewhere for concentrated solutions (Walton *et al*, 2004).

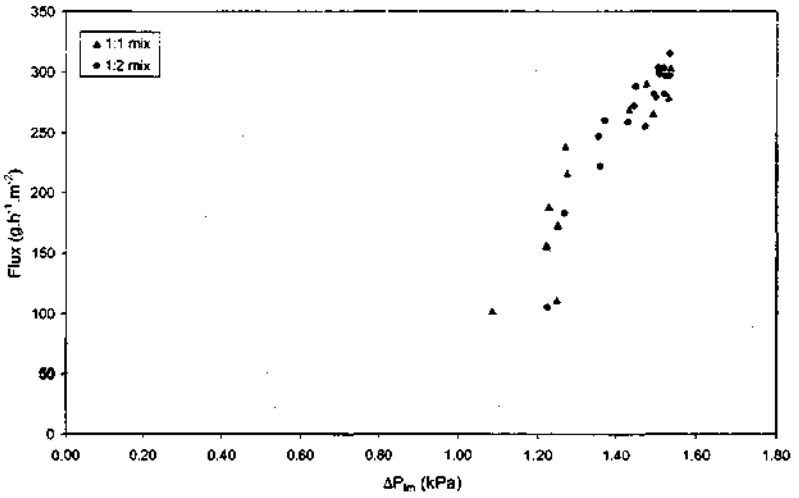

Figure 8: Transmembrane flux as a function of driving force during the distillation of 1:1 and 1:2 magnesium sulphate and sodium chloride solutions

Conclusions

The water activities during the membrane distillation of concentrated solutions of varying ratios of magnesium sulfate and sodium chloride were sufficiently accurately modeled using a computer program specific for geochemical calculations in concentrated brines. This program is limited to calculations within a temperature range of 0 to 60 °C which is inconsequential to our system, and membrane distillation in general, being an energy economic separation process which, within the norm, seldom exceeds an operating temperature of 40 °C. The resulting vapour pressure driving force showed notable similarity with the flux trend thus rationalizing the behaviour of the latter during the membrane distillation process.

An evaluation of the kinetics of crystallisation of the salts is necessary to complete the understanding of the process. These need to be well understood as the process must avoid crystallisation in the membrane module while producing a high quality final product which influences the performance of downstream processes (separation of crystals from mother liquor, drying, storage etc.)

Acknowledgements

The financial support of Sasol (Pty) Ltd., the National Research Foundation (NRF) and the Technology and Human Resources for Industry Programme (THRIP) which made the investigations possible is gratefully acknowledged. The assistance of the thermodynamics group at the University of KwaZulu-Natal, Durban, particularly that of Scott Clifford and Prathieka Naidoo, is highly appreciated.

References

Calabro V., Jiao B. L. and Drioli E. (1994) Theoretical and experimental study on membrane distillation in the concentration of orange juice. *Ind. Eng. Chem. Res.*, **33**, 1803-1808.

Curcio E., Criscuoli A. and Drioli E. (2001). Membrane Crystallizers. *Ind. Eng. Chem. Res.*, **40**, 2679-2684.

Franken A. C. M., Nolten J. A. M., Mulder, M. H. V., Bargeman D. and Smolders C. A. (1987) Wetting criteria for the applicability of membrane distillation. *J. Membr. Sci.*, **33**, 315-328.

Hsu S. T., Cheng K. T. and Chiou J. S. (2002) Seawater desalination by direct contact membrane distillation. *Desalination*, **143**, 279-287.

Joseph M. A., Raal J. D. and Ramjugernath D. (2001) Phase equilibrium properties of binary systems with diacetyl from a computer controlled vapour-liquid equilbrium still. *Fluid Phase Equilibria*, **182**, 157-176.

Lawson K. W. and Lloyd D. R. (1997). Membrane Distillation: review. *J. Membr. Sci.*, **124**, 1-25.

Liu C. and Lindsay W. T. (1971) Thermodynamics of sodium chloride solutions at high temperatures. *Journal of Solution Chemistry*, **1**(1), 1972.

Plummer L. N., Parkhurst D. L., Fleming G. W. and Dunkle S. A. (1988) *A computer program incorporating Pitzer's equations for calculation of geochemical reactions in brines*. U.S. Geological Survey Water-Resources Investigations, Report 88-4153, U. S. Department of the Interior, Reston, Virginia, USA.

Raal J. D. and Mühlbauer A. L. (1998) *Phase Equilibria: measurement and computation*, Bristol, PA.

Sparrow B. S. (2003) Empirical equations for the thermodynamic properties of aqueous sodium chloride. *Desalination*, **159**, 161-170.

Tzahi Y. C., Adams V. D. and Childress A. E. (2004) Experimental study of desalination using direct contact membrane distillation: a new approach to flux enhancement. *J. Membr. Sci.*, **228**, 5-16.

Walton J., Lu H., Turner C., Solis S. and Hein H. (2004) *Solar and waste heat desalination by membrane desalination*. Desalination and water purification research and development program report (DWPR) no. 81, Bureau of Reclamation, Denver Federal Center, USA.

PAPER 2

A Fully Integrated Membrane Operation for Sea Water and Brackish Water Desalination

Efrem Curcio[1,2], Gianluca Di Profio[1], Lynette Mariah[3], Enrico Drioli[1,2]

[1] *University of Calabria, Department of Chemical Engineering an Materials, Rende, Italy*
[2] *Institute on Membrane Technology, ITM-CNR, c/o University of Calabria, Italy*
Tel: +39.0984.492039 Fax: +39.0984.402103 Email: e.curcio@itm.cnr.it
[2] *Pollution Research Group, Department of Chemical Engineering, University of Kwa-Zulu Natal, Durban, South Africa*

Abstract

Water scarcity already represents the major problem in many countries. Considerable progresses have been reached by introducing pressure driven membrane operations as alternative to thermal desalination systems. Today, a large part of new desalination plants are almost completely based on Reverse Osmosis, eventually integrated with Microfiltration and Nanofiltration for pre-treatment. The introduction of these technologies has already evidenced interesting cost reduction and operational flexibility. However, membrane desalination technology still requires further improvements in the direction of: higher water recovery factors, further cost reduction, implementation of innovative strategies for brine disposal, improved process flexibility with respect to feed water composition, better quality of produced water for different potential end-users (ultrapure water, drinking water, agricultural and industrial water). In order to achieve these goals, the strategy of Process Intensification - that represent, today, one of the most realistic answer to a sustainable industrial growth – should be extended to the industrial segment of desalination. In this respect, fully integrated membrane operations seem to offer, in principle, interesting perspectives.
In this work, authors present the energetic and exergetic analysis of an integrated membrane desalination system and discuss some appropriate parameters for improving the performance of the desalination plant in the logic of process intensification. A preliminary cost analysis based on different combinations of the membrane units, including the possibility to produce crystals from brines, is also provided.

Keywords: *Integrated membrane systems; process intensification; desalination*

Introduction

Water shortage is now becoming acute in many countries so challenging governments to find solutions to the conflict over available water resources and rapid population increasing. In many arid zones, coastal or inland, desalination of sea or brackish water is the only solution to supply of fresh water. Due to the strategic nature of the product, several countries have drastically expanded the investments on desalination technologies. At the beginning of this millennium, the world production capacity was above 10^6 m^3/d and the number of operating units was more than 12,500. Desalination plants are today present in more than 120 countries and the current production capacity is almost twice what it was a decade ago [Drioli, E. and Romano, M., 2001]. Mediterranean countries, including Spain, Malta and Cyprus, as well as Israel, have reverted from traditional MSF to the RO method during the past two decades. Despite the great success of membrane systems in water treatment, some critical problems still remain open: improve the water quality, enhance the recovery factors in high-pressure membrane systems, reduce the global costs, minimize the brine disposal impact. In this work, authors aim to demonstrate that integrated membrane operations might be a solution for improving desalination and water treatment systems in the logic of Process Intensification (PI). Process Intensification represents today one of the most promising strategy believed to bring drastic improvements in manufacturing and processing, substantially decreasing equipment-size/production-capacity ratio, reducing raw materials, saving energy input, replacing

and reducing hazardous, recycling waste materials [Stankiewicz, A. and Moulijn, J.A., 2002]. In this contest, membrane science and technology is expected to give a substantial contribution to satisfy the PI goal and to develop sustainable pathways, thus providing reliable options for both industrial growth and environmental protection.

Membrane operations, with their intrinsic characteristics of efficiency and operational simplicity, high selectivity and permeability for the transport of specific components, compatibility between different membrane operations in integrated systems, low energetic requirements, good stability under operative conditions, environment-compatibility, easy control and scale-up, and large flexibility, can offer an interesting answer for the rationalisation of the chemical production. At present, the possibility to redesign important industrial production cycles by combining various membrane operations available in the separation and conversion units, so realizing highly integrated membrane processes, is an attractive opportunity because of the synergic effects that can be reached.

It is today well accepted that costs related to conventional pre-treatments can be minimized using pressure driven processes such as Microfiltration (MF), Ultrafiltration (UF) and Nanofiltration (NF). MF is a low energy-consuming technique extensively used to remove suspended solids and to lower COD/BOD and Silt Density Index (SDI) to values below 5. UF retains suspended solids, bacteria, macromolecules and colloids; although operating at higher pressure than MF, UF remains competitive against conventional pre-treatment. The use of NF leads to significant improvement in the reliability of Reverse Osmosis (RO): turbidity, microorganisms and hardness are strongly reduced, as well as the most part of multivalent ions; monovalent species are also retained by 10-50% depending on the membrane properties. As consequence, the osmotic pressure of the RO feed stream is decreased, thus allowing the unit to operate at high recovery factors without scaling problems.

Alternative designs and engineering approaches need to be developed not only to drive down the cost of water and to ensure the quality of water supply. Cost effective and environmentally sensitive concentrate management is today recognized as a significant hurdle to extensive implementation of desalination technologies. At present, a large part of desalination facilities discharge their concentrate waste stream back to surface waters or oceans. This disposal methods represents currently the least expensive option for both small systems and for larger systems located near coastal regions. However, the promulgation of more and more stringent environmental protection regulations will reduce progressively this opportunity. Recently, the R&D activity about concentrate disposal subject has been considered in the U.S. Roadmap on Desalination & Water Purification Technology [U.S. Bureau of Reclamation, 2003] as a research area of strategic importance, and alternative design pathways for brine concentration is encouraged as viable opportunity to obtain value from saline waste streams, with consequent benefits in terms of overall costs reduction. In this respect, authors of the present paper consider an innovative Membrane Crystallization device [Curcio, E. et al., 2001] as additional option for integrated membrane desalination systems able to recover dissolved salts present in seawater (NaCl, $MgSO_4 \cdot 7H_2O$), and to increase the yield of desalted water.

Membrane Crystallization (a schematic representation is reported in figure 1) has been recently proposed as one of the most interesting and promising extension of the MD concept: solutions, concentrated above their saturation limit, achieve a metastable state (supersaturation) in which crystals nucleate and grow. The driving force of the process, the vapour pressure gradient between both sides of the membrane, can be activated by a temperature or concentration gradients. Membrane Crystallizers, when working under forced solution flow regime, are characterized by an axial flux, in laminar regime, of the crystallizing solution through the membrane fibres. This is expected to promote a well ordered organization of the molecules, finally resulting in the formation of crystals with better structural properties. One of the main features of the MCr systems is that the membrane does not act simply as support for the solvent evaporation, but it also induces

heterogeneous nucleation starting at low supersaturation ratios, depending on the surface characteristics of the membrane.

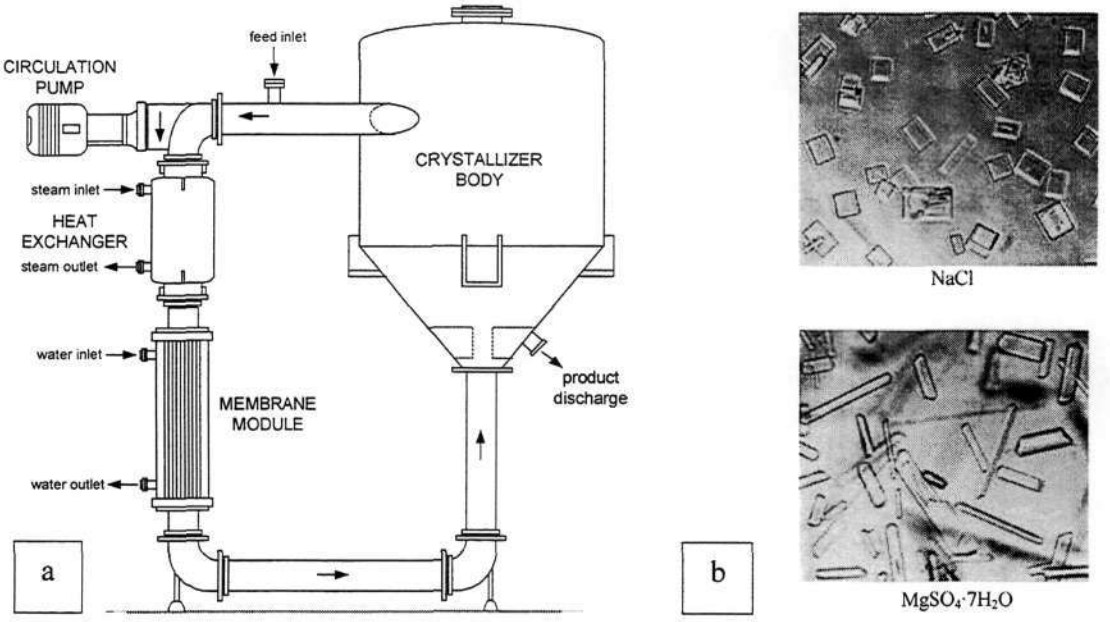

Figure 1- a) *Scheme of a Membrane Crystallizer;* ***b)*** *crystalline products of interest.*

Energy and exergy analysis for quantifying the energetic requirements of the various membrane systems and their efficiency – evaluated in terms of entropic losses – is carried out. The feasibility of different integrated flow sheets are discussed in terms of energy demand, productivity and quality of fresh water, brine disposal reduction and cost analysis.

Energy and exergy analysis

Three different flow sheets have been analysed; starting form the case study (FS1) that concerns the combination MF/NF/RO (figure 2), additional schemes include a Membrane Crystallization unit working: i) downstream the NF retentate (FS2, figure 3); ii) downstream the RO retentate (FS3, figure 4). In all cases, the same feed water flowrate (1000 kg/h) and composition (table 1) is considered.

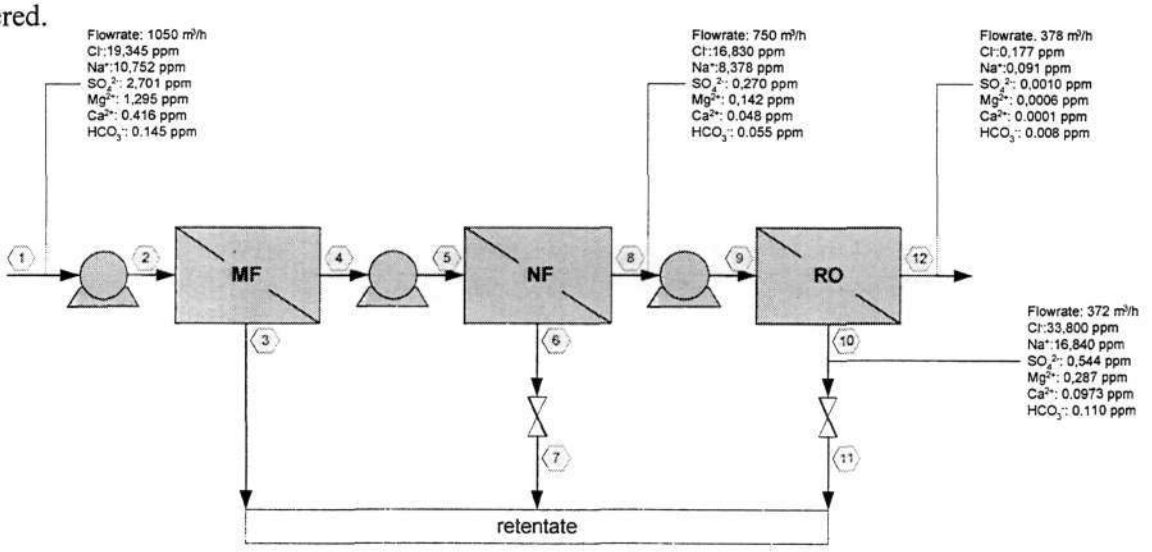

Figure 2*- Flow sheet 1 (FS1): an integrated MF/NF/RO system.*

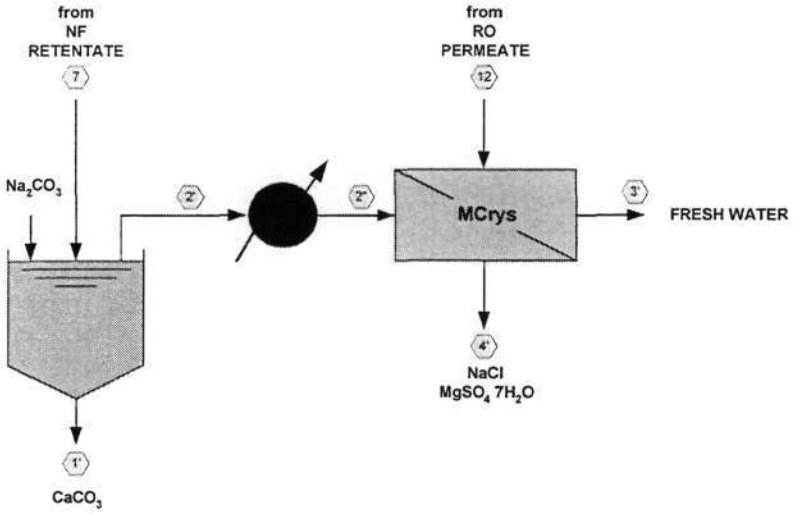

Figure 3- *Flow sheet 2 (FS2):the additional Membrane Crystallizer working downstream NF retentate completes FS1.*

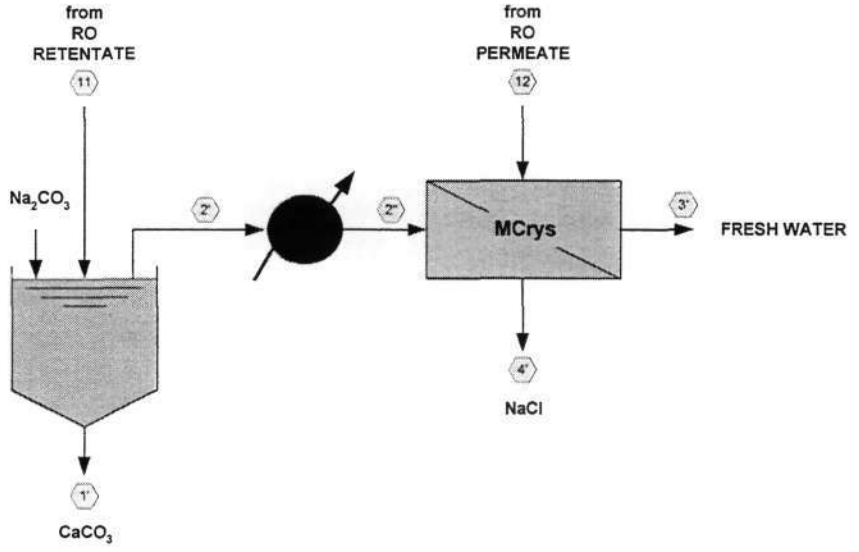

Figure 4 - *Flow sheet3 (FS3):the additional Membrane Crystallizer working downstream RO retentate completes FS1.*

Ion	Concentration (ppm)
Cl^-	19,345
Na^+	10,752
SO_4^{2-}	2,701
Mg^{2+}	1,295
Ca^{2+}	0,416
HCO_3^-	0,145

Table 1 – *Feed water composition*

Water recovery factors of the different pressure-driven membrane units are: 94.7% for Microfiltration, 75.3% for Nanofiltration, [Drioli, E. et al., 2004] and 50.5% for Reverse Osmosis (Nanofiltration reduces the scaling potential due to bivalent ions Ca^{2+} and Mg^{2+} and allows to operate RO at higher recovery factor). For what concerns the performance of a Membrane Crystallizer, the possibility to reduce up to 95% Ca^{2+} ions by reactive unseeded precipitation of calcium carbonates, to crystallize 78% of dissolved sodium chloride, and to produce 8.4 kg $MgSO_4 \cdot 7H_2O$ per cubic meter of NF retentate was experimentally verified in a previous work [Drioli, E. et al., 2004]. The fresh water coming out from RO is used as cold water stream in the Membrane Crystallizer.

The basic equations for energy and exergy analysis are below described [Criscuoli, A. et al., 1999]. Exergy (*Ex*), defined as the maximum useful work that a system can do when it passes from an actual state to the reference state where it is in equilibrium with the surroundings, is calculated as sum of three contributions:

$$Ex = Ex^T + Ex^P + Ex^c \quad (1)$$

- Temperature exergy term $Ex^T = G[(h - h_0) - T_0(s - s_0)]$ (1.a)
- Pressure exergy term $Ex^P = G[(P - P_0)/\rho]$ (1.b)
- Concentration exergy term $Ex^c = -G(N_s R T_0 \ln x_1)$ (1.c)

where G is the mass flowrate, s the specific entropy, h the specific entalpy, P the pressure, T the temperature, (subscript 0 indicates the reference status), ρ the density, R the gas constant, x_1 the molar fraction of the solvent, and N_s is:

$$N_s = (1000 - \Sigma c_i / \rho)/MW \quad (1.d)$$

$$x_1 = N_s / \{N_s + \Sigma[\beta_i c_i / (\rho MW_i)]\} \quad (1.e)$$

In equations (1.d-e), c_i concentration of i-th component, β is the number of particles formed by dissociation of i-th component in solution, MW the molecular weight.

The exergy balance is expressed as:

$$R_s T_0 = W_u - W_u' - \Delta Ex \quad (2)$$

where $R_s T_0$ is the entropy production, ΔEx is the exergy variation between inlet and outlet streams, W_u is the electrical exergy supplied to the cycle, W'_u is the thermal exergy supplied to the cycle, calculated assuming that saturated vapour loses its latent heat transferring exergy to the fluid to be heated:

$$W_u' = G_v[(h_v - h_c) - T_0(s_v - s_c)] \quad (2.1)$$

G_v is the steam mass flow rate; subscripts *v* and *c* refer to vapour and condensed steam, respectively. Primary energy (PE), defined as the energy supplied by fuel combustion to produce energy, is evaluated as:

$$PE = G_v \cdot 0.8 \quad (3)$$

Mass flowrate, total concentration of ionic species, pressure and temperature and exergy terms of each stream in FS1-3 are reported in tables 2-4.

Stream	1	2	3	4	5	6	7	8	9	10	11	12
G (kg/h)	1,050,000	1,050,000	55,000	995,000	995,000	245,000	245,000	750,000	750,000	372000	372,000	378,000
c (g/l)	34.654	34.654	34.654	34.654	34.654	61.852	61.852	25.733	25.733	51.679	51.679	0.270
P (MPa)	0.1	0.2	0.1	0.1	1.1	1.0	0.1	0.1	6.9	6.8	0.1	0.1
T (K)	293	293	293	293	293	293	293	293	293	293	293	293
Ex^c (kJ/h)	2,808,300	2,808,300	148,800	2,659,500	2,659,500	1,113,400	1,113,400	1,541,300	1,541,300	1,520,500	1,520,500	8,280
Ex^P (kJ/h)	0	105,000	0	0	995,000	2,213,000	0	0	5,097,000	2,476,000	18,600	0
Ex^T (kJ/h)	0	0	0	0	0	0	0	0	0	0	0	0

***Table 2** – Stream properties in FS1.*

Stream	1'	2'	2''	3'	4'
G (kg/h)	894	244,100	244,100	233,300	10,800
c (g/l)	-	62.270	62.270	0	-
P (MPa)	0.1	0.1	0.1	0.1	0.1
T (K)	293	293	323	313	293
Ex^C (kJ/h)	-	1,138,000	1,138,000	0	-
Ex^P (kJ/h)	-	0	0	0	0
Ex^T (kJ/h)	-	0	1,432,000	638,000	0

***Table 3** – Stream properties in FS2.*

Stream	1'	2'	2''	3'	4'
G (kg/h)	85.4	371,900	371,900	359,400	12,500
c (g/l)	-	51..705	51.705	0	-
P (MPa)	0.1	0.1	0.1	0.1	0.1
T (K)	293	293	323	313	293
Ex^C (kJ/h)	-	1,521,000	1,521,000	0	-
Ex^P (kJ/h)	-	0	0	0	0
Ex^T (kJ/h)	-	0	2,170,000	963,000	0

***Table 4** – Stream properties in FS3.*

Tables 5-7 report the results of the analysis for the three different flow sheets in terms of product characteristics, energy and exergy.

Brine flow rate	672 m^3/h
Brine concentration	53.986 g/l
Fresh flow rate	378 m^3/h
Fresh flow rate concentration	0.270 g/l
W_u	6,523,600 kJ/h
W_u'	0 kJ/h
R_sT_0	6,522,300 kJ/h
Electrical energy	1,812 kWh
G_v	0 kg/h
PE	0 Mcal/h

***Table 5** – Product characteristics and thermodynamic characteristics of FS1.*

Brine flow rate	426 m^3/h
Brine concentration	49.457 g/l
Fresh flow rate	624 m^3/h
Fresh flow rate concentration	0.166 g/l
W_u	6,524,000 kJ/h
W_u'	7,129,000 kJ/h
R_sT_0	14,764,000 kJ/h
Electrical energy	1,812 kWh
G_v	13,400 kg/h
PE	10,750 Mcal/h

***Table 6** – Product characteristics and thermodynamic characteristics of FS2.*

Brine flow rate	312 m^3/h
Brine concentration	56.827 g/l
Fresh flow rate	738 m^3/h
Fresh flow rate concentration	0.138 g/l
W_u	6,524,000 kJ/h
W_u'	10,803,000 kJ/h
R_sT_0	18,864,000 kJ/h
Electrical energy	1,812 kWh
G_v	20,350 kg/h
PE	16,300 Mcal/h

***Table 7** – Product characteristics and thermodynamic characteristics of FS3.*

The opportunity to improve the water recovery factor by using Membrane Crystallization is evident in both FS2 and FS3. In the latter case, fresh water flowrate increases by 95%,whereas brine flowrate decreases by 53% with respect to data from FS1. Globally, the recovery factors are of 36%, 59% and 71% in FS1, FS2 and FS3, respectively. A progressive enhancement of the fresh water quality, evaluated in terms of amount of dissolved salts, is also observed when analysing FS2 and FS3.
In addition to drinking water, FS2 offers the possibility to recover from NF retentate 8.7 tons NaCl/h and 2.1 tons $MgSO_4 \cdot 7H_2O$/h in crystalline form. Before the crystallization stage, a reactive precipitation is needed in order to eliminate calcium ions and related scaling problems due to gypsum precipitation. Because of bivalent ions are retained by NF, a Membrane Crystallizer working on RO retentate (FS3) is able to produce only NaCl crystals in larger quantity (12.5 tons/h).
From an energetic point of view, the integrated system related to FS1 is the most convenient: only electrical energy is requested to drive the medium- and higher- pressure pumps (1,812 kWh). The exergetic efficiency is also interesting and the entropic losses are moderate. With respect to conventional RO desalination plants, NF units allows to pre-pressurize the feed to RO train, leading to a reduction of the electrical power requested to drive the RO pumps. NF offers further benefits in terms of reduction of membrane fouling and, consequently, of related maintenance and replacement costs.
The integration of Membrane Crystallization in FS2 and FS3 introduces a thermally energy requirement which increases the globally energy demand; as from tables 6 and 7, additional 10,750 Mcal/h and 16,300 Mcal/h are needed for heating the NF retentate and RO retentate streams, respectively, up to 323K (inlet temperature to Membrane Crystallization modules). Entropic losses are also increased.
Although the estimation of energy saving is an important parameter, it could not be the determining factor in the selection of the more appropriate flow sheet. Plant economics and productivity, drinking water quality and disposal are additional key issues to be taken into account.

Cost analysis

Capital and operating costs for seawater and brackish water desalting tend to be high for small-capacity plants and to decrease for plant capacities above 3 MGD.
Principal components to direct costs are represented by membranes ($90/m^2 for Microfiltration membranes, also suitable for application in Membrane Crystallization, $30/m^2 for Nanofiltration and Reverse Osmosis membranes) and equipments (high-pressure pumps, tubes, controllers, heat exchangers etc.).
Additional costs must be included for chemicals, brine disposal, steam and electric power, labor and membrane replacement.
Cost analysis has been carried out using the following financial factors [Ettouney, H.M. et al., 2002; Peters, M.S. et al., 2002]:

- interest rate: 5%;
- plant life: 30 yr;
- amortization factor: 0.0651 yr^{-1} ;
- plant availability: 0.9;
- electric cost: 0.09 $/KWh;
- heating steam cost: 0.0032 $/lb;
- specific chemicals cost: 0.025 $/$m^3$;
- specific cost of operative labor: 0.05 $/$m^3$;
- specific cost of brine disposal: 0.0015 $/$m^3$;

The obtained results are summarised in tables 8-10.

Direct Capital Cost	$ 2,594,000
Plant Capacity	9.080 m^3/d
Electric Power Consumption	4.79 kWh/m^3
Fixed Charges	$ 100,900 /yr
Steam	-
Electric Power	$ 1,290,000 /yr
Chemicals	$ 74,600 /yr
Brine Disposal Cost	$ 7,930 /yr
Labor	$ 149,000 /yr
Membrane Replacement	$ 188,300 /yr
Total Annual Cost	$ 1,810,730 /yr
Unit Cost Water Production Basis	$ 0.61 $/m^3$

Table 8 – Cost analysis of FS1.

Direct Capital Cost	$ 5,898,000
Plant Capacity	14.800 m^3/d
Electric Power Consumption	2.94 kWh/m^3
Fixed Charges	$ 108,000 /yr
Steam	$ 738,400 /yr
Electric Power	$ 1,286,000 /yr
Chemicals	$ 655,600 /yr
Brine Disposal Cost	$ 5,030 /yr
Labor	$ 243,000 /yr
Membrane Replacement	$ 827,700 /yr
Total Annual Cost	$ 3,863,730 /yr
Unit Cost Water Production Basis	$ 0.80 $/m^3$

Table 9 – Cost analysis of FS2.

Direct Capital Cost	$ 7,563,000
Plant Capacity	17.700 m^3/d
Electric Power Consumption	2.46 kWh/m^3
Fixed Charges	$ 110,000 /yr
Steam	$ 1,119,000 /yr
Electric Power	$ 1,286,000 /yr
Chemicals	$ 196,400 /yr
Brine Disposal Cost	$ 3,500 /yr
Labor	$ 291,000 /yr
Membrane Replacement	$ 1,154,000 /yr
Total Annual Cost	$ 4,159,900 /yr
Unit Cost Water Production Basis	$ 0.72 $/m^3$

Table 10 – Cost analysis of FS3.

Conclusions

Three different flow sheets have been analysed for desalination purpose. In FS1, pre-treatment by MF and NF allows to increase the recovery factor of the RO stage up to 50.5%; the global recovery of fresh water is 36% with a unit cost water production of $ 0.61/m^3.

FS2 and FS3 require higher energy consumption due to the additional thermal demand; however, the increased overall performance makes them an attractive alternative with respect to conventional desalination schemes.

The introduction of a Membrane Crystallization unit downstream the NF retentate (FS2) enhances the global water recovery factor of water up to 58.6%, although the unit cost increases up to $0.80/$m^3$ as consequence of additional expenses for membrane replacement, chemicals and steam. However, this gap can be potentially offset by 8.4 M$/yr resulting form the production of 8.7 tons NaCl/h (0.044$/kg) and 2.1 tons Epsomite/h (0.33$/kg). In FS3, the membrane crystallizer works on RO retentate: the global water recovery factor of water increases up to 70.1%, and both cost and environmental impact of brine disposal operations are drastically reduced. Once more, the additional production of 12,5 tons NaCl/h might counterbalance the higher unit cost of water production (4.3 M$/yr, $0.72/$m^3$).

Bibliography

Criscuoli, A., Drioli, E., 1999.Energetic and exergetic analysis of an integrated membrane desalination system. *Desalination* (125) 243

Curcio, E., Criscuoli, A., Drioli, E., 2001. Membrane Crystallizers. *Ind. Eng. Chem. Res.* (40) 2679

Drioli, E., Curcio, E., Criscuoli, A., Di Profio, G., 2004. Integrated system for recovery of $CaCO_3$, NaCl and $MgSO_4 \cdot 7H_2O$ from nanofiltration retentate. *Journal of Membrane Science* (239) 27

Drioli, E., Romano, M., 2001. Progress and new perspectives on integrated membrane operations for sustainable industrial growth. *Ind. Eng. Chem. Res.* (40) 1277

Ettouney, H. M., El-Dessouky, H. T., Faibish, R. S., Gowin, P. J. 2002. Evaluating the Economics of Desalination. *CEP Magazine* (December) 32

Peters, M.S., Timmerhaus, K. D., West, R. E. *Plant Design and Economics for Chemical Engineers*, Mc Graw Hill, 2002

Stankiewicz, A., Moulijn, J.A., 2002. Process Intensification. *Ind. Eng. Chem Res.* 41(8) 1920

U.S. Bureau of Reclamation, Sandia National Laboratories. 2003. *Desalination and Water Purification Technology Roadmap- A Report of the Executive Committee*

PAPER 3

Available online at www.sciencedirect.com
SCIENCE DIRECT
ELSEVIER
Journal of Membrane Science 280 (2006) 937–947
journal of MEMBRANE SCIENCE
www.elsevier.com/locate/memsci

Membrane distillation of concentrated brines—Role of water activities in the evaluation of driving force

Lynette Mariah [a,*], Chris A. Buckley [a,**], Chris J. Brouckaert [a], Efrem Curcio [b,c], Enrico Drioli [b,c], Deogratius Jaganyi [d], Deresh Ramjugernath [a]

[a] School of Chemical Engineering, University of KwaZulu-Natal, Durban 4041, South Africa
[b] Institute on Membrane Technology (ITM-CNR), Via P. Bucci 17/C, c/o University of Calabria 87030, Rende (CS), Italy
[c] Department of Chemical Engineering and Materials, University of Calabria, via P. Bucci 45/A, 87030 Rende (CS), Italy
[d] School of Chemistry, Private Bag X01, University of KwaZulu-Natal, Scottsville 3209, South Africa

Received 15 December 2005; received in revised form 3 March 2006; accepted 7 March 2006
Available online 16 March 2006

Abstract

Membrane distillation crystallisation (MDC) can be used to recover crystalline products from solutions. MDC of a concentrated solution of magnesium sulphate of 375 g/l was investigated. It was found that the MDC of epsomite was achievable at a feed temperature of only 33 °C and a distillate temperature of approximately 17 °C. The orthorhombic crystals were formed at a growth rate of 1.6×10^{-8} m s^{-1}. The transmembrane flux was then measured for the membrane distillation (MD) of two concentrated solutions of mixed electrolytes, $MgSO_4$ and NaCl with concentrations of 225 and 225 g/l, respectively, for one mix; and 275 and 137.5 g/l, respectively, for the other mix. For the mixtures of salts, only sodium chloride was precipitated while magnesium sulphate remained in solution but increased in concentration. The geochemical equilibrium speciation program, PHRQPITZ, was used to determine solution activities. These results were verified by experimental vapour pressure values determined by dynamic vapour–liquid equilibrium (VLE) experiments to calculate the vapour pressures of the solution (and hence driving force) at each stage during the distillation. The accountability of water activities showed how the trend of decreasing flux fitted with that of the driving force for the distillation process. When operated in batch concentration mode the flux and driving force showed a constant initial rise (due to stabilisation of temperature and concentration profiles and fluid dynamics inside the module) after which it plateaus off before rapidly declining. Preliminary computer modelling has demonstrated how the understanding of membrane distillation processes can be improved by being able to predict driving forces.

Keywords: Membrane distillation; Crystallisation; Flux decline; Vapour pressure

1. Introduction

Salinity is one of the most critical environmental problems for water scarce countries, deteriorating water quality and threatening economic and social consequences. Some industries and mines currently have reverse osmosis (RO) and other plants producing usable water and waste brine, but brine disposal is a problem. If there is no intervention, the completed mining operations will produce saline aqueous effluents for hundreds of years. Exploiting the fact that inorganic concentrates can be separated into high value chemicals and reusable water, membrane distillation (MD) (and crystallisation) is a technique which potentially leads to an almost complete water recovery and the elimination of the brine disposal problem. Chemical manufacturing complexes frequently have an excess of low-grade heat. This energy can be used to create a temperature gradient across a hydrophobic microporous membrane. The resulting vapour pressure difference produces a flux of water vapour through the membrane thus aqueous brine solutions can be concentrated and crystallised [1,2]. Some of the main features of membrane distillation which distinguishes this process from more conventional desalination processes such as reverse osmosis and thermal evaporation are that this process (i) can operate at lower operating pressure and lower temperatures than the boiling temperature of the feed solutions [3–5], (ii) requires lower vapour space as the vapour–liquid interface is developed by a hydrophobic

* Corresponding author. Tel.: +27 33 3861007/+27 824539873.
** Co-corresponding author. Tel.: +27 31 2603131.
E-mail addresses: lynette.mariah@sasol.com (L. Mariah), buckley@ukzn.ac.za (C.A. Buckley).

0376-7388/$ – see front matter © 2006 Elsevier B.V. All rights reserved.
doi:10.1016/j.memsci.2006.03.014

membrane in MD as opposed to conventional distillation which relies on high vapour velocities to establish a vapour–liquid interface. Large membrane areas can be densely packed into a compact volume [6], (iii) is not limited by high osmotic pressure constraints and fouling as the membrane works at atmospheric pressure and is not directly involved in the separation process but acts merely as a support [7], (iv) has low sensitivity to feedwater concentrations therefore has potential applications for concentrating aqueous solutions or producing high-purity water even at very high feedwater concentrations [8,9] and (v) does not require elevated temperatures therefore the heat can be supplied by solar collectors or other forms of heat such as low-grade waste heat from factories or geothermal energy [10,11]. For these reasons MD has gained much popularity and its applications have grown in recent years. Amongst others, some of the main applications of MD include desalination, using low-grade thermal energy, the treatment of wastewater in the textile industry, the concentration of fruit juice and milk in the food industry and separation of alcohol–water mixtures [12–16]. MD is one of the membrane processes in which the membrane is not directly involved in the separation. The membrane acts only as a support for a vapour–liquid interface and does not contribute to the separation mechanism. Selectivity is determined by the vapour–liquid equilibrium involved. Hence the component with the highest partial pressure will show the highest permeation rate [17]. Solute with very low vapour pressures (or pressure differences) will have a low permeation rate. For this reason water with a very high purity can be separated from salt solutions by MD. This is because in water–NaCl mixtures, only water has a significant vapour pressure (the vapour pressure of NaCl can be neglected), which implies that only water can permeate through the membrane hence achieving very high selectivities [17].

During the late 1980s, advances in MD have lead to the extension of this process to the crystallisation stage. Crystallisation from solution is a widely used concentration and purification technique and is capable of producing large amounts of pure solid product, usually in a single processing step. However, some crystallisation techniques may require large energy inputs and process requirements in order to yield good product quality. Realising the importance of crystallisation as a purification technique the innovative technology of membrane crystallisation (MCr) was introduced by Wu and Drioli [18] who undertook investigations on MCr to produce crystals from solutions. As opposed to conventional crystallisers such as the circulating-magma crystalliser, in membrane crystallisers the solvent evaporation and solute crystallisation takes place at separate locations, i.e. the solvent evaporation takes place inside the membrane module (where the solution is below supersaturation) and crystallisation takes place in a separate tank (where the solution is in a metastable phase of supersaturation) [19,2]. This apparently induces a well organisation of the molecules thus resulting in crystals with improved quality and size distribution. This is important when crystals need to undergo further treatment or reactions. Wu et al. [20] used MCr for treating the wastewater of taurine. Tomaszewska [21] used MDC to concentrate sulphuric acid solutions subsequent to the extraction of apatite phosphogypsum. After concentrating the solution up to 40% he was able to recover the lanthane compounds which spontaneously precipitated under these conditions. Gryta [22] used MDC to concentrate sodium chloride solutions. Recently, Curcio et al. [23] used this emerging technology in the field of protein science for the crystallisation of lysozyme from supersaturated solutions. Another recent study performed by Drioli et al. [24] used the MCr to obtain epsomite ($MgSO_4{\cdot}7H_2O$) and sodium chloride as solid products from NF retentate streams. The kinetics of crystallisation for sodium chloride was well defined by Drioli et al. and in an earlier investigation by Curcio et al. [2]. The crystallisation of epsomite, has been performed but only preliminary data concerning the growth rate and morphological quality of the crystals has been evaluated. The addition of a crystalliser stage after the MD stage reduced both the cost and environmental impacts of brine disposal operations [19,25]. These results are consistent with the trend towards green chemistry and sustainable industrial development.

Despite the fact that much work has been performed in the field of membrane distillation within the last decade, the quantitative description of the decrease in transmembrane flux observed during a typical batch MD experiment has not been reported. Some authors have attributed the decrease to membrane wettability or membrane fouling [26,9,27]. Very few researchers have performed long-term experiments in order to quantify and characterise this phenomenon [28–31]. During their investigations the main drawback was the inability to evaluate the feed and permeate vapour pressures and hence driving force during the distillation process. To overcome this, theoretical approaches have been adopted in which a series of equations, derived from theoretical models of heat and mass transfer, were used to infer the flux [32,1]. Furthermore, for direct contact membrane distillation (DCMD), the theoretical analysis holds for solutions of low concentrations, certainly lower than saturation concentrations. A recent study undertaken by Tun et al. [33] which investigated the MDC of concentrated solutions of sodium sulphate and sodium chloride, found that the flux decreased gradually up to a critical saturation. They proposed a way of predicting the flux, only up to the critical condition, by interactive heat and mass transfer models. In our study it was realised that when dealing with solutions of extremely high concentration (close to saturation), it becomes necessary to take into account the activities of water on either side of the membrane. Seeing that literature does not contain extensive vapour pressure data for mixtures of electrolytes, the aim of this work was to accurately evaluate activity changes during the MD of concentrated mixed brines, and to show how these activities contribute to the overall trend of decreasing driving force and hence permeate flux.

2. Materials and methods

A series of methods was used to achieve the overall goal:

(1) MDC was first used to evaluate the production of solid magnesium sulphate heptahydrate ($MgSO_4{\cdot}7H_2O$, epsomite) from a concentrated solution of this salt. Thereafter, the MDC of mixed salt solutions of magnesium sulphate and

sodium chloride in varying ratios were investigated. The initial concentrations of the salts were chosen so that sodium chloride would precipitate while epsomite would remain in solution although increased in concentration.

(2) Vapour pressure measurements were conducted using a dynamic vapour–liquid equilibrium (VLE) still on brines with similar compositions of those studied in the MD experiments.

(3) The accuracy of a thermodynamic geochemical speciation program was evaluated by comparing the predicted vapour pressures with the experimentally derived values. The vapour pressure driving force during the course of the MD experiments was calculated using the geochemical speciation program and correlated with the distillate flux.

2.1. Membrane distillation crystallisation

The MDC unit (Fig. 1) induces supersaturation by removing pure water from the brine; thus creating a metastable state which leads to nucleation and crystal growth. The retentate (hot brine) and permeate (cold water) streams are held at different temperatures on either side of a hydrophobic microporous membrane. The membrane module, MD020CP-2N, supplied by Microdyn, contains 40 hydrophobic polypropylene hollow fibres of 0.1 m^2 total interfacial area. The nominal pore size of the polypropylene membranes was 0.2 μm and the external diameter was 1.8 mm. The water flux was evaluated by measuring the amount of water extracted at time intervals during the course of the experiment.

Crystallisation occurs in the brine recirculation tank from which the mother liquor was recirculated to the membrane module. A significant feature of membrane crystallisers is that the membrane does not merely serve as a support for the vapour–liquid interface, but it also induces heterogeneous nucleation initialising at low supersaturation ratios, depending on the surface characteristics of the membrane [19]. Samples were routinely withdrawn from the crystallisation tank and visually examined and photographed using a video-camera model, Axiovert 25, equipped with optical head 25X, to determine the crystal size distribution. Nucleation rate has been evaluated by microscopic visualization, i.e. monitoring the evolution in time of the crystal size distribution. The crystals obtained show good quality and size distribution which is important for the determination of the final product quality and influences the performance of downstream processes such as separation of crystals from mother liquor, drying and storage [24]. The performance of the membrane was evaluated in terms of transmembrane flux.

It has been shown [32] through a series of mass transfer models, that the mass flux, J, across the membrane in MD can be approximated to:

$$J = C\Delta P_m \tag{1}$$

where C is a membrane mass transfer coefficient for the system (obtained from a combination of flow models) and ΔP_m is the vapour pressure difference across the membrane. C is only slightly temperature-dependent and it is a function of the membrane pore geometry or the mole fraction of air within the pores, the discriminating factor being whether convective or diffusive transport, respectively, is dominant. Furthermore, as the vapour pressures within the membrane are not directly measurable it is more convenient to express Eq. (1) in terms of temperature [7,32]:

$$J = C\left(\frac{dP}{dT}\right)_{T_m}(\Delta T_m) \tag{2}$$

where ΔT_m is the temperature gradient across the membrane. When $\Delta T_m < 15\,^{\circ}C$ (dilute solutions), then dP/dT can be approx-

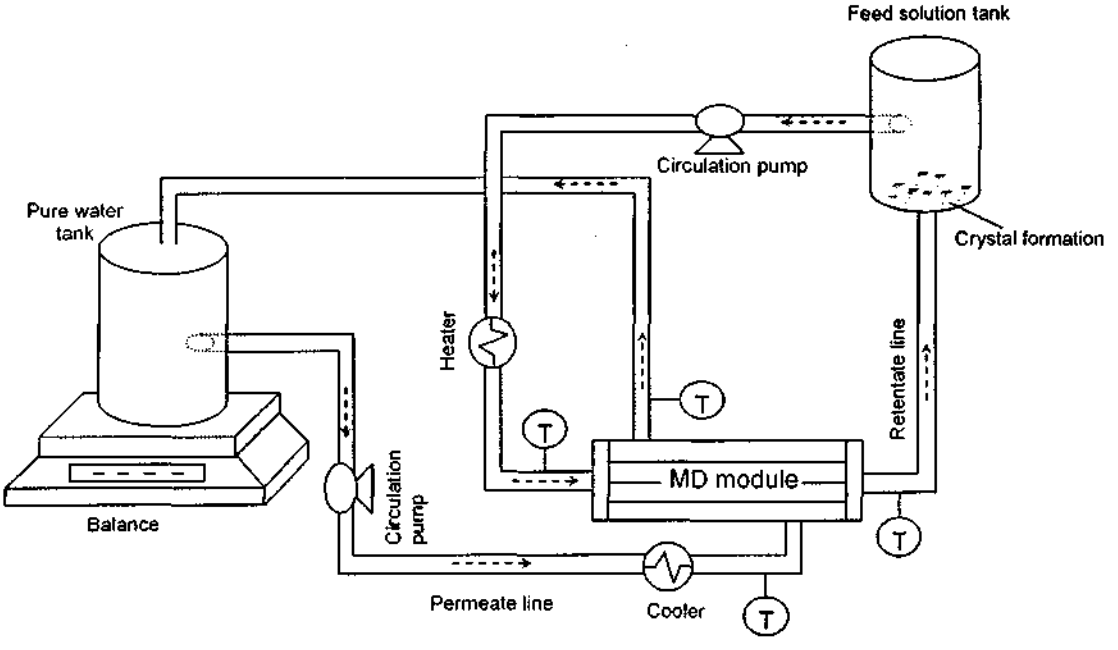

Fig. 1. Schematic of the membrane distillation–crystallisation experimental setup.

imately evaluated using the Clausius–Clapeyron equation:

$$\frac{dP}{dT} = \frac{P\Delta H_{vap} M}{RT_m^2} \tag{3}$$

where ΔH_{vap} is the molar heat of vapourisation and P can be evaluated from the Antoine equation:

$$\ln P = A + \frac{B}{T + C_A} \tag{4}$$

where P is the pressure in Pa, T the temperature in Kelvin and A, B and C_A are constants which vary from substance to substance.

It has been shown by Sarti et al. [4] that Eq. (2) must be modified to account for the reduction in vapour pressure caused by dissolved species before it can be used for more concentrated solutions. Eq. (2) then becomes

$$J = C\left(\frac{dP}{dT}\right)[\Delta T_m - \Delta T_{th}](1 - x_m) \tag{5}$$

where ΔT_{th} is a threshold temperature defined as

$$\Delta T_{th} = \frac{RT^2}{M\Delta H_{vap}} \frac{x_m^f - x_m^p}{1 - x_m} \tag{6}$$

where x is the mole fraction of dissolved species. If $\Delta T_m < \Delta T_{th}$, a negative driving force will be observed, giving rise to a dilution of the brine solution.

2.1.1. Experimental

For the single electrolyte system, experiments were performed with concentrated solutions of magnesium sulphate of 375 g/l by dissolving analytical grade magnesium sulphate heptahydrate ($MgSO_4 \cdot 7H_2O$) in demineralised water. A volume of 2.76 l of a 375 g/l solution was initially fed into the distillation plant which operated for approximately 15 h for the course of the experiment. For the mixed electrolyte system, solutions of magnesium sulphate and sodium chloride were prepared in mass ratios of 1:1 and 1:2, respectively, by dissolving the appropriate amount of analytical grade magnesium sulphate heptahydrate and sodium chloride in demineralised water. Concentrations of $MgSO_4$ and NaCl of 225 and 225 g/l, respectively, were prepared for the 1:1 mix; and concentrations of $MgSO_4$ and NaCl of 137.5 and 275 g/l, respectively, were prepared for the 1:2 mix. The volume of solution fed to the plant was 3 l and the duration of the experiment was, on average, 8 h. The system was operated in a batch concentration mode where the recirculating permeate stream was deionized water, and the retentate stream flowed countercurrent through the membrane module at a flowrate of the order 100 l/h. The temperature was set to an approximate value for the feed solution and the solution gradually heated before starting the MDC process. Once the appropriate temperature was reached the process was initialised. However, the temperature did fluctuate during the initial stages of the process as the temperature difference across the membrane was established. The average temperatures at module inlet on retentate and distillate sides for the 1:1 mix was 32.6 ± 1.7 and 16.0 ± 0.5 °C, respectively, and 32.6 ± 1.2 and 16.8 ± 0.4 °C for the 1:2 mix, respectively. The average temperatures at module outlet on retentate and distillate sides for the 1:1 mix was 29.3 ± 1.4 and 16.9 ± 0.7 °C, respectively, and 30.5 ± 1.0 and 17.4 ± 0.7 °C for the 1:2 mix, respectively.

2.2. Vapour–liquid equilibrium still

The vapour–liquid equilibrium (VLE) still developed by Raal and Mühlbauer [34] was used to measure the vapour pressures of the mixtures of sodium chloride and epsomite corresponding to the range of compositions of those used during the distillation process at different temperatures. The vapour pressures of pure sodium chloride as a function of temperature were also evaluated in order to test the accuracy of the procedure by comparison to literature.

The VLE still is shown in Fig. 2. The vapour–liquid mixture that is generated in the boiling chamber is forced upward through the Cottrell tube. The mixture then flows down through a stainless steel wire mesh packing onto the temperature sensing Pt-100 element. The packed section allows close contact between the vapour and liquid so the attainment of equilibrium is rapid. The equilibrium chamber consists of small holes at the

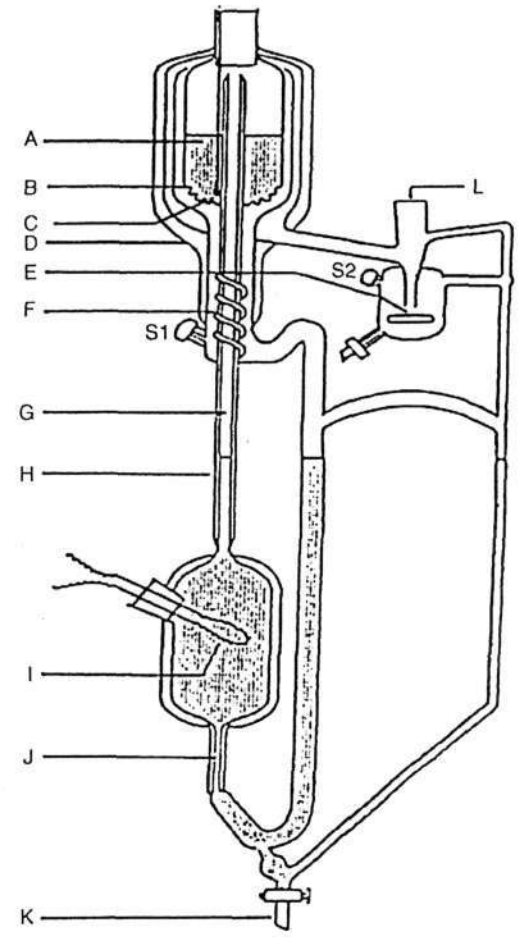

Fig. 2. Schematic diagram of vapour–liquid equilibrium still. A: SS wire mesh packing; B: drain holes; C: Pt-100 bulb; D: vacuum jacket; E: magnetic stirrer; F: SS mixing spiral; G: insulated Cottrell pump; H: vacuum jacket; I: internal heater; J: capillary; K: drain valves; S1: liquid sampling point; S2: vapour sampling point; L: condenser is attached here [34].

Table 1
Antoine's coefficients obtained for the pure magnesium sulphate solution and the binary systems, 1:1 and 1:2 mixes

Solution	A	B	C_A	$\sum r^2$
$MgSO_4$ (375 g/l)	16.552	4000.0	−40.123	5.11×10^{-4}
1:1 mix	16.019	4001.9	−34.319	7.06×10^{-2}
1:2 mix	16.058	3986.9	−34.506	7.97×10^{-2}

bottom which allows for the exit of the equilibrium mixture. Part of the equilibrium liquid is caught in a liquid trap before returning to the boiling chamber. The disengaged equilibrium vapour flows around the equilibrium chamber before being condensing in the condensate receiver [35].

The Antoine equation (Eq. (4)) was fitted to the experimental vapour pressure data by using a regression procedure to determine the parameters. The parameters for the solutions of importance are listed in Table 1.

2.2.1. Experimental

The preparation of the solutions followed the same procedure as that used for MD. The suitability of the VLE still to measure vapour pressures of concentrated salts was evaluated by comparing the experimental vapour pressure values of sodium chloride with those in literature. The temperature and pressure were measured with a multimeter (which measured the resistance of the Pt-100 bulb) and pressure transducer, respectively. The accuracies of temperature and pressure measurements were estimated to be ±0.02 K and ±0.03 kPa, respectively. The desired temperature was set and once vapour–liquid equilibrium was established, the corresponding pressure was recorded. The control of temperature was within 0.01–0.05 K, depending on the composition of the solution, according to a technique developed based on pulse-width modulation of the two solenoid valves with the aid of a computer [35].

2.3. Modelling using the geochemical equilibrium speciation program, PHRQPITZ

PHRQPITZ is a computer program which enables geochemical calculations in brines and other electrolyte solutions at high concentrations by making use of the Pitzer-virial coefficient approach for activity coefficient corrections [36]. In addition to being able to calculate the activity coefficients for the above solutions with temperature, the program is also able to model mineral solubility thus predicting the evaporation factor needed in order to reach supersaturation and crystallisation. For the purposes of this paper, this program was used to test its applicability for modelling vapour pressures by comparison to the data obtained from the VLE experiments. The activity of water, α_{H_2O}, in PHRQPITZ is computed from the osmotic coefficient, ϕ (estimated from the Pitzer equation [37]) according to:

$$\ln \alpha_{H_2O} = -\frac{\phi \sum_i m_i}{55.50837} \tag{7}$$

where m_i is the molality of the ith ion in solution and 55.50837 is the number of moles of water per kilogram of water. The effective vapour pressure of a solution is then defined as the product of the vapour pressure of pure water at the same temperature as the solution and the activity of water in the solution (Eq. (8)):

$$P_{soln} = P_{H_2O} \alpha_{H_2O} \tag{8}$$

There are some limitations concerning the use of this program for modelling purposes. One such limitation is that the temperature range for equilibria in the PHRQPITZ database is variable and is within the range 0–60 °C but the sodium chloride system is valid up to approximately 350 °C. However, this limitation did not apply to our MD system as the maximum retentate temperature did not exceed 33 °C.

3. Results and discussion

3.1. Membrane distillation

Crystals of epsomite and sodium chloride were obtained from crystallisation experiments on single electrolyte solutions of magnesium sulphate and mixed solutions of magnesium sulphate and sodium chloride, respectively. The epsomite crystals obtained (Fig. 3), at a supersaturation of 1.34 kg/l, display the typical orthorhombic geometry characteristic of this salt.

For the crystallisation of a single salt solution of epsomite, data in Fig. 4 show that the peak of particle size distribution progressively migrates towards increasing crystal size due to the crystal growth process. The indicated times (t) refer to the time passed after the first visual appearance of crystals.

The shape of the particle size distribution is governed by a coefficient of variation, CV, which is defined according to the following equation [38]:

$$\mathrm{CV} = \frac{F_{80\%} - F_{20\%}}{2F_{50\%}} \times 100 \tag{9}$$

where F is the cumulative crystal size distribution. Analysis of the experimental cumulative size distribution functions

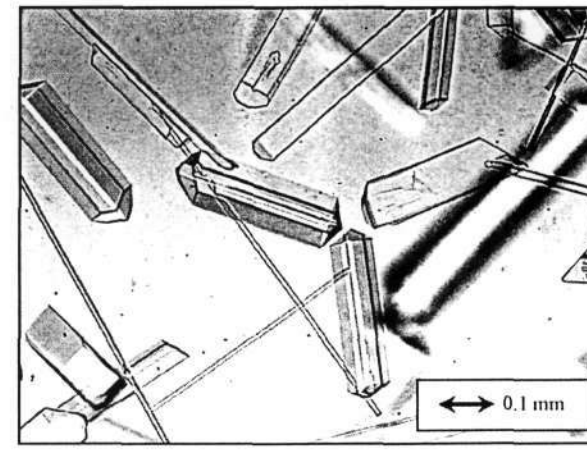

Fig. 3. Epsomite crystals obtained from the MDC of a single salt solution of an initial concentration of 375 g/l, sampled approximately 17 h from the start of the MD process. Concentration of magnesium sulphate at precipitation was 1.34 kg/l.

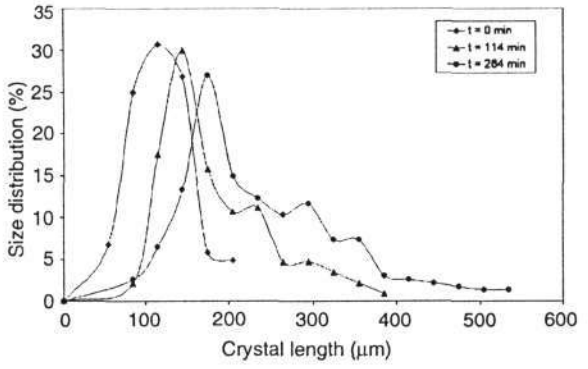

Fig. 4. Particle size distribution for the crystallisation of epsomite from a concentrated single electrolyte solution of magnesium sulphate using MDC. The indicated times refer to the experimental sampling times after the first visual appearance of crystals.

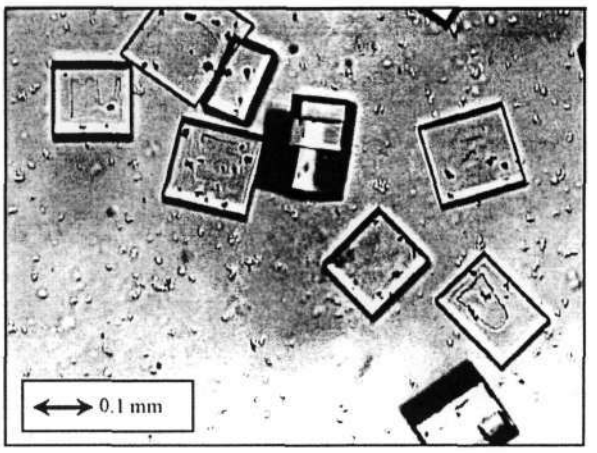

Fig. 5. Sodium chloride crystals obtained from the MDC of a mixed solution (1:1 mix) of sodium chloride and epsomite sampled at approximately 13 h after the start of the MD process.

enabled CV values to be calculated and was found to be in the range of 10–30%. A crystal growth rate of 1.6×10^{-8} m s^{-1} was observed for the crystallisation of epsomite. Al-Jibbouri et al. [39] reported a growth rate of 2.82×10^{-7} m s^{-1} for the crystallisation of epsomite at 24 °C at a supersaturation of 0.64 g epsomite/100 g H_2O. Ramalingom et al. [40] showed that epsomite, in the presence of urea, crystallised at a rate of 1.85×10^{-8} m s^{-1} through seeded crystallisation. Drioli et al. [24] reported a growth rate of 5×10^{-7} m s^{-1} of epsomite at 25 °C from a solution containing a mixture of salts representing that of seawater. Apart from the distinct highly concentrated solutions used in this work, the techniques and experimental conditions under which the mentioned crystallisations were performed differ from those used in this work. The kinetics of crystallisation as well as crystal morphology is strongly related to the different components present in the crystallising solution, degree of supersaturation, temperature and hydrodynamic conditions [39]. It is difficult to draw any meaningful conclusions from the comparison between the crystallisation rate observed in this study and those from the literature, because of the different composition of the solutions. For example, Al-Jibbouri et al. [39] showed that the presence of NaCl in the crystallising solution tends to increase the growth rate of epsomite which explains the increased growth rate observed by Drioli et al. [24] for the crystallisation of epsomite from a solution in which NaCl was present in an appreciable amount as opposed to that observed in this experiment where magnesium sulphate existed alone in solution.

For the mixed electrolyte systems, when MD was run in batch concentration mode with the crystalliser, sodium chloride crystals were precipitated from solution. This is featured in Fig. 5 which shows the characteristic cubic geometry displayed by this salt.

For the evaluation of the transmembrane flux, MD was run in a batch concentration mode, without the crystalliser, with the mixed electrolyte salt solutions at feed concentrations below saturation. The performance of the MD was evaluated by examining the water flux as illustrated in Fig. 6. This trend represents that of the 1:1 mix.

The experiments were performed in a closed (non-continuous) membrane system evolving with time. At the beginning of the experimental run depicted in Fig. 6, the brine heater, the permeate cooler and the circulating pumps for both streams were switched on. There was an initial rise in flux as the temperature difference across the membrane was established. Thereafter the flux declined as the brine concentration increased. Thus the initial rise in the flux that is observed in Fig. 6 is due to the stabilisation of concentration and temperature profiles as well as fluid dynamic conditions inside the membrane module. In general, it is typical that when a crystallisation run is carried out in a batch concentration mode i.e. the retentate line is not continuously replenished with fresh feed solution, the flux will decrease with time (once the system has stabilised) as the solution becomes more concentrated. A similar decrease in flux was obtained for the 1:2 mix. This has been variously attributed to the growth of crystals on the membrane thus blocking the membrane pores [33] and to the reduction of vapour pressure gradient due to the increase of the concentration of salts in the solution [24]. The latter explanation was investigated further by measuring these vapour pressures of these solutions.

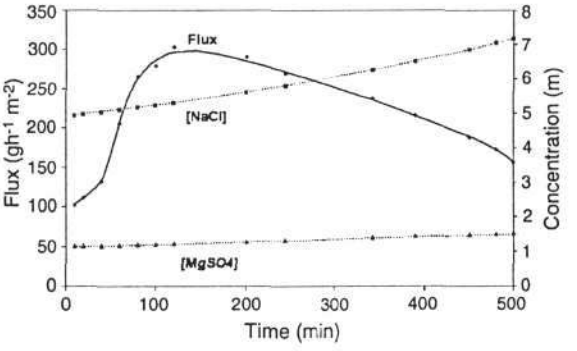

Fig. 6. Water transmembrane flux and the concentration of magnesium sulphate and sodium chloride with time for the 1:1 mix, up to the metastable state, just before crystallisation.

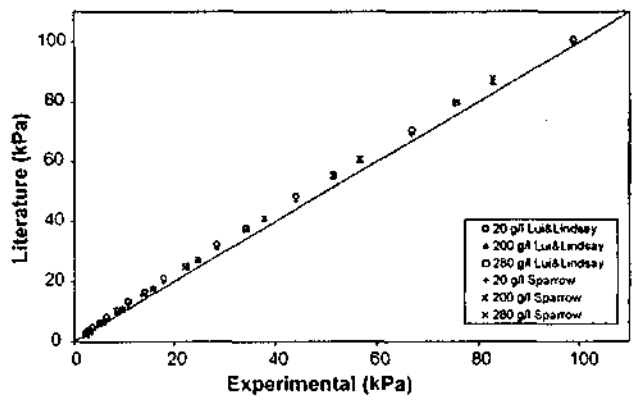

Fig. 7. Comparison of experimental vapour pressures obtained using VLE and those of literature.

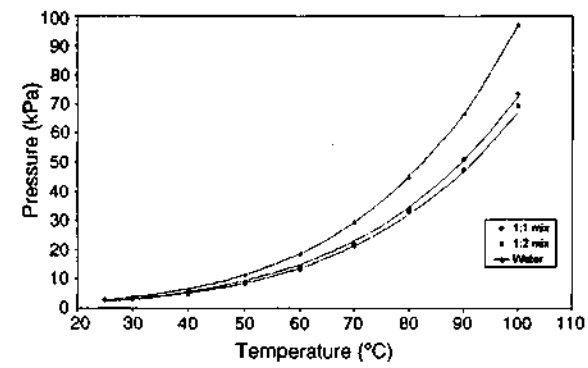

Fig. 8. Vapour pressures of the 1:1 and 1:2 salt mixes from VLE experiments together with the fitted Antoine curve and the vapour pressure curve of pure water.

3.2. Vapour–liquid equilibrium still

In order to test the performance of the VLE still the vapour pressure of aqueous solutions of pure sodium chloride was measured as a function of temperature and was compared to two literature sources. Liu and Lindsay [41] performed vapour pressure lowering experiments on concentrated solutions of sodium chloride (from 4 m to saturation) and at temperatures from 75 to 300 °C. The vapour pressure measurements performed in this work on the concentrated sodium chloride solutions were performed at temperatures from 25 to 100 °C and concentrations of 20, 200 and 280 g/l. As no literature data was found containing actual measurements of NaCl solutions within these precise concentration and temperature ranges, the data of Liu and Lindsay [41] was fitted to the Antoine equation (Eq. (4)) and then extrapolated to lower temperatures. The empirical equations presented by Sparrow [42] for thermodynamic properties of aqueous NaCl was used as a second comparison with the data obtained form these VLE experiments. The comparisons between the experimental vapour pressure measurements and those extrapolated from the data of Lui and Lindsay and those calculated from the empirical equations of Sparrow are shown in Fig. 7.

The relative error between the VLE experimental data and those extrapolated from literature range between −0.030 and −0.192 for the 20 g/l solution, −0.057 and −0.188 for the 200 g/l solution and −0.065 and −0.179 for the 280 g/l solution. Considering the accumulated error that would have occurred during the extrapolation procedures, it can be concluded that there is good agreement between the experimental and literature data.

The relative error between the VLE experimental data and those calculated from the empirical equations of Sparrow range between −0.021 and −0.107 for the 20 g/l solution, 0.003 and −0.105 for the 200 g/l solution and −0.035 and −0.100 for the 280 g/l solution. There is therefore good agreement between the measured vapour pressures and those calculated from literature.

From the above work, the agreement between literature and the measured vapour pressures for each of the sodium chloride solutions was substantial to acknowledge VLE as a suitably accurate apparatus for obtaining the vapour pressures of inorganic salt solutions. This apparatus was then used to measure the vapour pressures of the solutions of the mixed salts. The vapour pressures obtained for the subsequent mixes of salt solutions together with the Antoine fit, in addition to that of pure water are shown in Fig. 8. The values of the Antoine coefficients A, B and C_A obtained from the regression procedure are listed in Table 1.

It can be seen from Fig. 8 that the difference in vapour pressure between the hot (brine) and cold (pure water) sides drives the separation process.

3.3. PHRQPITZ

This program is designed to execute a series of simulations in a single computer run by solving two separate problems: (i) processing of an initial solution/s and (or) (ii) modelling of a reaction [36]. There are varieties of reactions that can be modelled but in each type of reaction the initial solutions must be specified. The total concentrations of elements as well as information such as pH and temperature are input into a specific solution given a unique number. Any further reactions or mineral equilibrations are then performed on this solution. The output of the calculations performed with PHRQPITZ includes the osmotic coefficient, water activity, mineral saturation indices, mean-activity coefficients, total-activity coefficients, and scale-dependent values of pH, individual ion activities and individual ion activity coefficients. For our purposes the activity of water was the crucial output required from PHRQPITZ which was then used to obtain the solution vapour pressures directly (Eq. (8)), of the two mixes of salt solutions at the range of temperatures used during the VLE experiments.

Fig. 9 shows the comparison of the vapour pressure trend obtained from both methods. The deviation of approximately 1.4% at a temperature of 100 °C of the experimental results from those of PHRQPITZ is attributed to the uncertainty in PHRQPITZ calculations above 60 °C. This uncertainty, however, does not affect the outcome of the results in this study as discussed above. It therefore appears that the vapour pressure can be sufficiently accurately modelled using PHRQPITZ for the analysis of the experimental MD results.

Knowing the temperature and concentration of the retentate and distillate streams during the course of a batch concentration, the vapour pressures of these streams was calculated using

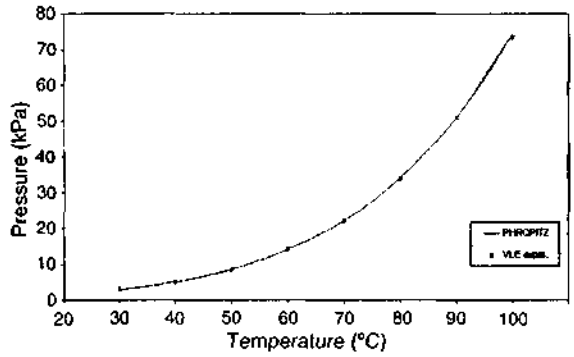

Fig. 9. Vapour pressures obtained for 1:1 salt mix from PHRQPITZ calculations and VLE experiments.

data from the speciation program. Fig. 10 shows the variation of the vapour pressures of each of the streams as indicated in the legend. The pure retentate (hot water) in and out streams, refers to the vapour pressure of pure water at the temperature of the brine at module inlet and outlet. Fig. 10 emphasises the significant change in these water activities at either end of the module. This is contrasted to the negligible change in the pure water vapour pressure for the distillate between the module inlet and outlet. For the pure water streams the vapour pressures do not change during the course of the distillation as opposed to the brine streams which decrease in vapour pressure due to an increase in the activity coefficients as the solution is concentrated. However, the curves in Fig. 10 all show a slight increase at the beginning of the distillation process. As mentioned above, this is again due to the instability in temperature during the start of the process.

The driving force, expressed as the logarithmic mean vapour pressure differences (ΔP_{lm}) between the high temperature and low temperature sides of the module, were calculated and plotted on the same graph as the transmembrane flux–time relationship. The logarithmic mean is generally considered as the most appropriate average driving force in a counter-current mass or

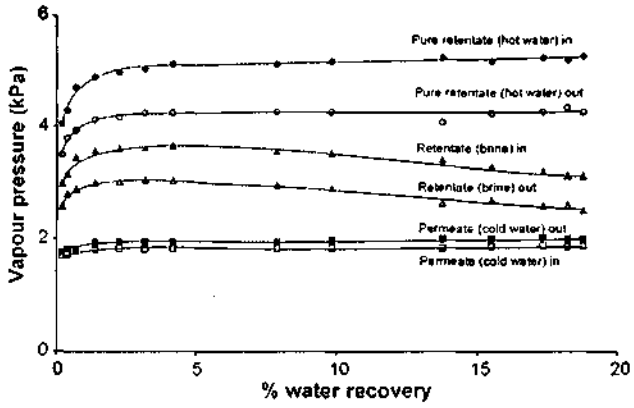

Fig. 10. Vapour pressures of respective streams in membrane distillation of a 1:1 mix emphasising the significant change in activities of the pure water retentate streams at outlet and inlet of the membrane module. The data are plotted against percentage water recovery, which represents the course of the MD run. The curves labelled "pure retentate (hot water)" are calculated for pure water at the same temperatures as the brine at that point in the run.

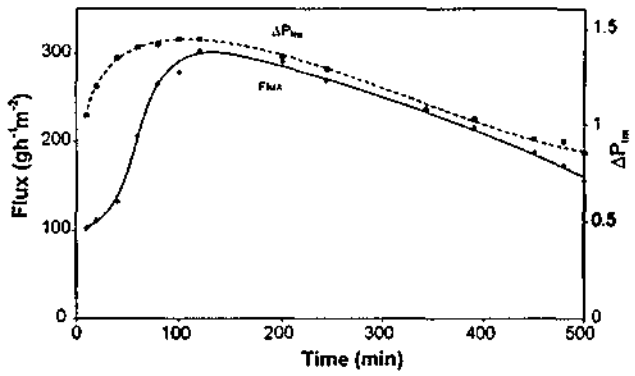

Fig. 11. Variation of transmembrane flux with the driving force as a function of time for the 1:1 mix indicating that the flux decline is due to a decline in driving force as seen from the similarity in these trends trend.

heat transfer device. Fig. 11 demonstrates the similarity in trend between the driving force and transmembrane flux for the distillation of the 1:1 mix after accounting for the change in water activities of both the streams at either end of the membrane. The flux and driving force show a constant rise after which it plateaus off before rapidly declining. As explained above, the initial rise in flux is due to the stabilisation of the system in terms of fluid dynamics and temperature profiles. However, Figs. 11 and 12 also demonstrate that a simultaneous rise in the driving force occurs during this period hence the relationship between flux and driving force also holds during this phase.

A similar trend is observed for the 1:2 mix (Fig. 12). As the initial salt content of this solution is lower than that of Fig. 11, the flux decline is less profound than before.

In Fig. 13 the data are replotted to show the relationship between flux and vapour pressure driving force.

The initial steep rising parts of the curves in Figs. 11 and 12 have been excluded in the construction of Fig. 13 as we believe that, because the temperatures were changing too rapidly to record an accurate measurement of the corresponding fluxes, this resulted in a lag in the measurement of flux relative to the measurement of temperature. A notable feature of this plot is the non-zero intercept where the flux is zero, although the apparent vapour pressure driving force is positive. This can be explained as an interaction between the transmembrane con-

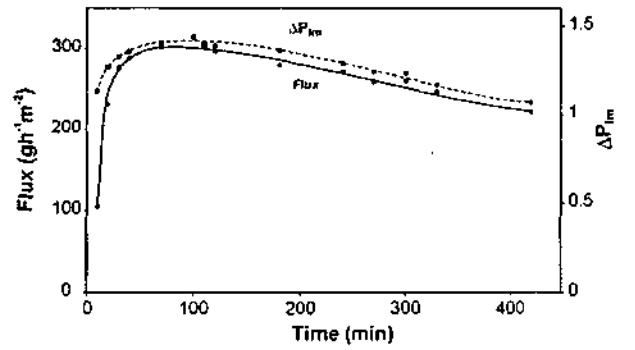

Fig. 12. Variation of transmembrane flux with the driving force as a function of time for the 1:2 mix indicating that the flux decline is due to a decline in driving force as seen from the similarity in these trends trend.

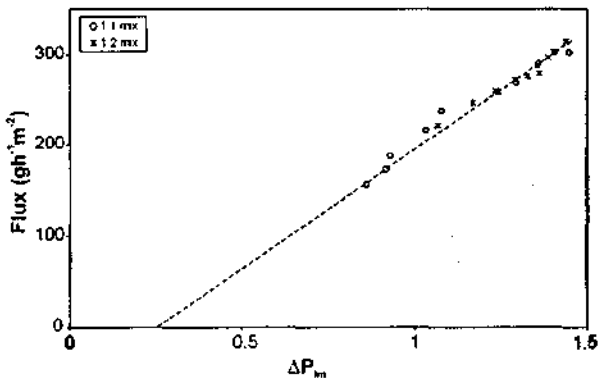

Fig. 13. Transmembrane flux as a function of driving force during the distillation of 1:1 and 1:2 magnesium sulphate and sodium chloride solutions. The graph seems to display a non-zero intercept.

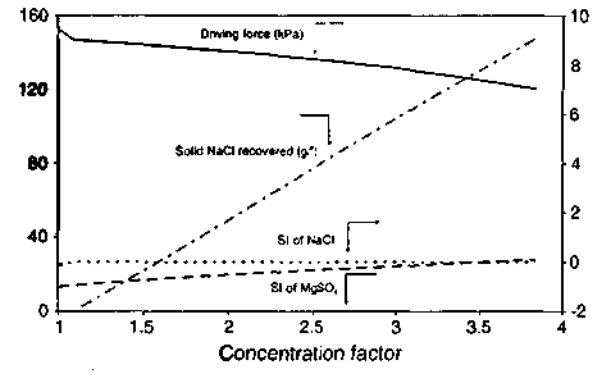

Fig. 14. MD process showing evolution of driving force and solid NaCl recovery for the 1:1 mix obtained from PHREQPITZ modelling, where concentration factor is the ratio between the initial volume of the solution and the amount of water remaining after each concentration step (or water recovery level).

centration and temperature differences, conductive heat transfer and temperature polarization [43]. In the case where the pure water and brine streams are at the same temperature, the brine vapour pressure is depressed by the salt concentration, causing a reverse flux of water across the membrane—i.e. from the pure water side to the brine side. As the brine temperature is raised, its vapour pressure is raised, counteracting the concentration effect. At the point where the temperature effect balances the concentration effect exactly, the flux is zero, which is the intercept point on the graph. Because there is no mass flux at this point, there is no concentration polarization; however the temperature difference across the membrane causes a conductive heat flux across the membrane, so there is temperature polarization. This means that the difference between the bulk temperatures of the brine and water streams is greater than the difference between the temperatures at the membrane surfaces. Hence the apparent vapour pressure driving force, calculated from the bulk stream temperatures, is greater than the true driving force based on the membrane surface temperatures. This effect is usually negligible for dilute solutions, but has been observed in concentrated solutions by other investigators [11].

Having obtained a way to accurately estimate the vapour pressures, it becomes possible to predict the course of a batch MD by accounting for the continual concentration of salts in the solution which subsequently decreases the vapour pressure and hence the driving force. Fig. 14 represents a MD concentration of a mixture of sodium chloride and magnesium sulphate each at a concentration of 225 g/l (1:1 mix described above). The solution is modelled so as to calculate the saturation index (SI) of the salts at each water recovery level according to the experimental findings. Once crystallisation of sodium chloride begins, i.e. $SI_{NaCl} = 0$, the system is modelled so as to keep the SI of sodium chloride at 0 (by continual removal of the crystals) while the concentration of magnesium sulphate increases. The saturation index (SI) of a salt is defined as the logarithm of the ratio of the ion activity product (IAP) and the solubility product (K_{sp}):

$$SI = \log \frac{IAP}{K_{sp}T} \quad (10)$$

With a brine temperature of 55 °C and a pure water temperature of 20 °C, if the crystals are continually removed from the recirculating solution, Fig. 14 illustrates how the initial rapid decline in driving force plateaus and then gradually declines when the crystal disengagement occurs thus enabling the process to proceed for an extended period of time. It can be seen that MD can concentrate the solution up to the point of sodium chloride crystallisation and beyond with approximately 150 g/l of pure crystalline sodium chloride being recovered and a 74% water recovery being achieved before epsomite would start to precipitate, while still maintaining an existent vapour pressure driving force.

This modelling stage, however, requires further development and experimental verification.

3.4. Conclusions

The water activities of the brine and distillate streams were sufficiently accurately modelled using a computer program specific for geochemical calculations in concentrated brines during the MD of concentrated solutions of varying ratios of epsomite and sodium chloride. The current database for this computer program is limited to a temperature range of 0–60 °C which is sufficient for our system, and MD in general, as seldom an operating temperature of 40 °C is exceeded. The calculated vapour pressure driving force was able to explain the flux trend during batch concentrations. Furthermore it has been found that, particularly in the case of concentrated solutions, the relationship between driving force and transmembrane flux is governed by interactions between the transmembrane concentration and temperature differences, conductive heat transfer and temperature polarization. Overall, the novel approach to predicting driving forces can enhance the understanding of MD experiments.

An evaluation of the kinetics of crystallisation of the salts is necessary to complete the understanding of the process. These need to be well understood as the process must avoid crystallisation in the membrane module while producing a high quality final product which influences the performance of downstream processes (solid–liquid separation steps, drying and storage).

Acknowledgements

The financial support of Sasol (Pty) Ltd., the National Research Foundation (NRF) and the Technology and Human Resources for Industry Programme (THRIP) which made the investigations possible is gratefully acknowledged.

Nomenclature

A, B, C_A	Antoine equation coefficients
C	membrane transfer coefficient
CV	coefficient of variation (%)
ΔH_{vap}	molar enthalpy of vapourisation (kJ mol^{-1})
IAP	ion activity product
J	transmembrane flux (g h^{-1} m^{-2})
K_{sp}	solubility product
m	molality (mol/kg H_2O)
M	molar mass (g mol^{-1})
P	pressure (kPa)
ΔP	vapour pressure difference between the feed and permeate streams (kPa)
R	gas constant (J K^{-1} mol^{-1})
SI	saturation index
T	temperature (°C)
T_{th}	threshold temperature (K)
x_m	mole fraction

Greek letters

α	activity
τ	temperature polarization coefficient
ϕ	osmotic coefficient

Subscripts

b	bulk
lm	log mean
m	membrane surface

Superscripts

f	feed
p	permeate

References

[1] K.W. Lawson, D.R. Lloyd, Review: membrane distillation. J. Membrane Sci. 124 (1997) 1.
[2] E. Curcio, A. Criscuoli, E. Drioli, Membrane crystallizers, Ind. Eng. Chem. Res. 40 (2001) 2679.
[3] S.I. Andersson, N. Kjellander, B. Rodesjo, Design and field tests of a new membrane distillation desalination process, Desalination 56 (1985) 345.
[4] G.C. Sarti, C. Gostoli, S. Matulli, Low energy cost desalination processes using hydrophobic membranes, Desalination 56 (1985) 277.
[5] M. Khayet, M.P. Godino, J.I. Mengual, Theoretical and experimental studies on desalination using the sweeping gas membrane distillation method, Desalination 157 (2003) 297.
[6] A.S. Jonsson, R. Wimmerstedt, C. Harryson, Membrane distillation—a theoretical study of evaporation through microporous membranes, Desalination 56 (1985) 237.
[7] S.T. Hsu, K.T. Cheng, J.S. Chiou, Seawater desalination by direct contact membrane distillation, Desalination 143 (2002) 279.
[8] A. Kubota, K. Ohta, I. Hayano, M. Hirai, K. Kikuchi, Y. Murayama, Experiments on seawater desalination by membrane distillation, Desalination 69 (1988) 19.
[9] A.M. Alklaibi, N. Lior, Membrane-distillation desalination: status and potential, Desalination 171 (2004) 111.
[10] P.A. Hogan, A.G. Sudjito, G.L. Fane, Morrison, Desalination by solar heated membrane distillation, Desalination 81 (1991) 81.
[11] J. Walton, H. Lu, C. Turner, S. Solis, H. Hein, Solar and waste heat desalination by membrane desalination, Bureau of Reclamation, Denver Federal Center, USA, Desalination and water purification research and development program report (DWPR) no. 81, 2004.
[12] S. Kimura, S.-I. Nakao, Transport phenomena in membrane distillation, J. Membrane Sci. 33 (1987) 285.
[13] V. Calabro, B.L. Jiao, E. Drioli, Theoretical and experimental study on membrane distillation in the concentration of orange juice, Ind. Eng. Chem. Res. 33 (1994) 1803.
[14] F. Laganá, G. Barbieri, E. Drioli, Direct contact membrane distillation: modeling and concentration experiments, J. Membrane Sci. 166 (2000) 1.
[15] C. Gostoli, G.C. Sarti, Separation of liquid mixtures by membrane distillation, J. Membrane Sci. 41 (1989) 211.
[16] G.C. Sarti, C. Gostoli, S. Bandini, Extraction of organic components from aqueous streams by vacuum membrane distillation, J. Membrane Sci. 80 (1993) 21.
[17] M. Mulder, Basic Principles of Membrane Technology, Kluwer Academic Press, The Netherlands, 1996.
[18] Y. Wu, E. Drioli, The behaviour of membrane distillation of concentrated aqueous solution, Water Treat. 4 (1989) 399.
[19] E. Curcio, G. Di Profio, L. Mariah, E. Drioli, A fully integrated membrane operation for sea water and brackish water desalination, in: Proceedings of the Seventh World Congress of Chemical Engineering, Glasgow, Scotland, 10–14 July, 2005.
[20] Y. Wu, Y. Kong, J. Liu, J. Zhang, J. Xu, An experimental study on membrane distillation–crystallization for treating waste water in taurine production, Desalination 80 (1991) 235.
[21] M. Tomaszewska, Concentration of the extraction fluid from sulfuric acid treatment of phosphogypsum by membrane distillation, J. Membrane Sci. 78 (1993) 277.
[22] M. Gryta, Concentration of NaCl solution by membrane distillation integrated with crystallisation, Sep. Sci. Technol. 37 (2002) 3535.
[23] E. Curcio, G. Di Profio, E. Drioli, A new membrane-based crystallization technique: tests on lysozyme, J. Crystal Growth 247 (2003) 166.
[24] E. Drioli, E. Curcio, A. Criscuoli, G. Di Profio, Integrated system for recovery of $CaCO_3$, NaCl and $MgSO_4 \cdot 7H_2O$ from nanofiltration retentate, J. Membrane Sci. 239 (2004) 27.
[25] A. Criscuoli, E. Drioli, Energetic and exergetic analysis of an integrated membrane desalination system, Desalination 124 (1999) 243.
[26] A.C.M. Franken, J.A.M. Nolten, M.H.V. Mulder, D. Bargeman, C.A. Smolders, Wetting criteria for the applicability of membrane distillation, J. Membrane Sci. 33 (1987) 315.
[27] M. Gryta, M. Tomaszewska, J. Grzechulska, A.W. Morawski, Membrane distillation of NaCl solution containing natural organic matter, J. Membrane Sci. 181 (2001) 179 (short communication).
[28] E. Drioli, Y. Wu, Membrane distillation: an experimental study, Desalination 53 (1985) 339.
[29] J.-M. Li, Z.-K. Xu, Z.-M. Liu, W.-F. Yuan, H. Xiang, S.-Y. Wang, Y.-Y. Xu, Microporous polypropylene and polyethylene hollow fiber membranes. Part 3. Experimental studies on membrane distillation for desalination, Desalination 155 (2003) 153.
[30] E. Drioli, Y. Wu, V. Calabro, Membrane distillation in the treatment of aqueous solutions, J. Membrane Sci. 33 (1987) 277.
[31] F.A. Banat, J. Simandl, Theoretical and experimental study in membrane distillation, Desalination 95 (1993) 39.
[32] R.W. Schofield, A.G. Fane, C.J.D. Fell, Heat and mass transfer in membrane distillation, J. Membrane Sci. 33 (1987) 299.

[33] C.M. Tun, A.G. Fane, J.T. Matheickal, R. Sheikholeslami, Membrane distillation crystallization of concentrated salts—flux and crystal formation, J. Membrane Sci. 257 (2005) 144.
[34] J.D. Raal, A.L. Mühlbauer, Phase Equilibria: Measurement and Computation, Bristol, PA, 1998.
[35] M.A. Joseph, J.D. Raal, D. Ramjugernath, Phase equilibrium properties of binary systems with diacetyl from a computer controlled vapour–liquid equilibrium still, Fluid Phase Equilibr. 182 (2001) 157.
[36] L.N. Plummer, D.L. Parkhurst, G.W. Fleming, S.A. Dunkle, A computer program incorporating Pitzer's equations for calculation of geochemical reactions in brines, US Geological Survey, Department of the Interior, Reston, Virginia, Water-Resources Investigations Report 88-4153, 1988.
[37] K.S. Pitzer, G. Mayorga, Thermodynamics of electrolytes. II. Activity and osmotic coefficients for strong electrolytes with one or both ions univalent, J. Phys. Chem. 77 (19) (1973) 2300.
[38] J.W. Mullin, Crystallization, 4th ed., Butterworth Heinemann, Oxford, 2001.
[39] S. Al-Jibbouri, C. Strege, J. Ulrich, Crystallization kinetics of epsomite influenced by pH-value and impurities, J. Cryst. Growth 236 (2002) 400.
[40] S. Ramalingom, J. Podder, S. Narayana, G. Bocelli, Habit modification of epsomite in the presence of urea, J. Cryst. Growth 247 (2003) 523.
[41] C. Liu, W.T. Lindsay, Thermodynamics of sodium chloride solutions at high temperatures, J. Sol. Chem. 1 (1971) 1972.
[42] B.S. Sparrow, Empirical equations for the thermodynamic properties of aqueous sodium chloride, Desalination 159 (2003) 161.
[43] K. Smolders, A.C.M. Franken, Terminology for membrane distillation, Desalination 72 (1989) 249.

PAPER 4

MEMBRANE DISTILLATION FOR THE RECOVERY OF CRYSTALLINE PRODUCTS FROM CONCENTRATED BRINES

L. Mariah[1], CA Buckley[1], CJ Brouckaert[1], D Jaganyi[2], E Curcio[3,4] and E Drioli[3,4]

[1]Pollution Research Group, University of KwaZulu-Natal, Durban, South Africa
E-Mail: Buckley@ukzn.ac.za, Tel: +27 31 260-3131, Fax: +27 31 260-3241
[2]School of Chemistry, University of KwaZulu-Natal, Pietermaritzburg
[3]Institute on Membrane Technology (ITM-CNR), Via P. Bucci 17/C, c/o University of Calabria, 87030, Rende (CS), Italy.
[4]Department of Chemical Engineering and Materials, University of Calabria, via P. Bucci 45/A, 87030, Rende (CS), Italy

Membrane distillation and crystallisation (MDC) is a useful adjunct to seawater and other desalination processes in order to further process the resulting brine streams. MDC becomes particularly valuable when treating solutions of extremely high concentration which other processes such as reverse osmosis are incapable of handling. The process uses low grade heat and operates at about atmospheric pressure. This work demonstrates how membrane distillation and crystallisation is used to obtain pure crystalline products and pure water from solutions of sodium chloride and magnesium sulphate of concentrations near to saturation. Furthermore, a new approach to the modelling of the MDC process has been achieved which enables the prediction of driving force for the process by estimating the vapour pressure from chemical speciation calculations.. These modelling procedures are used to illustrate the gradual decline in the driving force during the membrane distillation process of solutions containing high concentrations of salt in contrast to the drastic decline in driving force in reverse osmosis. Further simulations are performed which illustrate how membrane distillation could be used to recover solid products from a mixed solution of salts whilst maintaining a driving force at extremely high solute concentrations.

1. BACKGROUND

Salinity is one of South Africa's most critical environmental problems, threatening economic and social consequences. Industries such as Sasol and Eskom currently have reverse osmosis (RO) plants producing waste brine, but brine disposal is a problem. If there is no intervention, the completed mining operations will continue to produce saline aqueous effluents for hundreds of years after mine closure. In the past most of the waste streams arising from the various mining and manufacturing activities were discharged to surface waters or the ocean. However, more rigid current and future environmental regulations will make these disposal routes less feasible therefore other disposal options need to be sought. It seems that technologies that are available for managing these waste products are either prohibitively uneconomic (exceeding the cost of water treatment or desalination) or unsatisfactory because of long term liabilities and associated risks they pose to water resources. Evaporation ponds appear to be one of the widely used means of disposal. However, low rates of evaporation due to highly concentrated waste streams or insufficient

driving force for evaporation, especially in areas where the humidity is relatively high, has resulted in a build-up in the inventory of these facilities. Much work has been performed on being able to solve this salinity crisis. However, bearing in mind the concept of sustainable development, we can deem these saline waters an environmental problem or we can turn this environmental problem into an economic resource by viewing these saline waters as a sustainable resource of salts. Several of the waste streams contain potentially recoverable and saleable products. Some of these include calcium carbonate, magnesium sulphate and calcium sulphate. Sustainable salt sinks can be achieved by considering the formation of valuable salts when designing a saline water circuit and the composition of the streams that enter the circuit. The separation and concentration processes need to be combined to produce high-value products. The chlor-alkali salt preparation circuit is an example of a process that requires a pure sodium chloride feed for a subsequent synthesis step (electrolysis) (1). Suitably purified and concentrated brine streams could substitute for the imported raw salt which is used as the feed chemical. A technique is therefore required in order to separate and recover these concentrates with the concomitant release of pure water.

Many techniques have been investigated for the desalination of water and separation of salts. The most commonly used is that of reverse osmosis although other techniques such as thermal desalination and evaporation have been investigated (2). The main shortcoming of reverse osmosis is the high osmotic pressure of the feed stream at high solute concentrations. In reverse osmosis an excess pressure is required to overcome the solution osmotic pressure in order to concentrate the feed. In processes such as thermal evaporation, for example, elevated temperatures are required in order to achieve evaporation and salt recovery. Large heat transfer areas are required and scaling of the heat transfer surfaces reduces the efficiency of the process. There is a need for a process which would achieve the recovery of crystalline products and pure water and is capable of operating at high solute concentrations.. Exploiting the fact that inorganic concentrates can be separated into high value chemicals and reusable water, membrane distillation and crystallization (MDC) is a technique which potentially leads to a 100 % water recovery and the elimination of the brine disposal problem (3). This is achieved by the production of pure water by concentrating aqueous solutions through a vapour pressure difference induced by a transmembrane temperature gradient resulting in highly concentrated mother liquors in which nucleation and crystal growth occurs in a controlled fashion. This process does not have the limitations of reverse osmosis as this process can operate at higher concentrations, at low concentration gradients and atmospheric pressure. The advantage over distillation is that the mass transfer and heat transfer surfaces are combined, they consist of polymer fibres which have a higher packing density and lower cost that conventional corrosion resistant heat transfer surfaces.

This paper therefore proposes the technique of membrane distillation crystallisation (MDC) for the recovery of crystalline products from brine concentrates and the production of pure water. The benefits of MDC as opposed to other membrane processes such as RO are discussed. Furthermore, a step is taken which is new to the MDC process is that of being able to computational model the process in terms of the evaluation of driving force and to examine some of the constraints of the latter.

2. MEMBRANE DISTILLATION

As the name implies, the process combines both the use of distillation and membranes. In the process, saline water is heated to increase the vapour of water, and this vapour is exposed to

a hydrophobic polymeric membrane that can pass water vapour but not water. After the vapour passes through the membrane, it is condensed on a cooler surface (or in a cold water stream) to produce fresh water. In the liquid form, the fresh water cannot pass back through the membrane, so it is trapped and collected at the output of the plant. The main advantages of membrane distillation lie in its simplicity and the need for only small temperature differentials. One important advantage of membrane distillation in contrast to reverse osmosis, is because of the independence of the quality of the permeate from the feed solution concentrations, membrane distillation can handle highly concentrated feed solutions without a reduction in membrane selectivity. Reverse osmosis, however, is strongly affected by the osmotic pressure if the feed solution is highly concentrated resulting in higher applied pressure demands furthermore, increasing the susceptibility of the membrane to fouling.

Recent innovative designing of integrated membrane systems (IMS) have lead to process intensification and reduction in pre-treatment costs (4). Integration of various single membrane units might assist in overcoming the shortfalls otherwise experienced if these units operate independently, i.e. many specialised separations as opposed to one big concentration step. Figure 1 shows an integrated system proposed by Drioli et al. (5). This system consisted of a *pre-treatment* stage which included MF/UF-NF-MC and a *processing* stage consisting of RO-MD. The pre-treatment stage included a gas-liquid membrane contactor unit (MC). This MC operation serves to reduce the amount of dissolved gases such as CO_2 and O_2 that is present in the feed solution, if deemed necessary. An energetic and exergetic analysis of this IMS indicated that the recovery factor of the MD unit was 77 % and the RO unit alone yielded a recovery factor of 40 %. However, by coupling these two membrane units the global recovery factor was a high of 87.6 % (6).

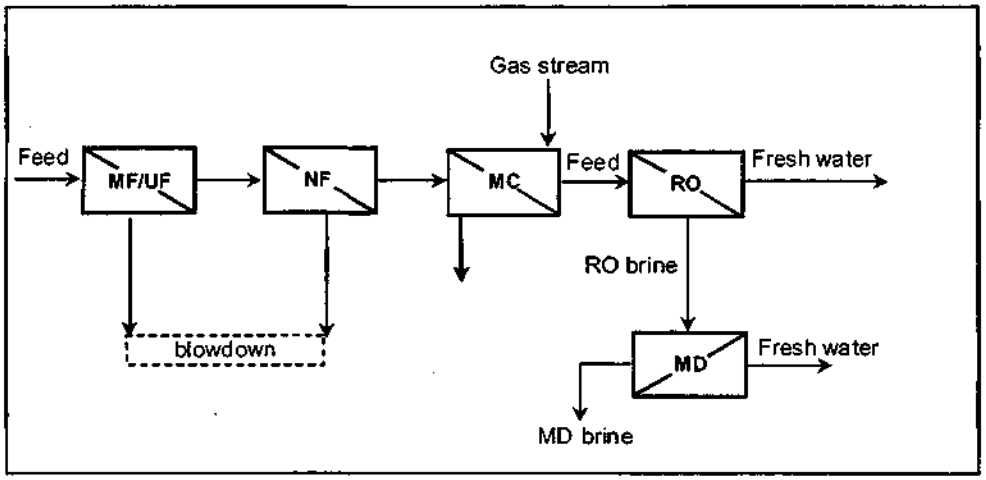

Figure 1: *Proposed ideal integrated membrane system for seawater desalination (5)*

Furthermore, from their analyses it was found that by placing NF ahead of RO the osmotic pressure of the feed solution is lowered and hence a lower applied pressure is required to move water through the membrane. The added electrical energy that is required to operate the NF as a pre-treatment to RO can be offset by using the NF concentrate to pre-pressurise the feed water thus reducing the RO electrical energy requirements. For the coupling of RO with MD a higher thermal demand arises because of MD. However, when these two units are further coupled with NF it was found that this energy demand is lowered. If excess thermal energy is already present in the plant (as is the case in most industries such as Sasol where

there is an excess of low-grade thermal energy), then the surplus energy required by this system can be offset.

Following the proposal of the ideal integrated system of Figure 1, later work performed by Drioli et al (4) incorporated a membrane crystalliser to form the NF-RO-MCr integrated system. The membrane crystalliser achieves the complete recovery of desalted water and solid salts. Feeding the MD unit with RO retentate represents the brine as the concentrated mother liquor which promotes nucleation and crystal growth. Curcio et al. (7) performed an energetic, exergetic and cost analysis on the systems MF-NF-RO and NF-MC-RO-MCr. In one instance, the NF retentate from the integrated system represented in Figure 1 was mixed with Na_2CO_3, produced from the reactive adsorption of CO_2 via MC, for the removal of Ca^{2+} ions as $CaCO_3$, before entering the MCr unit. In the second instance the RO retentate was subjected to $CaCO_3$ precipitation before reaching the crystalliser. In the former case a global recovery factor of water of up to 58.6 % is achieved and in the latter case a 70.1 % global water recovery is achieved. Although the membrane crystalliser system represents a higher thermal energy requirement, it does, however, considerably reduce both the cost and environmental impacts of brine disposal operations thus favouring the concepts of green chemistry and moving towards sustainable industrial growth and, as already stated, if there is excess thermal energy already available within the plant, it could be used to supplement this added energy demand of the MCr unit making the overall energy requirement then comparable to an NF-RO coupled system (4).

The main advantages of MD over conventional membrane and distillation processes can be summarised as follows:

Membrane distillation,

- Can be performed at lower operating pressure and lower temperatures than the boiling point of the feed solutions (8-10) and a relatively low temperature difference between the two liquids in contact with the membrane surface gives relatively high fluxes.
- Requires lower vapour space as the vapour-liquid interface is developed by a hydrophobic membrane in membrane distillation as opposed to conventional distillation which relies on high vapour velocities to establish a vapour-liquid interface (11). As such they are very compact and very little equipment space is required. Furthermore, the possibility to overcome corrosion problems by using plastic equipment exists (12).
- Is unlimited by high osmotic pressure and fouling as the membrane works at atmospheric pressure and is not directly involved in the separation process but acts merely as a support. As such there is reduced chemical interaction between the membrane and process solution (13). Furthermore, due to this characteristic membranes can be fabricated from a variety of chemically resistant polymers (14).
- Displays selectivity higher than any other membrane process (15). MD therefore allows very high separation factors for ions, macromolecules, colloids, cells and other non-volatile solutes in comparison to UF, NF and RO processes (16,17)
- Has low sensitivity to feedwater concentrations and has potential applications for concentrating aqueous solutions or producing high-purity water even at very high feedwater concentrations (15, 18, 19)
- Does not require elevated temperatures therefore the heat can be supplied by solar collectors or other forms of heat such as low-grade waste heat from factories or geothermal energy (20).

Membrane distillation is one of the membrane processes in which the membrane is not directly involved in the separation. The membrane acts only as a support for a vapour-liquid interface and does not contribute to the separation mechanism. Selectivity is determined by the vapour-liquid equilibrium involved.

One of the most important applications of MD is in the production of pure water. Studies have shown that a high quality permeate can be obtained during MD. This feature of MD makes this process invaluable in the desalination of seawater, in industry for boiler feedwater and in the semiconductor industry (21). Other areas in which MD is used to treat waste water is in the textile industry (22-23). In the case of a solution containing non-volatile components, e.g. NaCl, only water vapour flows through the membrane. Therefore, the retention degree of solutes in MD is close to 100 % (24). This allows the concentration of solutions up to solute saturation. The concentrating process of MD may be exploited in the food industry for the concentration of fruit juices and milk (25-27). Gostoli and Sarti (28) and later Sarti et al. (29) have found vacuum membrane distillation to be very useful for the separation of alcohol-water mixtures such as the extraction of organic components, ethanol and methylterbutyl from aqueous streams. Criscuoli et al. (30) evaluated MD for the treatment of uraemia by employing this process for the purification of human plasma ultrafiltrate and the re-circulation of the purified water to the patients. The feasibility of breaking down azeotropic mixtures by the removal of water using MD has been explored by Udriot et al. (31). Gryta et al. (24) used MDC for the treatment of NaCl solutions subsequent to use in the food industry. The concept was to produce pure water together with a concentrate containing substances present in the initial solution which could be separated by crystallisation thus facilitating their disposal and potential recycling of the water produced.

3. EXPERIMENTAL

The experimental plant design that was used during these series of MDC experiments is depicted in Figure 2. The distillation plant was operated in a batch concentration mode where the recirculating permeate stream, consisting of deionised water, and the retentate stream flowed counter current through the membrane module. The membrane module, MD020CP 2N, supplied by Microdyn, contained 40 hydrophobic polypropylene hollow fibres of 0.1 m^2 total interfacial area. The nominal pore size of the polypropylene membranes was 0.2 μm and the external diameter was 1.8 mm. During the process the solution in the retentate line is heated and flows toward the membrane and converges in a counter current manner with the cold permeate stream. A vapour-liquid interface is established at the membrane surface and water vapour molecules from the retentate stream diffuse across the membrane and condenses in the cold permeate. Continual removal of water in the retentate line leads to the concentration of the remaining solution resulting in a mother liquor in which nucleation and crystal growth is initialised. Crystallisation occurs in a vessel in which a centrifugal pump receives and returns the mother liquor to the membrane module on the retentate line. The crystallisation vessel operated at room temperature and atmospheric pressure. Samples were routinely withdrawn from the crystallisation tank and visually examined and photographed using a video-camera model, Axiovert 25, equipped with optical head 25 X, to determine the crystal size distribution.

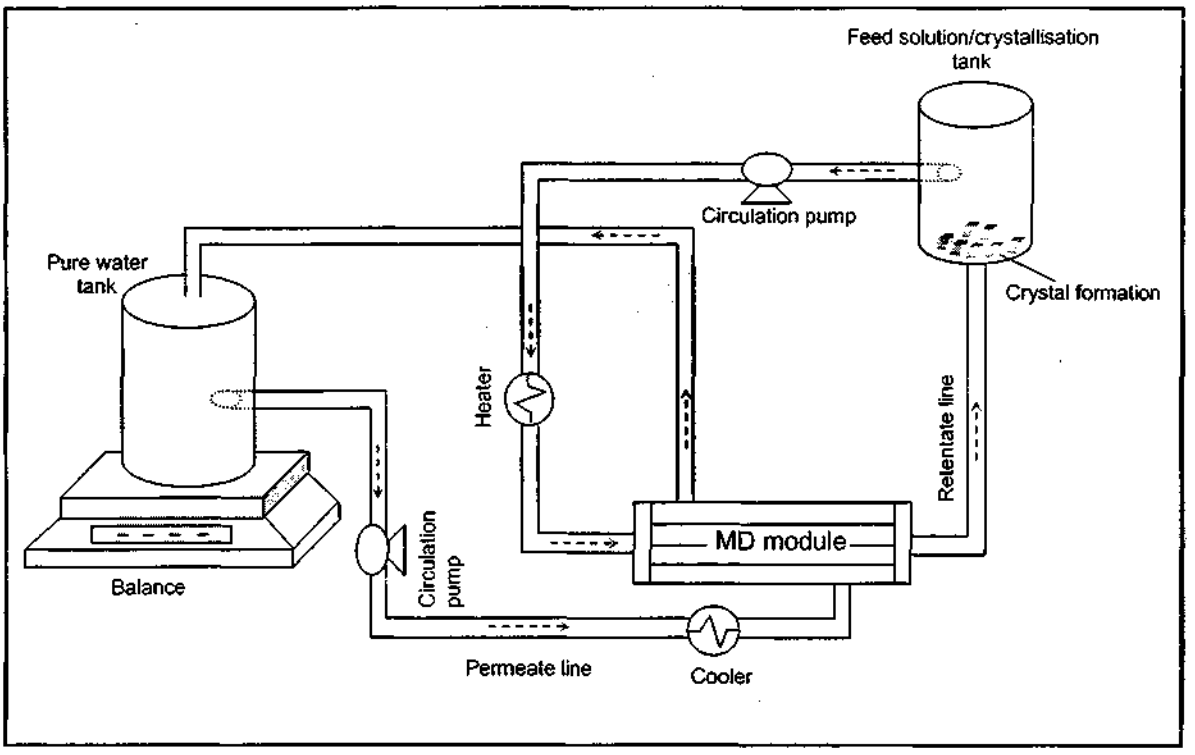

Figure 2: *Experimental setup for membrane distillation-crystallisation of concentrated salts*

For the series of MDC experiments, two types of systems were investigated. Although some work has been done concerning the MDC of epsomite for the recovery of crystalline product (32), solutions of high concentration (close to saturation) have not been performed. Therefore, the first part of this work investigates the MDC of concentrated solutions of epsomite of concentrations 375 g/ℓ and 625 g/ℓ. This is then followed by the MDC of concentrated solutions of a mixture of sodium chloride and epsomite, in varying ratios, aimed at the crystallisation of sodium chloride. For this purpose aqueous solutions of analytical grade epsomite and sodium chloride were prepared in mass ratios of 1:1, 1:2 and 1:3, respectively, with initial concentrations of 225 g/ℓ of epsomite and NaCl for the 1:1 mix; 137.5 g/ℓ and 275 g/ℓ of epsomite and NaCl, respectively, for the 1:2 mix; and 93.3 g/ℓ and 280 g/ℓ of epsomite and NaCl, respectively for the 1:3 mix. The average temperatures at module inlet on retentate and distillate sides were 29.8 ± 1.6 °C and 17.6 ± 4.4 °C, respectively, for the MD of the pure magnesium sulphate solutions. The average temperatures at module inlet on retentate and distillate sides for the 1:1 mix was 32.6 ± 1.7 °C and 16.0 ± 0.5 °C, respectively; for the 1:2 mix 32.6 ± 1.2 °C and 16.8 ± 0.4 °C, respectively; and for the 1:3 mix 33.6 ± 2.6 °C and 14.8 ± 0.5 °C, respectively. The average temperatures at module outlet on retentate and distillate sides for the 1:1 mix was 29.3 ± 1.4 °C and 16.9 ± 0.7 °C, respectively; for the 1:2 mix 30.5 ± 1.0 °C and 17.4 ± 0.7 °C, respectively; and for the 1:3 mix 27.6 ± 1.0 °C and 16.1 ± 0.6 °C, respectively. The water flux was evaluated by measuring the amount of water extracted at time intervals during the course of the experiment. The flux of pure water through the membrane is more fully described in (33) but ranged from 0.1 to 0.3 L/m^{2}h for temperatures of 55 and 20 °C.

4. RESULTS

The detailed results of the MD experiments have been described in a previous work by the authors (33). Therefore only a brief discussion of the results will be considered here. Figure 3 shows the photographs of the crystals that were taken during the crystallisation of magnesium sulphate from a pure solution of this salt and the crystallisation of sodium chloride from a mixture of sodium chloride and magnesium sulphate in equal mass ratios. The crystals display the characteristic geometries associated with their crystal forms, i.e. orthorhombic magnesium sulphate and cubic sodium chloride crystals.

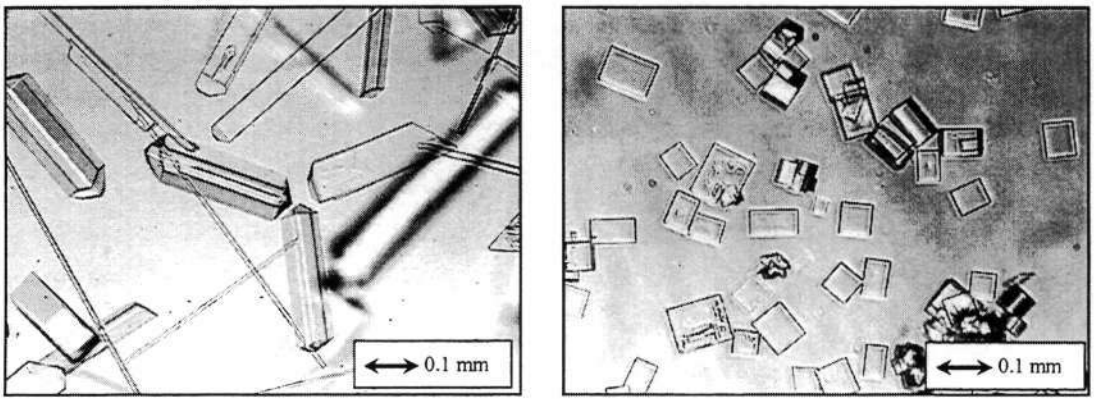

Figure 3: Magnesium sulphate and sodium chloride crystals obtained from MDC

For the crystallisation of magnesium sulphate the evolution of the particle size distribution shows that the initial peak progressively migrates towards increasing crystal size due to the crystal growth process. The shape of the particle size distribution is governed by a coefficient of variation, CV, which is defined according to Equation 1,

$$CV = \frac{F_{80\%} - F_{20\%}}{2F_{50\%}} \times 100 \qquad [1]$$

where F is the cumulative particle size distribution. Analysis of the experimental cumulative size distribution functions enabled CV values to be calculated and was found to be in the range of 10 – 30 %.

5. MODELLING

A computer program, PHRQPITZ, is able to perform geochemical calculations in brines and other electrolyte systems to high concentrations (34). This is possible as the main code of this program uses the Pitzer virial coefficient approach for activity coefficient corrections according to the works of Harvie (35) and Harvie et al. (36) for the prediction of mineral solubilities in natural waters for the Na-K-Mg-Ca-H-Cl-SO_4-OH-HCO_3-CO_3-CO_2-H_2O system to high ionic strengths. The water activity values can be used to calculate water vapour pressures and osmotic pressures. The computer program PHRQPITZ was tested for its suitability of modelling vapour pressures. The details of the program and modelling and measurement procedures of vapour pressures have been described in a previous work by the

authors (37). The suitability of the program for modeling vapour pressures was verified by experiments performed with the aid of a dynamic vapour liquid equilibrium (VLE) still. A fit of the modelled vapour pressures to those measured experimentally is shown in Figure 4.

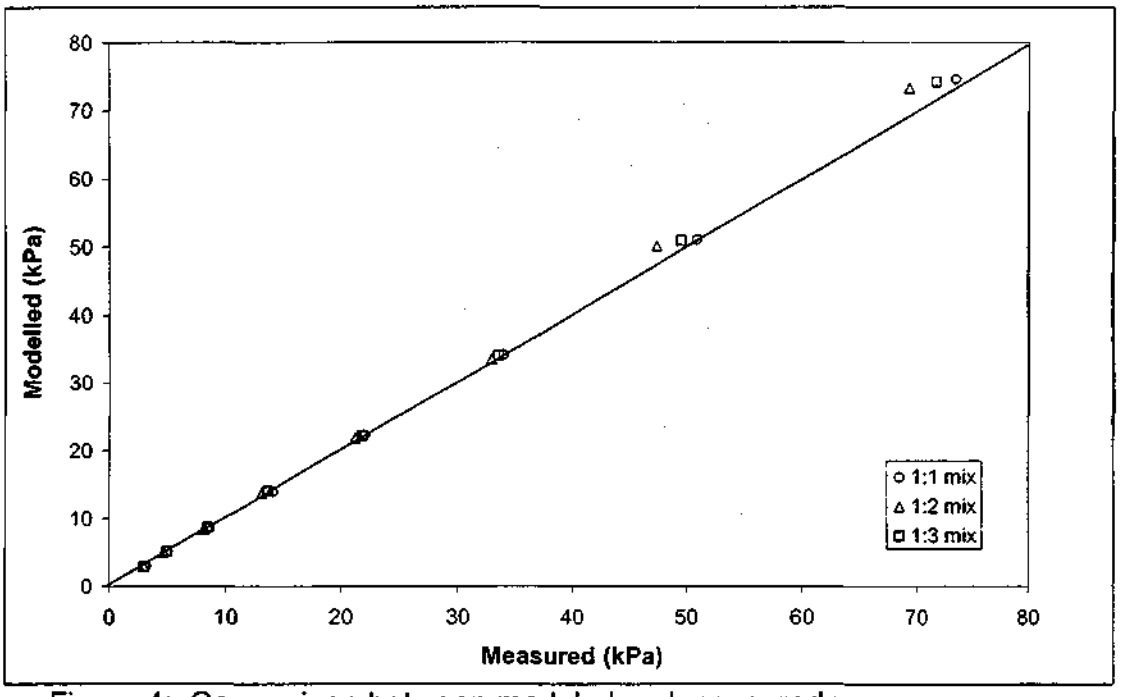

Figure 4: Comparison between modeled and measured vapour pressures

The relative errors between the vapour pressures modelled and those obtained experimentally range between -0.0014 to 0.0956 for the 1:1 mix, -0.0191 to -0.0576 for the 1:2 mix and -0.0136 to -0.0333 for the 1:3 mix. There therefore appears to be excellent agreement between the modelled and measured vapour pressures. The larger deviations are those at higher temperatures. This is due to the limitation of the input data to PHRQPITZ, with regards to the uncertainty in PHRQPITZ calculations above 60°C. Hence, the program PHRQPITZ was deemed suitably accurate for modelling vapour pressures.

Having a program capable of modelling the vapour pressures and osmotic pressures and hence driving force during MD (and RO) is a powerful tool which enables the prediction of the MD process. Figure 5 represents the vapour pressure driving force that was modelled for a solution containing approximately 100 g/ℓ of sodium chloride. This is compared to a driving force that would be obtained using RO on the same solution. The net driving force in RO is calculated as the difference in the applied pressure and that of the osmotic pressure of the solution calculated from the water activity according to Equation 2 (38, 39).

$$\pi = -\frac{RT}{V_w}\ln \alpha_w \qquad [2]$$

where π is the osmotic pressure in kPa, α_w the activity of water, R the universal gas constant (= 8.314 ℓ.kPa.mol^{-1}K^{-1}), T is the absolute temperature in Kelvin and V_w is the molar volume of water in ℓ.mol^{-1}.

The vapour pressure of the initial solution was 14.75 kPa and the osmotic pressure was 9.86 MPa. Thus a minimum applied pressure of approximately 10MPa is required in order to exceed the osmotic pressure. In Figure 5 an initial pressure of 10.5 MPa was applied. This applied pressure however, becomes insufficient at a concentration factor of less than 1.13 % whereas MD (with a brine temperature of 55 °C and a pure water temperature of 20 °C) maintains a vapour pressure driving force of approximately 12.3 kPa which extends to very high concentration factors with only a gradual decline. It has been calculated that in order for RO to maintain a positive driving force at higher concentration factors, pressures of up to12 MPa and over would have to be applied.

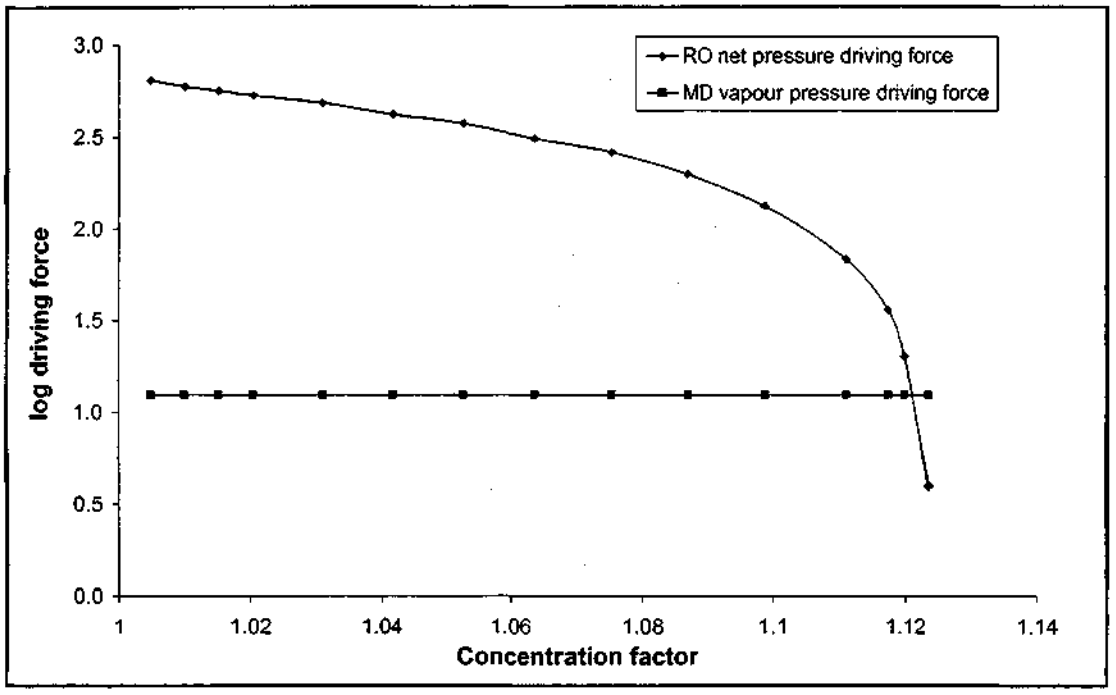

Figure 5: Comparison of RO and MD driving force for a 100 g/ℓ sodium chloride solution

In order to further illustrate the capability of MD to concentrate a solution up to saturation and crystal formation is shown in Figure 6. This plot represents a MD concentration of a mixture of sodium chloride and magnesium sulphate each at a concentration of 225 g/ℓ (1:1 mix described above). The initial vapour pressure of this solution is 11.8 kPa and the osmotic pressure is 43MPa. With a brine temperature of 55 °C and a pure water temperature of 20 °C, it can be seen that MD can concentrate the solution up to the point of sodium chloride crystallisation and beyond with approximately 150 g/L of pure crystalline sodium chloride being recovered and a 74 % water recovery being achieved before magnesium sulphate would start to precipitate, while still maintaining an existent vapour pressure driving force. It was calculated that in order for reverse osmosis to perform at these levels of concentration, an enormously elevated applied pressure of approximately 50 MPa is required in order to obtain a positive driving force. Furthermore, this applied pressure would become insufficient at an extremely low water recovery factor.

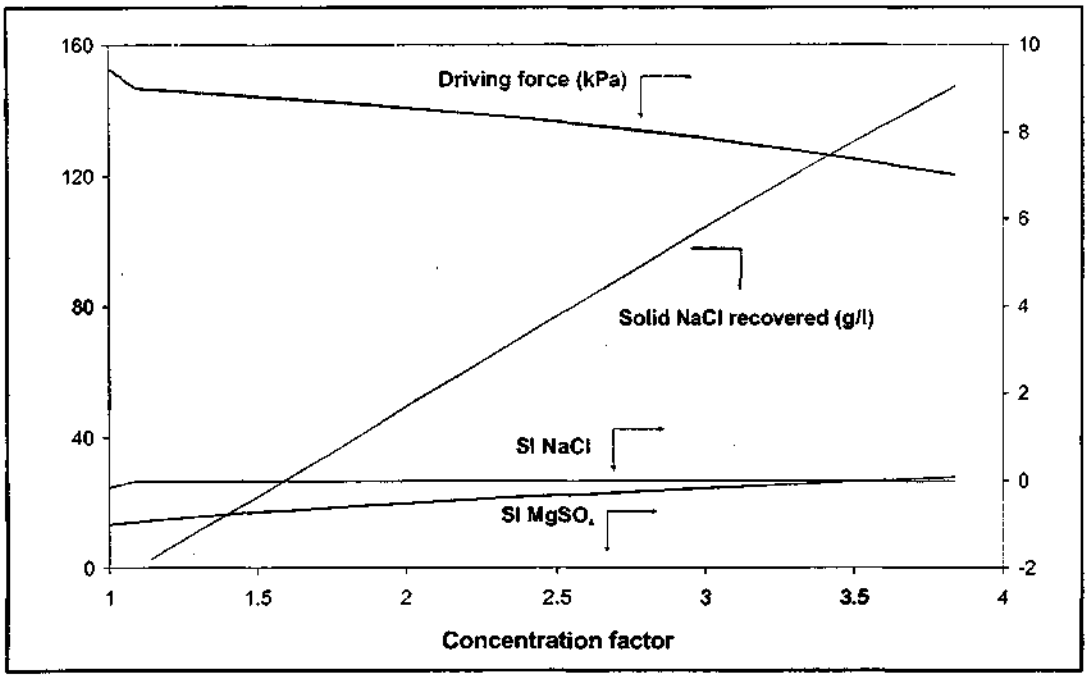

Figure 6: MD process showing evolution of driving force and solid NaCl recovery with water recovery

6. CONCLUSION

The computer program PHRQPITZ has facilitated the modelling of driving forces in MD and RO processes thereby illustrating the incapacity of the latter to operate at extremely high solute concentrations without the application of excessively high pressures. Furthermore, the vapour pressure driving force during MD allows a solution to be concentrated up to saturation and beyond thus facilitating the recovery of crystalline products. MD is a relatively new technique and its applications are imminent.

7. ACKNOWLEDGEMENTS

The financial support of Sasol (Pty) Ltd., the National Research Foundation (NRF) and the Technology and Human Resources for Industry Programme (THRIP) which made the investigations possible is gratefully acknowledged.

8. REFERENCES

1. P Giannadda, *The development and application of combined water and materials pinch analysis to a chlor-alkali plant* PhD thesis, Pollution Research Group, University of Natal, South Africa (2002).
2. J Kurbiel, W Balcerzak, MS Rybicki and K Swist, Desalination, 106 p.415 (1996).
3. E Curcio, A Criscuoli and E Drioli, Ind. Eng. Chem. Res., 40, p.2679 (2001).
4. E Drioli, A Criscuoli and E Curcio, Desalination, 147, p.77 (2002).
5. E Drioli, F Lagana, A Criscuoli and G Barbieri, Desalination, 122, p.141 (1999).
6. A Criscuoli and E Drioli, Desalination, 124, p.243 (1999).

7. E Curcio, G Di Profio, L Mariah and E Drioli, Proc. 7th World Conference for Chemical Engineers, Glascow, 2005.
8. SI Andersson, N Kjellander and B Rodesjo, Desalination, 56, p.345 (1985).
9. M Khayet, MP Godino, and JI Mengual, Desalination, 157, p.297 (2003).
10. GC Sarti, C Gostoli and S Matulli, Desalination, 56, p.277 (1985).
11. AS Jonsson, R Wimmerstedt and AC Harryson, Desalination, 56, p.237 (1985).
12. FA Banat and J Simandl, Desalination, 95, p.39 (1993).
13. ST Hsu, KT Cheng and JS Chiou, Desalination, 143, p.279 (2002).
14. V Gekas and B Hallstrom, J. Membr. Sci., 30, p.153 (1987).
15. AM Alklaibi and N Lior, Desalination, 171, p.111 (2004).
16. L Martinez-Diez and FJ Florida-Diaz, Desalination, 137, p.267 (2001).
17. KW Lawson and DR Lloyd, J. Membr. Sci., 124, p.1 (1997).
18. Y Wu, Y Kong, J Liu, J Zhang and J Xu, J. Membr. Sci., 69, p.72 (1992).
19. A Kubota, K Ohta, I Hayana, M Hirai, K Kikuchi and Y Murayama, Desalination, 69, p.19 (1988).
20. PA Hogan, Sudjito, AG Fane and GL Morrison, Desalination, 81, p.81 (1991).
21. M Mulder, Basic principles of membrane technology, Kluwer Academic Press, p. 48 (1996).
22. V Calabro, E Drioli and F Matera, Desalination, 83, p.209 (1991).
23. Y Wu, Y Kong, J Liu, J Zhang and J Xu, Desalination, 80, p.235 (1991).
24. M Gryta, M Tomaszewska, J Grzechulska and AW Morawski, J. Mebr. Sci., 181, p.179 (2001).
25. S Kimura and S-I Nakao, J. Membr. Sci., 33, p.285 (1987).
26. F Lagana, G Barbieri and E Drioli, J. Membr. Sci., 166, p.1 (2000).
27. V Calabro, BL Jiao and E Drioli, Ind. Eng. Chem. Res., 33, p.1803 (1994).
28. C Gostoli and GC Sarti, J. Membr. Sci., 41, p.211 (1989).
29. GC Sarti, C Gostoli and S Bandini, J. Membr. Sci., 80, p.21 (1993)
30. A Criscuoli, E Drioli, A Capuano, B Memoli and VE Andreucci, Desalination, 147, p.147 (2002).
31. H Udriot, A Araque and U Von Stockar, The Chemical Engineering Journal, 54, p.87 (1994).
32. E Drioli, E Curcio, A Criscuoli and G Di Profio, J. Membr. Sci., 239, p.27 (2004).
33. L Mariah, CA Buckley, CJ Brouckaert, E Curcio, E Drioli, D Jaganyi and D Ramjugernath, submitted J. Membr. Sci (2005)
34. LN Plummer, DL Parkhurst, GW Fleming and SA Dunkle, US Geological Survey, Water-Resources Investigations Report 88-4153, Reston, Virginia (1988).
35. CE Harvie and JH Weare, Geochimica et Cosmochimica Acta, 44, p.981 (1980).
36. CS Harvie, N Møller and JH Weare, Geochimica et Cosmochimica Acta, 48, p.723 (1984).
37. L Mariah, CA Buckley, CJ Brouckaert, E Curcio, E Drioli, D Jaganyi and D Ramjugernath, Proc. IWA/WISA Conference: Management of Residues Emanating from Water and Wastewater Treatment, Johannesburg, South Africa (2005).
38. RA Robinson and RH Stokes, Electrolytes Solutions, 2nd Edition, Butterworths Scientific Publications, London (1959).
39. CJ Brouckaert, S Wadley and QE Hurt, Research on the Modelling of Tubular Reverse Osmosis, WRC Report No 325/1/95 (1995).